Turbulent Drag Reduction by Polymers, Surfactants and Their Mixtures in Pipeline Flow

by

Ali Asghar Mohsenipour

A thesis
presented to the University of Waterloo
in fulfillment of the
thesis requirement for the degree of
Doctor of Philosophy
in
Chemical Engineering

Waterloo, Ontario, Canada, 2011

AUTHOR'S DECLARATION

I hereby declare that I am the sole author of this thesis. This is a true copy of the thesis, including any required final revisions, as accepted by my examiners.

I understand that my thesis may be made electronically available to the public.

Abstract

Although extensive research work has been carried out on the drag reduction behavior of polymers and surfactants alone, little progress has been made on the synergistic effects of combined polymers and surfactants. A number of studies have demonstrated that certain types of polymers and surfactants interact with each other to form surfactant-polymer complexes. The formation of such complexes can cause changes in the solution properties and may result in better drag reduction characteristics as compared with pure additives.

A series of drag-reducing surfactants and polymers were screened for the synergistic studies. The following two widely used polymeric drag reducing agents (DRA) were chosen: a copolymer of acrylamide and sodium acrylate (referred to as PAM) and polyethylene oxide (PEO). Among the different types of surfactants screened, a cationic surfactant octadecyltrimethylammonium chloride (OTAC) and an anionic surfactant Sodium dodecyl sulfate (SDS) were selected for the synergistic study. In the case of the cationic surfactant OTAC, sodium salicylate (NaSal) was used as a counterion. No counterion was used with anionic surfactant SDS. The physical properties such as viscosity, surface tension and electrical conductivity were measured in order to detect any interaction between the polymer and the surfactant. The drag reduction (DR) ability of both pure and mixed additives was investigated in a pipeline flow loop. The effects of different parameters such as additive concentration, type of water (deionized (DI) or tap), temperature, tube diameter, and mechanical degradation were investigated.

The addition of OTAC to PAM solution has a significant effect on the properties of the system. The critical micelle concentration (CMC) of the mixed surfactant-polymer system is found to be different from that of the surfactant alone. The anionic PAM chains collapse upon the addition of cationic OTAC and a substantial decrease in the viscosity occurs. The pipeline flow behaviour of PAM/OTAC mixtures is found to be consistent with the bench scale results. The drag reduction ability of PAM is reduced upon the addition of OTAC. At low concentrations of PAM, the effect of OTAC on the drag reduction behavior is more

pronounced. The drag reduction behavior of polymer solutions is strongly influenced by the nature of water (de-ionized or tap).

The addition of OTAC to PEO solution exhibited a week interaction based on the viscosity and surface tension measurements. However, the pipeline results showed a considerable synergistic effect, that is, the mixed system gave a significantly higher drag reduction (lower friction factors) as compared with the pure additives (pure polymer or pure surfactant). The synergistic effect in the mixed system was stronger at low polymer concentrations and high surfactant concentrations. Also the resistance against mechanical degradation of the additive was improved upon the addition of OTAC to PEO.

The mixed PEO/SDS system exhibited a strong interaction between the polymers (PEO) and the surfactant (SDS), Using electrical conductivity and surface tension measurements, the critical aggregation concentration (CAC) and the polymer saturation point (PSP) were determined. As the PEO concentration is increased, the CAC decreases and the PSP increase. The addition of SDS to the PEO solution exhibits a remarkable increase in the relative viscosity compared to the pure PEO solution. This increase is attributed to the changes in the hydrodynamic radius of the polymer coil. The pipeline flow exhibited a considerable increase in DR for the mixed system as compared to the pure PEO solution. The addition of surfactant always improves the extent of DR up to the PSP. Also the mixed PEO/ SDS system shows better resistance against shear degradation of the additive.

Acknowledgements

I would like to express my sincere appreciation to my supervisor, Professor Rajinder Pal whose encouragement, guidance and support from the initial to the final level enabled me to develop an understanding of the subject. I am grateful to him not only for his valuable suggestions but also for his extensive assistance during the preparation of the thesis.

Furthermore I would like to thank greatly the other members of the supervising committee, Professor Sean Sanders, Professor João Soares, Professor Ali Elkamel and Dr. Nasser Lashgarian Azad for their time and invaluable comments.

I gratefully acknowledge the technical staff of the Chemical Engineering Department. The technical support of Bert Habicher, Ravindra Singh, Jennifer Moll, Siva Ganeshlingam, Ralph Dickhout, Rick Hectus and Dennis Herman was very helpful to me during making of the experimental set-up, bench scale and pipeline experiments. I also appreciate Ketan Prajapati for allowing me to use a few graphs from his work for mixed polymer and surfactant in bench scale system. I also thankful to co-op students who help me during the experiments specially Sadman Ayub and also Abel Sy, Daniel Filiatrault and Kathy Wang.

I would like to express my heartfelt appreciation to my parents, my wife Negar Parva, my daughter Kiana for their support and understanding and my brother Ali Akbar Mohsenipour for his great support.

I would like to pass my special thanks to my best friends and supporter during preparation of this thesis and my defense presentation Dr. Abolfazl Maneshi, Dr. Sohrab Zendehboudi and Dr. Nima Rezaei and also great support of my other colleagues Dr. Saeideh Naderi, Dr. Saeid Mehdiabadi, Dr. Ali Shafiei, Dr. Mousa Jafari and Dr. Majid Soltani at University of Waterloo.

I would also like to convey thanks to the Natural Sciences and Engineering Research Council of Canada (NSERC) for providing the financial support through my supervisor.

This thesis is dedicated:

To my parents,
my wife and my daughter
for their love.

and
to my brother Abbas
his love and his memory
are always in my heart.

Table of Contents

List of Figures

List of Tables

NOMENCLATURE

Roman Symbols

Symbol	Denotes
% DR	Measured percent drag reduction
a_0	The head group cross-section area
C	Concentration
CAC	Critical aggregation concentration
CMC	Critical micelle concentration
D	In pipe flow DR measurement, the inner diameter of the test tube
DI	Deionized water
DR	Drag reduction, drag reducing
DRA(s)	Drag reducing agent(s)
f	Friction factor in DR solutions
f_0	Friction factor in Newtonian solvents
k	The flow consistency index
L	In pipe flow DR measurement, the length of the test tube
l_0	Hydrophobic chain length of surfactant molecules solutions
MDRA	Maximum drag reduction asymptote
MR	Molar ratio of counterion to surfactant
MW	Molecular weight
N	The slope of Ln $\boldsymbol{\Omega}$ versus Ln (torque)
n	The flow behaviour index
p	packing factor
Q	Flow rate
R_0	Rotor inside diameter in Fann viscometer
R_i	Bob outside diameter in Fann viscometer
Re	Reynolds number

Re_G	General Reynolds number at which onset of DR occurs
$S=R_0/R_1$	ratio of rotor to bob radius
SIS	Shear induced structure, represented by a local increase in shear viscosity
t_p	Time flow of polymer
t_w	Time flow of water
TLM	Threadlike micelle
u	Mean flow velocity
u*	Friction velocity
u’	Instantaneous fluctuating axial velocity
u+	Dimensionless velocity
V	Mean flow velocity
v’	Instantaneous fluctuating velocity perpendicular to the flow direction
WLM	Worm-like micelle
y	Distance from the wall
y+	Dimensionless distance from the wall
ΔB	Dimensionless shift in turbulent core velocity profile for DR solutions
ΔP	Pressure drop

Greek Symbols

Symbol Denotes

γ	Shear rate
$\boldsymbol{\Omega = 2\pi(rpm)/60}$	Angular velocity
$\boldsymbol{\pi}$	PI number
τ_{Total}	Total stress in turbulent flow
τ_w	Wall shear stress
η	Shear viscosity, dynamic viscosty
η_0	Zero shear viscosity

$\boldsymbol{\eta_r}$	Relative viscosity
$\boldsymbol{\eta_r}$	Relative viscosity
ρ	Density
ν	Kinematic viscosity

Chapter 1
Introduction and Objectives

1.1 Introduction

It has been known for over fifty years that adding a small quantity of additive such as a polymer or surfactant can lead to a reduction in friction in turbulent pipe flow. This phenonmenon has been classified as drag reduction (DR). The first publication on this subject is credited to Toms, for which reason the DR effect is sometimes referred to as the "Toms' effect" (1948). Drag reduction has a broad range of important applications; including transport of oil, wastewater treatment, firefighting, transport of solids in water, heating and cooling loops, hydraulic and jet machinery, and also biomedical applications (Gasljevic et al. 2001; Harwigsson and Hellsten 1996; Hellsten 2002; Zakin et al. 1996).

For the past few decades, a substantial amount of research effort has been put into the study of polymers for the purpose of drag reduction. Several studies have been performed to discover the mechanisms of DR. Lumley (1969) suggested that there is a critical value of wall shear stress at which the macromolecules become stretched due to the fluctuating strain rate. However, in the viscous sub-layer close to the wall, polymer coils are not greatly deformed and viscosity does not increase greatly above solvent viscosity. Lumley (1973) also concluded that the stretching of randomly coiled polymers due to strong turbulent flow is relevant for DR. Variation in turbulent structure in the buffer layer was also discussed by Tiederman (1989). Virk (1975) suggested, based on experimental evidence, that DR is limited by an asymptotic value. Warholic et al. (1999) conducted experiments with polymer solutions and concluded that the Reynolds shear stress becomes negligible near the maximum DR asymptote. Polymer DR was also explained by viscoelastic effects of the polymer chains in the solution (Hinch 1977; Metzner and Metzner 1970). The high shear conditions of turbulent flow induce stretching of the polymer chain and increase the elongational viscosity, which in turn increases effective viscosity in the buffer layer of the turbulent flow. Due to this increase, the buffer layer thickness increases causing a reduction in wall friction (Lumley

1973). The stream-wise and span-wise fluctuations are suppressed, velocity profile is modified, and the shear in the boundary layer is redistributed in case of polymer solution. Tesauro *et al.* (2007) proposed that energy is transported by the velocity fluctuations to the polymer chain; which is stored in the form of stretching of the polymer chain (which in turn dissipates the energy into heat), and by relaxation of the polymer chain from its extended to equilibrium state.

Mysels (1949) is noted to be the first scientist to have studied the effect of surfactant on DR. However, the area of DR did not receive enough attention for a decade until it was considered in the studies of Dodge and Metzner (1959). Surfactants are categorized into four groups: anionic, cationic, zwitterionic, and non-ionic. It was not until recently that bio-degradable surfactants have received special attention as drag reducing additives. Surfactants are known to exhibit lower mechanical degradation and most of them can be classified as environmentally safe chemicals (Harwigsson and Hellsten 1996; Zakin and Lui 1983; Zakin et al. 1996). Threadlike or wormlike micelles are believed to be necessary for surfactant solution to perform as a drag reducer (Qi and Zakin 2002; Zakin et al. 1998; Zakin et al. 1996). Micelles morphology can be changed from spherical to threadlike by addition of an oppositely charged surfactant, organic counterions, or uncharged small compounds like alcohols to the cationic solutions. This was reported by many researchers (Zakin et al. 1998; Zhang et al. 2009). Exact mechanism of DR by surfactants solutions is still unclear; however, some researchers have proposed that viscoelastic effects of surfactant solution could be responsible for turbulent DR. Bewersdorff & Ohlendorf (1988) showed using micro and integral scale of turbulence axial velocity fluctuations that both the scales increase substantially relative to that of the Newtonian solvent.

In spite of five decades of research, the fundamentals of DR phenomenon still require further clarification. Given the nature of turbulent flow, the lack of progress in the understanding is reasonable as the rheology of viscoelastic fluids in much simpler flow fields is still under investigation(Aguilar et al. 2006).

Many variables have been considered while exploring the field of drag reduction: the type of drag reducing additive, additive concentration, molecular weight, additive structure, temperature, and solvent quality are some of these variables.

Most of the reported studies on DR suffer from various issues some of which are listed as follows:

a. Several studies were done under extreme range of concentrations which are not applicable in practical situations (very low or very high concentration of drag reducers)
b. The addition of DR additives can change the solution viscosity. Many researchers have used solvent viscosity in DR calculations which makes the interpretation of results difficult.
c. In most studies the Blasius equation is used as the base line for friction factor comparison in turbulent regime. All the graphs and calculated data such as percent of DR are based on the Blasius equation. This assumption is correct for only those solutions which show same viscosity as the solvent.
d. In only a few reports the effect of pipe diameter on DR has been taken into consideration. In most studies, the selected diameters are small and far from what is required in the real application.

Despite a great deal of effort having been put into the research of surfactant and polymers DR, there is no report which evaluates the benefits as well as the disadvantages in using one as opposed to the other as the drag reducer. Most of the research work was conducted separately for polymers and surfactants under different conditions or at a different scale. To address some of these issues, the current research work was planned and conducted in a pilot plant to simulate practical situation.

To the best of our knowledge, there is a thin literature on study of the drag reduction by combination of surfactants with polymers in the pipeline flow and no systematic study has been done yet to relate the bench scale experiment to pipeline flow behavior. One aim of this work is to investigate the drag reduction capability of different surfactant/ polymer complexes compared to that achieved by pure polymer and pure surfactant in pipeline flow.

The combination of polymer and surfactant additives has been used in variety of applications such as drug delivery, oil recovery and cosmetics industries (Bai et al. 2010; Dan et al. 2009; Harada and Kataoka 2006; Stoll et al. 2010; Villetti et al. 2011; Zhang et al. 2011). The majority of these studies are focused on the methodology, and the feasibility to attain polymer-surfactant aggregation at very low surfactant concentration (Goddard and Ananthapadmanabhan 1993; Kwak 1998; Touhami et al. 2001; Trabelsi and Langevin 2007). Many studies have attempted to control the properties of the mixtures. The polymer-surfactant interaction depends on the type of polymer and surfactant and also the physical and chemical properties of the solution; such as pH and temperature (Feitosa et al. 1996; Jönsson et al. 1998). The interaction between polymers and surfactants usually starts at a well-known surfactant concentration called critical aggregation concentration (CAC). Polymer and surfactants can interact in two ways. First, the interaction is possible for polymers with negative or positive charge with oppositely charged ionic surfactant. Here the electrostatic interactions play a profound role. In this case, CAC has been reported to be several orders of magnitudes lower than the critical micelle concentration. The second possible interaction type is the interaction between non-ionic polymer and ionic surfactant, where the CAC can be close to the CMC of surfactant. A hydrophobic interaction between the hydrophobic parts of both polymer and surfactant is the driving force for the interaction in this category (Diamant and Andelman 1999; Goddard and Ananthapadmanabhan 1993; Hansson and Lindman 1996). In spite of the extensive studies conducted on the understanding of polymer-surfactant interactions, their complex behavior in solution has prevented a true understanding of the interaction mechanism involved.

1.2 Objectives

The main objectives of this work are as follows:

1-To study and to compare the DR ability of pure polymers and pure surfactants in pipeline turbulent flow

Different types of polymers and surfactants were considered in the experiments. Several polymers and surfactants were selected and after screening, two polymers and two surfactants were chosen for further investigation. The polymers which were selected for this study are: A copolymer of acrylamide and sodium acrylate referred to as PAM and polyethylene oxide (PEO). These two polymers are widely used as drag reducer agents. The surfactants selected are: Octadecyltrimethylammonium Chloride (OTAC) which is a cationic surfactant and sodium dodecyl sulfate (SDS) as an anionic surfactant. A pipeline set-up with different pipe diameters was designed and constructed for this purpose. Effect of various parameters such as polymer concentration, type of water (e.g. deionized (DI) or tap water), temperature, tube diameter, and mechanical degradation were investigated.

2- To study the combination of polymers and surfactants and to determine their synergistic effect on drag reduction

Some studies have demonstrated that certain polymers can interact with surfactants to form polymer-surfactant complexes consisting of surfactant micelles bound to the polymer backbone. The formation of such complexes can cause changes in the solution properties such as viscosity due to the increase in hydrodynamic volume of the polymer molecules (Goddard and Ananthapadmanabhan 1993; Jiang and Han 2000). The formation of complexes between polymers and surfactants has the potential to offer better drag reduction than the pure additives. In this project mixtures of different types of surfactant and high molecular weight polymers were investigated. Screening of different mixtures of polymers and surfactants were done at bench-scale. Physical properties such as viscosity, surface tension and conductivity were studied. Based on bench-scale experiments some of the combinations were selected and investigated in pipeline flow.

3- To study the effect of mechanical shear on polymer degradation

Polymers undergo degradation at high shear stress. Degradation of polymers was studied under different conditions. The effect of surfactant on polymer degradation was also

studied. The goal was to develop methods to decrease or to postpone the degradation of polymers in turbulent flow.

1.3 Outline of This Study

This thesis consists of nine chapters including the introduction. Chapter 2 gives some basic information on fluid flow. The equations used in this study are discussed. A literature review on drag reduction of polymers and surfactants is presented in Chapter 3. Chapter 4 describes experimental setup and its calibration. This chapter includes procedures for bench-scale and pipeline flow experiments.

Chapter 5 presents the experimental results and discussion for pure polymers and surfactants. The results of related mixtures of anionic polymer (PAM) and cationic surfactant (OTAC) are presented in Chapter 6. In Chapter 7 the interaction of non-ionic polymer (PEO) and cationic surfactant (OTAC) along with pipeline results are explained. The mixed non-ionic polymer (PEO) and anionic surfactant (SDS) systems are discussed in Chapter 8. The conclusions and recommendations for future work are listed in Chapter 9.

Chapter 2
Background

2.1 Fluid Flow Equations

The conservation of mass for a differential fluid element can be expressed as:

$$\frac{\partial \rho}{\partial t} + \nabla . (\rho \vec{V}) = 0 \qquad (2\text{-}1)$$

where ρ is fluid density and V is the velocity vector. For a fluid element the linear momentum equation is obtained by applying Newton's second law of motion:

$$\rho \frac{\partial \vec{V}}{\partial t} + \rho \vec{V} . \nabla \vec{V} = -\nabla P + \rho \vec{g} + \nabla . \underline{\underline{\tau}} \qquad (2\text{-}2)$$

P is pressure and $\underline{\underline{\tau}}$ is viscous stress tensor. The stress tensor is described by a constitutive equation. By considering the constitutive equations two main categories of fluids can be introduced: Newtonian and non-Newtonian fluids.

In Newtonian fluid the relationship between shear stress and shear rate is linear. It reads:

$$\tau = \mu \dot{\gamma} \qquad (2\text{-}3)$$

where μ is constant and is referred to as fluids shear viscosity and $\dot{\gamma}$ is shear rate exerted on the fluid.

For non-Newtonian fluid, the shear stress is a non-linear function of shear rate and the linear relationship between shear rate and shear stress is no longer valid. In this case an apparent viscosity has been defined .The relationship between shear rate and shear stress by analogy to the Newtonian flow is expressed as:

$$\tau = \eta \dot{\gamma} \qquad (2\text{-}4)$$

where η is apparent viscosity and function of $\dot{\gamma}$. Some models such as Sisko, Ellis, Williamson, Carreau and power law have been developed which show the trend of shear viscosity (Carreau 1972).

$$\tau = K\dot{\gamma}^{n} \quad (2\text{-}5)$$

$$\eta = K\dot{\gamma}^{n-1} \quad (2\text{-}6)$$

K and n are power law constants. The n (flow behaviour index) indicates the degree of non-Newtonian behaviour and the K (flow consistency index) shows the viscosity level at certain shear rate.

Figure 2-1 shows different behaviors of fluids. The power law model has been widely used to express the viscosity behavior of many non-Newtonian fluids at intermediate shear rates (Pal 1992).

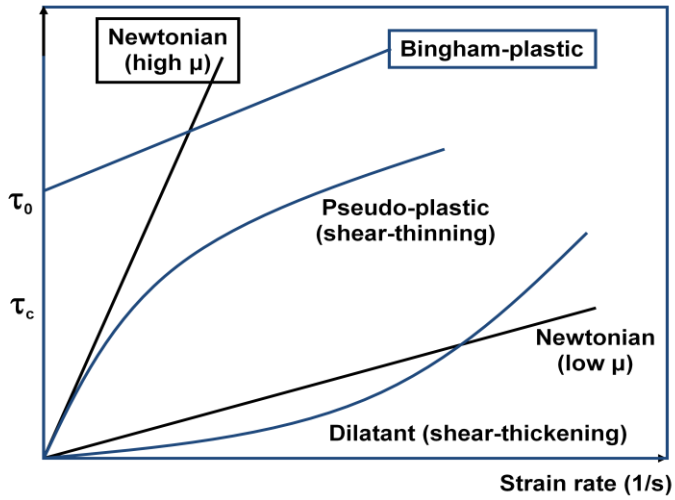

Figure 2-1: Shear stress vs. Shear rate for viscous fluid (Revised from Streeter et al., 1998)

2.2 Fluid Flow in Pipelines

All fluid flow is classified into one of two broad categories or regimes; laminar or turbulent. The flow regime, whether laminar or turbulent, is important in the design and operation of any fluid system. The amount of fluid friction, which determines the amount of energy required to maintain the desired flow, depends on the flow condition.

Laminar flow is also referred to as streamline or viscous flow. In laminar flow, layers of fluid flow over one another at different speeds with virtually no mixing between the layers. At this time fluid particles move in definite and observable paths or streamlines. The viscosity plays a significant role in fluid flow for this type of fluid (Streeter et al. 1998).

Turbulent flow is characterized by the irregular movement of particles of the fluid. The particles travel in irregular paths with no observable pattern and no definite layers.

Fluid flow in pipes can be described through defining its boundary layer and velocity profile. In the boundary layer, (the region adjacent the walls of the pipe) viscous effects are most important. Turbulent flow has a different velocity profile than laminar flow. The velocity profile, as shown in Figure 2-2, will also vary due to the growth of this boundary layer. When the velocity profile reaches a constant (i.e., velocity profile no longer changes along the pipe), the flow is said to be fully developed. The length required for the flow to reach fully developed conditions is referred to as entrance length (Le), and it can be determined from the following empirical relations for different types of flows:

For laminar flow: $$L_e/_D = 0.06Re \qquad (2\text{-}7)$$

For turbulent flow: $$L_e/_D = 0.06Re^{1/6} \qquad (2\text{-}8)$$

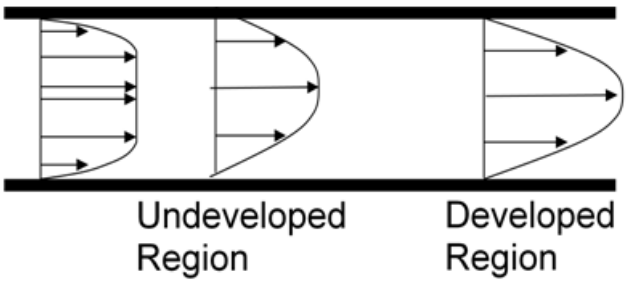

Figure 2-2: Parabolic velocity profile in laminar flow

When fluid flows through pipes, a certain amount of power is needed to overcome the wall friction. The wall shear stress (τ_w) in fully developed pipe flow can be related to the pressure drop (ΔP) over a given length (L) of pipe having a diameter (D) using the following equation:

$$\boldsymbol{\tau_w} = \frac{\boldsymbol{\Delta P . D}}{\boldsymbol{4L}} \qquad (2\text{-}9)$$

The Fanning friction factor is defined as:

$$f = \frac{\tau_w}{\frac{1}{2}\rho V^2} \qquad \textbf{(2-10)}$$

where V is the mean flow velocity. Substituting of equation (2-9) into equation (2-10) gives:

$$f = \frac{\Delta P D}{2\rho V^2 L} = \frac{\pi^2 D^5 \Delta P}{32 \rho L Q^2} \qquad (2\text{-}11)$$

where Q is the volumetric flow rate. *f* can be calculated if ΔP and Q are measured.

Fully developed laminar pipe flow is generally known as Hagen-Poiseuille flow. The velocity profile of a fully developed laminar flow in a horizontal circular pipe can be derived from the Navier-Stokes equations and is given by

$$V_z = \frac{1}{4\mu}\frac{dP}{dZ}\left(r^2 - R^2\right) \qquad (2\text{-}12)$$

By integrating the velocity profile over the cross-sectional area and applying to the volumetric flow rate (Q):

$$Q = \frac{\pi R^4}{8\mu L}\Delta P \qquad (2\text{-}13)$$

where ΔP is the pressure drop across a pipe length of L and radius R. The above equation is known as Hagen-Poiseuille's law.

Equation (2.11 – 2.13) lead us to the Fanning friction factor law for laminar flow:

$$f = \frac{16}{Re} \qquad (2\text{-}14)$$

For Newtonian laminar flow:

$$\tau_w = \frac{\Delta P . D}{4L} = \mu \frac{8V}{D} \qquad (2\text{-}15)$$

Turbulent fluid motion is highly random, unsteady, and three-dimensional. It consists of many eddies with different lengths and time scales. Due to these complexities, the turbulent motions are extremely difficult to describe and thus to predict theoretically. The exact equations describing the turbulent motion are believed to be the Navier-Stokes

equations, and numerical procedures are available to solve these equations. The storage capacity and speed of present-day computers is still not sufficient to allow a solution for exact equation. This approach is known as direct numerical simulation (DNS).

The turbulent transport process cannot be calculated with an exact method so that it must be approximated by a turbulence model. This model is determined with the aid of empirical information. In the Reynolds-averaged procedure, the Navier-Stokes equations are averaged over a time period. The physical variables are decomposed into mean and fluctuating components. Only the mean values are solved and therefore it is necessary to express the fluctuating values as functions of the mean values. Equation (2.16) shows time averaged motion equation:

$$\boldsymbol{\rho}\frac{\partial\bar{\vec{V}}}{\partial t} + \boldsymbol{\rho}\bar{\vec{V}}.\nabla\bar{\vec{V}} = -\nabla\bar{P} + \boldsymbol{\rho}\vec{g} + \nabla.\underline{\bar{\tau}} - \nabla.(\rho\,\overline{\vec{v}'\vec{v}'}) \qquad (2\text{-}16)$$

The time-averaged component is indicated by overbar and the prime shows fluctuating component. The term $\rho\,\overline{\vec{v}'\vec{v}'}$ is called Reynolds or turbulence stress. In order to solve the turbulent problem by this method, a constitutive equation should be applied. One of the best equations has been introduced by Prandtl (1963). By applying the Prandtl constitutive equation to the time-averaged motion equation in fully developed pipe flow, one can derive the velocity equation and eventually Prandtl's law (Prandtl-Karman) of friction. This equation is the most common equation for Newtonian fluid in turbulent flow. It is:

$$\frac{1}{\sqrt{f}} = 4.0\,\log_{10}\left(Re\sqrt{f}\right) - 0.4 \qquad (2\text{-}17)$$

Alternatively, the friction factor for turbulent flow of Newtonian fluid in smooth pipes can be estimated by some empirical equations. Three different equations, which are accurate in specific Re ranges, have been experimentally developed. These equations can be found in the form:

$$f = a + \frac{b}{Re^n} \qquad (2\text{-}18)$$

Table 2.1 shows the equation names and parameter value. Among them the Blasius equation is the most popular. It reads:

$$f = \frac{\mathbf{0.079}}{\boldsymbol{Re}^{\mathbf{0.25}}} \qquad (2\text{-}19)$$

Table 2-1: Empirical equation coefficients for turbulent flow with Re (Jhon, 2001)

Equation name	a	b	n	Re range for each equation
Blasius	0	0.079	0.25	$4x10^3 < Re < 10^5$
Colburn	0	0.046	0.20	$10^5 < Re < 10^6$
Koo	0.0014	0.125	0.32	$4x10^3 < Re < 3x10^6$

The Prandtl-Karman law has been modified by Colebrook for pipe with roughness:

$$\frac{\mathbf{1}}{\sqrt{\boldsymbol{f}}} = 4.0\ \mathbf{log_{10}}[\frac{\varepsilon/_D}{\mathbf{3.7}} + \frac{\mathbf{1.255}}{\boldsymbol{Re}\sqrt{\boldsymbol{f}}}] \qquad (2\text{-}20)$$

where $\varepsilon/_D$ is relative roughness.

Metzner and Reed (1955) derived Equation 2-21 for steady state, a fully developed laminar flow of a time-independent non Newtonian fluid.

$$\boldsymbol{\tau_w} = \frac{\boldsymbol{\Delta P.D}}{\boldsymbol{4L}} = \mathbf{k'}(\frac{\mathbf{8V}}{\mathbf{D}})^{\mathbf{n'}} \qquad (2\text{-}21)$$

If n' does not change with shear stress n and n' will be equal and k and k' have following relationship:

$$\boldsymbol{k = k'}(\frac{\boldsymbol{4n}}{\boldsymbol{3n+1}})^{\boldsymbol{n}} \qquad (2\text{-}22)$$

For a power-law non-Newtonian fluid, Re_G is defined differently than the Newtonian Re number. It reads:

$$\mathrm{Re} = \frac{\rho D^{n} \bar{V}^{2-n}}{8^{n-1} k \left(\frac{(3n+1)}{4n}\right)^{n}} \qquad (2\text{-}23)$$

where n and k are power-law model parameters.

For flow of non-Newtonian fluids there is not any universally accepted equation in turbulent flow. Dodge and Metzner (1959) studied on Prandtl-Karman law and applied power law to introduce a new equation as shown in equation 2-24.

$$\frac{1}{\sqrt{f}} = \frac{4}{n^{0.75}} \log\left(Re_G f^{1-\frac{n}{2}}\right) - \frac{0.4}{n^{1.2}} \qquad (2\text{-}24)$$

Figure 2-3 shows friction factor chart for Newtonian and non-Newtonian fluids based on Dodge and Metzner equation (D&M).

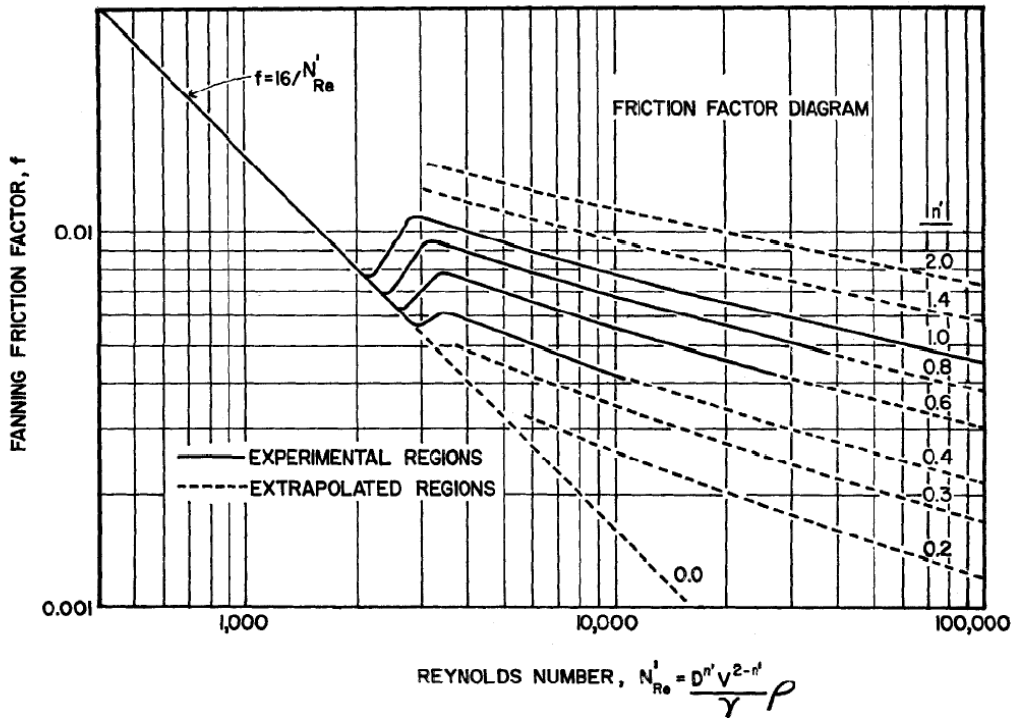

Figure 2-3: Friction factor chart for Newtonian and non-Newtonian fluids (Dodge and Metzner 1959)

Subsequently, an explicit equation giving good agreement with Eequation 2-24 was proposed by Yoo (1974) shown in 2-25.

$$f=0.079n^{0.675}Re^{-0.25} \qquad (2\text{-}25)$$

Some other models were proposed by Wilson and Thomas in term of power law fluids and Bingham plastic (Thomas and Wilson 1987; Wilson and Thomas 2006; Wilson and Thomas 1985).

The behavior of viscoelastic fluids in turbulent pipe flow is different from purely viscous non-Newtonian fluid and also from solvent. Different friction factor is observed for these types of fluid under turbulent flow conditions. This value in most cases is much lower than the values for the pure solvent or purely viscous non-Newtonian fluids with same viscosity (Cho and Harnett 1982).

Chapter 3
Literature Survey

3.1 Introduction and Drag Reduction Concepts

Turbulent drag reduction due to the addition of a small amount of dilute polymer was observed by Toms (1948). As a result of his pioneering contribution, drag reduction is often termed as Tom's effect in the literature. Gyr and Bewersdorff have given a very detailed description of the drag reduction phenomenon (Gyr and Bewersdorff 1995). Numerous studies have been conducted in recent decades to explore drag reduction in various system and to provide at least a qualitative understanding of drag reduction and its mechanisms. Among these studies the early studies of Metzner and Park (1964), Lumley (1969; 1973), Virk (1975), Zakin et al. (1978; 1971), Berman (1978) and Tabor and Gennes (1986) and the recent contributions of Escudier et al. (1998), Zakin (2010; 1998), Sreenivasan et al. (2000), Ptaskinski et al (2001), Kim (2003), Vanapalli et al. (2006), Shah and Zhou (2009), and Tamano (2010) should be mentioned. There are also some experimental studies which provide important information about modifications of the statistical properties of turbulence flows in the presence of a drag reducer (Frohnapfel et al. 2007; Jovanovi et al. 2006; Ptasinski et al. 2001; Wei and Willmarth 1991; Yu and Kawaguchi 2006).

With the addition of an additive to a turbulent flow system; drag reduction occurs if the pressure drop is reduced at constant flow rate or the flow rate is increased at constant pressure. It is common to define drag reduction as

$$\%\mathrm{DR} = \frac{f_0 - f}{f_0} \times 100 \qquad (3\text{-}1)$$

where %DR is percentage of drag reduction and f and f_0 represent the friction factors of the solution and the solvent respectively (Zakin et al. 1998).

Additives causing drag reduction can be divided into three groups: polymers, surfactants and fibers. In this study drag reduction of turbulent pipe flow by polymers and surfactants was investigated.

3.2 Velocity Profile of Drag Reduction Flow and Maximum Asymptote

3.2.1 Mean velocity profiles

Many researchers have divided the turbulent flow velocity profile for Newtonian fluids into three regions in pipe flow (Zakin et al. 1998): the viscous sublayer, the buffer layer, and the turbulent core. To represent velocity profiles in pipe flow, friction velocity is defined as:

$$U^* = \sqrt{\tau_w / \rho} \qquad (3\text{-}2)$$

and two dimensionless parameters are defined as:

$$U^+ = U / U^* \qquad (3\text{-}3)$$

$$y^+ = U^* y / \nu \qquad (3\text{-}4)$$

where U is the local mean velocity and varies with the distance from the wall (y), ν is kinematic viscosity and ρ is density.

1. Viscous sublayer

$$U^+ = y^+ \qquad (0 < y^+ < 5) \qquad (3\text{-}5a)$$

2. Buffer layer

$$U^+ = 5.0 \, \mathrm{Ln} y^+ + 3.05 \qquad (5 < y^+ < 30) \qquad (3\text{-}5b)$$

3. Core

$$U^+ = 2.5 \, \mathrm{Ln} y^+ + 5.5 \qquad (y^+ > 30) \qquad (3\text{-}5c)$$

Studies have shown that the velocity profile in the viscous sublayer of drag reducing fluid is similar to Newtonian fluids (Ohlendorf et al. 1986; Virk 1975; Wilson and Thomas 1985). For drag reducer fluid the buffer layer is mostly a part of the turbulent core velocity profile. For the core section thr profile can be expressed by equation 3-6.

$$U^+ = 2.5\ \mathrm{Ln}y^+ + 5.5 + \Delta B \qquad (3\text{-}6)$$

Figure 3-1 shows turbulent core velocities for a Newtonian fluid and a drag reducing fluid in pipe flow. In this figure and equation 3-6 , ΔB is an added part to show the parallel profile for fluids with moderate drag reduction. This term causes a revision from the Newtonian profile.

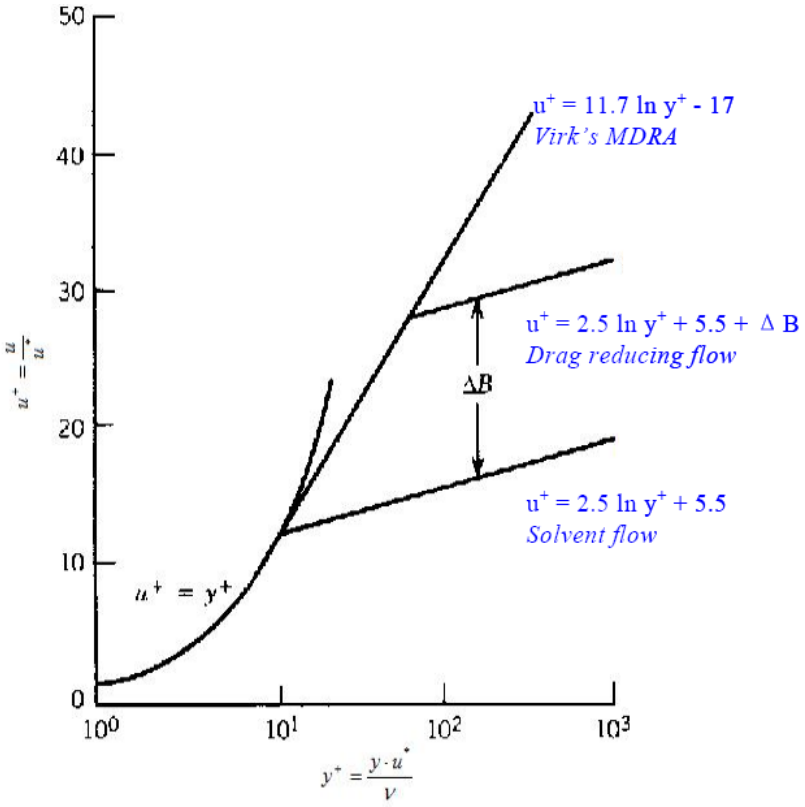

Figure 3-1: Turbulent core velocities for Newtonian fluids and fluid with drag reducer (Zakin et al. 1998)

3.2.2 Drag Reduction Asymptote (MDRA)

As previously mentioned, for Newtonian turbulent pipe flow of non-DR solutions, friction factors are predicted by the von Karman equation (2.18) or Blasius equation (2.20).

Both polymer and surfactant drag reducer agent have Maximum Drag Reduction Asymptote (MDRA). Virk (1975) defined a MDRA for polymers. (Equation 3.7)

$$\frac{1}{\sqrt{f}} = 19.0 \log_{10}\left(Re\sqrt{f}\right) - 32.4 \qquad (3.7)$$

this equation can be estimated as follows:

$$f = \frac{0.58}{Re^{0.58}} \quad (4000 < Re < 40000) \qquad (3.8)$$

Zakin et al. (1996) introduced another MDRA for surfactants. They studied several surfactant systems and showed that their friction factors are over 40 percent less than Virk's MDRA for high polymers and more than 90% less than for Newtonian solutions. Equation (3.4) shows their MDRA for surfactants:

$$f = \frac{0.32}{Re^{0.55}} \qquad (3.9)$$

Aguilar et al. (2001) proposed another asymptote as follows:

$$f = \frac{0.18}{Re^{0.50}} \qquad (3.10)$$

3.3 Drag Reduction by Polymer Solutions

Polymers have been under numerous studies for the past decades for the purpose of drag reduction. In this case a few parts per million of soluble high-molecular weight polymers in both aqueous and organic solvents are used as a drag reducer. This amount of polymer has been found to be very effective. Most studies have revealed that polymer with a linear structure and high molecular weight, above 500, 000 (g/gmole), can be good drag reducers (Den Toonder et al. 1997).

The trans-Alaska pipeline system was one of the largest successes in utilizing polymer applications for drag reduction by using oil-soluble polymers. In this case the flow rate was increased by 32,000 m^3 /day for the same pipe line system (Zakin et al. 1998).
Lumley (1969) suggested that there is a critical value of wall shear stress, at which macromolecules become stretched due to the fluctuating strain rate. However, in the viscous sublayer close to the wall, polymer coils are not greatly deformed and viscosity does not increase greatly above the solvent viscosity. It was also mentioned that the stretching of randomly coiled polymers due to the strong turbulent flow, is relevant for drag reduction (Lumley 1973). Virk (1975) by his experimental evidence suggested that drag reduction was limited by an asymptotic (Equation 3.2). The changes of turbulent structures in the buffer layer are also discussed by some other researchers (Tiederman 1989).

Warholic et al. (1999) presented their experimental evidence of drag reduction of polymer solutions and suggested that the Reynolds shear stress can be considered negligible near the maximum drag reduction .

Kim (2003) studied the pseudo plastic behaviour of CMC polymer as a drag reducer in straight pipes. He used power law model for laminar flow and extended this model to non-Newtonian turbulent flow.

Many studies have been done regarding Direct Numerical Simulation (DNS) of the turbulent flow of polymer solutions. Graham (2004) has provided a comprehensive review of more recent numerical investigations on drag reduction aspects.

3.4 Drag Reduction by Surfactants

Physical chemistry of surfactants

Surfactants have a hydrophilic head group and a hydrophobic tail group. The hydrophilic head group is an ionisable polar group (except for non-ionic surfactants) and is capable of forming hydrogen bonds. The hydrophobic tail group is a non-polar group which is typically a long chain alkyl group. A usual characteristic of surfactants is their ability to lower the surface tension of liquids. In an aqueous solution, the hydrophobic group repels water while the hydrophilic group is attracted to the polar water molecules. This causes the hydrophobic groups to aggregate together in a hydrocarbon phase in order to prevent contact with water. At the same time the hydrophilic polar groups surround them and are in contact with the water. The formed aggregates are called micelles. Depending on system conditions, the micelle shape can be globular/spherical, disk-like, cylindrical or rod/worm/thread-like, bilayer spherical (vesicle), and hexagonal, lamellar and cubic crystal which can transform from one shape to another when the solution conditions change (Zakin et al. 1998; Zhang et al. 2009; Zhang 2005). Figure 3-2 shows different type of micelle forms.

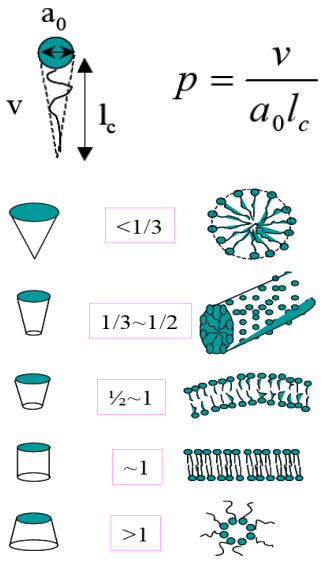

Figure 3-2: Schematic diagram of geometric packing of surfactant micelles (Zhang 2005)

Micelle shapes are determined by a packing factor ($p= v/a_0l_0$) where v is hydrodynamic group, l_0 is length of the group and a_0 is the head group cross-section area. When p is equal to 1/3 or less, the surfactant will be cone shape and the micelles will be spherical. This situation is the most common type of micelle shape. For p close to or equal to 1/2 the micelles will be in cylindrical shape (rod like). Figure 3-3 shows rod-like micelles.

Figure 3-3: Spherical and rod-like micelles (revised from (Rothstein 2008))

A simplified phase diagram for an aqueous surfactant solution is shown in Figure 3-4. The Kraft point is the temperature at which the solubility is equal to the critical micelle concentration (CMC). When the temperature is lower than Kraft point, the surfactants will be partially in gel or crystal form in the solution. For temperatures above the Kraft point and concentrations higher than the CMC point, the micelles will be in spherical form within the surfactant solution. Any increase in concentration or upon addition of counterions will change the micelles shape to the thread-like (Zakin et al. 1998).

The concentration at which surfactants form rod-like micelles sometimes is called CMCII. CMC is almost independent of temperature but CMCII increases with temperature.

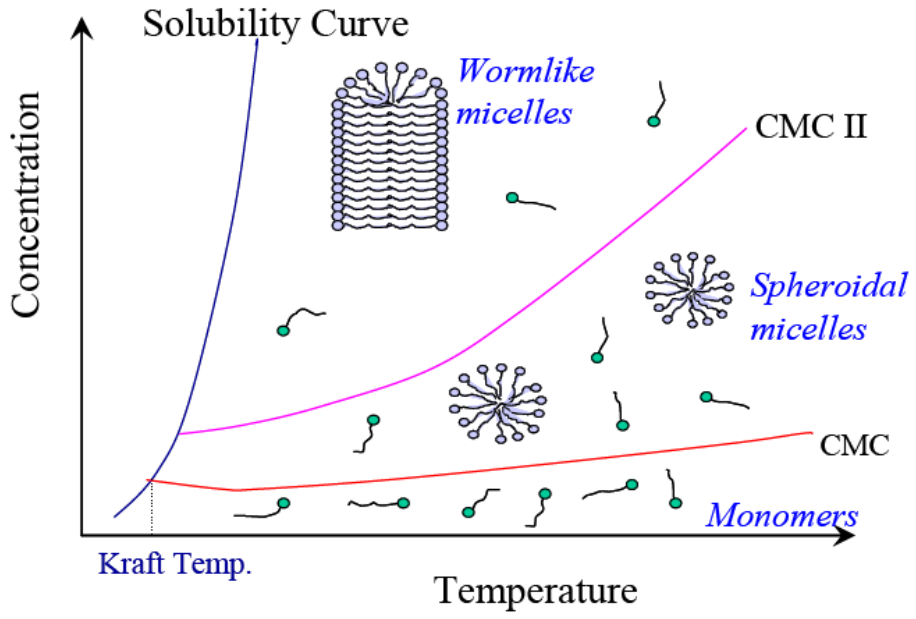

Figure 3-4: Simplified phase diagram of surfactant aqueous solution (Zakin et al. 1998)

Spherical micelles, rod-like or thread-like micelles and vesicles are the three forms of microstructures visualized in dilute DR surfactant solutions (Qi and Zakin 2002; Zakin et al. 2007; Zakin and Lui 1983; Zakin et al. 2006; Zhang et al. 2009). Salts or counterions have been used to promote the formation of rod-like micelles. These type of materials disperse the positive repulsive charges on the ionic head groups and stabilizes the micelles allowing them to grow in size (Zhang et al. 2005).

Mysels (1949) studied the effect of surfactant solutions on drag reduction for the first time, but this area did not receive much attention until 10 years later in the studies of Dodge and Metzner (1959).

Surfactants are categorized into four groups: anionic, cationic, zwitterionic, and non-ionic. A summary of some of the studies using different type of surfactants is presented in the following section.

Anionic surfactants

Anionic soap surfactants are water soluble and have a negative charge when they are in aqueous solutions.

Mysels (1949) was the first who used anionic aluminum soaps during the flow studies of gasoline. He published the finding much later in 1949. Savins (1967) did extensive work on anionic surfactants as drag reducers in aqueous solutions. He used alkali metal and ammonium soaps to achieve a reasonable DR by 0.2% sodium oleate solutions. Savins also reported that the addition of KCl can accelerate association of the soap molecules to form rod-like micelles. He observed that DR increased with increasing shear stress up to a critical value and rapidly decreases with a further increase in shear stress. This indicates that the network of micelles collapses if the shear stress exceeds a critical shear stress. The drag reducing ability of solution will return back when the shear stress decrease under the critical value.

Anionic surfactant is stable and inexpensive which make them good candidate to consider as drag reducer. The only problem regarding this surfactant is their interaction with calcium and other cations that are generally present in tap water (Dodge and Metzner 1959; Hellsten 2002).

Cationic surfactants

Cationic surfactants are relatively expensive compared to anionic surfactants. On the other hand they do not precipitate in tap water which is a remarkable advantage.

Zakin et al. (1971) studied the capability of Cetryltrimethylammonium bromide (CTAB) for drag reduction as the first cationic surfactant. They reduced drag up to 70 % by adding different amounts of 1-naphtol to CTAB. They studied the shear-thinning characteristics of CTAB-naphthol mixture to forecast the possibility of drag reduction ability of this mixture. Similar to anionic surfactant solutions, the drag reducing ability of the CTAB-naphthol solution vanished at high Re numbers.

Chou and Zakin [1991] studied effectiveness of mixed cations and mixed counterions on drag reduction. They noted that the effective drag reduction temperature range for long

chain cationic surfactants usually extends to high temperatures. Zakin and Lu (1998) found out that drag reduction is only effective at low temperatures for short chain molecules.

Rehage and Hoffmann (1991) found that spherical micelles can change to threadlike micelles when an oppositely charged surfactant, organic counterions, or uncharged small compounds (like alcohols) are added to the solution. Later Bewersdorff (1996) found that these additives give a much smaller interfacial charge density on the micelle, and allow denser packing of surfactant molecules in the micelles. Organic counterions, typically hydroxy- or halo-substituted benzoates, at equimolar or higher concentrations are the most effective counterions for cationic DR surfactant solutions (Prud'homme and Warr 1994).
Thread-like or worm-like micelles are believed to be necessary for surfactant solutions to be drag reducing (Qi and Zakin 2002; Zakin et al. 1998). Zheng et al. (2000) found that vesicle microstructures can transform to thread-like micelles under shear. Qi and Zakin (2002) found that rod-like micelles set themselves along the flow direction, causing drag reduction in pipeline flow.

Microstructures of aqueous cationic surfactant solutions vary with surfactant chemical structure and concentration, counterion chemical structure and concentration, temperature, shear and pH. Zhang et al. (2005) studied co-solvent effects on drag reduction, rheological properties, and micelle structures of cationic surfactants. The effect of headgroup structure of quaternary ammonium cationic surfactants on their DR, rheological properties and microstructures was investigated at certain counterion and surfactant concentrations by Zhang and Qi et al. (2005). In their research they concluded that surfactants with larger head groups had lowered upper temperature limits for drag reduction.

Non-ionic Surfactants

Non-ionic surfactants have no charge on their head groups. Zakin and Chang (1972) were pioneer researchers who investigated non-ionic surfactants as drag reducers. They used three non-ionic surfactants and investigated the effects of temperature, electrolyte concentration, surfactant concentration and the effect of mechanical shear stress. For Alfonic 1214 they found that 1% solutions were more effective than 0.5 % solutions. The molecular

structure of non-ionic surfactant has an important effect on its micelle size and shape. This profoundly influences the drag reducing ability of the surfactant. Plenty of research has been conducted on drag reduction by different non-ionic surfactants containing saturated and unsaturated C12 to C18 alkyl group. It was found that the maximum drag reduction is close to the cloud point of surfactant solution (Cho et al. 2007; Zakin and Lui 1983). Harwigsson and Hellsten (1996) examined ethoxylated fatty acid ethanolamide as drag reducer. Kim (2003) studied the effect of Alfonic surfactant on drag reduction in a closed loop. The alcohol ethoxylate (Alfonic 1412-7), a type of non-ionic surfactant, was used to investigate the effect of molecular conformational change on the pseudo plastic behaviour of fluid and eventually on the drag reduction behaviour. They found that 2% solution had the best drag reduction and stability in a closed loop.

In comparison to anionic and cationic surfactants, non-ionic surfactants have some advantages. They can be used in the presence of calcium ions without any precipitation. They are both mechanically and chemically stable. This type of surfactant is biodegradable and has low toxicity compared to other types (which is very important in district cooling systems). Thus if a leak occurs within the system, the environment would not be polluted because of the additive.

Despite these merits, more studies are needed to exploit the potential of non-ionic surfactants to their fullest extent as drag reducers.

Zwitterionic surfactants

This type of surfactants has both negative and positives charges on the head group of the molecule. It may cause the surfactant molecule to be sensitive to the ions present in water or solutions.

Harwigsson and Hellsten (1996) studied zwitterionic surfactants with C16 to C18 and achieved a good drag reduction at low concentrations and high temperatures.

Drag reduction ability for mixtures of two types of zwitterionic surfactants (amine oxide and betaine type) was studied by Nobuchika et al. (2000). They found that mixing of zwitterionic surfactants results in better drag reduction.

3.5 Interaction of Polymers and Surfactants

Surfactants and polymers are used almost in every application and industry. For the past few decades, many researchers have been involved in this area of technology. Interactions of aqueous solution of polymers and surfactants have been studied as part of that kind of research. Most of the ongoing studies being conducted for different applications such as drug delivery, oil recovery and cosmetics industry (Bai et al. 2010; Dan et al. 2009; Harada and Kataoka 2006; Stoll et al. 2010; Villetti et al. 2011; Zhang et al. 2011). The majority of these studies are focused on the methodology, and the feasibility to accomplish polymer-surfactant aggregation at very low surfactant concentration (Goddard and Ananthapadmanabhan 1993; Kwak 1998; Touhami et al. 2001; Trabelsi and Langevin 2007). Researchers are inspired to accomplish ways to control the properties of the solution resulting from the interaction of polymer and surfactant (Kwak 1998). This interaction depends on the type of polymer, the type of surfactant and the solution conditions such as pH and temperature. (Feitosa et al. 1996; Jönsson et al. 1998)

Surfactant monomers start assembling at CMC point. When surfactant monomers are introduced to polymers, interaction of polymers and surfactants usually starts at a well-known surfactant concentration. This concentration is called critical aggregation concentration (CAC). Most of the experimental efforts have shown that CAC is lower than the critical micelle concentration of the surfactant solution alone (Deo et al. 2007; Goddard and Ananthapadmanabhan 1993; Jönsson et al. 1998).

Some studies have categorized these systems in two groups: The first group consists of the interaction of polymers with negative or positive charge with oppositely charged ionic surfactant. In this case CAC has been reported to be several orders of magnitudes lower than the critical micelle concentration. The second group referred to the interaction of non-ionic polymer and ionic surfactant, where the CAC is the same or close to what observed for CMC in surfactants or solution or (Diamant and Andelman 1999; Goddard and Ananthapadmanabhan 1993; Hansson and Lindman 1996).

Based on what was stated earlier it can be expressed that polymers and surfactants can interact in two ways:

1. Electrostatic Interactions (when the polymer and the surfactant are oppositely charged).

2. Hydrophobic Interactions (between the hydrophobic parts of both the polymer and surfactant)

Nagarajan (1980) explained the possible polymer –surfactant association structures. Several theoretical aspects have been considered for polymer-surfactant aggregation (Bai et al. 2005; Jönsson et al. 1998; Nikas and Blankschtein 1994; Nilsson et al. 2000). Most of these theories have been developed for the system of surfactants when polymers were added to solutions.

In this research, different experimental methodology is utilized. Here, we investigate the effect of addition of surfactant, on the properties of polymer solution instead of the conventional methodology which is to study the effect of polymer addition on micelle formation in a surfactant solution. These properties can be monitored below and at the onset of self-assembly. Question may raise if there is any differences between these two mythologies. In a simple case addition of anionic polymers into cationic surfactant can cause precipitation of polymer chains. In this case high amount of surfactant concentration (high in number) at the early stage of addition can attack to limited number of polymer chains and completely neutralize the negative sites on backbone of chains. Toward this electrostatic reaction polymer chains are collapse and precipitate.

There are several analytical techniques available which can be employed to study the interaction between polymers and surfactants. Techniques such as viscosity, conductivity, surface tension, turbidity, fluorescence, NMR, SANS are widely used. For more information one can refer to work of Goddard & Ananthapadmanabhan (1993). For this research work viscosity (relative and shear viscosity), conductivity, surface tension have been utilized to detect interaction behaviour.

The electrical conductivity measurements can be used to detect any changes in the solution behavior when an ionic surfactant is added to the aqueous solution. Figure 3-5 can be a typical conductivity plots for pure ionic surfactant and a mixed polymer / ionic surfactant system.

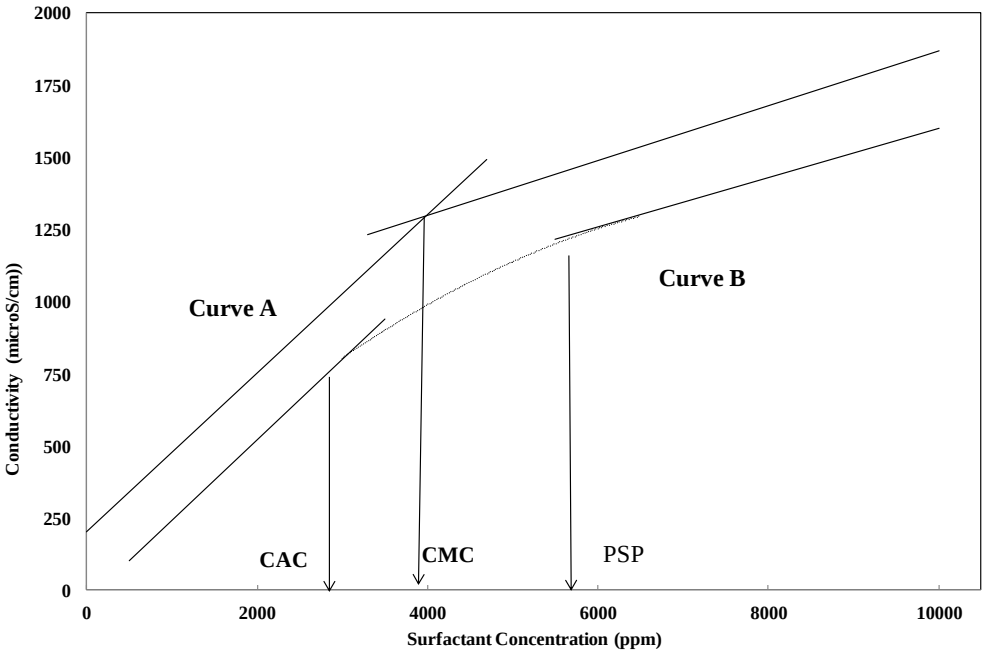

Figure 3-5: Schematic conductivity plots for pure surfactant and mixture of surfactant and polymer

This plot represents the systems which show good interaction. Curve A shows the trend for pure ionic surfactant in aqueous solution whereas curve B demonstrates the conductivity trend for a mixture of polymer/ionic surfactant. For pure surfactant solution (curve A), the conductivity is a linear function of the surfactant concentration below the CMC (CMC is the minimum surfactant concentration where micellization takes place). The ionic surfactant is completely dissociated below the CMC. Above the CMC, micelles are formed. The micellar contribution to conductivity is less than that of the same number of free surfactant molecules. Consequently the slope of the conductivity plot above CMC is lower than that below CMC although the conductivity continues to increase with the increase in the surfactant concentration. For the mixed surfactant and polymer systems, the conductivity plot shows two breakpoints. The first break point is known to occur at CAC, the concentration of surfactant where surfactant monomers begin to associate with the polymer chains. The second break point occurs at PSP (polymer saturation point) where the polymer molecules

are saturated with surfactant. Above the PSP, the addition of surfactant results in the formation of free micelles. For those systems with weak interaction the CAC and PSP are not easily detectable.

Figure 3-6 shows qualitatively the surface tension versus surfactant concentration plots for pure surfactant solution and for mixtures of polymer and surfactant at a fixed polymer concentration. For the pure surfactant solution, a sharp decrease in the surface tension occurs with the increase in surfactant concentration up to the CMC. At surfactant concentrations higher than the CMC, the surface tension remains constant. When polymer is present in the system, the solution behavior is different. The surface tension plot now shows two break points. The first point is the CAC point where interaction between the polymer and the surfactant begins. The second point is the PSP point where the polymer chains become saturated with the surfactant. CAC and PSP in most system with weak interaction are the same as CMC point.

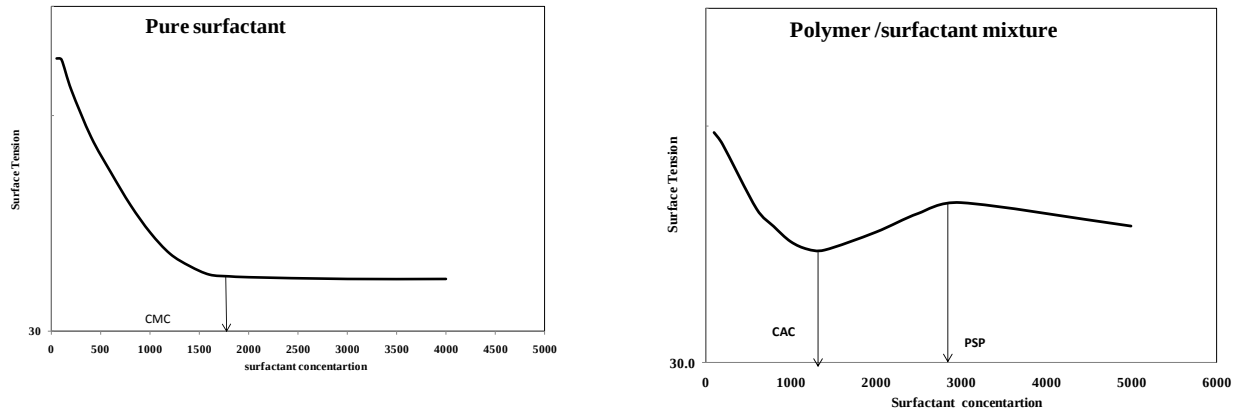

Figure 3-6: Qualitatively plots of surface tension for pure anionic surfactant and surfactant mixed with non- ionic polymer

Polymer and surfactant can have positive, negative or neutral charge. The interaction of polymers and surfactants is affected by their charge. This introduces a new property for consideration to the mixture solution. The main aim of this research work is to study the interactions of polymers and surfactants for drag reduction point of view. Different

combinations of polymers and surfactants have been studied in bench scale and best combinations were selected for further investigation in pipeline flow experiments. Different combinations were taken in consideration for screening test and finally combinations shown in Table 3-1 were selected for more bench scale and pipeline flow investigations.

Table 3-1: Different mixtures of polymer and surfactant

Polymer / surfactant	Anionic Polymer (PAM)	Non-ionic polymer (PEO)
Cationic Surfactant (OTAC)	DONE	DONE
Anionic Surfactant (SDS)	----------	DONE

3.5.1 Interaction of anionic polymers with cationic surfactants

Cationic surfactant and anionic polymer interact in two ways; Electrostatic charge interaction and hydrophobic interaction. Positive charge on cationic surfactant head groups interacts with negative charge of anionic polymers. This interaction is fast and starts even with addition of small amount of surfactant to polymer solution. The aggregation of polyelectrolyte and surfactant with opposite charges highly depends on both polyelectrolyte and surfactant properties (Goddard and Ananthapadmanabhan 1993).

Addition of cationic surfactant to aqueous solution of anionic polymer can effectively reduce the critical micelle concentration (CMC) of the surfactant-free polymer solution. Cationic surfactant monomers can interact with anionic polymer to form micelle-like clusters on the backbone of the polymer at critical aggregation concentration (CAC). The mixture may cause cluster precipitation if ratio of surfactant to polymer approaches 1. This is the consequence of the higher hydrophobicity when more surfactant monomers bind to the negative charge sites on the polymer (Thalberg et al. 1990). Excessive surfactant concentration may help the precipitates to re-dissolve because additional surfactants

monomer would be attached on the precipitates and increase the hydrophilicity of these clusters (Goddard and Ananthapadmanabhan 1993)

Electrostatic bonding is the main driving force for formation of polymer–surfactant complexes. The hydrophobic interaction of surfactant tail with the polymer also helps to improve the reaction but is not key to the process (Kogej and Škerjanc 1999).

3.5.2 Interaction of nonionic polymers with cationic and anionic surfactants

In the case of non- ionic polymers, a considerable effort has been put to understand their interaction with different surfactants types (Fishman and Elrich 1975; Jiang and Han 2000; Ma and Li 1989). The studies confirm that anionic surfactants are much more effective in binding to nonionic polymers. These studies support the idea that the size of anionic head group and their hydrophobicity conditions significantly contribute to the overall interaction. The early attempts reveal that the nonionic and cationic surfactants do not interact with the polymer molecules, generally speaking. However, in presence of some type of ions such as SCN- or I- as counterion a weak interaction was reported. The bulkiness of the cationic head group (compare to anionic surfactants) could be the main rational for such observations (Nagarajan 1989; Witte and Engberts 1987).

Hydrophobicity was also reported to be one of the key factors and plays an important role in the interaction between nonionic polymers and cationic surfactant. Typically polymers with more extent of hydrophobicity show a better interaction (Anthony and Zana 1996; Thuresson et al. 1995; Thuresson et al. 1996). Zana et al. (1992) reported that when hydroxyethyl cellulose interacts with Hexadecyltrimethylammonium chloride and bromide , the CAC is less than CMC and aggregation number of surfactant is also less compared to the polymer-free solution. No interaction was observed by Brackmanand et al. (1992) in the case of PEO and PVP polymers with the cationic surfactant.

Mya et al. (2000) reported that combination of cationic surfactant hexadecyltrimethylammonium and PEO could result in strong interactions when temperature is above 25 °C. In this case, the hydrodynamic radius (R_h) increases due to chain expansion.

This expansion occurs because of electrostatic repulsions between the bonded micelles on the backbone of the polymer chain. This observation is consistent with the work of Hormnirun et al. (2000).

Small-angle neutron-scattering experiments have proven that the surfactant molecules will attach to the polymer chains in the micelle, similar to the micelle aggregation in the polymer-free solution. The only difference arises in the aggregation number which is less for surfactant-polymer compare to the polymer-free solution. On the other hand, the radius of gyration of the polymer molecule is comparable to that of a "free" macromolecule (Ruckenstein et al. 1987).

Two models were proposed for nonionic polymer and ionic surfactant by Nagarajan (1980) and Ruckenstein et al. (1987). In the so-called "necklace model" proposed by Nagarjan, a complex consisting of the polymer molecule wrapped around surfactant micelles forms. In this case, the polymer segments will partially penetrate into the polar head group region of the micelles. This can cause a reduction in the micelle core-water contact area. Such a structure can describe the interaction of a nonionic polymer with surfactant micelles (Figure 3-7).

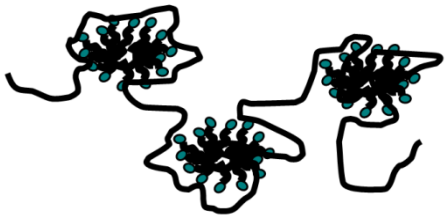

Figure 3-7: Necklace model

Ruckenstein's model is based on the adsorption of polymer on the micelle surface. The presence of polymer molecules in water changes the micro-environment of the surfactant molecules. This will change the surface free energy between micellar hydrocarbon core and the solvent in the "free space" of the coiled macromolecule. This will contribute the most to the overall interaction of polymer with the surfactant micelles. In this model, the interfacial free energy increases as the polymer provides higher hydrophobicity. If the head group is small (such as anionic surfactant head group) the overall surface free energy is decreased and

consequently, the micellization process is amplified. In such cases, free aggregation starts only after the polymer molecules are saturated with bound micelles. If the head group is large (such as for cationic surfactant head groups) the surface free energy is increased and the presence of the polymer has no effect on the micellization.

Suksamranchit et al. (Suksamranchit et al. 2006) investigated the turbulent wall shear stress of aqueous solutions of PEO, hexadecyltrimethylammonium chloride (HTAC), and their mixtures at 30 °C in Couette flow. They used different molecular weight of PEO which ranged from 0.91×10^5 g/mol to 17.9×10^5 g/mol. They found that the critical molecular weight of PEO required to observe drag reduction was reduced in mixtures of PEO/HTAC compared to pure systems. In this case, in the presence of HTAC, a low molecular weight PEO can result drag reduction similar to that achieved by a higher molecular weight PEO in pure solution. They observed that the maximum drag reduction happened at a surfactant concentration close to the maximum binding concentration (MBC) of HTAC to PEO. Suksamranchit and the co-workers also claimed that the interaction between the polymer and surfactant starts at a lower surfactant concentration as a result of high turbulent shear stress which causes polymer chains to stretch (Suksamranchit et al. 2006). In later research, Suksamranchit & Sirivat (2007) studied the influence of ionic strength on the solution of PEO and HTAC. They concluded that addition of NaSal causes an improvement in stability of the HTAC micelles and binding between PEO and HTAC. They also mentioned that in presence of NaSal, the micelle size increases due to the shielding of electrostatic charge of the ionic headgroup of the surfactant.

Matras et al. (2008) have reported drag reduction results in pipe flow using mixture of PEO and Cetyltrimethylammonium bromide (CTAB) with sodium salicylate (NaSal) as counterion. Their experiment was done for a specific concentration of polymer (30 ppm), a mixture of CTAB/NaSal and combination of two systems. They reported that combination showed better drag reduction compared to pure polymer and pure surfactant in a small range of Re. This range and behavior of combination is very close to surfactant system behavior which make the results uncertain.

In the case of non-ionic polymer /anionic surfactant interaction the study of Jones on the properties of mixed polyethylene oxide (PEO)/sodium dodecyl sulfate (SDS) systems has had a major impact on polymer/surfactant system field. Jones formalized the concept of this field and defined CAC and PSP for polymer system when surfactant was added to the solution (Jones 1967). Schwuger (1973) investigated the effect of PEO molecular weight on the surface tension of SDS solutions. He found that in case of PEO with a MW of 600, interaction was weak, but for a MW of 1550 it was reasonable. For Molecular weights higher than 4000 the interaction was strong and independent of molecular weight.

Chari et al. (1994) examined the effect of SDS on both local chain motions and long range dimensions of the coil. They showed that a PEO coil saturated with SDS micelles is swollen compared to free coils in good solvent. They also reported that these swollen chains are not fully stretched. Their results showed that the coil at saturation is more like a swollen cage rather than a necklace.

Minatti and Zanette (1996) reported that the critical aggregation concentration (CAC) and polymer saturation point (PSP) of PEO and SDS mixtures were changed in the presence of salt (NaCl). Masuda et al. (2002) studied the swelling behaviour of poly(ethylene oxide) (PEO) gels in aqueous solutions of sodium dodecyl sulfate (SDS). They observed that in the absence of salt, PEO gels start to swell from a concentration lower than the CMC of SDS. This concentration was in agreement with CAC value reported for the aqueous PEO solution.

Benrraou et al. (2003) studied the interaction between poly(ethylene oxide) or poly(vinylpyrrolidone) and cesium and tetraalkylammonium (tetramethyl to tetrabutyl ammonium) dodecylsulfate. They used the electrical conductivity method to determine the CAC for different polymer surfactant systems. They concluded that the value of the CAC/CMC ratio increased with the radius of the counterion in the sequence as follows:

Na+ < Cs+ < tetramethylammonium+ < tetraethylammonium+ = etrapropylammonium+ = tetrabutylammonium+ = 1.0

The results showed that the strength of the interaction decreases upon increasing counterion radius.

Yan and Xiao (2004) checked the effect of anionic surfactant headgroup on interaction with non-ionic polymer (PEO). Their report revealed that differences between $C_{12}SO_3$ and $C_{12}SO_4$ in interacting with PEO were obvious. They also concluded that both of the hydrophobic and electrostatic interactions play important roles in the $C_{12}SO_3$/ PEO and $C_{12}SO_4$ / PEO interactions.

Romani et al. (2005) investigated the effect of addition of different combination of polyethylene glycol (Mw = 8000 g/mol) / polyvinylpyrrolidone ((PVP),Mw = 55 000) g/mol on CMC of SDS. They measured electrical conductivity, zeta potential, viscosity and used fluorescence spectroscopy, and small-angle X-ray scattering (SAXS). The results showed that SDS−polymer interaction takes place at low surfactant concentration, and the CAC dependents on polymer composition. The average aggregation number varies with surfactant concentration and is highly unstable compared to pure SDS micelles. The zeta potentials were increased linearly with the fraction of PVP at constant SDS concentration. The results of the SAXS indicated that the PVP/PEG/SDS system is in the form of cylindrical shape with an anisometry ratio of about 3.0.

To our knowledge, there is a very thin literature on study of the drag reduction by combination of ionic surfactants and nonionic polymers in the pipeline flow and no systematic study has been done yet to relate the bench scale experiment to pipeline flow behavior.

Based on literature survey, one can conclude that the increase in the length of the hydrophobic group of surfactant and the increase in molecular weight of polymer will enhance the binding interaction between nonionic polymer and cationic surfactant. PEO with highest available molecular weight (7×10^5 g/mol) and a cationic surfactant Octadecyltrimethylammonium Chloride (OTAC) (which has a long enough tail of hydrophobic group) were chosen. The bench-scale and pipeline results have been presented in chapter 7.

In the case of anionic surfactant, SDS was used and it's interaction with PEO was investigated at the bench-scale. Bench scale and pipeline flow results of SDS /PEO mixtures have both been presented in chapter 8.

Chapter 4
Experimental Set-up and Calibrations

4.1 Bench Scale Experiments

Experimental procedure

All the chemicals in this research study were used as received without any further purification. To investigate the interaction between polymer and surfactant in bench-scale, the polymers were dissolved in DI or tap water and prepared as stock solution at 0.3%- %0.5 polymer concentration. DI water conductivity was 2 – 5.5 μS/cm and for tap water conductivity was 650 – 700 μS/cm. Surfactants and salt were dissolved separately in DI water before added to the polymer solution. 400ml of surfactant/polymer/ water solution at various concentrations was synthesized and mixed to ensure homogeneity throughout the solution. The characterizations of the surfactant and polymer/surfactant solutions were conducted in the following order: conductivity, surface tension, relative viscosity .

4.2 Pilot Plant Experiments

Experimental set-up

The experiments were performed in a closed loop system. Figure 4-1 and Figure 4-2 show a schematic diagram and a photo of the experimental set-up.

The test fluid was prepared in a large mixing tank which was installed in the flow loop. The tank had a jacket and a temperature controller to maintain a constant temperature during the experiments. Two different capacity centrifugal pumps were used to circulate the test fluid. Three straight tubes, with different diameters were installed horizontally. Each tube was equipped with three pressure taps which were made by drilling small holes (1/10 of tube diameter) through the tube walls. The pressure transducers were configured in such a manner that a desired pressure transducer could be easily connected to the pressure taps while they were in use. The pressure taps were located far enough from the tube entrance to ensure that the flow of test fluid was fully developed in a section of the tube where measurements were taken place. The first pressure tap was used as the reference tap for measuring the differential

pressure between two taps. The loop has been equipped with a data acquisition system. The data acquisition system consisted of an electronic board for input and output signals, a computer to process the signals using the LABVIEW software. Table 4-1 and Table 4-2 show the setup layout with more details. The Technical Data such as accuracy and other information for apparatuses used in the set-up have been gathered in Appendix B.

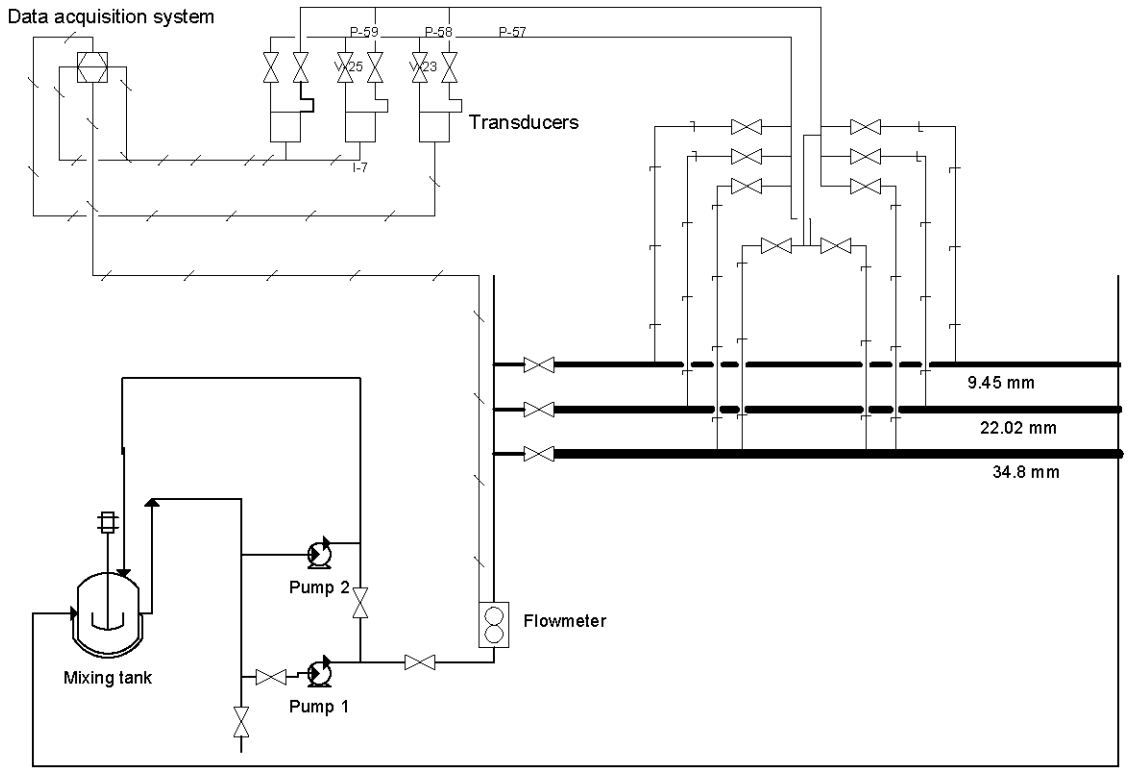

Figure 4-1: Schematic diagram of experimental setup

Table 4-1: Equipments and tubes installed in the closed loop

Item#	Equipments and test sections	Description
1	Mixing tank	Stainless still with Jacket
2	Pump 1	Centrifugal ,1.5 Hp
3	Pump 2	Centrifugal 7.5 HP
4	Coriolis flow meter	KROHNE-7050 series (one tube), nominal flow1200 1b/min
7	Straight pipe	Pipe #1 stainless still pipe (see table 4-2)
8	Straight pipe	Pipe #2 stainless still pipe (see table 4-2)
9	Straight pipe	Pipe #3 stainless still pipe (see table 4-2)
10	Pressure transducers	Rosemount Model 3051 (0-0.5 psi, 0-5 psi) and Cole-Parmer Model 68071-52 (0-10 psi)
11	Control panel for transducers connection	Gives flexibility for transducer to pressure tap connections
12	Data acquisition system	Consisting of: PC, USB Measurement Computing Interface Model 1680 FS and LABVIEW software

Table 4-2: Tube dimensions and tap locations

Pipe #	Nominal diameter (in)	Inside diameter (mm)	Entrance length (mm)	Test section length (m)
1	1.5	34.8	154.2	3.048
2	1.0	22.02	154.2	3.048
3	0.5	9.45	91.44	1.219

Figure 4-2: Pipeline flow loop

4.3 Experimental Tests and Equipments for Measuring Fluid Parameters

4.3.1 Coriolis flowmeter

The flow rate is measured by a Coriolis flowmeter which has been installed in flow loop. The flowmeter was calibrated by measuring (weighing) the amount of water passing the flowmeter in a certain time. Then different points were graphed and calibration equation was

obtained. Figure 4-3 shows calibration graph and equation for this flow meter. Other related information regarding this flowmeter has been presented in Appendix B.

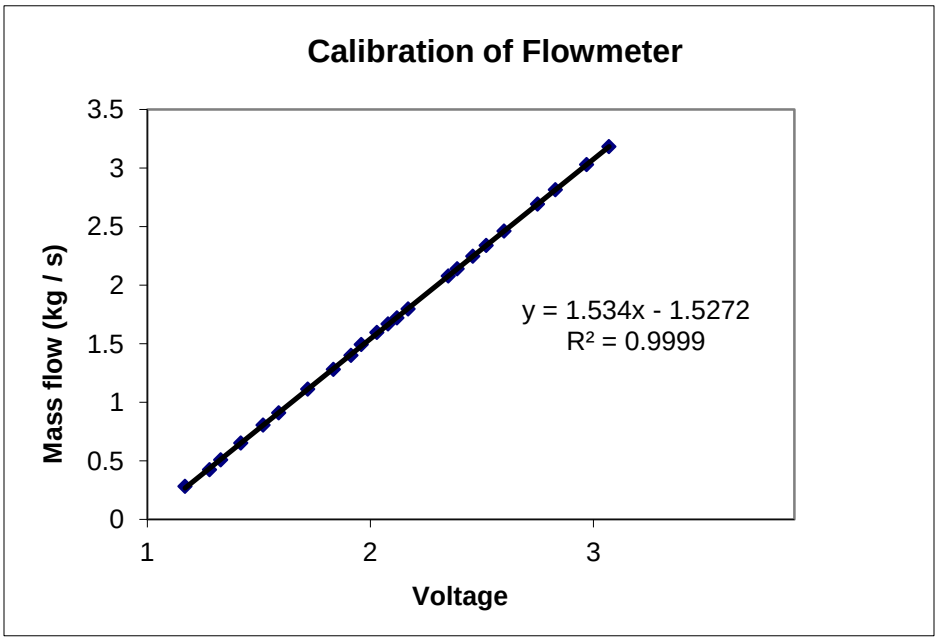

Figure 4-3: Flowmeter calibration

The equation used for mass flowmeter is:

Mass flow (Kg/s) = 1.534 × (Reading volt) - 1.5272 (4-1)

4.3.2 Pressure transducers

Three pressure transducers with different measurement ranges were installed. Each transducer was mounted on a panel independently so that they could easily be removed or added without disturbing whole set-up. Each transducer was equipped with two shut-off valves and one bypass valve. The whole line can be purged with water. Figure 4-4 shows a schematic diagram for pressure transducer valve connection. A panel was designed to give more flexibility in connecting taps to transducers. More technical data about the pressure transducer used in this research work have been brought in Appendix B.

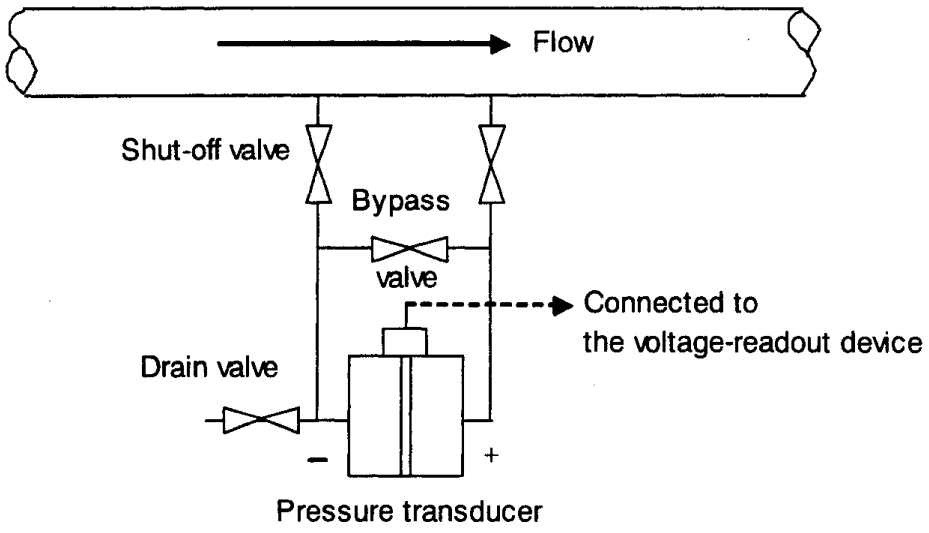

Figure 4-4: Pressure transducer connection diagram (Revised from Kim (2003))

Calibration of pressure transducers

Pressure transducers relate the pressure or pressure difference with a voltage output. Figure 4-5 shows pressure transducer calibration set-up. The accuracy of the pressure transducers was ensured by calibrating them with a manometer and a digital pressure calibrator. Since the pressure transducers were mounted in a horizontal position any deflection in voltage reading was removed. The air pressure is incrementally increased from atmospheric to the maximum transducer pressure corresponding to a voltage signal of 1-5 volts. At the same time, the average pressure and voltage are recorded for that pressure increment. Figure 4-6, Figure 4-7 and Figure 4-8 show calibration graphs using this method.

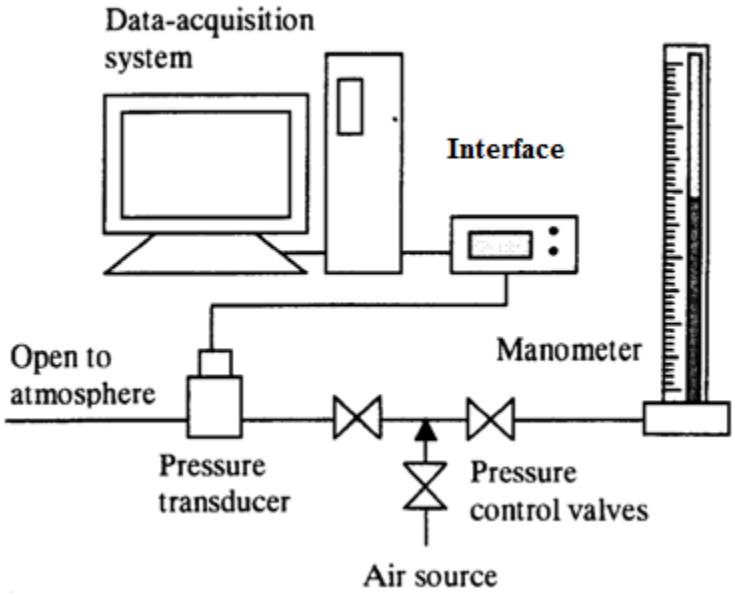

Figure 4-5: Pressure transducer calibration set-up

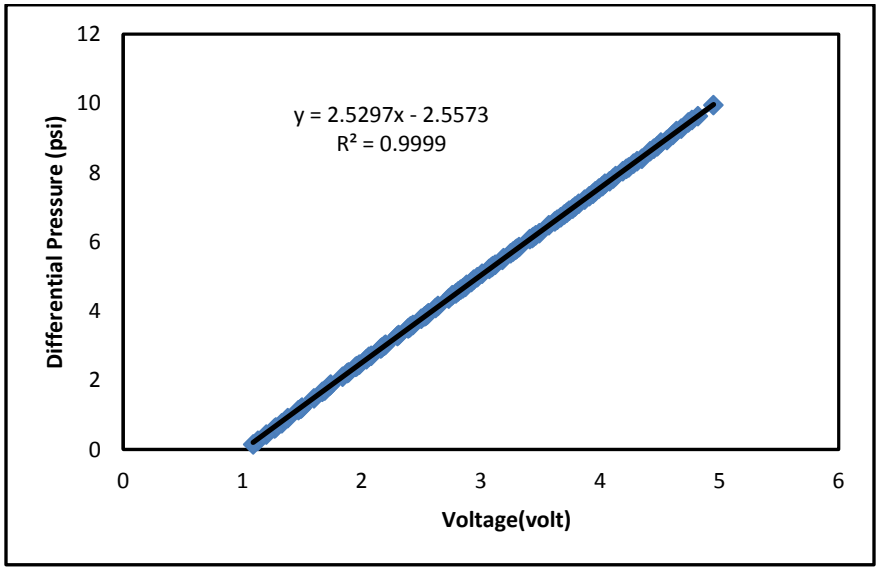

Figure 4-6: 0-10 psi pressure transducer calibration graph

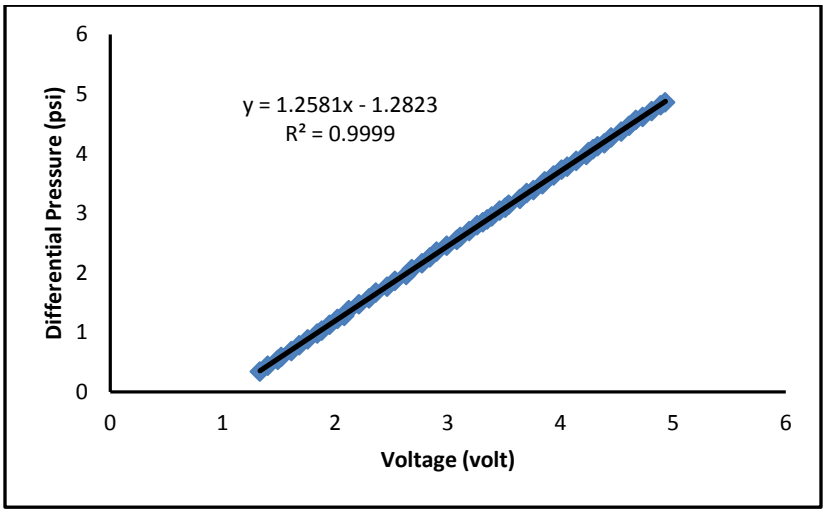

Figure 4-7: 0-5 psi pressure transducer calibration graph

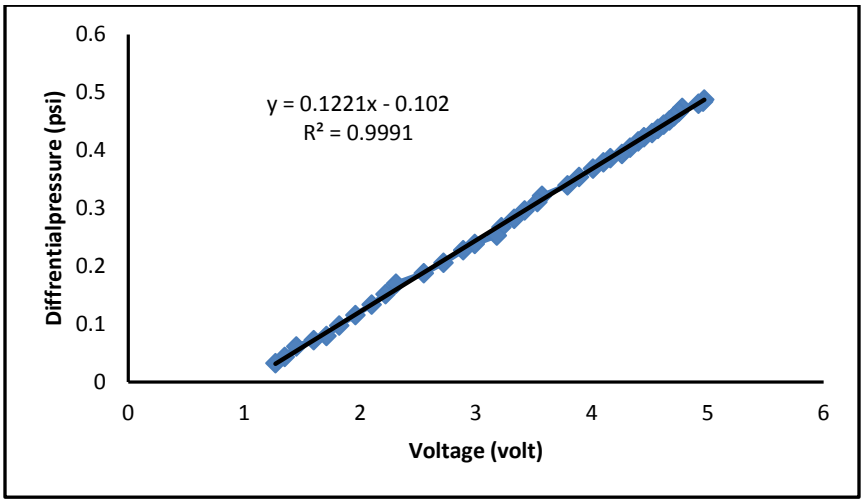

Figure 4-8: 0 - 0.5 psi pressure transducer calibration graph

Table 4-3 Shows the pressure transducer calibration equations which have been applied to the pipe flow.

Table 4-3: pressure transducer calibration equations

Range	Differential Pressure Calibration
0-10 psi	Differential pressure = 2.5297×(Reading voltage) - 2.5573
0-5 psi	Differential pressure = 1.2581×(Reading voltage) - 1.2823
0-0.5 psi	Differential pressure = 0.1221×(Reading voltage) - 0.102

4.3.3 Viscosity measurements

Viscosity measurement by Ubbelohde viscometer

Relative viscosity of solution was determined using an Ubbelohde viscometer. The relative viscosity is defined as ratio of flow time of test solution to flow time of water through the capillary of viscometer.

Relative Viscosity

$$\eta_{r=\frac{t_p}{t_w}} \qquad (4\text{-}2)$$

Specific Viscosity

$$\eta_s = \frac{t_p - t_w}{t_w} \qquad (4\text{-}3)$$

To measure flow time of a solution, it is loaded very gently to reservoir C (see Figure 4-9) where it has to be sucked to bulb A in there all trapped air should be realized. The flow time between point D and point E are measured and compared to flow time of reference fluid (water).

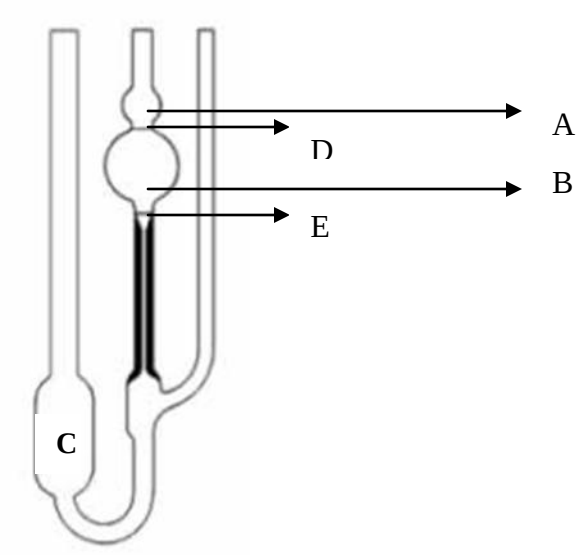

Figure 4-9: Capillary viscometer

Coaxial cylinder viscometer

A Fann coaxial cylinder viscometer Model No35A/SR12 was used for measuring the shear viscosity. Figure 4-10 shows schematic diagram for the viscometer. The information has been gathered in Table 4-4. The viscometer had a gap width of 0.113 cm. The Bob was fixed and rotor would rotate.

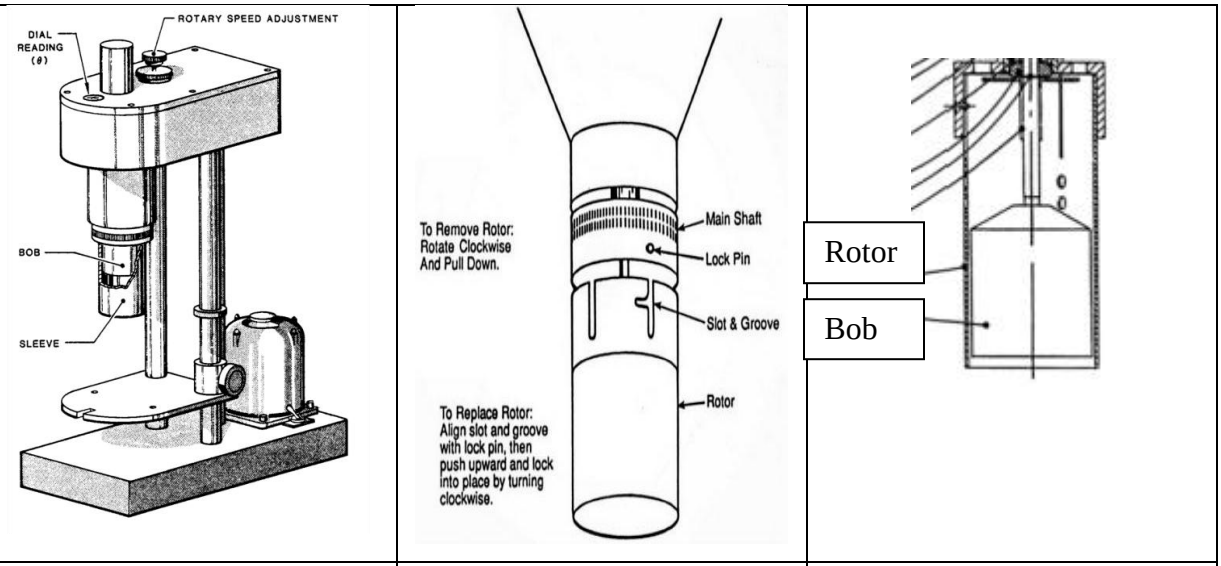

a) Full view of apparatus	b) Rotor	c) Rotor and Bob

Figure 4-10: Fann viscometer Model 35A/SR12 (revised from apparatus manual)

Table 4-4: Bob and Rotor dimensions

	OD(mm)	Length (mm)	ID	Thickness(mm)
Bob	34.5	45.12		
Rotor	40.67	87.33	36.76	1.96

The shear rate is calculated using these equations:

Newtonian fluids

$$\dot{\gamma}_{Ri} = \frac{2S^2}{S^2 - 1}\Omega_0 \tag{4.5}$$

Non-Newtonian fluids

$$\dot{\gamma}_{Ri} = \frac{2N}{1 - S^{-2N}}\Omega_0 \tag{4-6}$$

where Ω is defined as:

$$\Omega = 2\pi(rpm)/60 \tag{4-7}$$

S, in equation 4.5, is the ratio of rotor to bob radius (R_0/R_i =1.06551) and N is the slope of Ln $\boldsymbol{\Omega}$ versus Ln(torque) for the viscometer.

The procedure is very simple. The provided stainless steel sample cup has a line at 350 ml test fluid level. The cup has to be filled up to that line with test fluid. By loosing the height adjustment knob somebody can insert the bob and rotor inside the test solution up to a scribe line on the rotor which indicates proper immersion depth. By changing the rotor speed different shear rates can be produced and at the same time different dials can be read on the dial-reading.

The calibration of shear stress vs. dial-reading was done for a fluid with known viscosity of 8.7 cP for this viscometer showing Table 4-5 in and following equation was obtained:

$\boldsymbol{\tau} = \mathbf{0}.0881\times$ (Dial reading) - 0.3694 (Pa) (4-4)

Table 4-5: Calibration of Fann coaxial viscometer

speed	Omega(rad/s)	Dial Reading	Shear rate (1/s)	Shear stress (Pa)
0.9	0.09	3.5	1.58	0.0138
1.8	0.19	3.5	3.16	0.0275
3	0.31	4	5.27	0.0459
6	0.63	4	10.54	0.0917
30	3.14	9	52.72	0.4587
60	6.28	14.5	105.44	0.9173
90	9.42	21	158.16	1.3760
100	10.47	22.5	175.73	1.5288
180	18.85	36.5	316.31	2.7519
200	20.94	40	351.46	3.0577
300	31.42	58.5	527.19	4.5865
600	62.83	106	1054.37	9.1730

4.3.4 Conductivity

The conductivity plots can yield useful information such as critical micelle concentration, critical aggregation concentration (CAC) and polymer saturation point (PSP). To perform the conductivity measurements, Thermo Scientific conducto-meter (Orion 3 star) was used. The conducto-meter should be calibrated by standard solution provided by company. The information regarding this instrument have been gathered in Appendix B. To measure the conductivity for a provided sample the probe has to be cleaned by DI water and dried with fine lab tissue. Then the conducto-meter probe is inserted inside the sample solution and measure button is pressed. The apparatus will read the electrical conductivity after several blinking. This procedure has to be repeated three times and average is reported.

4.3.5 Surface tension

To measure the surface tension, CSC Du NOUY tensiometer (Model No. 70535) was used. This tensiometer uses a ring method. To measure the surface tension between a liquid and the air, the Du Noüy ring is placed below the surface of the liquid. This test is performed by pulling the ring upward through the surface of the liquid.

The use the instrument first a calibration should be done. The calibration procedure can be find in manufacturer's instructions. The ring should be cleaned before each test (which normally is done by flame). A standard sample dish (provided by manufacturer) with a diameter of at least 4.5 cm, to a minimum depth of 1.0 cm is used to measure the surface tension. The dish is cleaned by DI water and dried by air. The ring is attached to the lever arm. Sample is placed on the sample table which is raise until the ring is immersed approximately 5 mm into the liquid. The ring should be roughly centered in the test vessel. At this stage using the fine adjustment screw one lowers the sample table keeping the index reading at approximately zero. The wire should be under torsion while slowly lowering the sample table until the liquid film breaks, and the ring breaks free. The scale reading reads directly the surface tension (dyne/cm). More information has been provided in Appendix B.

There are some limitations in use of the ring method. As our intention is to study the trend of interaction between polymer and surfactant, the results of surface tension obtained from the ring method are accurate enough for comparison.

4.4 Data collection and calculation approach

To collect the pipeline flow data, the flow was changed by two valves 1 and 2 in the pipeline setup. The highest possible flow was measured at the start for every solution and then the flow was decreased to lower flowrates. The pressure drop signal was registered for each flow rate. To ensure that flow is stable a series of signals for flowrate and corresponding pressure drop were collected. The average values of series over time (while the signal line was smooth and had almost no noise) was registered and used for calculation. Figure 4-11 shows calculation approach for friction factor and Re_G.

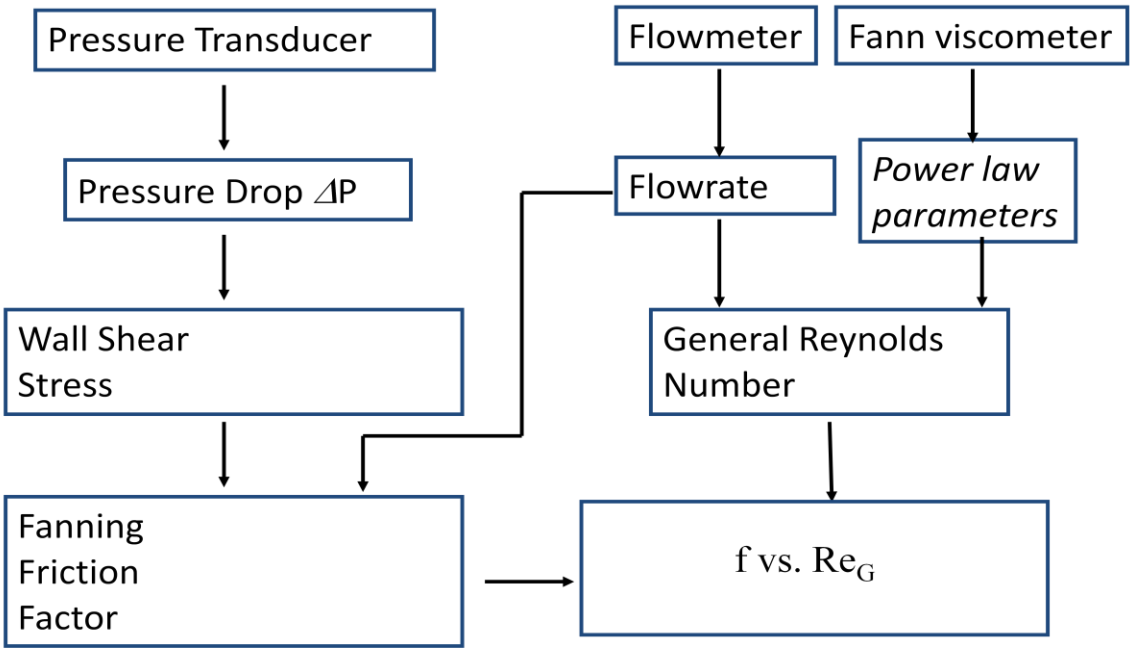

Figure 4-11: Flow chart showing calculation procedure for friction factor and Re_G

To calculate the %DR, based on viscosity experiment, corresponding Dodge and Metzner (D&M) values for different Re_G were calculated by equation (2-24). Using equation (3-1) %DR was calculated in which f_0 is corresponding D&M values at same Re_G.

4.5 Single phase flow of water through experimental set-up

Experimentally, it is important to calibrate and verify that the experimental apparatus yields comparable results for water. Figure 4-12 shows the baseline experimental results of water flowing through different size pipes. The resulting friction factors are compared with the Blasius equation. As shown, there is a good agreement between the results of water flow through the experimental setup and the Blasius equation indicating that the experimental set-up and methodology is satisfactory. In this research water line was used as base line for comparison between friction factor data. In the case of DR graphs, the values were calculated using Dodge and Mentzer (1959), from corresponding graphs shown in Figure 2-3.

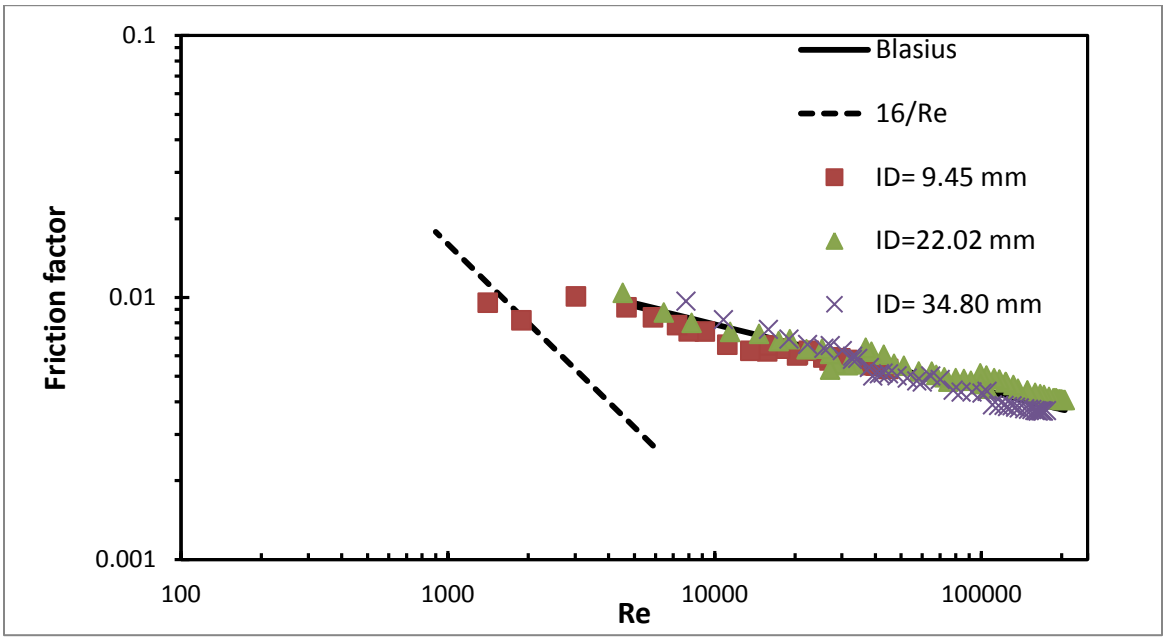

Figure 4-12: Comparison between pipeline flow results and Blasius equation for water in different pipes

4.6 Solution preparation for pipeline flow experiments

4.6.1 Polymer solution preparation

Stock solution was prepared to make test polymer solution for the pipeline. An agitation system consisting of a tank, an impeller and small motor were employed to prepare the stock solution. The impeller was selected from those which insert low shear on the solution to ensure that low degradation will happen while polymer is dissolved in water. In the case of PAM a stock solution of 0.3% was always prepared to keep consistency in the procedure. To prevent the polymer clumping on the solution surface, PAM powder was gradually was added to the bulk of the water during the first 15 min of agitation. Agitation was continued for 15 hr with a low speed motor. In the case of PEO, stock solutions were made by 0.5% of PEO. The same procedure as for PAM was applied.

The test solutions were prepared using polymer stock solution in the main system tank. The tank was calibrated for different amount of water (Kg) and each amount was assigned to

a level. A calibration equation was elaborated and used during this research. To make different polymer solutions the final amount of polymer solution was chosen and based on that, the amount of polymer stock solution which should be added to the main tank was calculated. More information along with a sample calculation has been gathered in the Appendix C. For pipeline flow a sample was taken before each run for viscosity check.

4.6.2 Surfactant solution preparation

In the case of pure surfactant experiment, solutions were made inside the main system tank. Proper amount of water, surfactant and salt were added to the tank where they were mixed using an electrical propeller installed to mix the solution inside the tank. Pipeline flow of surfactant systems were started with lower surfactant and salt concentration. To make the higher surfactant concentration more surfactant was added to the old solution to adjust the surfactant concentration inside the tank.

4.6.3 Polymer-surfactant mixture preparation

To prepare solution of polymer and surfactant mixture for pipeline flow test these steps are applied:

1- Polymer solution is prepared as same procedure as section 4.6.1 except that total solution is polymer + surfactant

2- A sample is taken from polymer solution

3- Surfactant is dissolved in 10-20 kg water and added gradually to the tank in 5 min while impeller is on.

4- Solution is left for few hours (2-3 hr) and a sample is taken before each experiment is stared.

Chapter 5

Experimental Results for Pure Polymers and Pure Surfactants

5.1 Experimental Results on Polymers

Polymers are categorized as either non-ionic polymers or ionic polymers. Polymers with positive or negative charges on their structures are referred as polyelectrolyte polymers. Most polyelectrolyte polymers are soluble in water but insoluble in organic solvents. These polymers are classified into two groups of weak and strong polyelectrolyte. Weak polyelectrolytes dissociate partially in solution at intermediate pH values. Strong polyelectrolyte polymers however, dissociate completely in solution for most ranges of pH values.

Based on what was found in the literature survey, the screening tests and the objectives of this research, two polymers were selected from the available drag reducing polymers. Polyethylene oxide (PEO), a widely used non-ionic polymer drag reducer, was chosen. As an anionic polymer a copolymer of acrylamide and sodium acrylate (PAM) was used.

PEO, (-O-CH2-CH2-), the backbone consists of carbon-carbon (C-C) and carbon-oxygen (C-O) bonds. PAM has a $CONH_2$ group in its backbone. The (C-C) and (C-O) bond strengths and lengths are almost the same for these two polymers. Therefore, same DR stabilities, and breaking of the backbones (chain scission) can be expected to occur at approximately the same shear rates. In this study DR was investigated in DI water and tap water for both polymers. For PEO, only the DI water results have been presented as the results in tap water were almost the same as the result of PEO in DI water. Effect of polymer concentration, pipe diameter, and mechanical degradation is discussed in the following sections. All experiments have been done at $25^{o}C \pm 0.5$.

PEO (WSR 303) with Molecular weight of 7×10^{6} gm/mol was supplied by DOW Company USA in powder form. PAM was supplied by Hychem Inc., USA which is a copolymer of acrylamide and sodium acrylate with average molecular weight of $10 - 12 \times 10^{6}$ gm/mol and charge density of 30%. DI water (2.0 – 4.0) μm/cm conductivity) and tap

water (670 – 800 μm/cm conductivity) was used as solvent. More information about these two polymers is available in Appendix A.

5.1.1 Anionic polymer (PAM)

5.1.1.1 Viscous behavior of PAM in DI and tap water

Figure 5-1 shows the specific viscosity vs. PAM concentration in DI and tap water. At the concentration of almost 250 ppm a sharp increase in viscosity was observed for DI water (C^*). This is the concentration (ppm) at which polymer molecules overlap each other in the solution. For tap water, observed C^* was 770 ppm. Table 5-1 shows average value measured by ICP for total cations presented in tap water. The table shows that the main cations are Ca, Mg, K ,Na.

When PAM is dissolved in tap water the cations present will neutralize a part of the charge on the polymer chain. This will cause that polymer chain to collapse, making tap water a poor solvent for PAM.

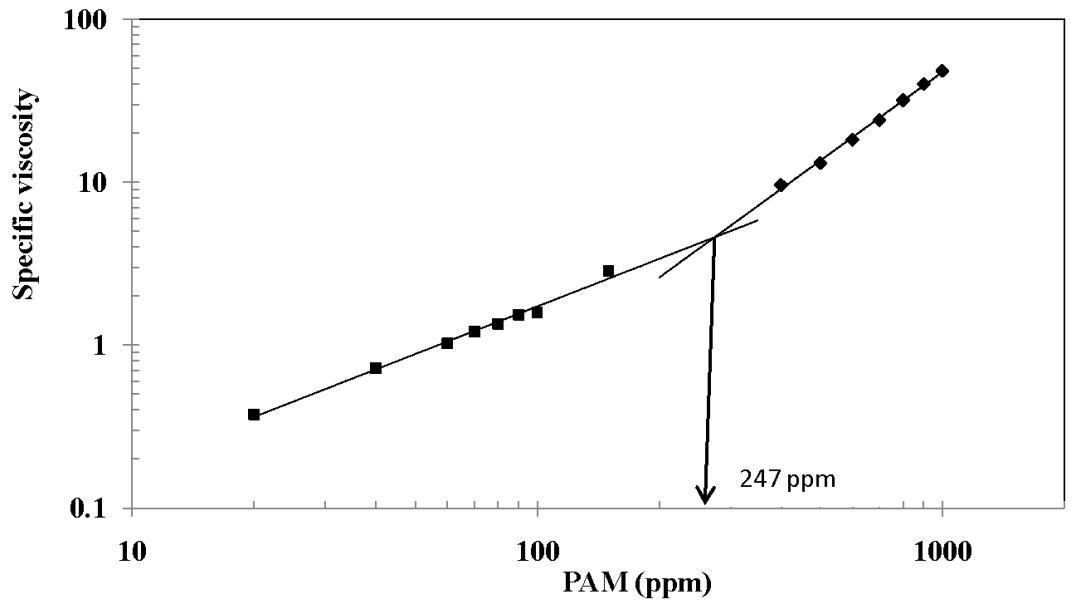

a) PAM in DI water

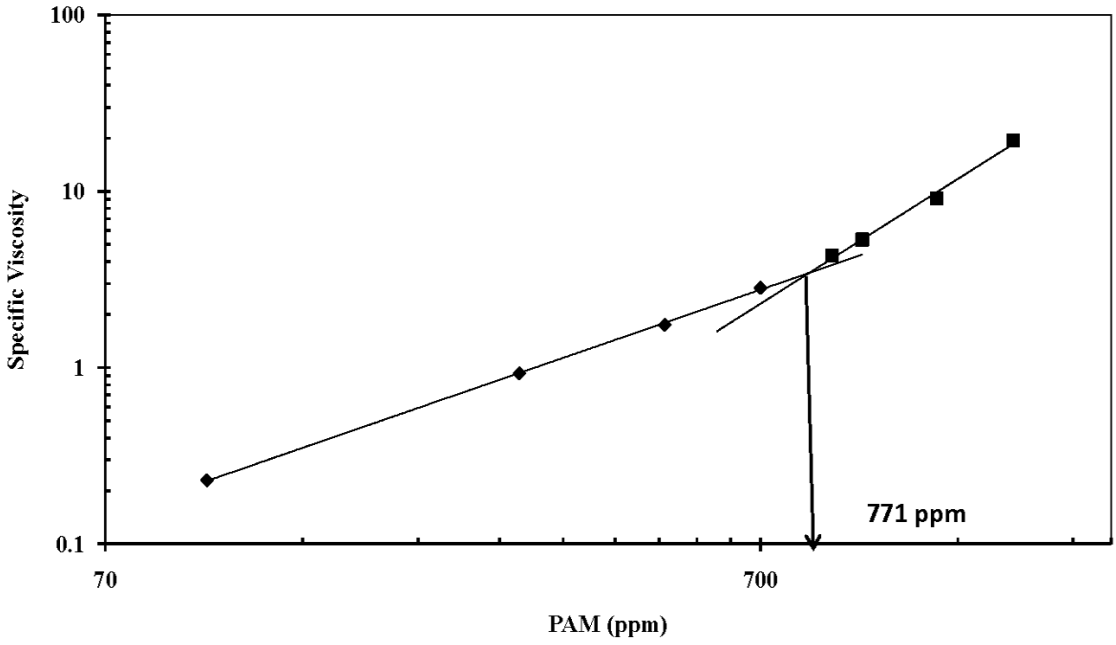

b) PAM in tap water

Figure 5-1: Specific viscosity vs. PAM concentration in (a) DI and (b) tap water

Table 5-1: Analysis of tap water (k=669 µS/cm)

Main cations in used tap water and average value (mg/L)									
Ca	Mg	K	Na	Mn	Zn	Fe	Cu	Ni	Pb
74.3	23.0	79.1	33.9	0.0	0.0	0.0	0.0	0.0	0.0

5.1.1.2 Pipeline flow behavior

Concentration effect

Figure 5-2 shows friction factor vs. generalized Reynolds number (Re_G) for different concentrations of pure PAM in DI water. For particular Re_G in the turbulent regime, the friction factor decreases substantially with the addition of PAM to DI water, especially when the PAM concentration is below 250 ppm. When the PAM concentration is increased above

250 ppm, no further decrease in friction factor is observed. Also note that with the increase in PAM concentration, a change in drag reduction behavior occurs from Type A to Type B.

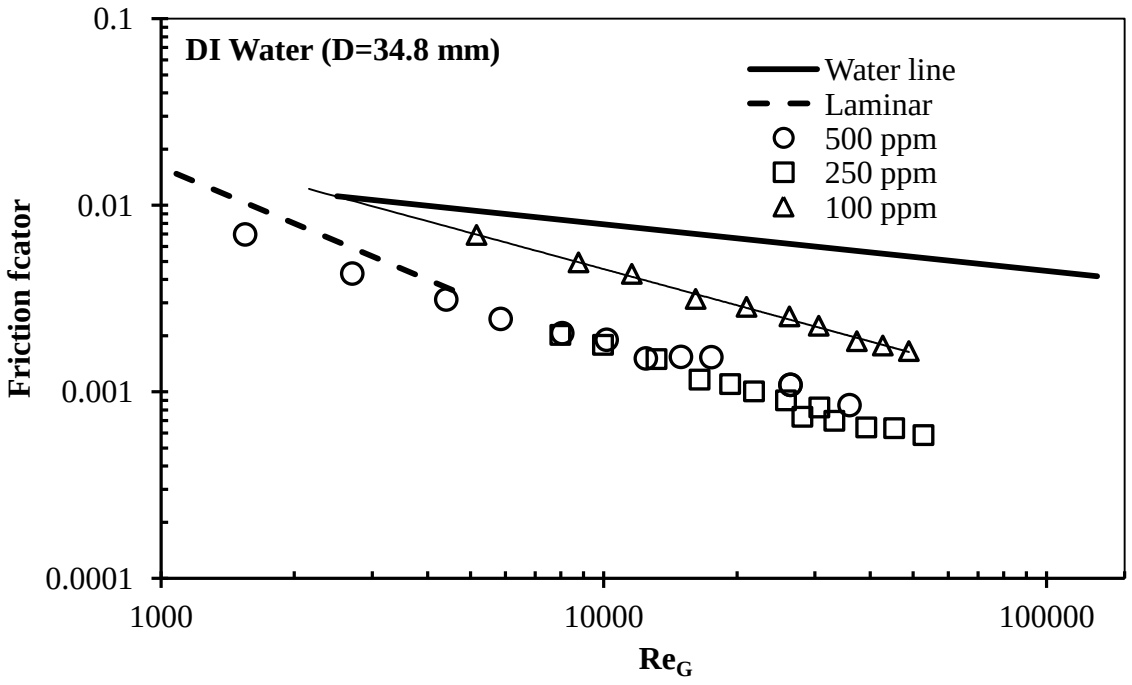

Figure 5-2: Friction factor vs. Re_G for different concentrations of PAM in DI water

In Type A drag reduction (100 ppm PAM), the usual transition from laminar to turbulent regime takes place and drag reduction (DR) occurs after an onset point. This type of DR can be due to uncoiling of the polymer chains in extensional flow field at the onset of DR, or due to entanglements of polymer chains when they reach the size of turbulent eddies (Virk and Merrill 1969; Virk and Wagger 1989). In Type B drag reduction, there is no transition region and the turbulent region data lie on a gradual extension of the laminar line. This phenomenon was also reported by Liaw et al. (1971).

Friction factor vs. Re_G for different concentrations of PAM in tap water is presented in Figure 5-3. The degree of drag reduction is almost the same for PAM concentrations of 100 ppm and 250 ppm. With further increase in polymer concentration to 500 ppm, the DR increases significantly. Referring back to Figure 5-1b), it can be seen that the overlap concentration(C*) for PAM solution dissolved in tap water was 770 ppm. This slight

increase in DR can be related to stretching of highly coiled polymer molecules at higher Re numbers.

Virk (1975) reported that the impact of polymer concentration on onset of DR was negligible, but this appears less obvious in the current study. In this study the Re_G at which onset of DR for 500 ppm occurred was changed from 3950 to 7350 for 250 ppm and 100 ppm, respectively.

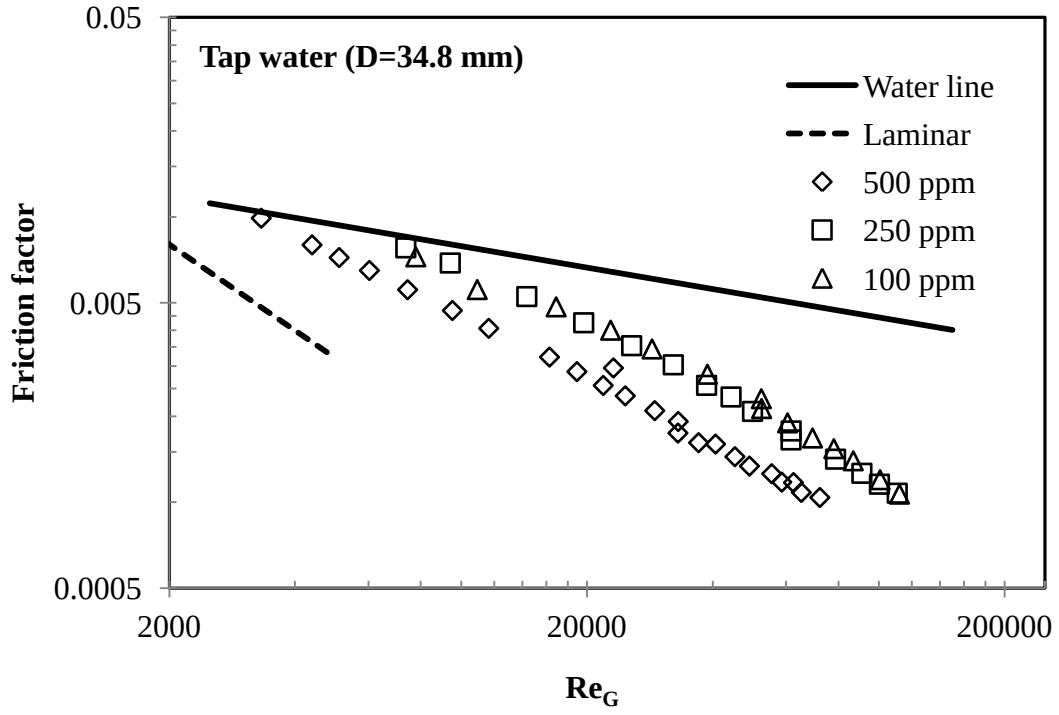

Figure 5-3: Friction factor vs. Re_G for different concentration of PAM in tap water

Figure 5-4 compares the friction factor vs. Re_G for 500 ppm PAM solutions in DI water and tap water. Lower %DR is observed in the case of tap water. In this case, the polymer solution exhibits Type A drag reduction, that is, DR begins after transition from laminar to turbulent regime (DR shows an onset point). As noted earlier, the polymer solution in DI water exhibits Type B drag reduction at the same PAM concentration. This difference in the drag reduction behaviour for DI water and tap water based polymer solutions is due to the presence of cations in tap water. The cations present in tap water cause the polymer chains to

convert from stretched shape (due to repulsive charges on the chain) to coiled shape. Sellin and Loeffler reported that $MgCl_2$ causes a sharp decline in the DR of polyacylic acid. They also concluded that the polymer chains will change from a completely stretched shape to a coiled shape if the salt is added to the chain. This leads to a lower DR (Sellin and Loeffler 1977).

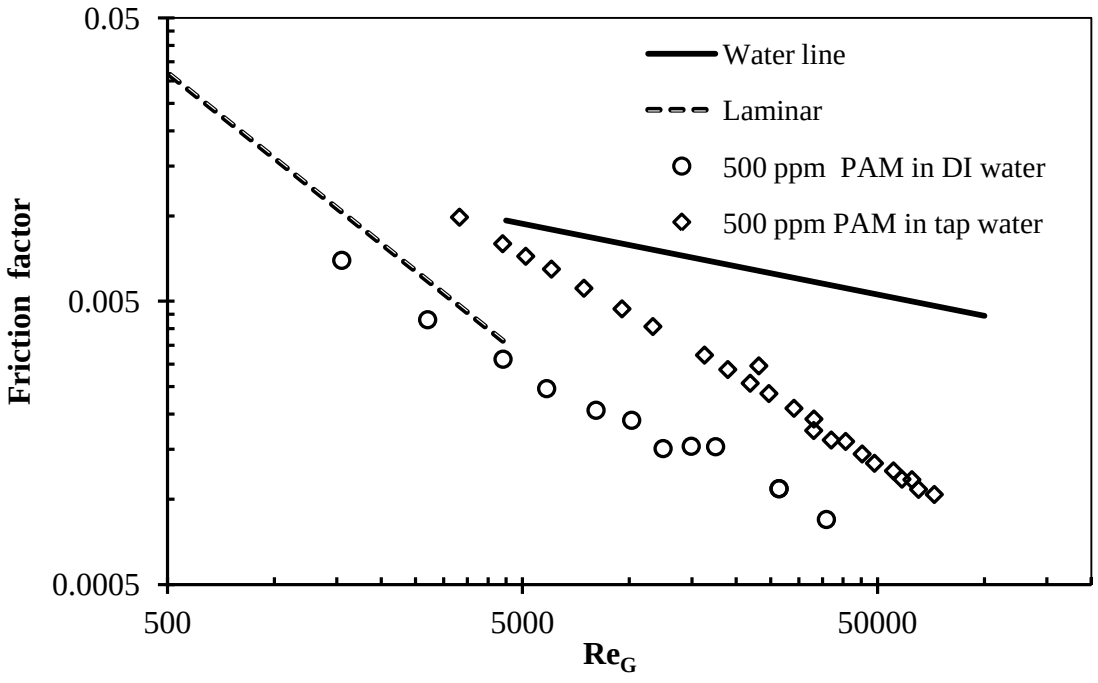

a) Friction factor vs. Re_G

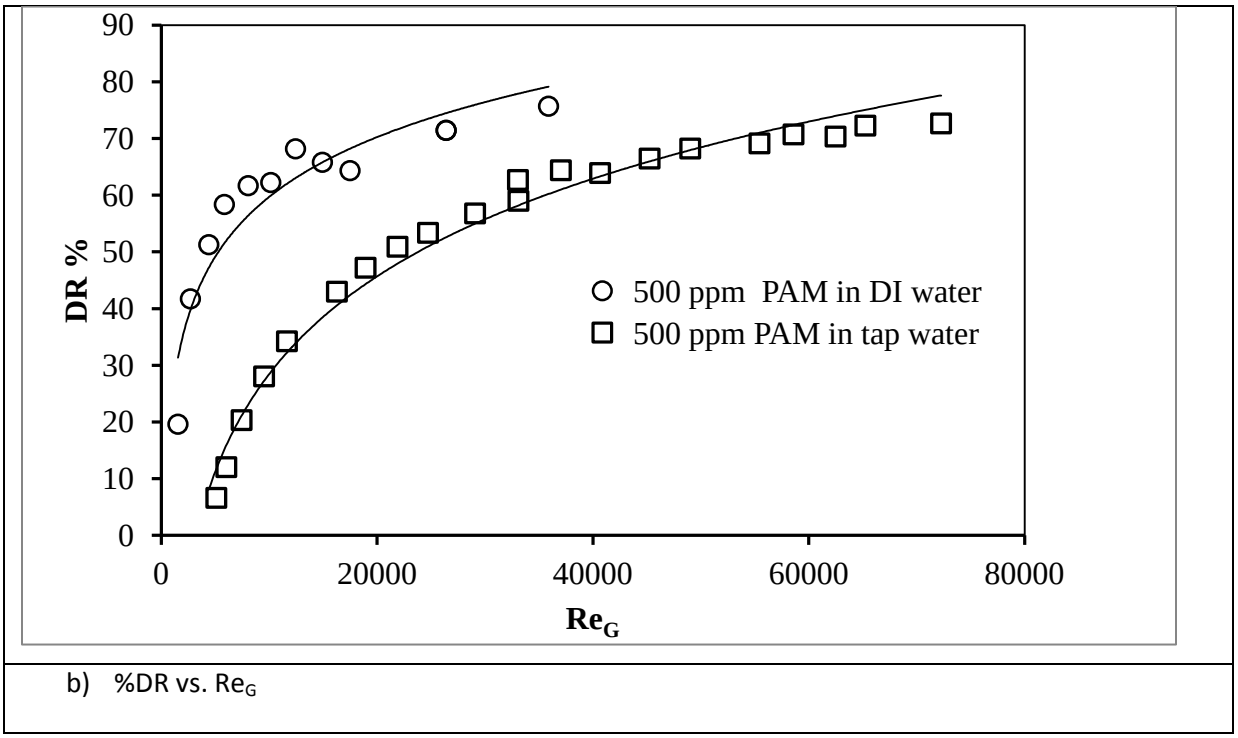

b) %DR vs. Re_G

Figure 5-4: Comparison between (a) friction factor and (b) %DR Vs. Re_G for 500 ppm in DI and tap water (D= 34.8 mm)

Diameter effect

The effect of pipe diameter on DR was investigated in this study for PAM solution. For each pipe a new solution was prepared to exclude the effect of degradation on DR. Figure 5-5 shows friction factor vs. Re for 500 ppm of PAM in tap and DI water, measured for the flow through the pipes with different diameters.

For PAM/DI water solution, there is no significant difference between the %DR measured using 22.02 mm and 34.8 mm diameter pipes at 500 ppm PAM (Figure 5-5a). Compared with other diameter pipes, higher %DR (lower friction factor) is attained in a 9.45 mm diameter pipe.

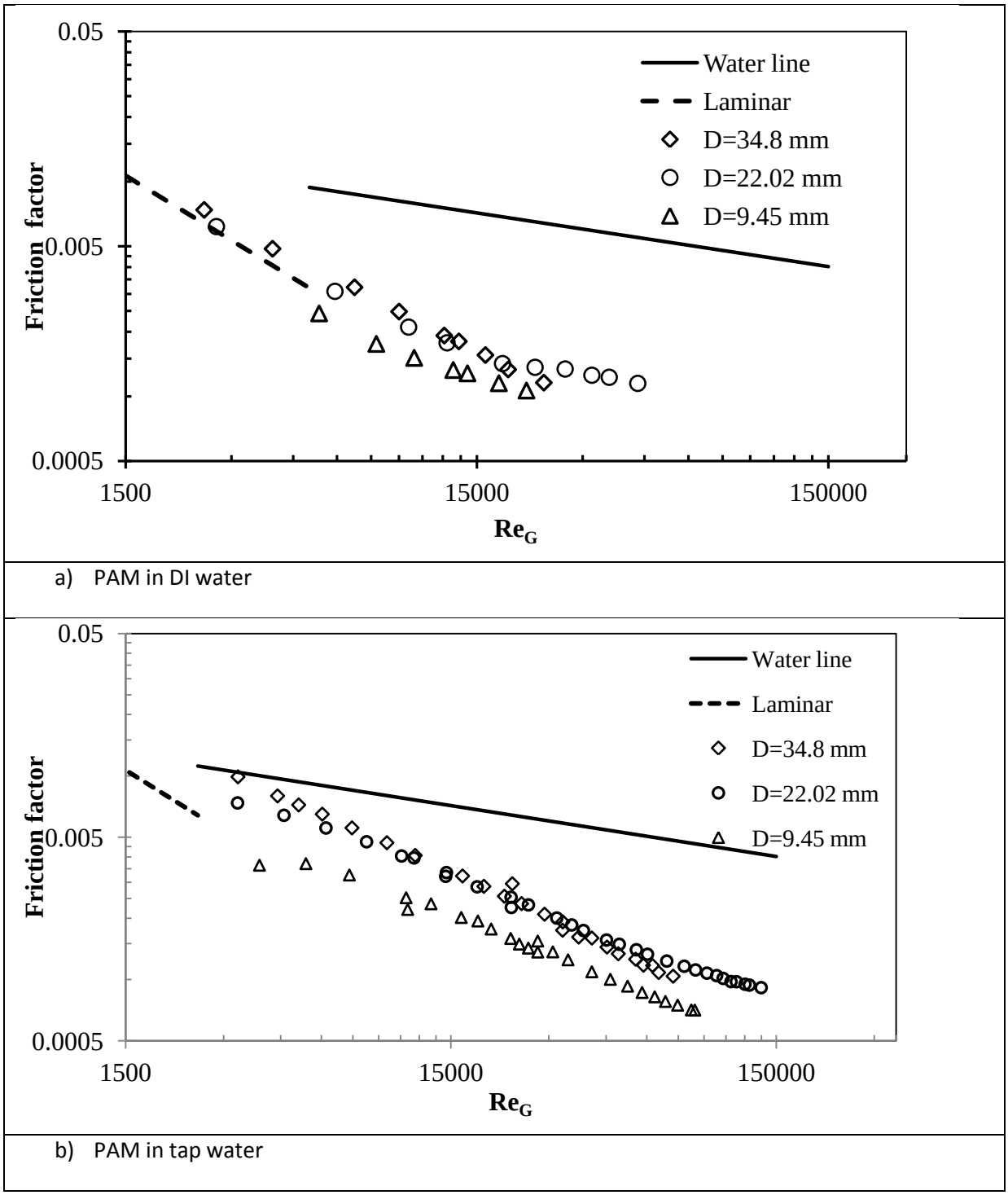

Figure 5-5: Friction Factor Vs. Re_G for 500 ppm PAM in DI and tap water for different pipes

The effect of pipe diameter on DR is illustrated in Figure 5-5b for PAM/tap water solutions. While there is no significant difference between the DR measured with 34.8 mm and 22.02 mm diameter pipes, a higher DR was attained using the 9.45 mm diameter pipe. Furthermore, PAM/tap water solutions exhibited drag reduction behavior of Type A in the pipes with large diameters.

Mechanical degradation of PAM

During mechanical degradation of polymers, the energy for the breaking of polymer molecules is supplied partly by mechanical shearing of the polymer. This results in severe limitations on their usage as drag reducing agents (Hunston and Zakin 1980).

Mechanical degradation of PAM in DI and tap water was studied for various concentrations of polymer. Polymer was sheared by passing through the pipe with diameter of 34.8 mm. During the degradation, the pressure drop and flow rate were measured and recorded accordingly. All the results presented in this section were obtained for the pipe with diameter of 34.8mm.

Figure 5-6 shows friction factor and %DR vs. Re_G for 500 ppm PAM in DI water, when the polymer was under degradation for certain time periods. At this particular concentration, %DR remains almost the same value for early degradation, however gradually starts to decrease with time after 28 hours. The PAM solution shows the same %DR at higher Re_G in DI water. This can be attributed to uncoiling of portion of PAM chains that have not been degraded yet. After 150 hr of degradation , result shows that %DR decreases (almost 25%) compared to that of the fresh PAM solution for $Re_G > 5000$.

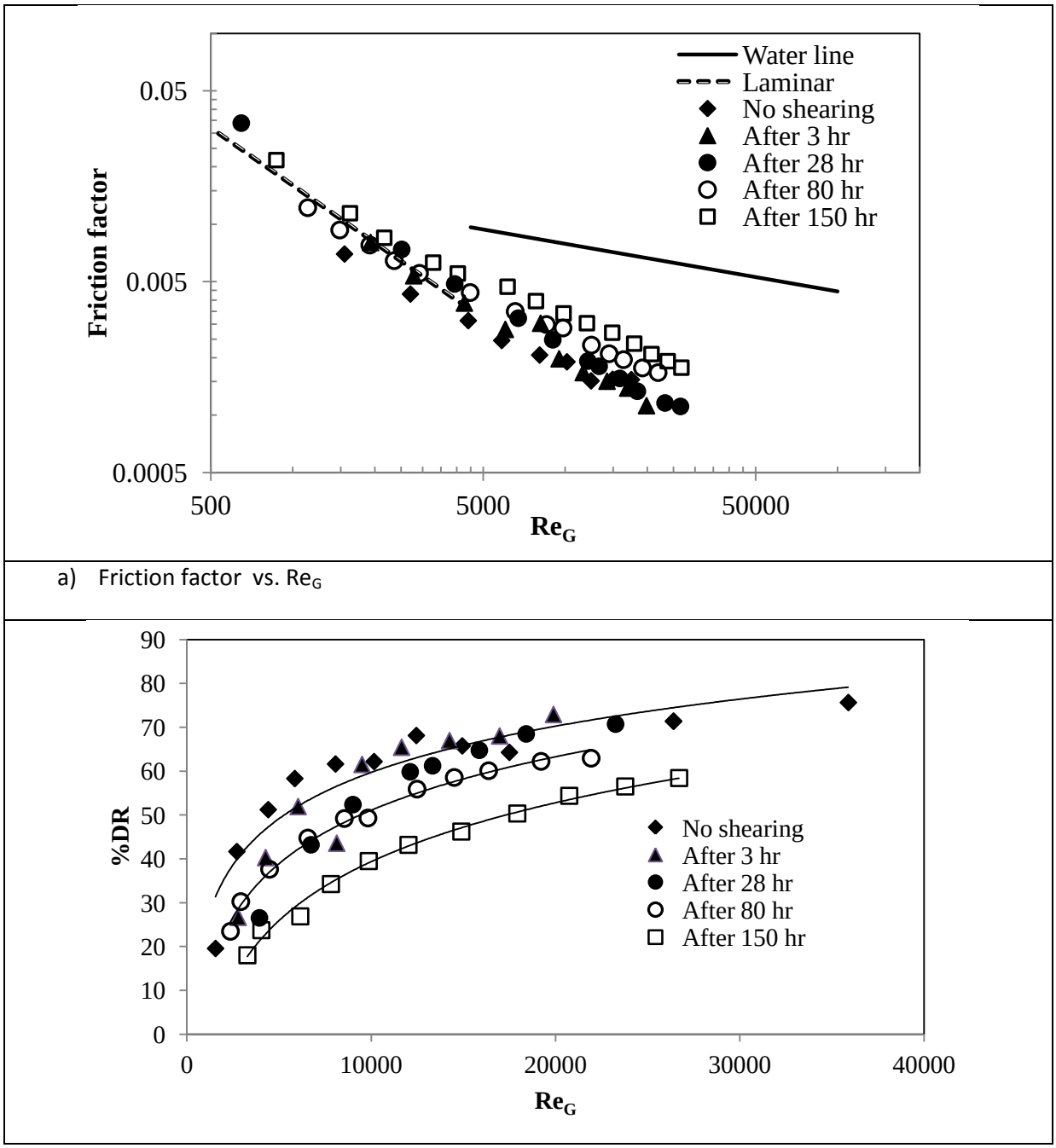

a) Friction factor vs. Re_G

b) %DR Vs. Re_G

Figure 5-6: Friction factor and %DR vs. Re_G for 500ppm PAM in DI water for different time

Influence of mechanical degradation is less for higher concentrations compared with lower concentrations. As seen in Figure 5-2, the magnitude of %DR is greater for fresh 250 ppm in comparison with 500 ppm of PAM. After 28 hours of degradation, %DR for a 500 ppm PAM was higher than that for the degraded 250 ppm polymer solution as shown in Figure 5-7. The degradation for a 100 ppm PAM in DI water is much faster than that for the 250 ppm solution. Mechanical degradation can change the flow behaviour of PAM solution in DI water when concentrations is lower than C*. This was observed for 100 ppm of PAM when its DR behaviour is turned from Type B to Type A. The solution was degraded for 20 hours. Some studies have shown that the mechanical degradation rate increases with the increase in wall shear stress, and decreases with the increase in polymer concentration (Yu et al. 1979; Zakin and Hunston 1978). For degraded 500 ppm PAM in DI water, the solution exhibits a Type B behaviour even if the degradation proceeds for 150 hours.

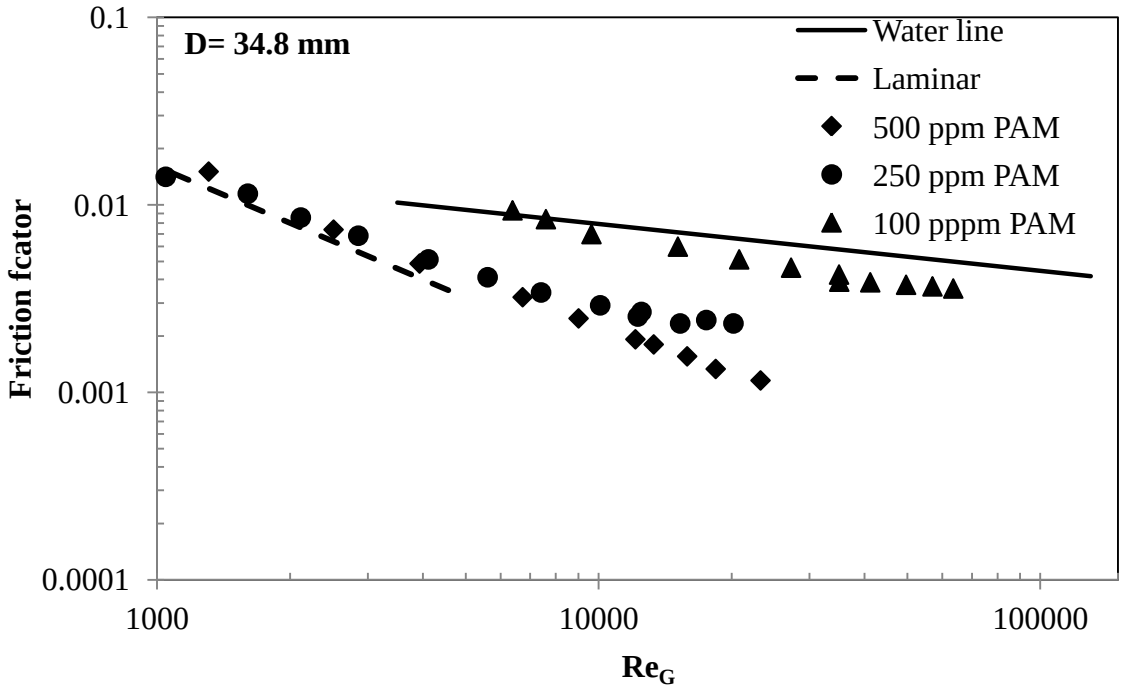

Figure 5-7: Friction factor vs. Re_G for different PAM concentrations after 28 hr of degradation

In Figure 5-8, DR for different concentration of PAM in tap water for non-degraded and degraded solutions is compared. Although 100 and 250 ppm PAM solutions show almost equal %DR, but the 100 ppm solution was degraded with higher rate after 24 hr degradation. The average difference in %DR between 250ppm and 100ppm solutions before degradation was almost 5%. This value was changed to 15% after a 24 hr -degradation for Re_G >50000. Degradation does not have any impact on the onset of DR such that the same onset of DR was observed for PAM solution before and after degradation at this particular concentration.

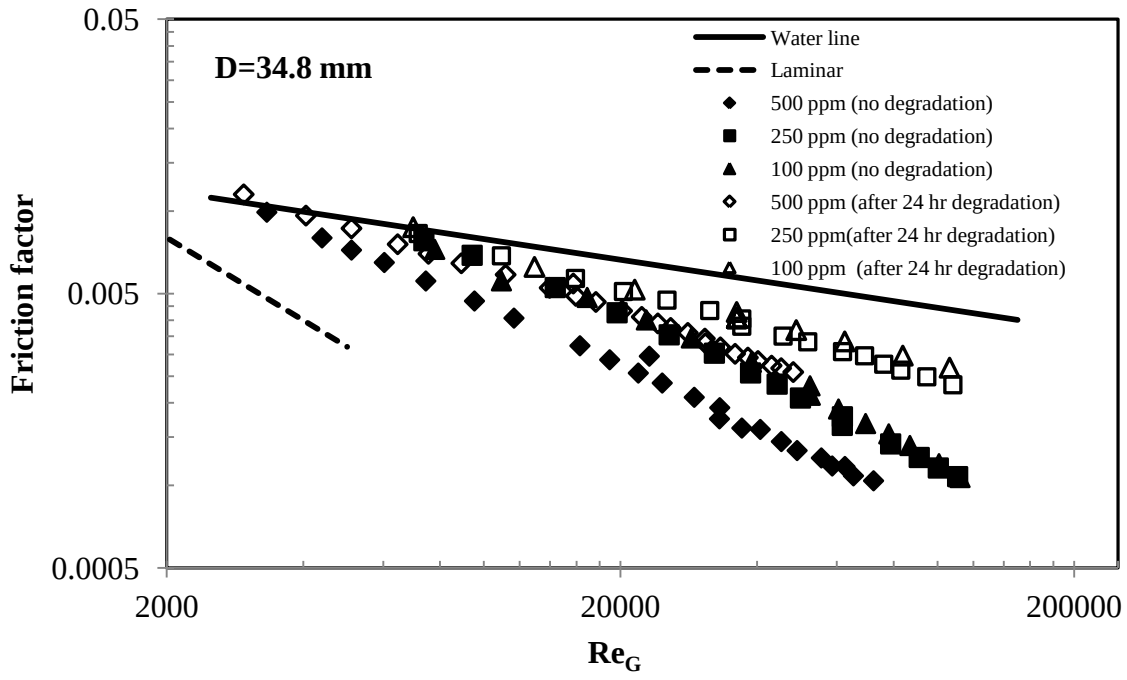

a) Friction factor vs. Re_G

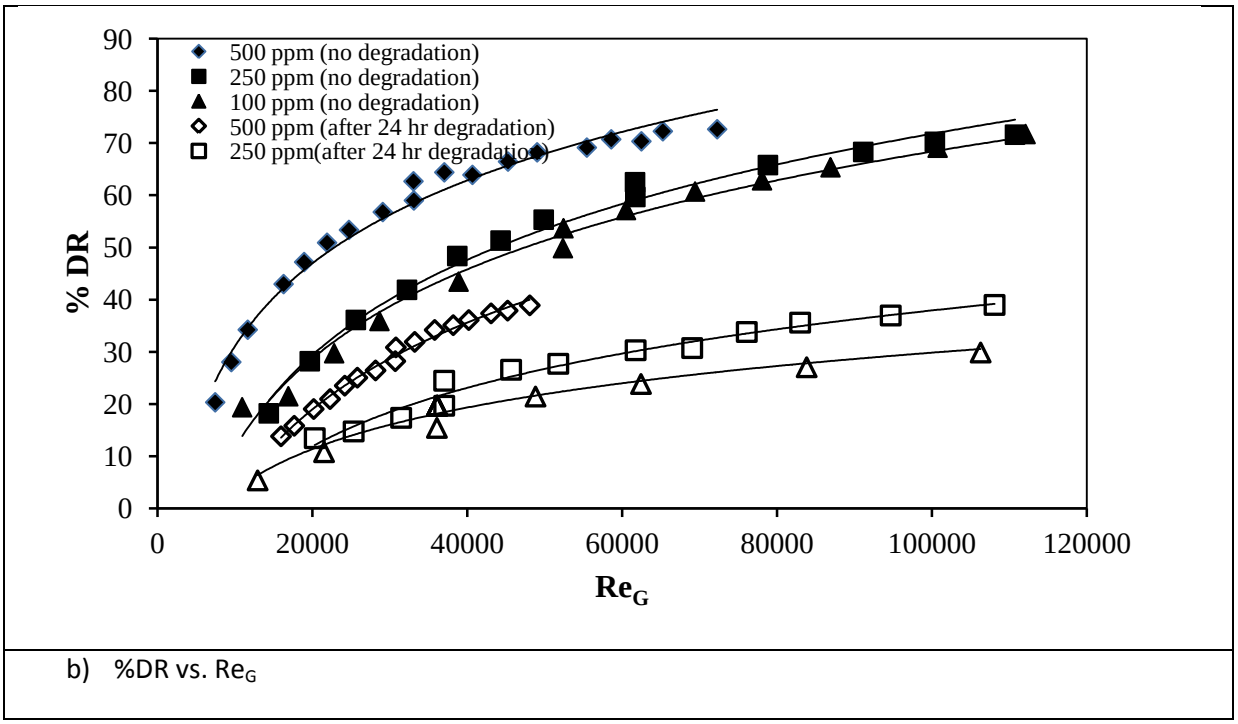

b) %DR vs. Re_G

Figure 5-8: Effect of degradation on friction factor and %DR for different concentrations of PAM in tap water

Figure 5-9 shows % DR vs. time for PAM in tap and DI water. For 500 ppm, %DR decreases gradually in tap and DI water compared to other concentration values. In this concentration (500 ppm), PAM solution in tap water was degraded faster than PAM solution in DI water. This is a challenging issue, since polymer chains are more compact in tap water and they are expected to be less exposed to mechanical degradation compared to the PAM chains in DI water (which own more expanded molecules).

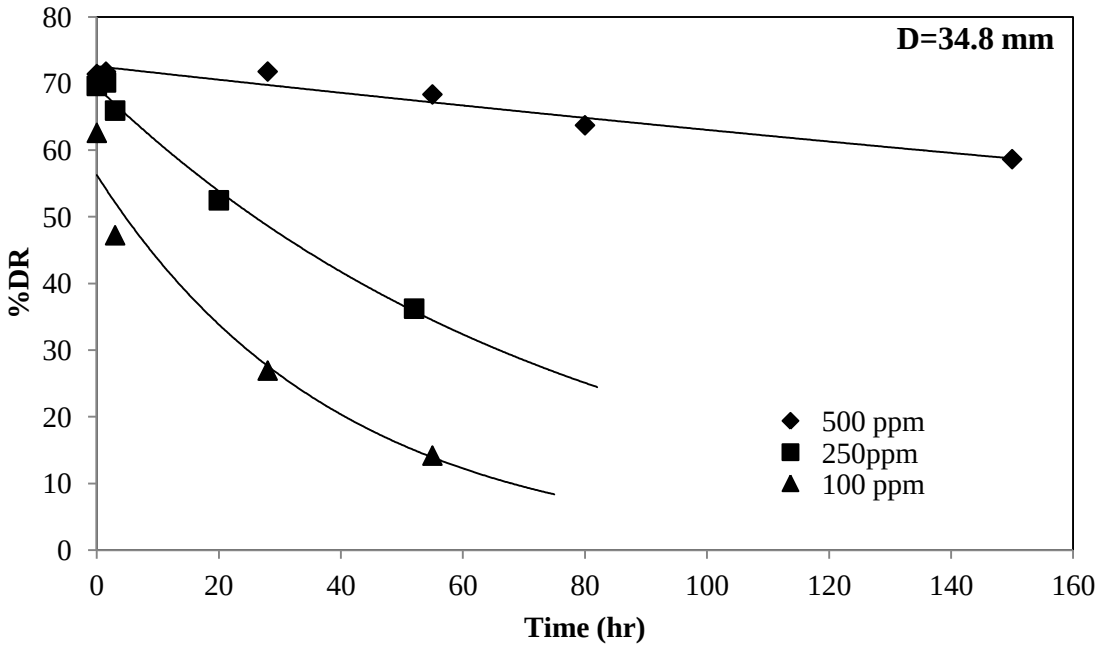

a) PAM in DI water

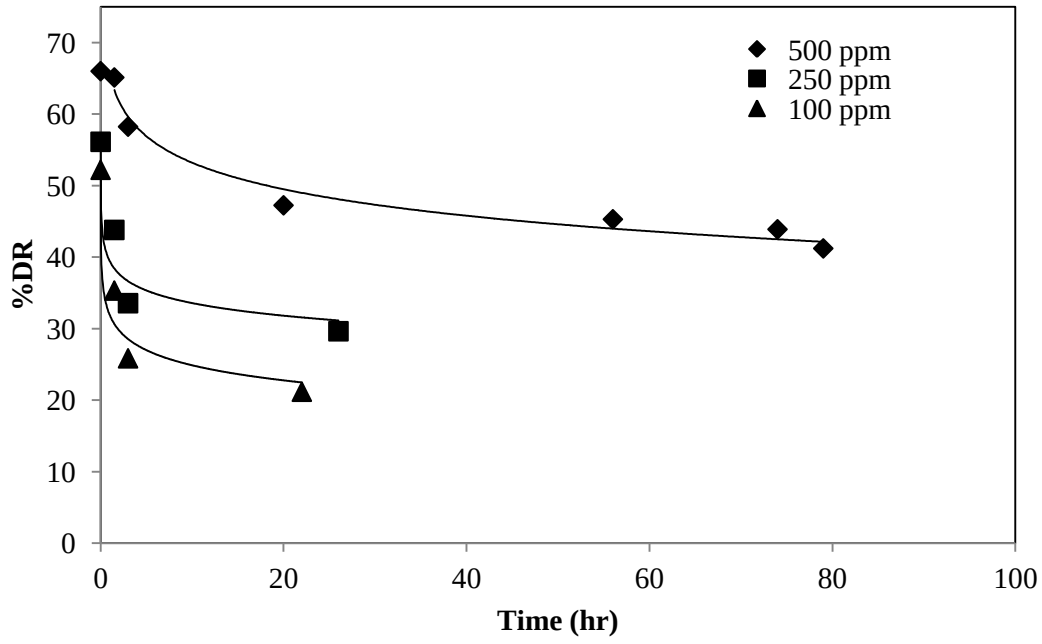

b) PAM in tap water

Figure 5-9: %DR vs. time for PAM in DI and tap water

Brostow et al. (1990) proposed a model, assuming two types of sequences in each polymer. The first one is that the chains are oriented along the flow direction, and strongly solvated. In the other one the polymer chains are oriented approximately perpendicular to the flow, and weakly solvated. They concluded that not only the solvent effectiveness, but also the goodness of the polymer chain sequences has a very important effect on the mechanical degradation and stability. Moreover, they made an effort in another study and derived an equation which predicts drag reduction as a function of time and the concentration (Brostow et al. 2007).

In general, mechanical degradation rates are rapid at the very early stage of degradation for PAM in DI and tap water. Choiet et al. and Sung et al. investigated the degradation of some types of polymer including PAM. It was found that the degradation process can be expressed by an exponential decay expression in terms of time (Choi et al. 2000; Sung et al. 2004). In the current study, we determined that degradation of PAM solution in DI water can be characterized by an exponential decay model, but this model is not applicable for the same polymer in tap water.

5.1.2 Nonionic polymer (PEO)

5.1.2.1 Viscous behavior of PEO in DI water

Figure 5-10 shows specific viscosity versus PEO concentration. Specific viscosity shows a sharp increase at concentration near to 1550 ppm. This concentration corresponds to C* for PEO_WESR303 at which polymer molecules begin to overlap in polymer solution.

Figure 5-11 shows apparent viscosity vs. shear rate for different concentrations of PEO. The polymer solution shows shear thinning behaviour at the PEO concentration equal to 2000 ppm. Shear thinning effect is much less in a 1000 ppm solution. For a 500 ppm solution no shear thinning effect was observed.

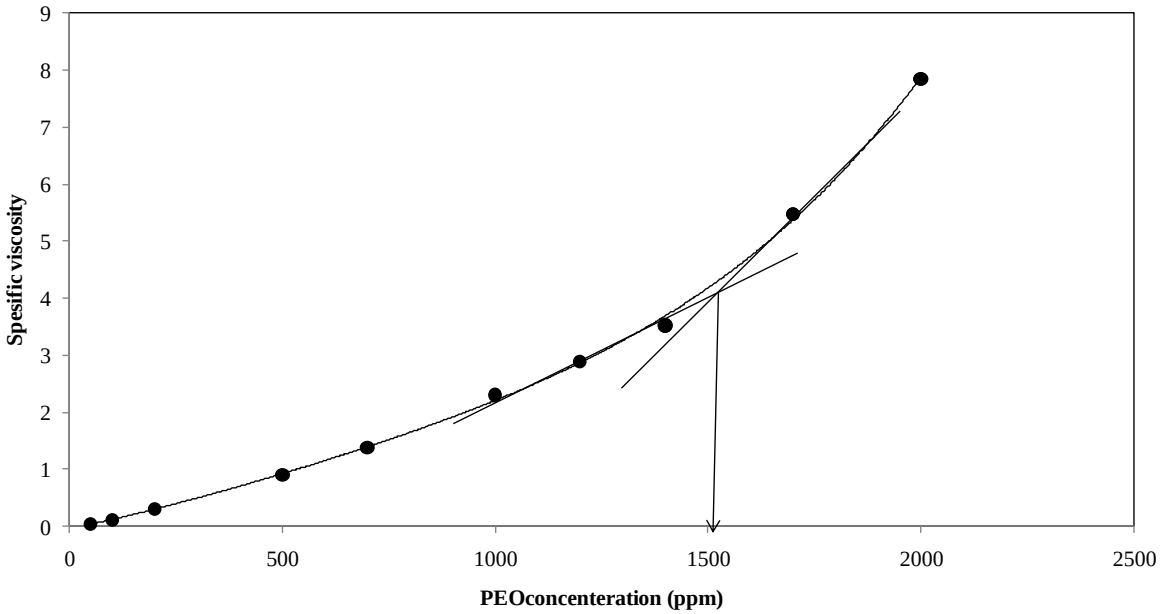

Figure 5-10: Specific viscosity vs. PEO concentration

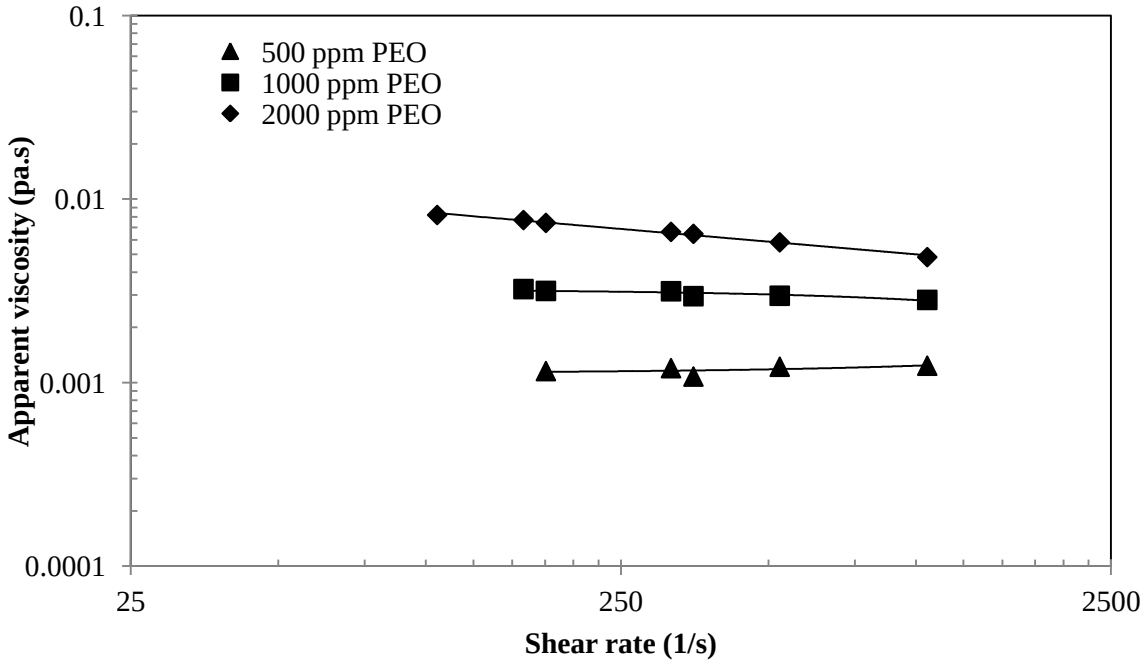

Figure 5-11: Apparent viscosity vs. shear rate for PEO solutions in DI water

5.1.2.2 Pipeline flow behavior

Concentration effect

Figure 5-12 depicts variations of friction factor and %DR with Re_G for various concentrations of PEO in DI water. This particular polymer shows Type A behavior in DI water, while PAM exhibits Type B for concentration about C* and higher concentrations. For PEO (WSR303), C* is about 1550 ppm. %DR increases with an increase in PEO concentration. However, this increase is not remarkable after C*.

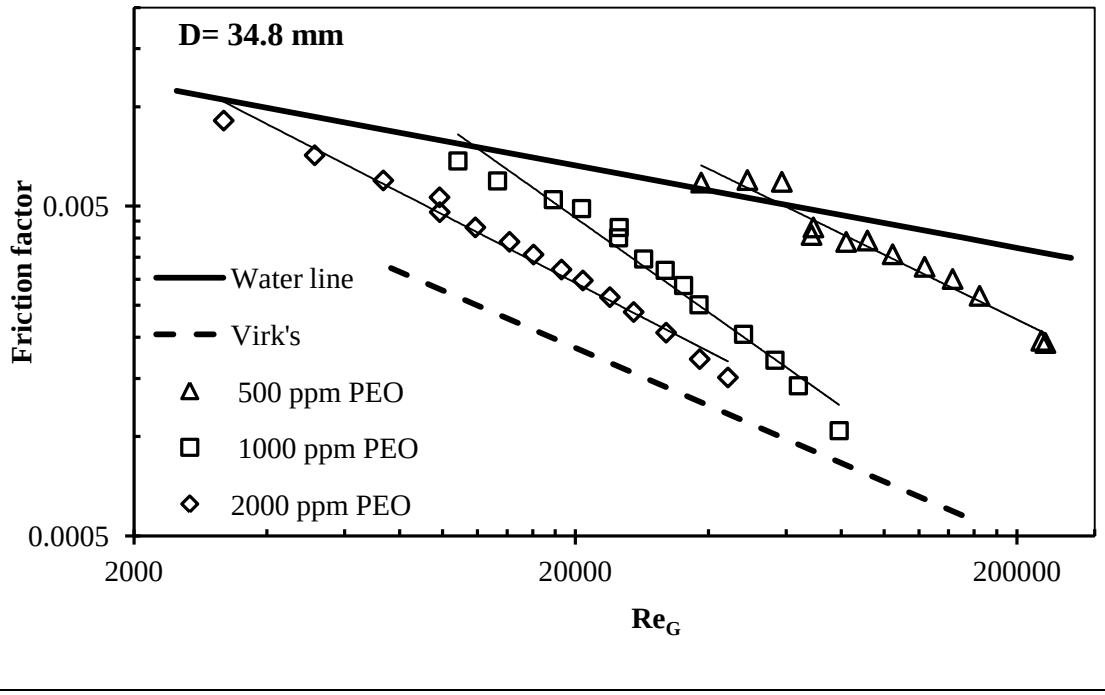

a) Friction factor vs. Re_G

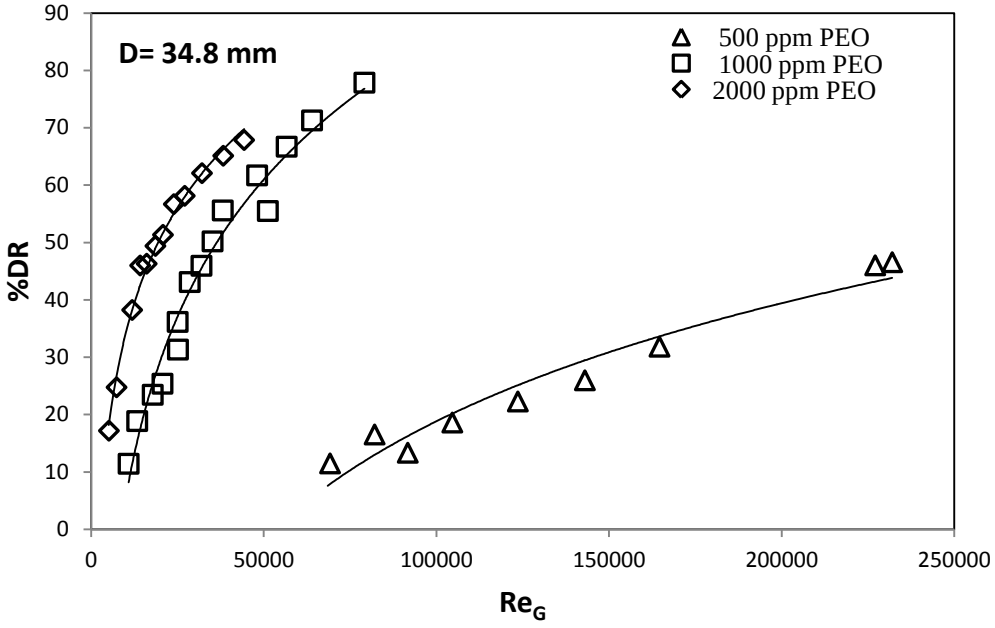

b) %DR vs. Re_G

Figure 5-12: Effect of PEO concentration on friction factor and %DR

Figure 5-13 shows variation of onset of DR with PEO concentration. Onset of DR decreases substantially by increasing polymer concentration from 500 ppm to 1000ppm. The onset of DR will continue to decrease for 2000ppm but it is not as sharp as before.

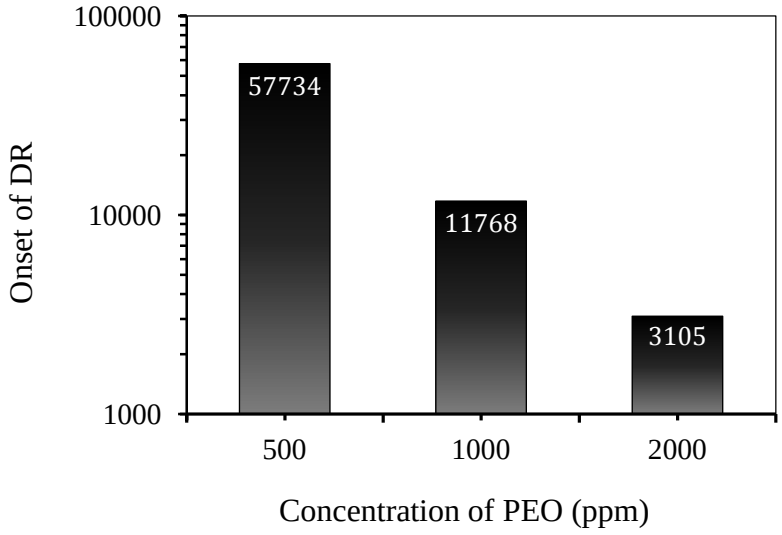

Figure 5-13: Effect of PEO concentration on onset of drag reduction

Diameter effect

The effect of pipe diameter on DR of PEO solution in DI water was studied. Like the PAM solution experiments, a new solution was prepared for each pipe to exclude the impact of degradation on the DR in the PEO solutions. Figure 5-14 shows friction factor vs. Re for 500 ppm of PEO in DI water, measured in different pipe diameters. For the PEO/DI water solution, there is no significant difference between the %DR values for 22.02 mm and 34.8 mm diameter pipes at 500 ppm PEO. But, higher %DR (lower friction factor) is attained in a 9.45 mm diameter pipe compared to other pipes with different diameter sizes.

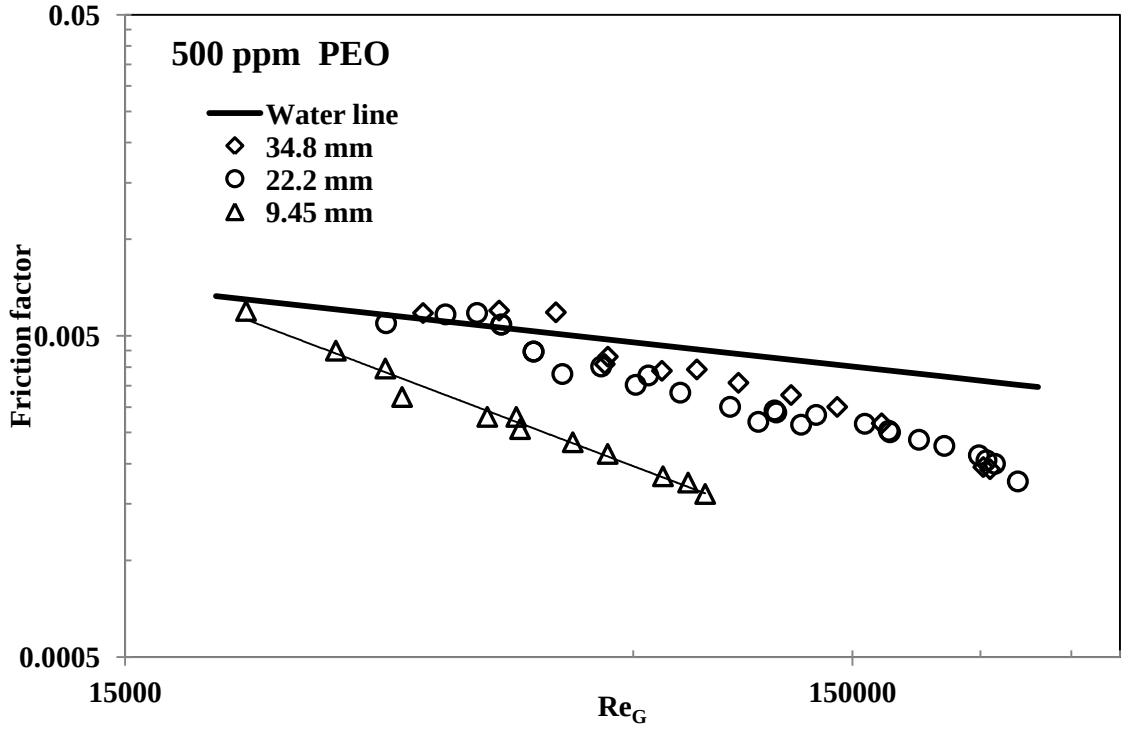

Figure 5-14: Diameter effect on friction factor data for 500 ppm PEO

For fully developed turbulent flow of a Newtonian fluid in smooth pipe, the friction factor is function of only Reynolds number and can be expressed satisfactorily by the Blasius equation. However, this is not true for drag-reducing fluids. For drag-reducing fluids, the friction factor depends on pipe diameter as well (in addition to the Reynolds number). This diameter-dependence of friction factor is referred to as "diameter effect". The effect of pipe diameter on friction factor in drag-reducing systems has been reported by several researchers (Indartono et al. 2005; Sellin and Ollis 1983; Usui et al. 1998; Zakin et al. 1998). In some cases the effect diminishes for larger diameter pipes. The magnitude of the diameter-effect may vary from one system to another (Zakin et al. 1998).

Mechanical degradation

Figure 5-15 shows friction factor and %DR for fresh PEO and degraded PEO for a wide range of Re_G. Polymer loses its DR ability when it flows through a pipe with diameter of

34.8 mm for a short time period. It was observed that at Re = 40000, %DR decreases from 70 % to 35%, which means almost a 50% drop in DR ability. At this time onset of DR increases to 13500 from 3100 for the polymer solution. Also, %DR approaches to a low value around 10 % after 28 hr.

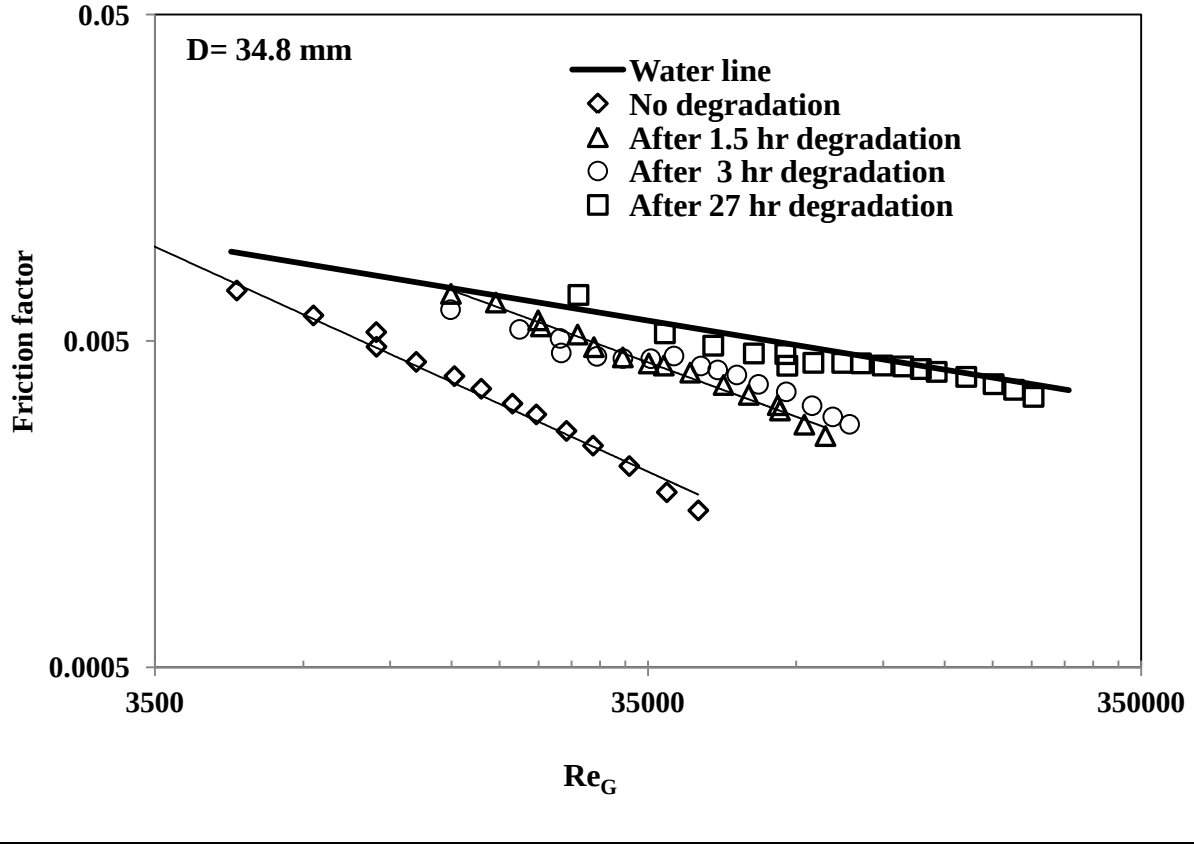

a) Friction factor vs. Re_G

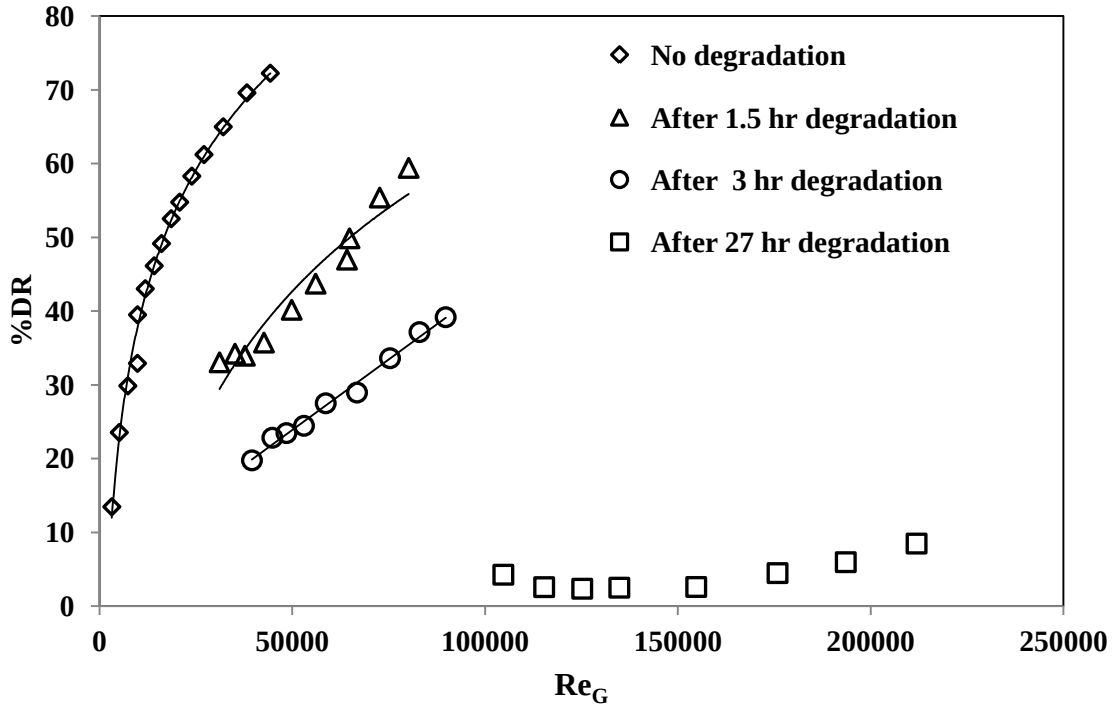

b) %DR vs. Re_G

Figure 5-15: Effect of degradation on friction factor and %DR of 2000 ppm PEO

Molecular weight of PEO in this study was about 7×10^6 g/mole. This number was lower than the molecular weight of PAM (10-12 million). There are a number of research works in the literature focusing on degradation of these two polymers with similar molecular weights for DR purpose (Martin, E., 2000). The same results were found in those researches. It conveys the message that PAM is much more stable against mechanical degradation compared to PEO.

5.2 Drag Reduction Study of Surfactants

A variety of surfactants with different charges were studied trough a screening test. Based on the literature survey and the bench-scale results, a cationic and an anionic surfactant were selected.

Octadecyltrimethylammonium chloride (OTAC) with molecular formula of $C_{21}H_{46}N^{\cdot}Cl$ was used as a cationic surfactant. OTAC with purity of 98% was supplied by Molekula, UK. The counterion used here was 99.5% sodium salicylate (NaSal), in crystalline powder form, supplied by Wintersun Chemical, USA. The level of salt was changed in the experiment to find out the effective and optimum amount of NaSal. This level is defined as molar ratio (MR) of Salt/Surfactant (NaSal/OTAC) in this work.

In this work, sodium dodecyl sulfate $C_{12}H_{25}SO_4Na$ (SDS) was employed as an anionic surfactant. SDS is an anionic surfactant with a tail of 12 carbon atoms, attached to a sulfate group giving the molecule amphiphilic properties. More information about structure and physical properties of these two surfactants and counterions can be found in Appendix A.

5.2.1 Cationic surfactant (OTAC)

To track the effects of important variables on drag reduction, based on the literature review three factors were considered in experimental works. Surfactant concentration, salt concentration and temperature were the most important factor affecting DR capability of surfactants. Three levels for each factor were chosen.

5.2.1.1 Rheology of OTAC solutions

Relative viscosities are presented in Figure 5-16. There is no change in relative viscosity for lower surfactant concentration. If salt is added to the solution considerable change is experienced for the solutions with higher surfactant concentration. According to the figure, the solutions including small amounts of surfactant have a viscosity near the viscosity of water, even if the molar ratio (MR) is doubled during the test runs.

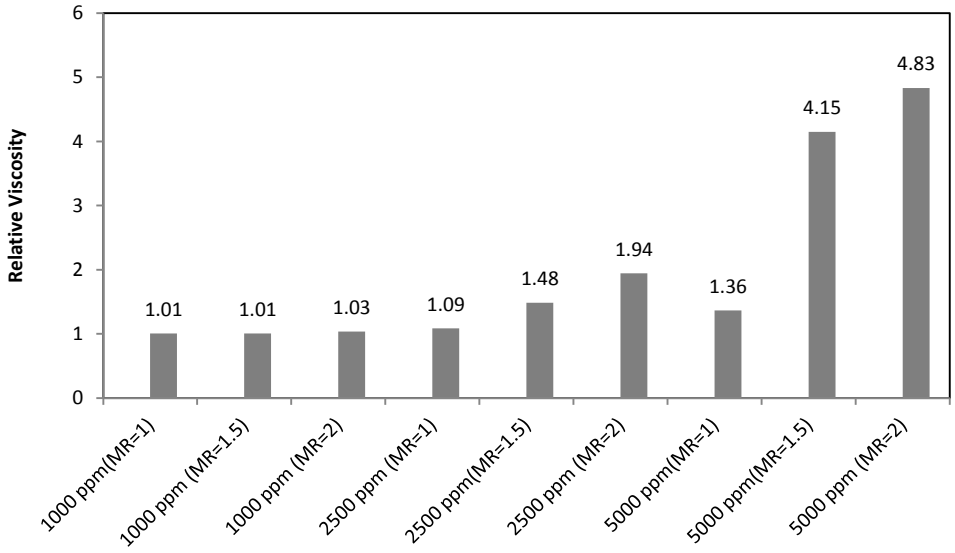

Figure 5-16: Relative viscosity for different concentrations of OTAC with different molar ratios of NaSal at 25 ^{o}C±0.5

Figure 5-17 shows the effects of salt amount on dial reading for 1000 ppm – 2%wt. of OTAC concentration. Dial reading increases if the counterion concentration increases. For higher surfactant concentration, salt addition by double molar ratio (MR=2) has the same effect as it does for low surfactant concentrations. Further addition of salt causes a reduction in dial reading for high surfactant concentrations. This effect has been observed in literature for cationic surfactants (Usui et al. 2004). Sodium salicylate reduces the electrostatic interactions between the surfactant head groups and thus enhances micelle growth. Meanwhile micelles are given this chance to form rod-like network. This structure formation leads to an increase in the shear viscosity (dial reading).

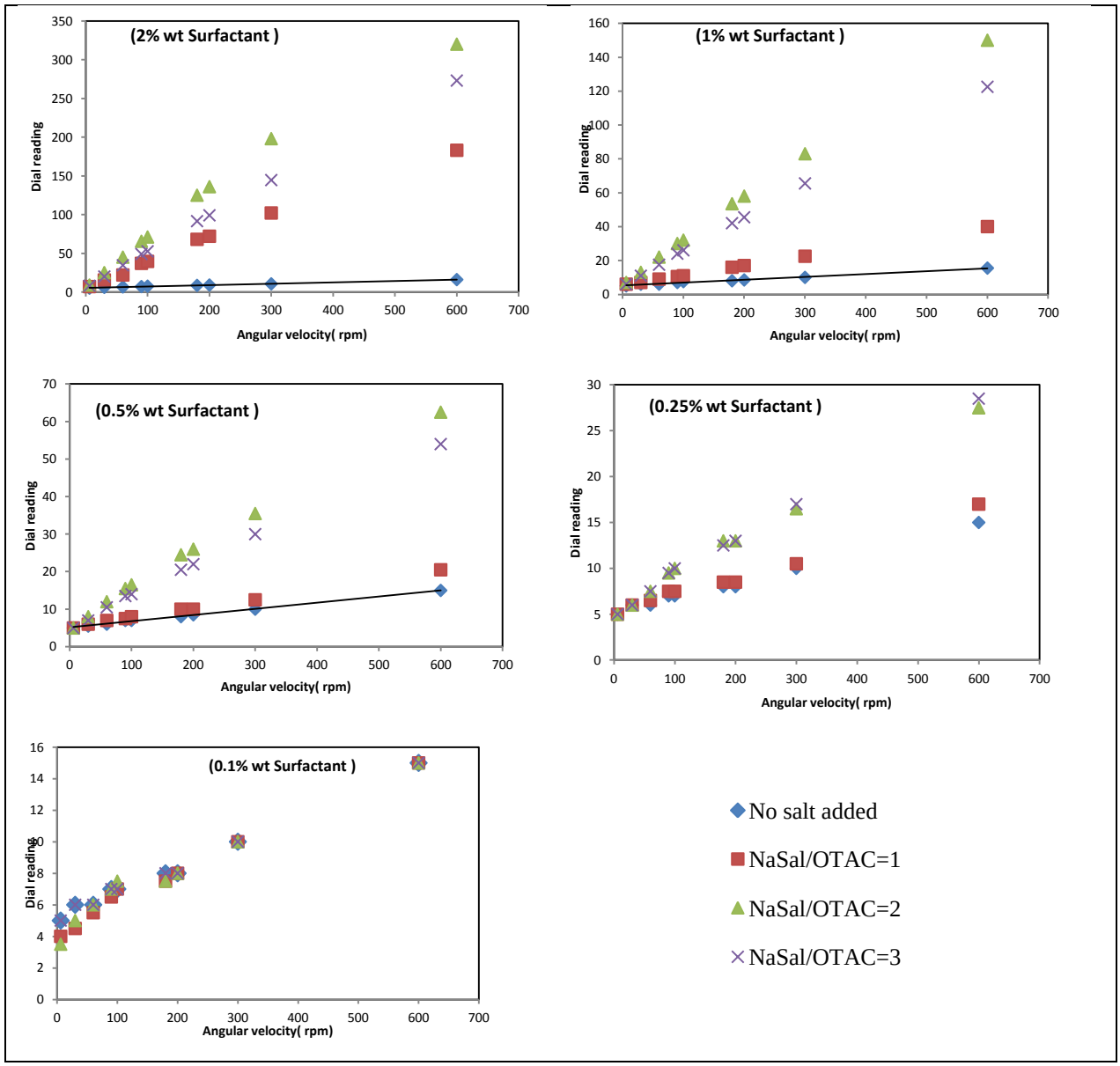

Figure 5-17: Dial reading Vs. Angular velocity for different concentrations of OTAC and NaSal

Figure 5-18 shows apparent viscosities for the surfactant solutions. When surfactant concentration is 1000 ppm, the solutions behave like a Newtonian fluid. For higher concentrations, shear thinning behavior was observed. When amount of surfactant and salt concentrations simultaneously change, a drastic change in apparent viscosity is observed

(compared to when just surfactant concentration in the solution is increased). In each case shear stress vs. shear rate was plotted. Assuming power law behavior, parameters are computed using curve fitting technique for the cases under study. If apparent viscosity value decreases with increasing shear rate, the behavior of fluid is closer to that of a shear thinning fluid. The parameters are presented in Figure 5-19. The values of 'k' and 'n' parameters indicate the behavior of a fluid under shear stress. The results shows that a number of solutions with surfactant concentration of 1000ppm do not display any shear thinning effect.

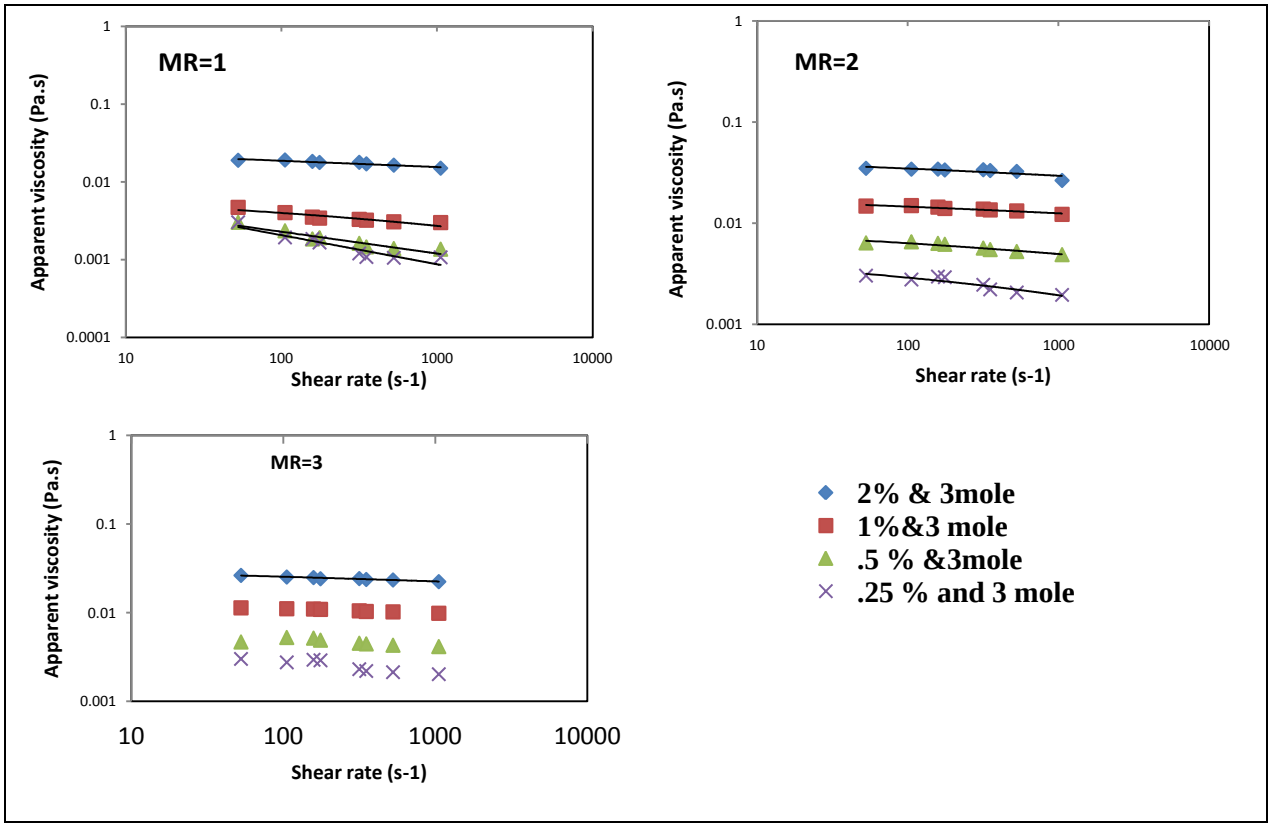

Figure 5-18: Apparent viscosity for OTAC / NaSal

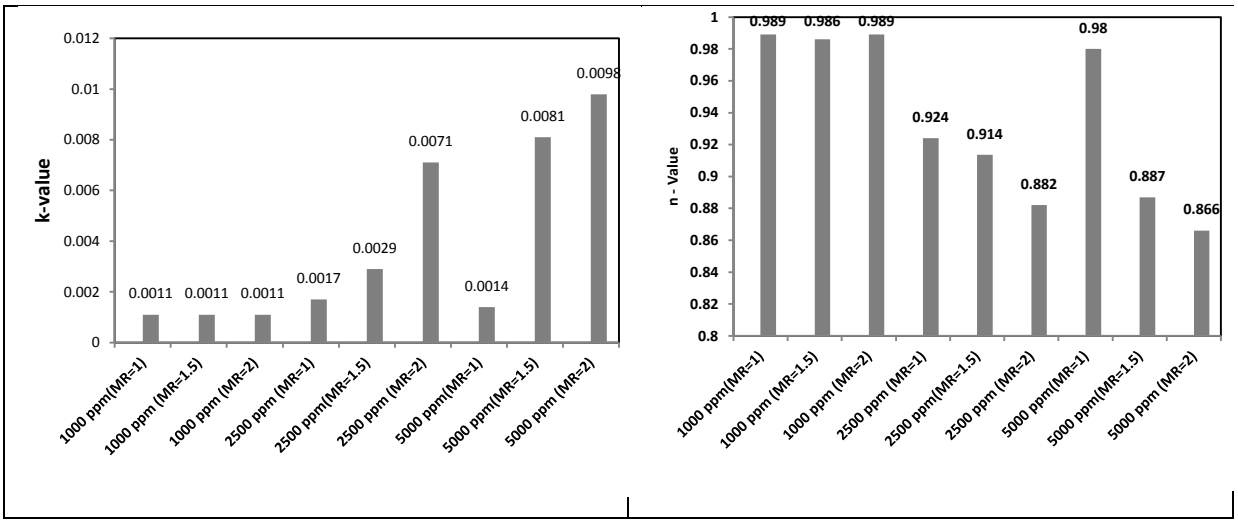

Figure 5-19: Variation of power law model parameters for different concentrations of OTAC and different molar ratios of NaSal

5.2.1.2 Conductivity

Figure 5-20 shows conductivity measurement for pure OTAC and OTAC / NaSal (MR=2). The CMC point will change from 5645 ppm to 773 ppm. This drastic change is related to the formation of rod-like micelles in presence of NaSal. Addition of salt (NaSal) disperses the positive repulsive charges on the ionic head groups and stabilizes the micelles allowing them to grow in size (Zhang et al. 2005).

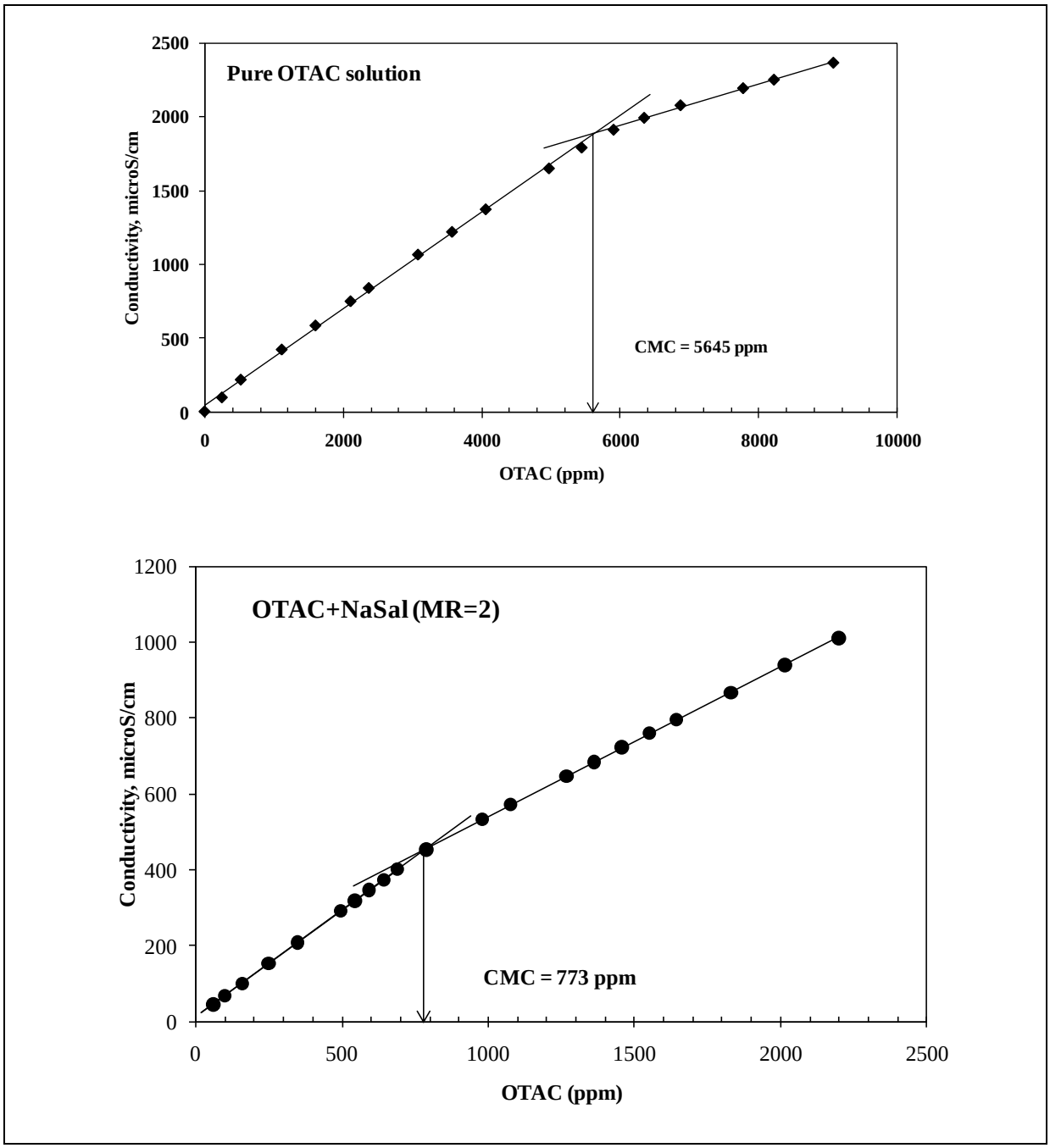

Figure 5-20: Effect of NaSal on CMC of OTAC solution

5.2.1.3 Pipeline flow behavior

Effect of salt and surfactant concentration on DR

In this study, the surfactant solutions with different concentrations and different molar ratios (MR) of NaSal/OTAC were tested. The solutions without salt do not cause a considerable drag reduction (i.e. lower than 10%). No DR was also observed for the surfactant concentrations lower than 500 ppm even if different values of MR were used in the experimental work. It should be noted here that DR was started at 500 ppm but the value was not considerable.

Drag reduction by surfactant solution is an ongoing area in the literature. A number of studies have shown that formation of worm-like micelles (WLM) is the main reason for DR (Gasljevic et al. 2001; Zakin et al. 2007; Zakin et al. 2007). In some cases, DR was observed without viscoelasticity or elongation viscosity (Lin et al. 2000). Some researchers emphasized on the influence of extensional viscosity and viscoelasticity on DR. Others concluded that both shear thinning and rod-like micelles act as important factors for DR (Ohlendorf et al. 1986; Zakin et al. 2006). Also, the SIS (shear induced superstructure) formation in surfactant systems under turbulent conditions has been proposed in many studies (Ohlendorf et al. 1986; Qi and Zakin 2002; Zakin et al. 1998).

In this experimental study, viscosity data showed that the solution with 1000ppm surfactant concentration displays Newtonian behaviour under low shear rates, while it could form a shear induced structure (SIS) if high shear stresses are applied (Qi and Zakin 2002). This new structure is the main cause for drag reduction at this stage. There is a lower bond critical value (LBCV) for wall shear stress at which SIS forms. This value depends on salt concentration, but it does not vary significantly upon this parameter. Although drag reduction increases when salt/surfactant molar ratio is equal to 2, but viscosity data do not show any considerable change in the value of %DR. This could be related to the chance of SIS formation and its stability.

The friction factor and %DR vs. Re_G for different concentrations of salt and surfactant is presented in Figure 5-21 for the pipe with diameter of 22.02 mm at 20^oC. The figure was plotted based on three levels of surfactant and also three levels of salt concentrations.

Figure 5-21a&b) depicts friction factor and %DR in 1000ppm OTAC/NaSal for different values of MR. When Re_G is higher than ~ 70000, %DR increases at a higher rate for MR=2 in comparison to MR=1.5. For Re_G lower than 70000, %DR is almost the same for MR=1.5 and MR=2. This supports the idea that in addition to SIS formation, the stability of this new structure can affect DR. This justification is valid for DR that occurs at MR equal to 1. In this case, %DR decreases when Re reaches the magnitude of ~ 70000. It means there is an upper value of critical Re at which SIS starts to break down. Existence of the Upper Bond Critical Value (UBCV) has been reported in the literature. At this level of surfactant and salt for flow inside the 1 inch pipe at 20 ^oC, UBCV is equal to 70000. Almost the same trend as 1000ppm was observed for 2500 ppm of OTAC, except that LBCV and UBCV for wall shear stress were different compared with that of 1000 ppm level (Figure 5-21c&d).

In general, as the salt concentration increases, the drag reduction increases if the surfactant concentration is in the range of 1000 - 2500 ppm. Solutions with molar ratio (MR) of salt/surfactant equal to 1.5 were shown almost the same drag reduction as those with MR=2 at f 20^oC.

Figure 5-21e&f) show the friction factor and %DR for the solutions with surfactant level of 5000 ppm with respect to Re_G. Increasing of MR from 1 to 1.5 results in an increase in %DR. Adding further salt has negative effect on %DR. %DR decreases slightly for MR=2 compared to MR=1.5 when Re_G is at lower bound. This phenomenon is due to the viscosity effect. At lower Re_G viscosity is much more effective compared to higher Re_G (high turbulence). The reason for this phenomenon, as mentioned before, can be the reshaping of rod-like micelles to spherical shape (Usui et al. 2004). High values of MR cause insolubility in some mixture systems (Qi and Zakin 2002). The effect of MR on worm like micelles (WLM) formation is complicated, depending on molecular structures of both the cationic surfactant and the counterion (Zhang 2005).

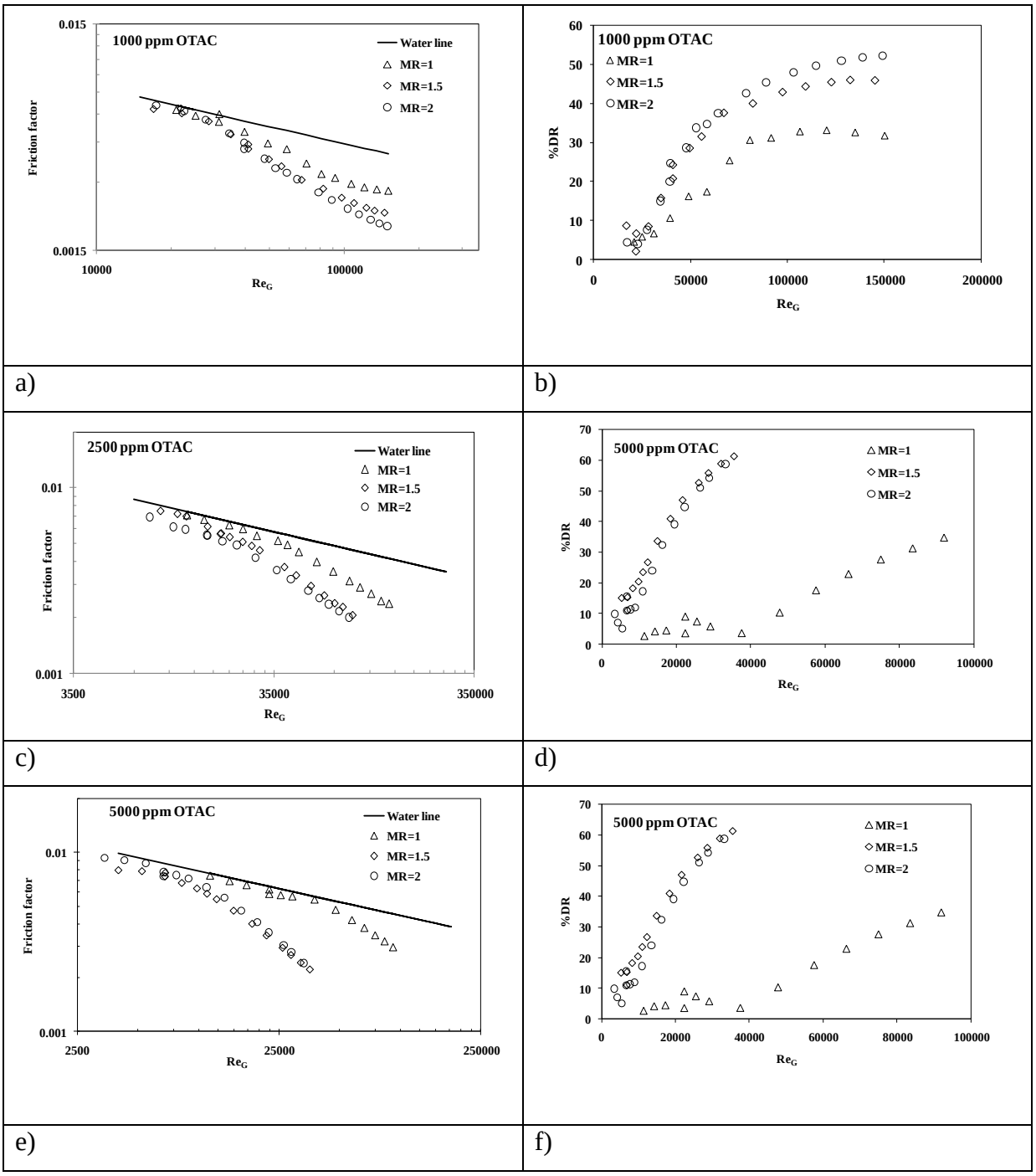

Figure 5-21: Friction factor and %DR vs. Re_G for different concentration of OTAC and NaSal at 20 ± 0.5 °C

Figure 5-22 depicts the effect of surfactant concentration on the friction factor and drag reduction. The level of salt concentration and also temperature were kept constant at MR=2 and 20^{o}C±.0.5 during the experiments, respectively.

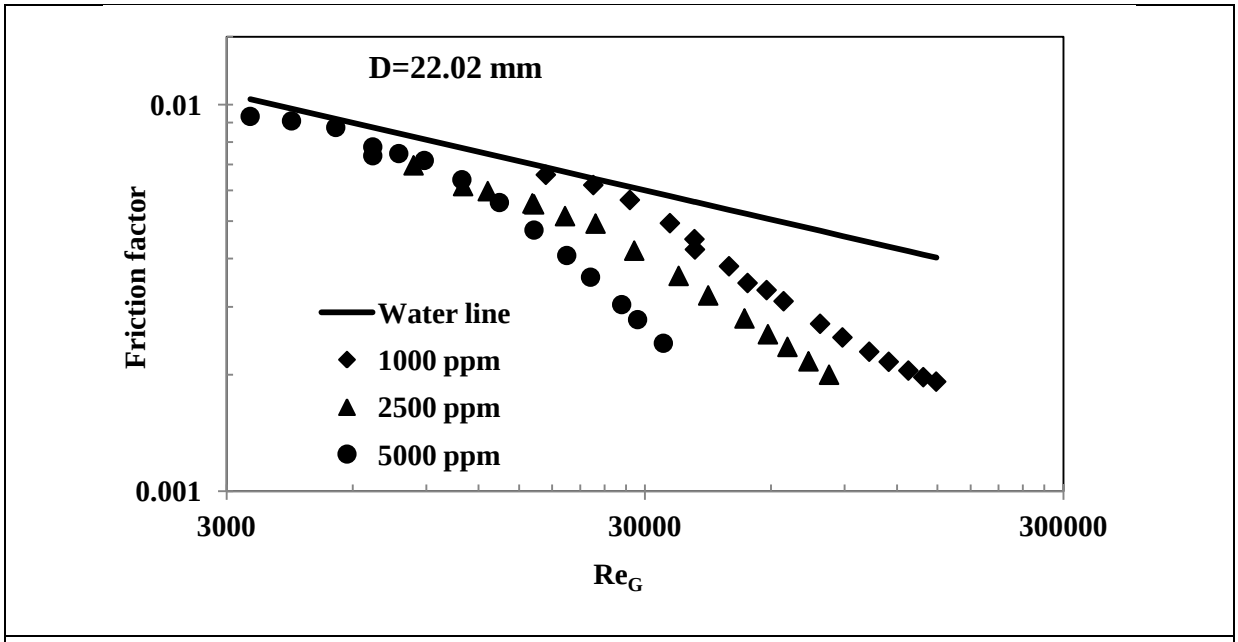

a) Friction factor

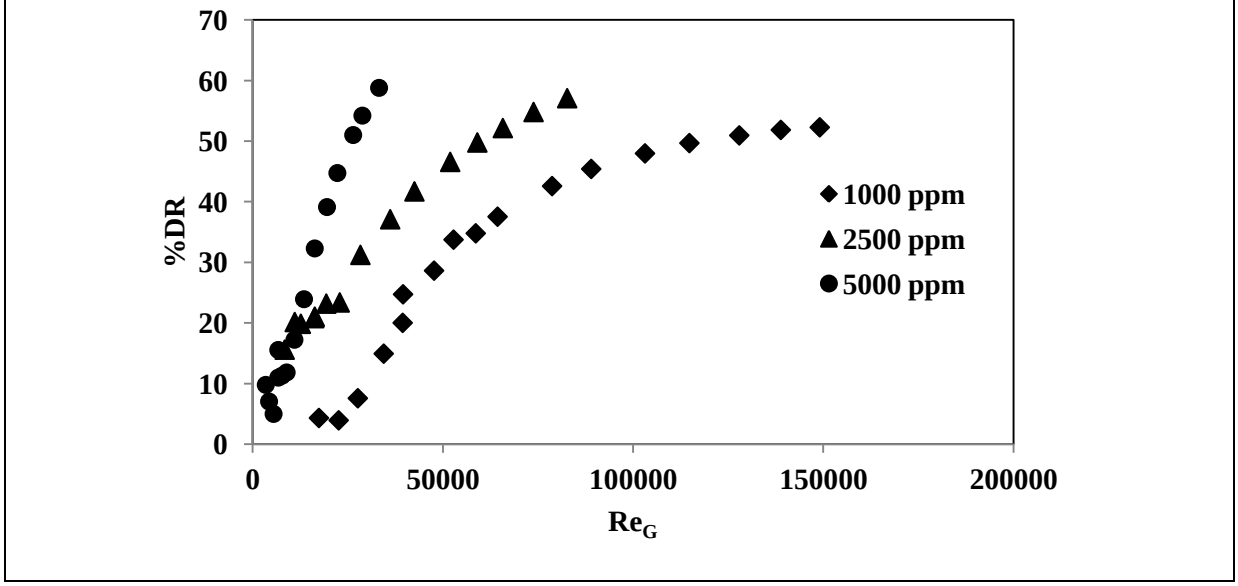

b) %DR

Figure 5-22: Effect of OTAC concentration on friction factor and %DR at 20^{o}C and MR=2

Increase in OTAC concentration results in an increase in %DR for a constant MR. The onset of DR decrease from ~$Re_{G=}$17000 to Re of 5500 in the case of 1000 ppm when the OTAC concentration reaches 2500 ppm. Onset of DR remains unchanged for higher OTAC concentration. According to the phase diagram for cationic surfactant solutions (see Figure 5-23), one would expect to see an increase in viscosity when surfactant concentration increases. When the solution is located above the state of CMCII, this change is more noticeable. Formation of Rod-like micelle improves DR considerably, compared with other circumstances.

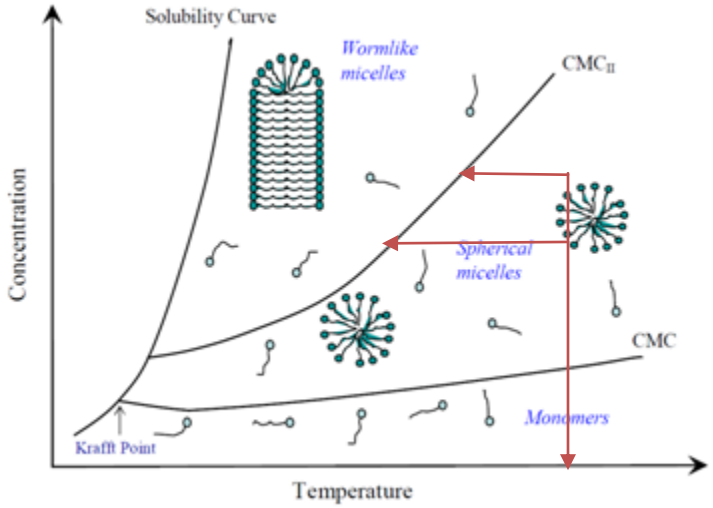

Figure 5-23: Schematic phase diagram for cationic surfactant solutions (Chou 1991)

Effect of temperature

The effect of temperature on friction factor and %DR for different concentration of OTAC has been presented in Figure 5-24. For different OTAC concentrations, increase in temperature has negative impact on DR. The negative effect is more significant for lower concentration (1000ppm). Since temperature does not affect onset of DR, the value of Re_G for onset of drag reduction remains similar for all conditions.

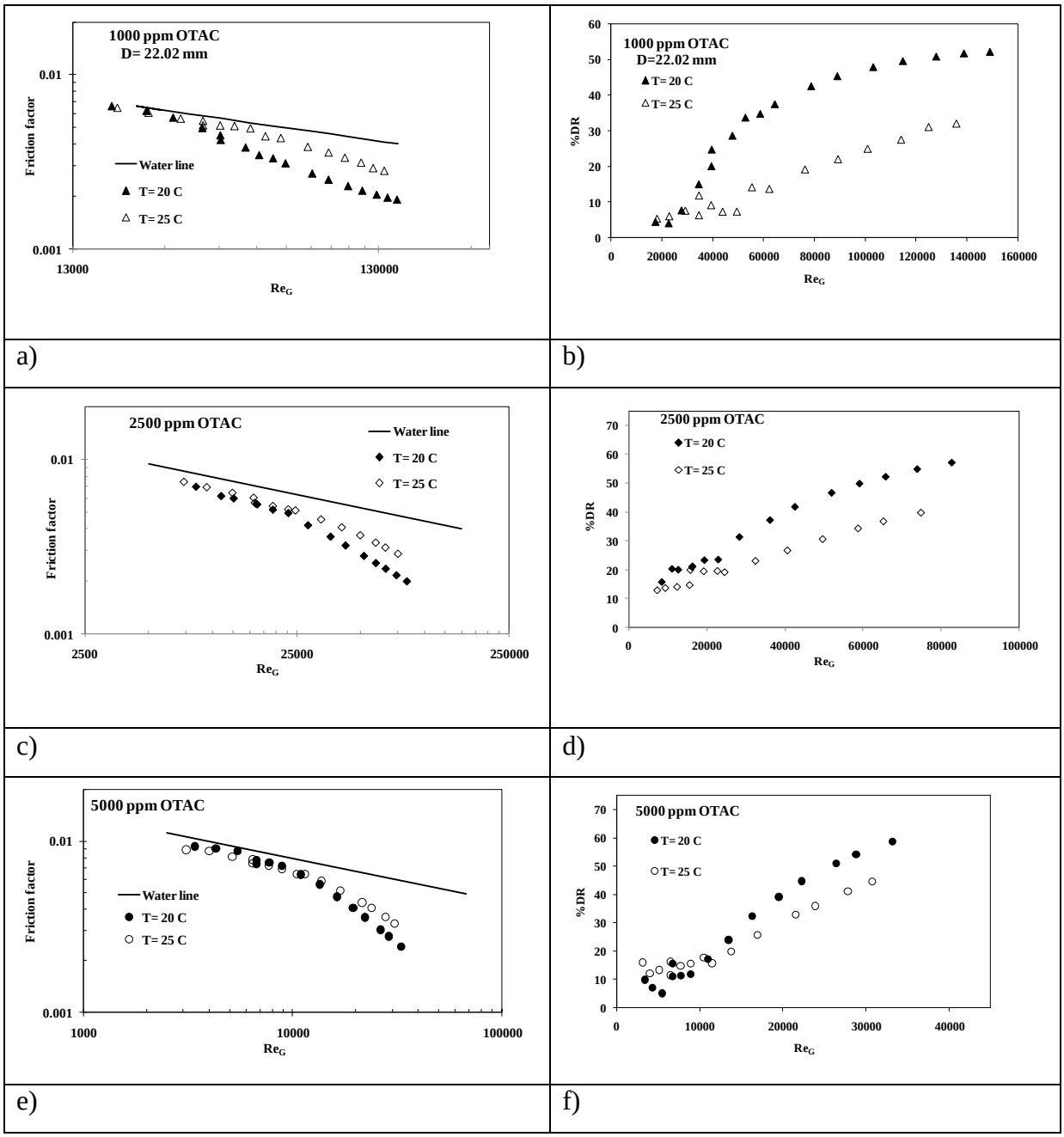

Figure 5-24: Effect of temperature on friction factor and %DR of OTAC solutions

As depicted in Figure 5-23, surfactants form rod-like micelles when the conditions are above CMCII. For a certain surfactant and salt concentration, the spherical micelles are more

likely to restructure to rod-like form as the temperature lowers. This depends on state of the solution in terms of concentration and temperature based on the phase diagram.

Diameter effect

Variation of friction factor against Re for different pipe diameters is presented in Figure 5-25. The temperature and MR were kept constant throughout the experiments. Various surfactant concentrations were employed in the experiments. The results show that larger pipe diameters have lower %DR. For the concentrations of 1000 ppm and 2500 ppm, %DR are very similar to each other especially for high values of Re_G. Increasing the surfactant concentration to 5000 ppm leads to a reasonable change in %DR while using different pipes.

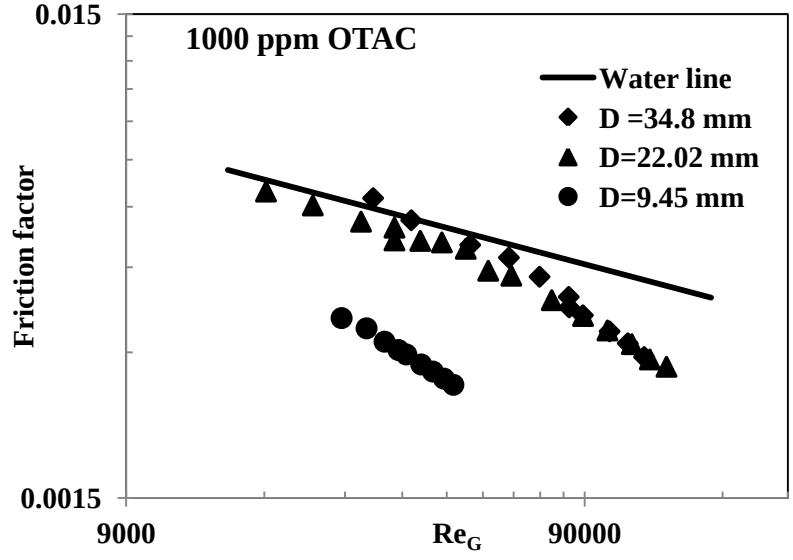

a)

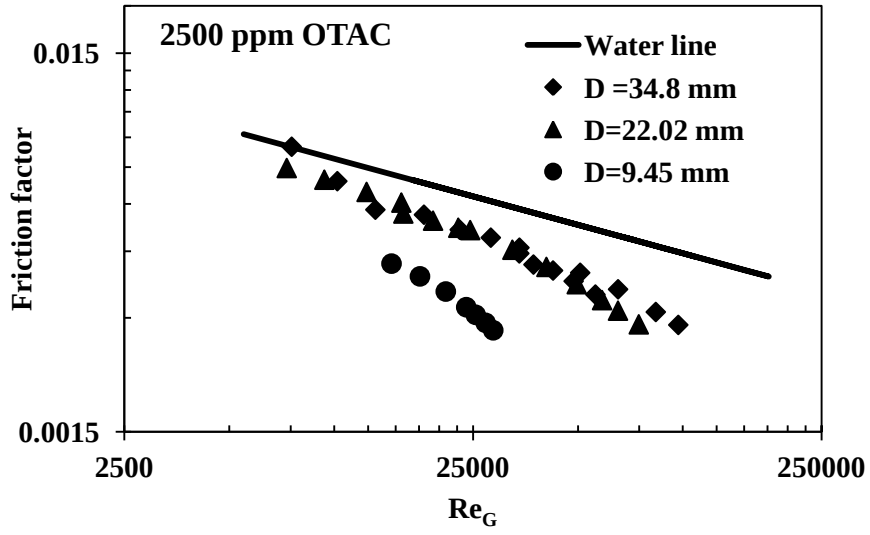

b)

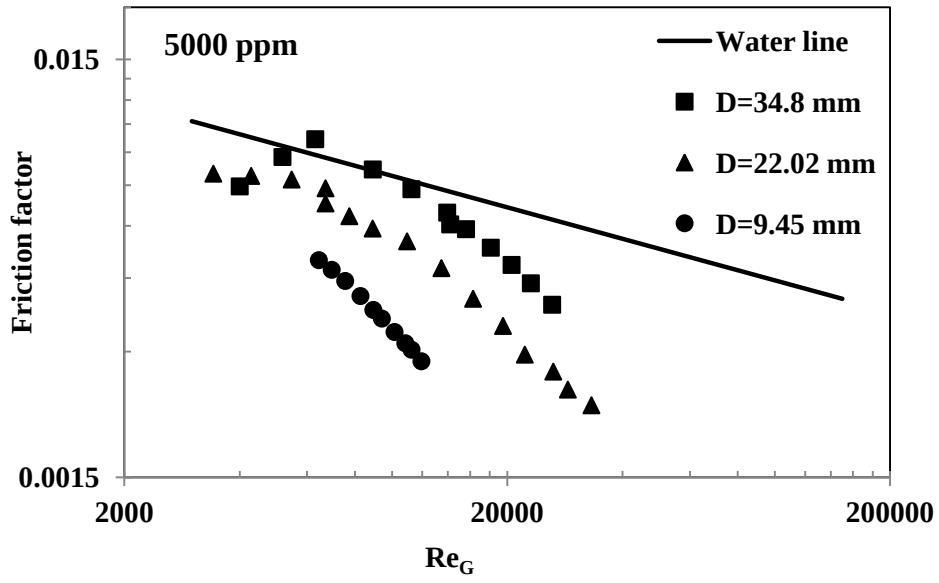

c)

Figure 5-25: Effect of pipe diameter on friction factor of OTAC+NaSal (MR=2) solutions at 20 ^{o}C

Effect of pump shearing

Figure 5-26 shows the effect of pump shearing on the value of DR. The hollow circles were collected using pump 2 which is more powerful (7.5hp) than pump 1 (1.5 hp). For 1000 ppm and MR=2 at 20^{o}C pump 2 has negative effect on %DR. Surfactant concentration of 5000 ppm at MR=2 had lower impacts compared with the the 1000 ppm- solution. The reason for this behavior is that the 5000 ppm solution has stronger micelles and network.

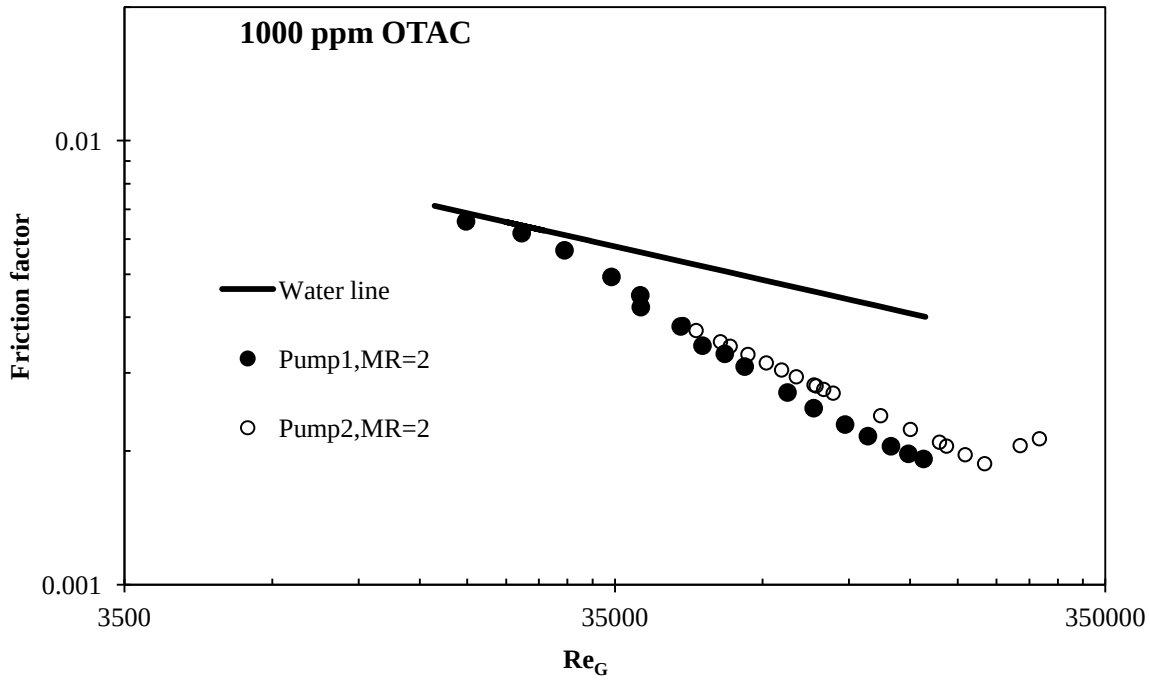

Figure 5-26: Effect of pump shearing for 1000 ppm of OTAC

Experimental work was carried out at MR=1.5 for 5000 ppm. Slight effects were observed for this MR compared with MR=2, under the same conditions. This means that the micelles for MR=1.5 (5000 ppm) are more stable in this solution than in solution with MR=2 (Figure 5-27).

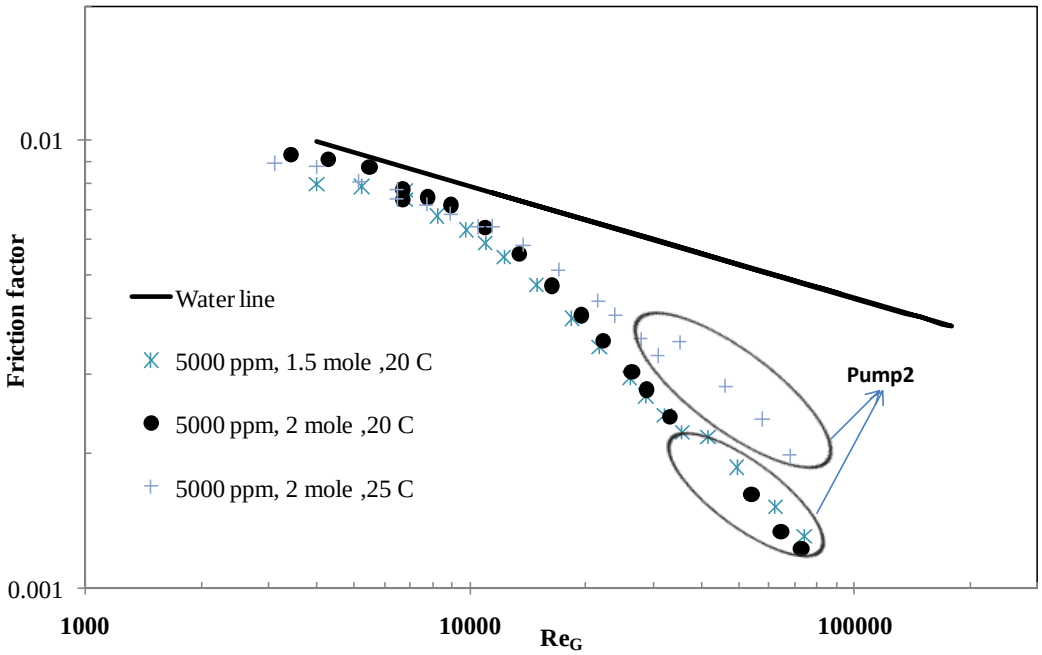

Figure 5-27: Effect of pump shearing on friction factor

5.2.2 Anionic surfactant

Figure 5-28 shows friction factor vs. Re_G for different concentrations of SDS in DI water. No drag reduction was observed for SDS at these concentration levels. Some studies have shown that SDS can demonstrate DR with high amount of some type of salts such as NaCl or KCl. Pure SDS produce globullar micelles in DI water especially at these levels of concentration. One wouldn't expect to observe drag reduction as rod like micelles seems to be necessary for drag reduction (Zakin et al. 1998; Zhang 2005).

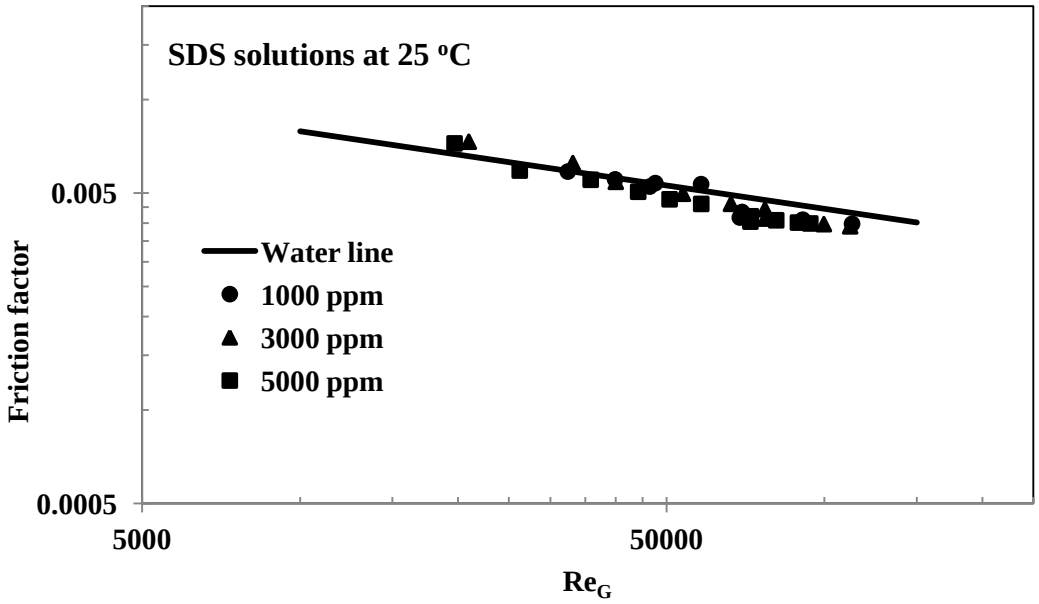

Figure 5-28: Friction factor vs. Re_G for different concentration of SDS in DI water

In this study no DR was observed with addition of 5% NaCl as salt. Temperature change (20-30^{o}C) did not have any effect of on observed DR behaviour. Therefore no more results are presented for SDS pipeline flow in this section.

5.3 Reproducibility

To check the reproducibility of data some methodology were applied to ensure that data were enough accurate for interpretation. During the pipe line flow data collection the flow was picked randomly. However the procedure was from highest flow to lowest one, to randomize the process time to times flow was picked randomly from every arrange (highest to lowest or reverse).

Some of experiment reaped under random condition. In this case different solutions from different stock solution of polymer were made and flow was randomly picked and pressure drop was measured and compared to each other. Figure 5-29 shows friction factor for different runs of 250 ppm of PAM in DI water.

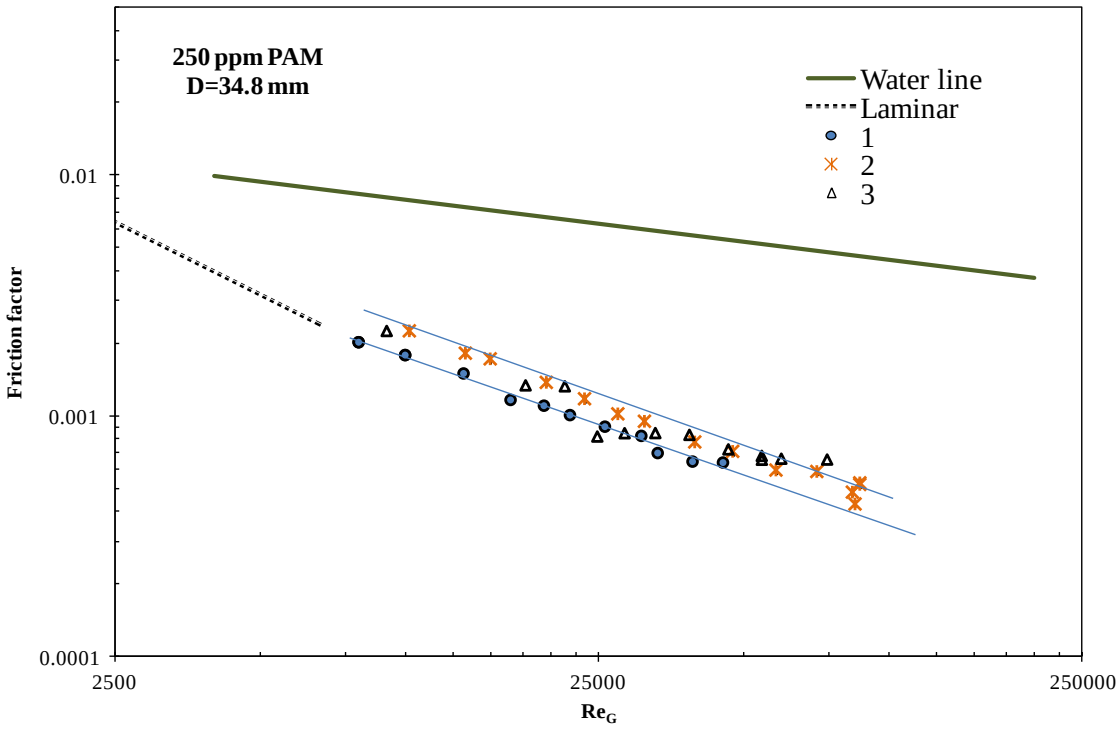

Figure 5-29: Reproducibility of drag reduction of polymer solution

In the case of surfactant, reproducibility was much better as surfactant solution will not degrade. Figure 5-30 shows reproducibility of OTAC solution for an identical condition. Data shows good agreement in two series of experiments.

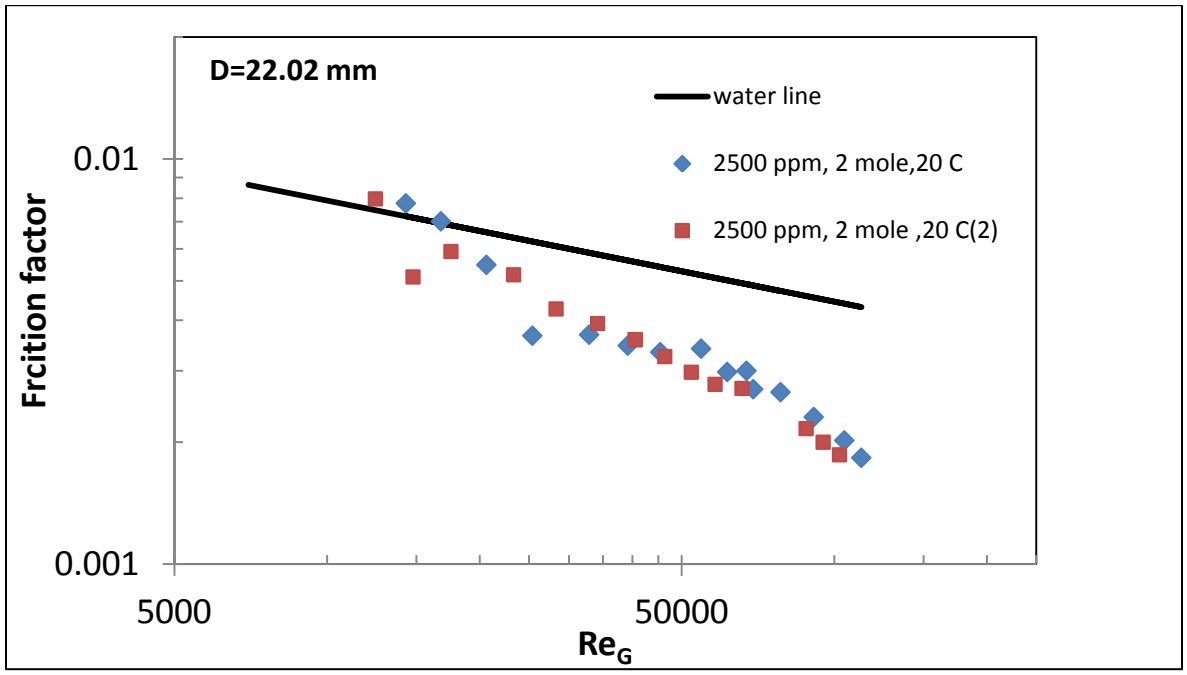

Figure 5-30: Reproducibility of OTAC solutions

5.4 Summary

Following results can be summarized for the studied surfactant DR:

Results of these different types of drag reducers conducted us to find out differences and similarities among OTAC as a cationic surfactant and PEO and PAM as two widely used polymers for DR. The following conclusions can be drawn based on results from the current study:

- Considerable energy savings resulting from a reduction in pumping power can be achieved using both polymers and some type of surfactants
- DR requires higher concentrations of surfactant compared with the required polymer concentration
- Salt and surfactant concentrations greatly affect DR like what polymer concentration does.
- When surfactant and salt concentration increase, the flow behaves as polymeric solution with shear thinning effect.

- Onset of DR is highly dependent on concentration of polymer.
- In case of surfactant DR onset of DR depends on salt and surfactant concentration.
- DR by low surfactant concentration (e.g. 1000 ppm) is caused by different mechanism compared to the low concentration polymer solutions.
- Shear stress effect on surfactant DR, before critical wall shear stress, is negligible compared with the polymer DR.
- The advantage of surfactant over polymer additives is due to the different nature of the mechanical degradation they experience. Mechanical degradation is the permanent loss of drag-reducing ability of a polymeric solution after exposure to supercritical shear or elongation stresses. Surfactants regain their DR ability when the supercritical shear remove or decrease to lower values.
- Temperature can negate the effects of DR from surfactants. For all levels of OTAC / Salt, increasing temperature causes DR to decrease, even though the decrease in DR for higher concentration is not as sharp as others.
- Temperature does not have a big effect on onset of DR for in case of DR by surfactant
- Effect of diameter is dominant in the small diameter range, only. At large diameters the effect is negligible.

Chapter 6
Interaction of Cationic Surfactant (OTAC) with Anionic Polymer (PAM)

For bench-scale experiment same procedure mentioned in section 4.1 was used. Temperature was kept constant in bench scale and pipeline flow experiments at $25^{o}C \pm 0.5$.

6.1 Bench Scale Results

6.1.1 Viscous Behavior of Solutions

Viscosity is one of the best ways to detect the conformational behavior of polymer chain and surfactant solution. As mentioned in section 3.5 the main reason for interaction of oppositely charged polymer and surfactant is their electrostatic charges. The electrostatic interaction between oppositely charged polymer and surfactant is expected to have a strong influence on the viscous behaviour of polymer-surfactant solutions.

As shown in Figure 6-1, addition of OTAC into PAM solution (DI water) can cause a drastic change in relative viscosity. The low shear relative viscosity of the polymer solution, measured using a capillary viscometer, decreases substantially with the addition of OTAC to PAM solution. This decrease in viscosity is due to strong interactions between negatively charged polymer chains and positively charged surfactant molecules. The interaction is significant even when a small amount of surfactant is added to the polymer solution.

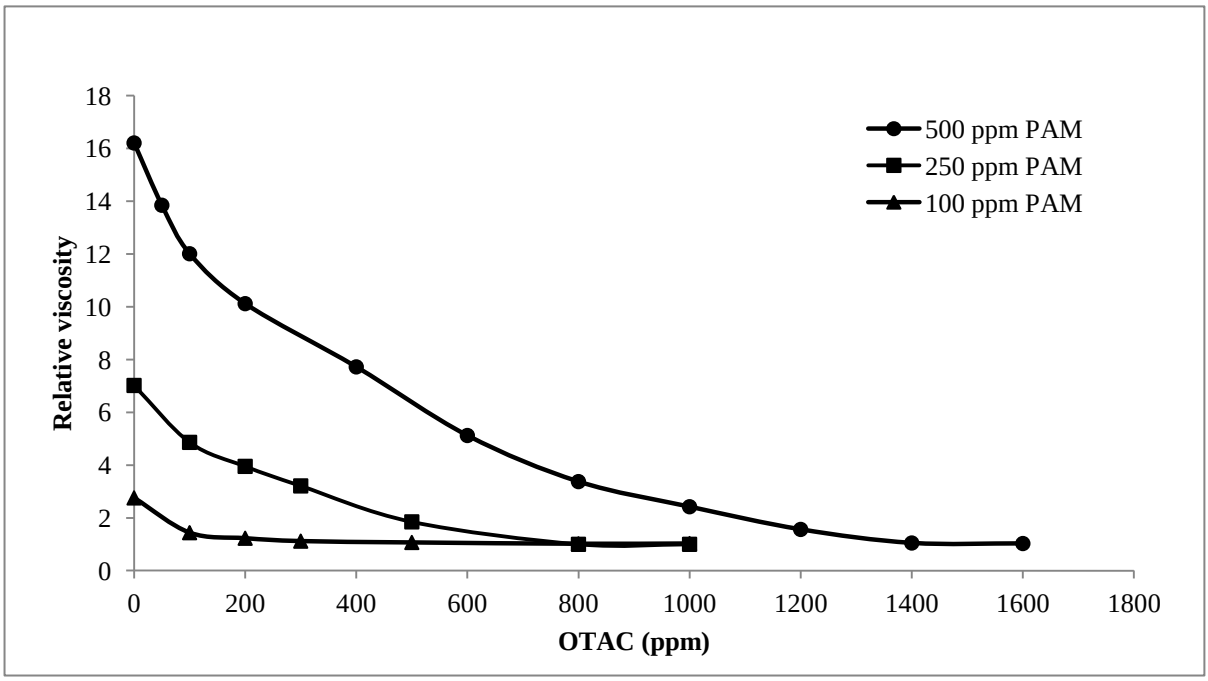

Figure 6-1: Relative viscosity of anionic PAM with OTAC in DI water

Referring to Figure 5-1a, overlap concentration of PAM (C*) in DI water is almost 250 ppm. At PAM concentration higher than C^*, the polymer molecules form a three dimensional network structure. The decrease in relative viscosity with the addition of surfactant is slow at polymer concentration higher than C^* due to inaccessibility of negatively charged sites of PAM molecules by OTAC monomers.

Figure 6-2 shows variation of apparent viscosity versus shear rate for 500 ppm PAM solution containing different concentrations of OTAC. The viscosity data over the shear rate range investigated can be described by a power-law model. The flow behavior index (n) of the solutions is shown in Figure 6-3. The mixture of polymer and surfactant approaches Newtonian behavior (n = 1) when the surfactant concentration is relatively high (800 ppm OTAC for 500 ppm PAM solution and 1000 ppm OTAC for 1000 ppm PAM solution).

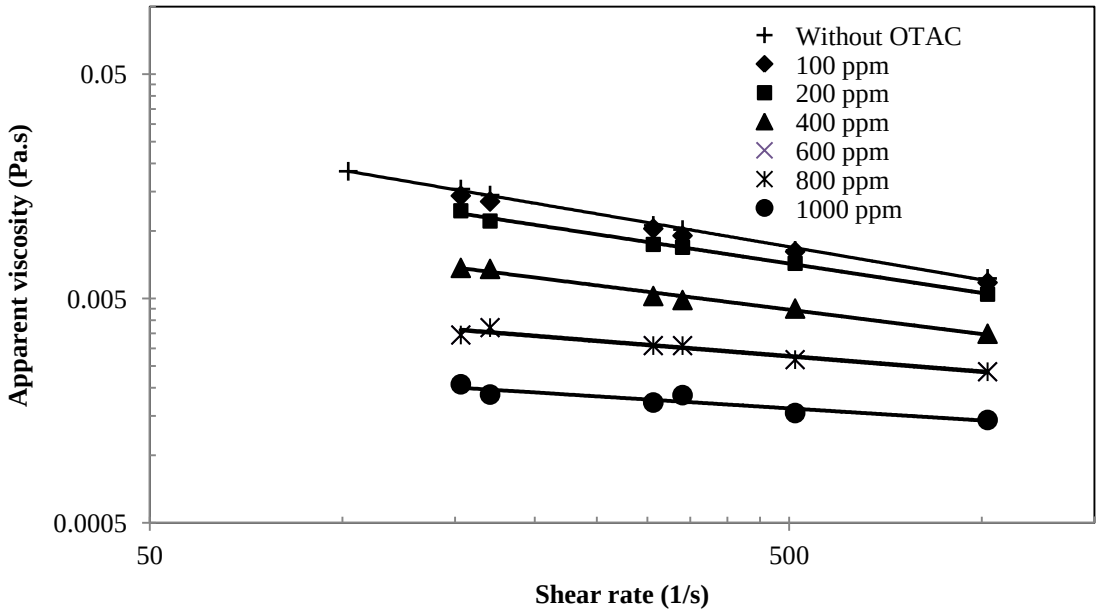

Figure 6-2: Effect of OTAC concentration on the apparent viscosity vs. shear rate for PAM-OTAC mixtures

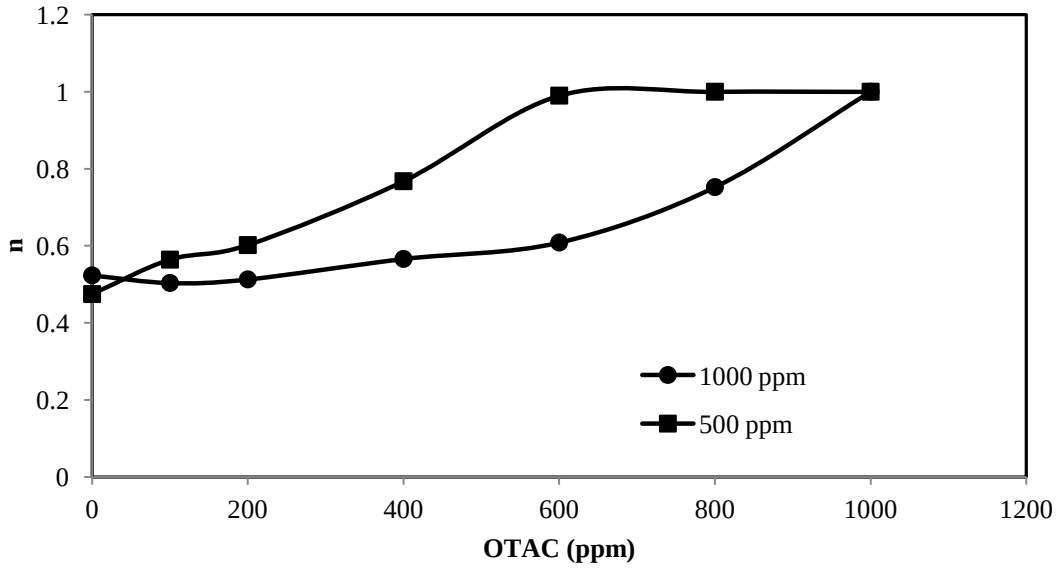

Figure 6-3: flow behavior index (n) of power law vs. varying concentration of OTAC

Figure 6-4 shows the interaction between anionic PAM and cationic OTAC schematically. The polymer molecules collapse upon interaction with OTAC monomers.

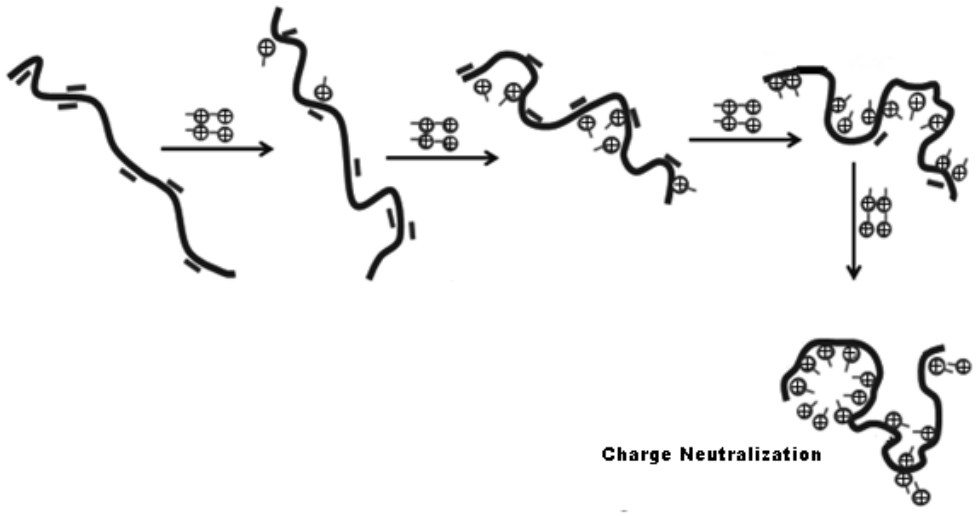

Figure 6-4: Schematic representation of interaction between anionic PAM and Cationic OTAC (Prajapati 2009)

Referring to Figure 5-1b) - which shows the specific viscosity vs. PAM concentration plot when tap water is used instead of DI water- the overlap concentration (C*) of polymer molecules is about 770 ppm. Note that the overlap concentration of polymer molecules is much higher when tap water is used. The presence of cationic ions in the tap water makes it a poor solvent for PAM compared to DI water. PAM chains are not fully extended in tap water which causes a very low relative viscosity for this solution compared to PAM solution in DI water. In this case, it is expected that the addition of cationic surfactant not having a significant effect on relative viscosity. Figure 6-5 shows relative viscosity vs. OTAC concentration for PAM / OTAC in tap water. At low surfactant concentrations, the relative viscosity does not change with the addition of surfactant. When a surfactant concentration is higher than 500 ppm, the relative viscosity drops sharply to a value of unity.

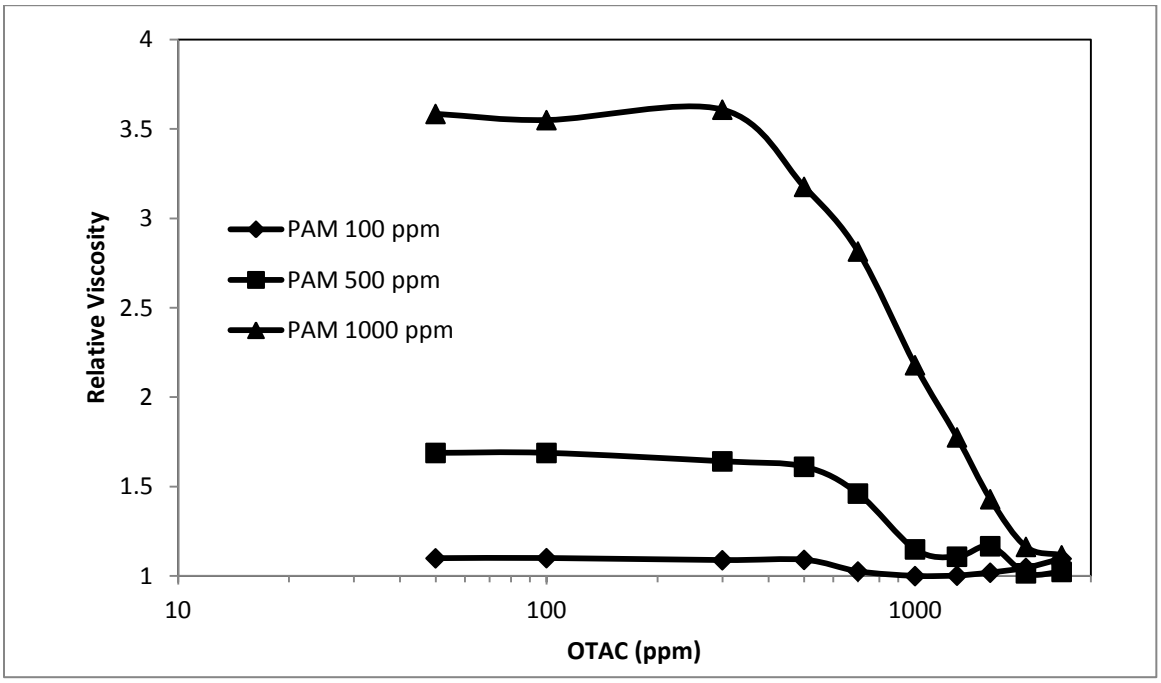

Figure 6-5: Relative viscosity vs. OTAC concentration for PAM / OTAC in tap water

The highly coiled PAM chains in tap water do not allow the OTAC monomers to easily access the charged sites on the polymer chains. Therefore, no interaction between PAM and OTAC is observed up to about 500 ppm. When the OTAC concentration exceeds a certain value, the OTAC monomers diffuse into coiled PAM chains resulting in a sharp decrease in relative viscosity.

6.1.2 Conductivity

The interaction between the surfactant and the polymer is also reflected in the conductivity measurements. Figure 6-6 shows the conductivity versus surfactant concentration plots for given polymer concentrations. The change in the slope of the conductivity plot occurs at CMC of surfactant. The CMC of surfactant increases from 5700 ppm in DI water to 6800 ppm in 500 ppm PAM solution, and to 7100 ppm in 1000 ppm PAM solution. These data are very close to those reported by Prajapati(Prajapati 2009). The observed increase in the CMC value with the increase in PAM concentration is expected. The interaction between the ionic part of OTAC and negative charge of PAM chain results in a

decrease in the amount of free OTAC monomers in the solution. Consequently, OTAC micellization is delayed to higher concentrations. When tap water is used, the OTAC micellization begins at 4800 ppm, compared to ~5700 ppm in DI water. The ions present in tap water tend to stabilize the OTAC monomers in the solution and therefore, a lower CMC value is observed with tap water.

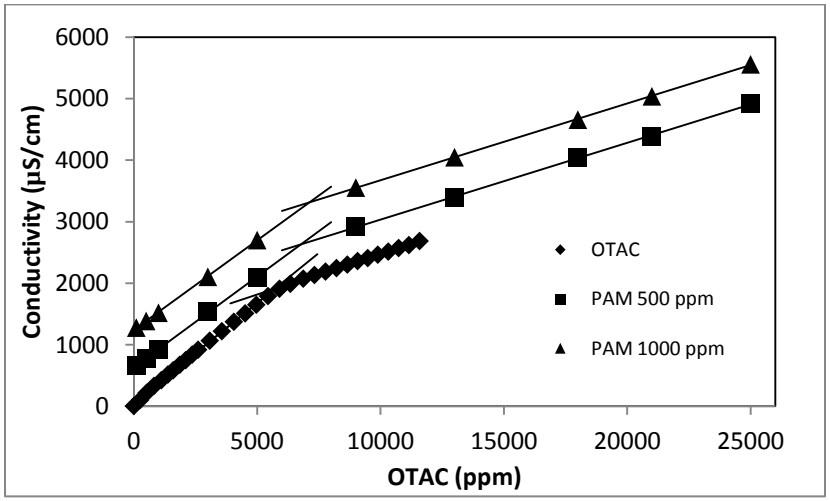

Figure 6-6: Conductivity change observation for PAM / OTAC solution vs. OTAC concentration

6.2 Pipeline flow of solutions

6.2.1 Solution in DI water

6.2.1.1 Effect of OTAC concentration

To study the effect of combination of anionic polymers and cationic surfactants on drag reduction, the anionic PAM and cationic OTAC were mixed in tap water and DI water. Then drag reduction behavior was monitored in previously designed and constructed pipeline set-up.

Figure 6-7 show the effect of OTAC concentration on drag reduction behaviour of PAM solution in DI water. No change in drag reduction ability of 500 ppm PAM solution is observed upon the addition of 300 ppm and 500 ppm of OTAC. As observed earlier, the C* for PAM is about 250 ppm. The PAM macromolecules at 500 ppm form a three dimensional network. In this situation, OTAC monomers cannot easily reach the negative charge sites of PAM. However, at an OTAC concentration of 800 ppm, the concentration gradient of OTAC is high enough for OTAC molecules to diffuse to the negative sites of polymer chains. Consequently, a decrease in %DR is observed at 800 ppm OTAC. Also note that the type of drag reduction behavior changes from Type A to Type B at 800 ppm OTAC. Similar trends were observed with different diameter pipes (Figure 6-8).

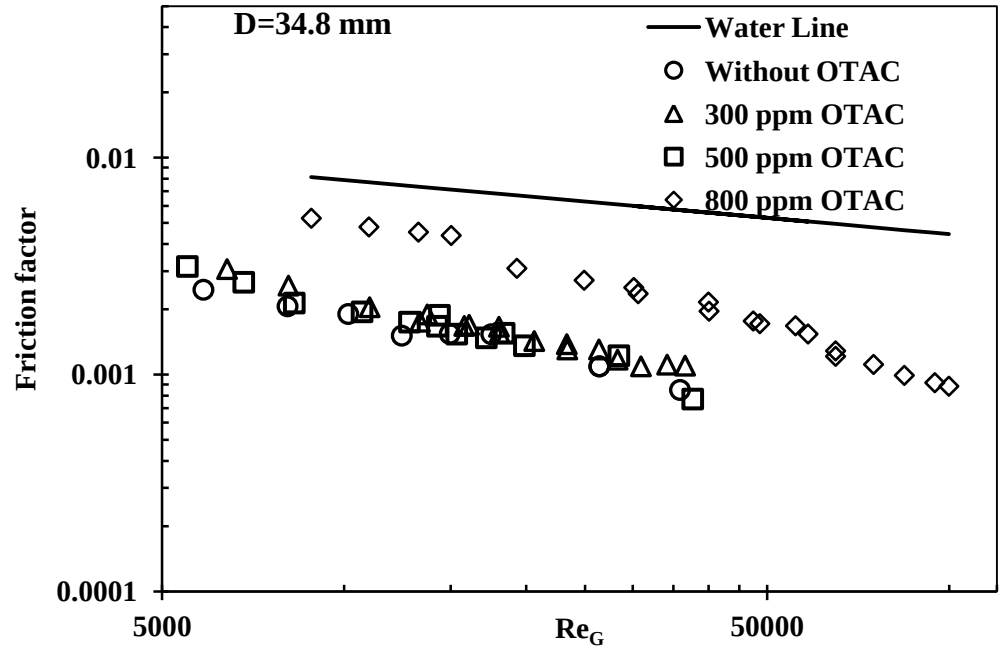

a) Friction factor vs. Re_G

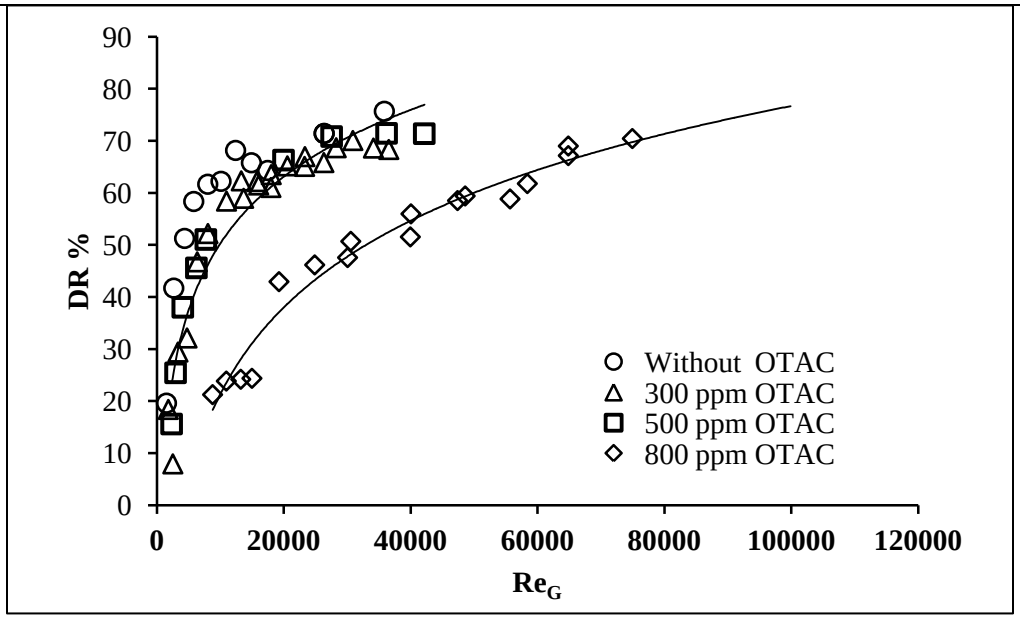

a) %DR vs. Re_G

Figure 6-7: Effect of OTAC on friction factor and %DR of 500 ppm PAM solution in DI water

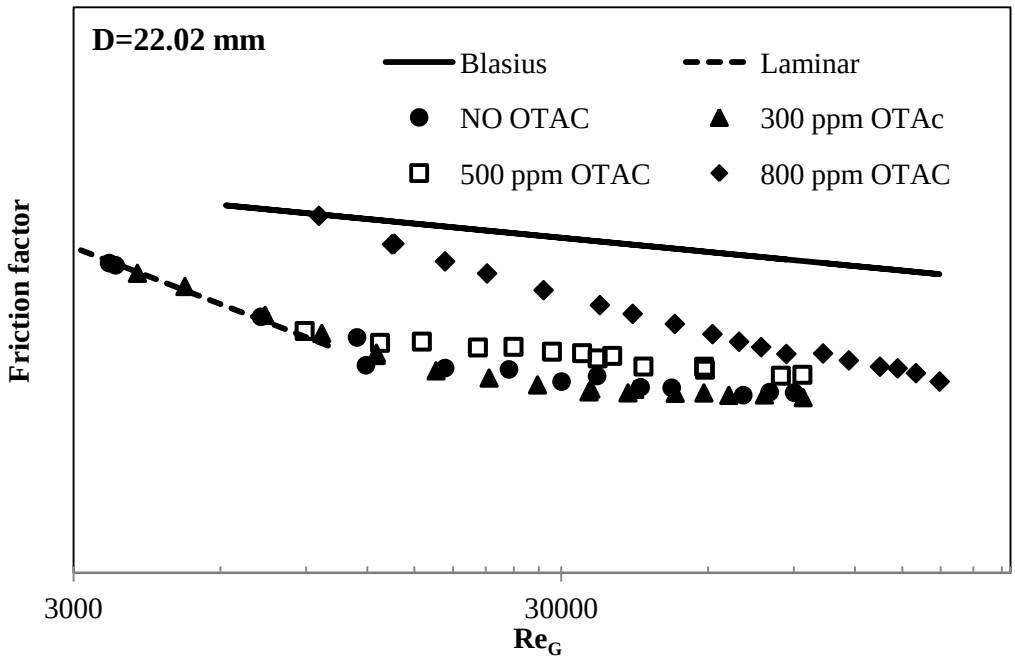

Figure 6-8: Effect of OTAC on drag reduction of 500 ppm PAM solution in DI water

Figure 6-9 shows friction factor and %DR vs. Reynolds number for 250 ppm PAM solution in DI water with different amounts of OTAC. In this case (where the polymer concentration is lower than that of the previous case), a lower concentration of OTAC (500 ppm) is needed to influence the drag reduction behaviour.

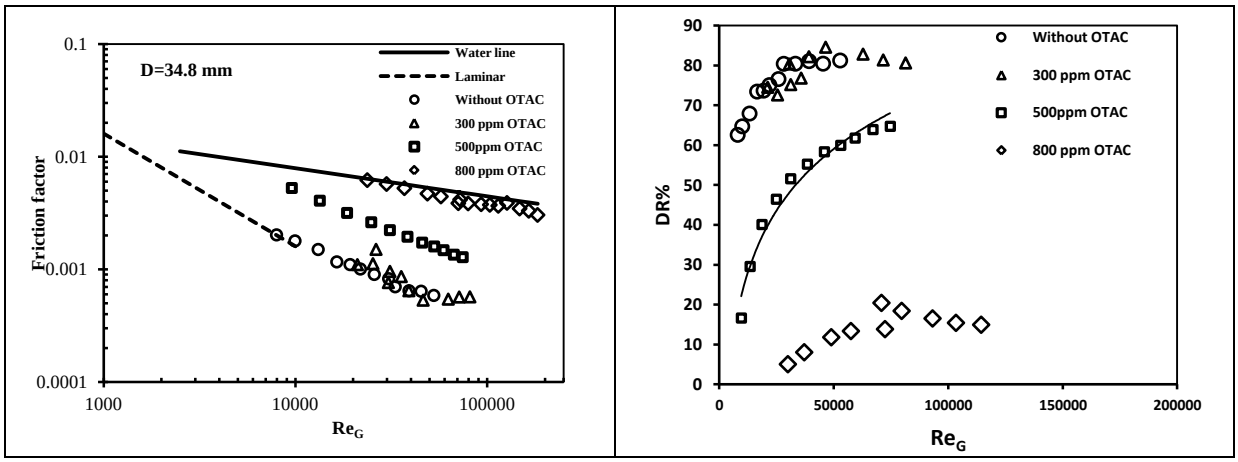

Figure 6-9: Effect of OTAC concentration on friction factor and %DR for 250 ppm of PAM solution in DI water

Based on bench-scale experiments for 100 ppm PAM solution, impact of OTAC addition is expected to be much more than 500 ppm and 250 ppm PAM solutions. A higher ratio of OTAC/PAM means higher accessibility of polymer anionic sites by OTAC molecules and hence a larger degree of electrostatic neutralization of polymer molecules.

Figure 6-10 shows friction factor vs. Reynolds and %DR for 100 ppm PAM with different concentrations of OTAC. As it was expected, friction factor and hence drag reduction behaviour is now affected even at a low OTAC concentration of 300 ppm. Friction factor is higher for all PAM / OTAC system compare to pure PAM solution. For 100 ppm PAM / 300 ppm OTAC solution the friction factor value is the same as that of pure PAM solution at lower Reynolds numbers. At lower Reynold and lower PAM concentrations, the concentration of fully extended polymer chains is not enough to damp the turbulence fluctuation.

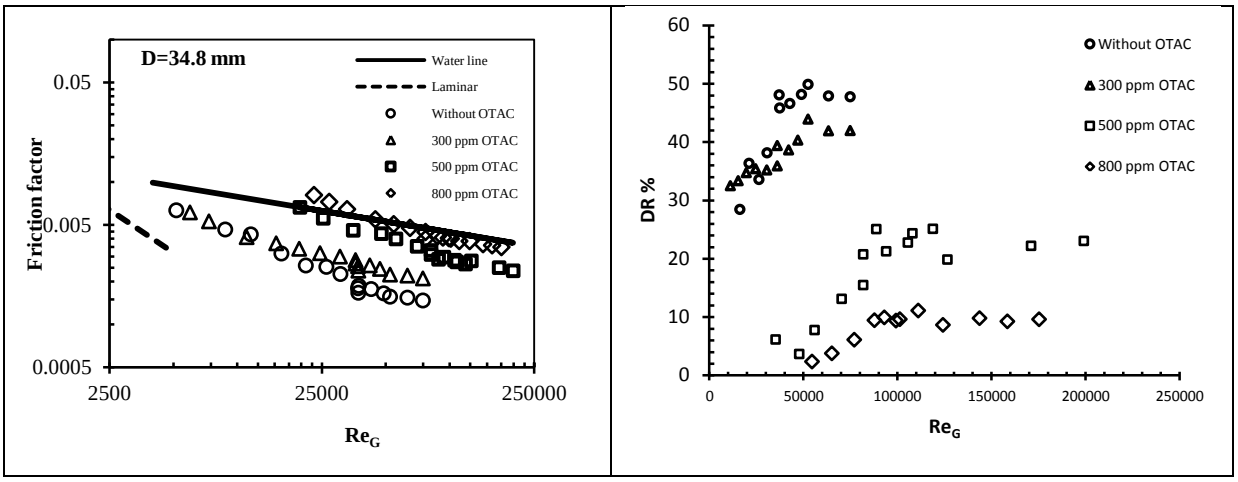

Figure 6-10: Effect of OTAC on %DR of 100 ppm PAM solution in DI water

Figure 6-11 compares friction factor for different concentration of PAM with a fixed value of 500 ppm OTAC. It's clear that the most impact is on the lower concentration of PAM (100 ppm). Other PAM solution receive less effect compare to 100 ppm which is much lower than C*.

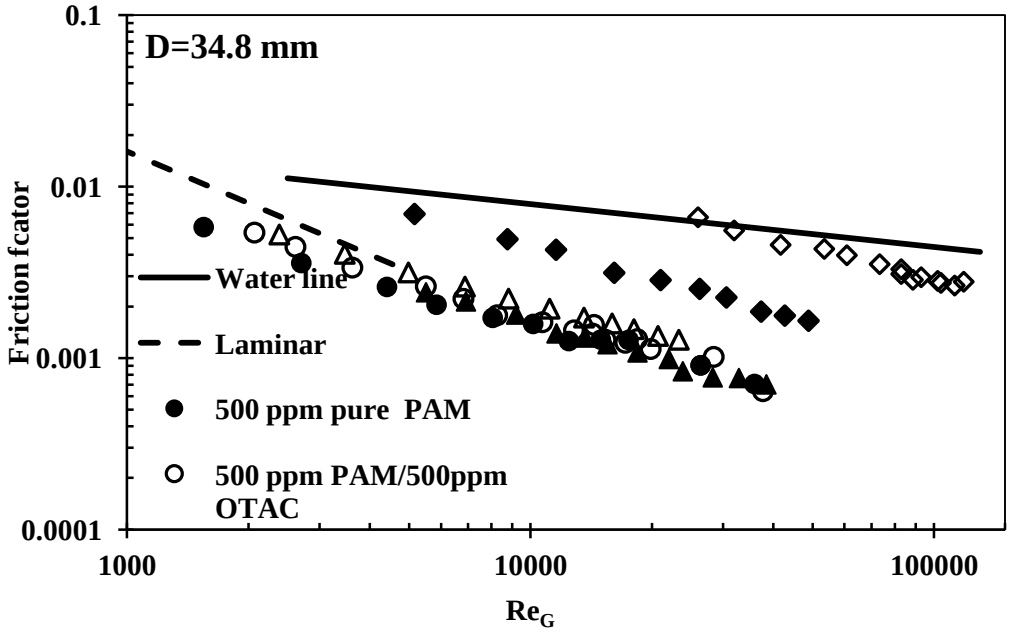

Figure 6-11: Comparison among (PAM /500 ppm OTAC) series

6.2.1.2 Mechanical degradation

Figure 6-12 shows friction factor versus Reynolds number for 250ppm PAM and different amount of OTAC (obtained after 20 hr degradation). Addition of 300 ppm OTAC does not have any considerable effect on degradation of PAM. This system behaves like pure PAM solution. For 500 ppm and 800 ppm OTAC, the degradation has much more impact on drag reduction.

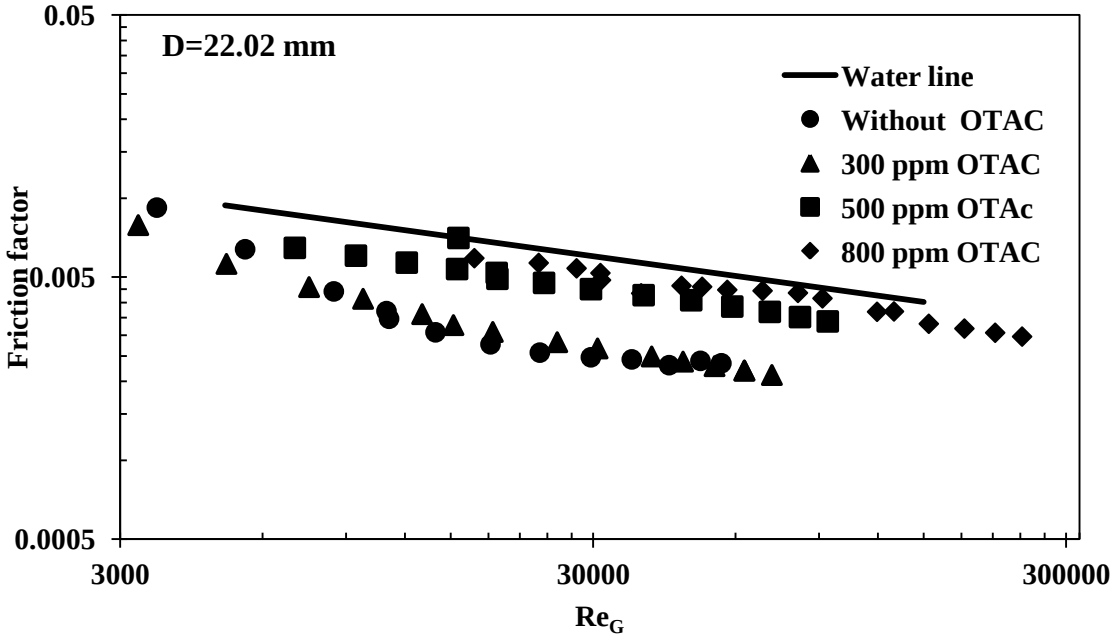

Figure 6-12: Friction factor vs. ReG for degraded 250 ppmPAM / OTAC systems after 20 hr

Extensional viscosity is another factor which can affect the drag reducing capability of the polymer. Solutions with higher extensional viscosities are believed to be better drag reducers (Zakin et al. 1998). Low concentration polymer solutions mostly behave as non-Newtonian fluids. They also have a higher extensional viscosity in comparison to Newtonian fluids such as water. However, a pure PAM solution behaves as shear thinning fluid. When OTAC monomers react with anionic charges on the backbone of the polymer, macromolecule chains collapse. Later, the behavior of the solution may change from non-Newtonian to Newtonian behavior. Table 6-1 and Figure 6-13 show flow behavior index for different APM / OTAC systems in DI water. n index increases exponentially for all PAM

concentrations; however, the slope increases in order of 100ppm>250 ppm>500 ppm. These results are in agreement with friction factor and %DR data shown in pervious figures.

Table 6-1: Flow behavior index for PAM /OTAC system in DI water

OTAC (ppm)	500 ppm PAM		250 ppm PAM		100 ppm PAM	
	k	n	k	n	K	n
0	0.1918	0.4738	0.0922	0.5121	0.0506	0.5296
300	0.1255	0.5261	0.038	0.5965	0.0132	0.6735
500	0.0629	0.5826	0.013	0.6769	0.0041	0.774
800	0.0102	0.7526	0.002	0.8907	.0012	~1

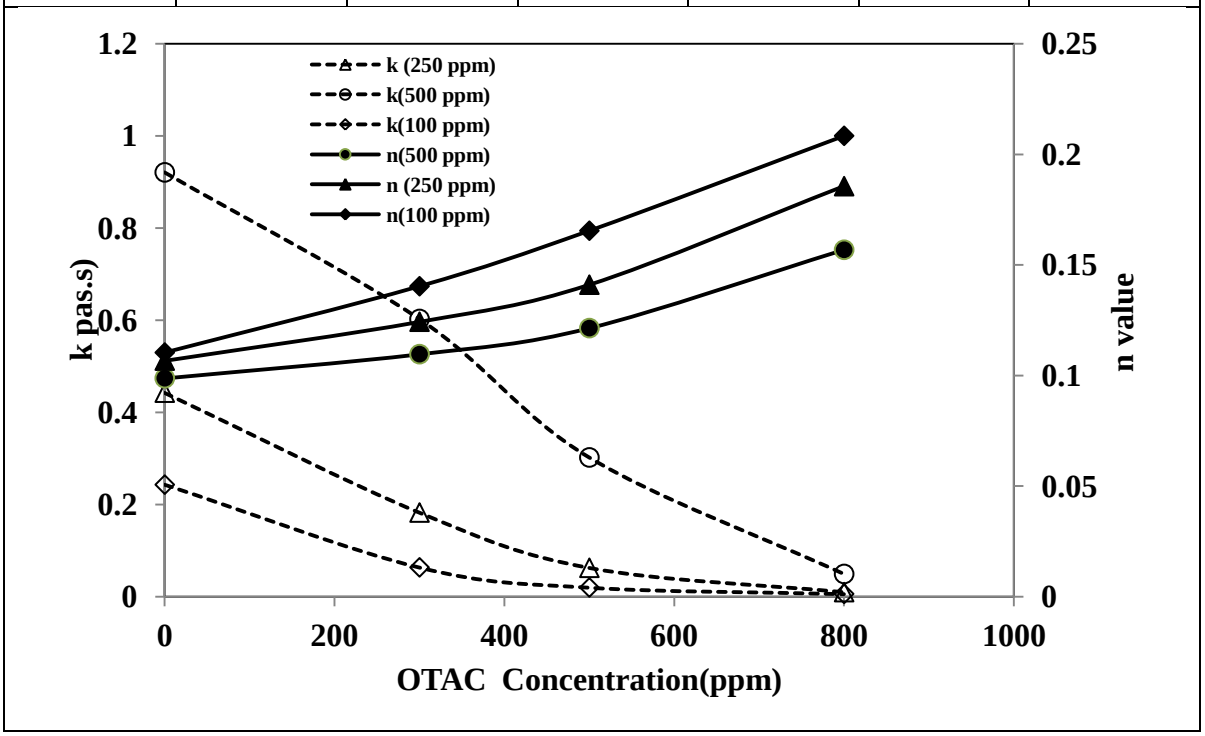

Figure 6-13: Flow behavior index for different PAM /OTAC in DI water

Some researchers believe that the coiling phenomenon protects polymer macromolecules against shear degradation in comparison to a fully extended one. Some others support this idea that extended model, in which the polymer molecules are fully

stretched, is more stable under high shear stress (Brostow et al. 1990; Brostow et al. 2007). In this case, a stretched polymer chain can be protected from shear degradation when it is under ultimate shearing.

Figure 6-14 shows variation of flow indexes for 500 ppm PAM / OTAC with time when is under degradation. The n values for 300 ppm and 500 ppm of OTAC are not changed with time and remains almost the same as fresh solutions for the first few hours, whereas the n value changes exponentially for 800 ppm OTAC. Based on this information, it is expected to observe a sharp decrease in %DR with time at higher concentrations of OTAC such as 800 ppm (See Figure 6-12 and Figure 6-15).

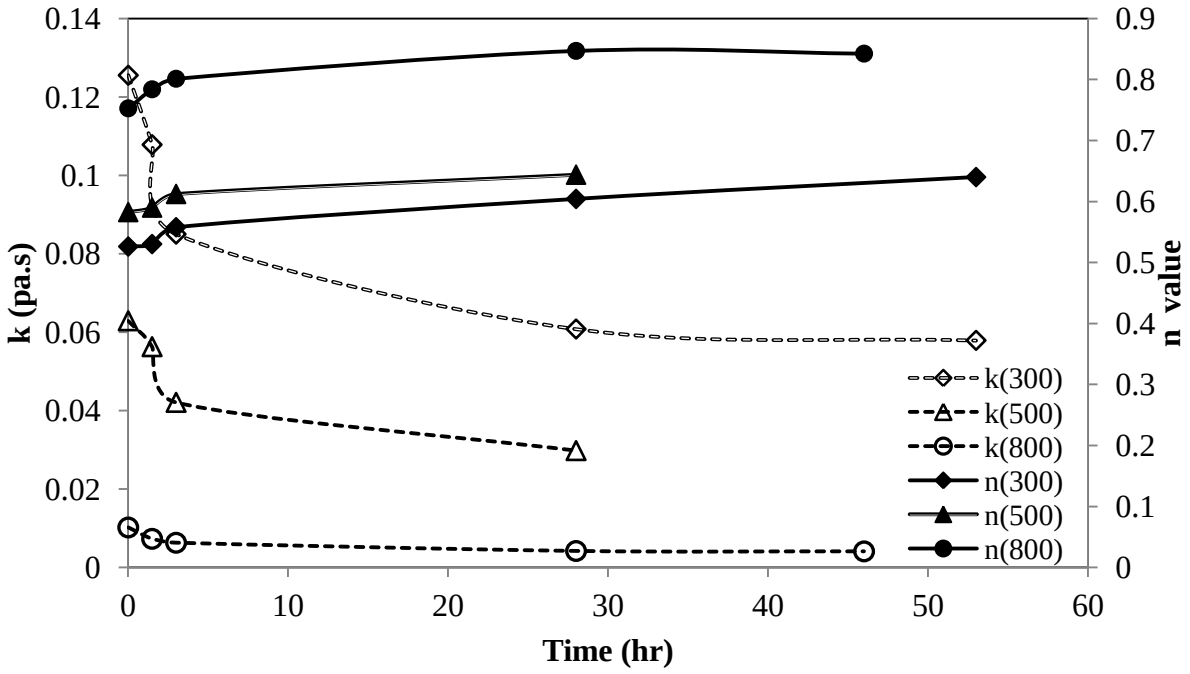

Figure 6-14: Variation of flow index versus time for 500ppm PAM and different concentration of OTAC

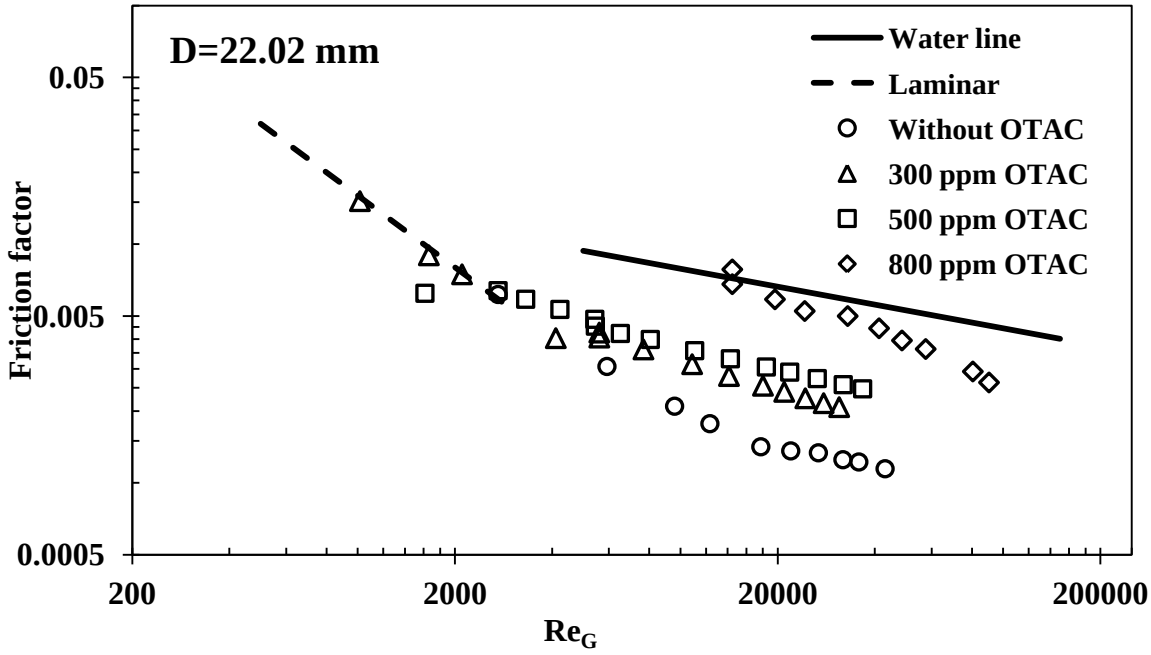

Figure 6-15: Friction factor vs. Reynolds number for 500ppm PAM with different concentrations of OTAC after 30 hr degradation

More results are presented in Figure 6-16 to show the degradation phenomenon in PAM / OTAC solutions in detail. It is obvious that the coiling of polymer can cause more degradation especially for those solutions with PAM concentrations lower that C* and higher OTAC concentration.

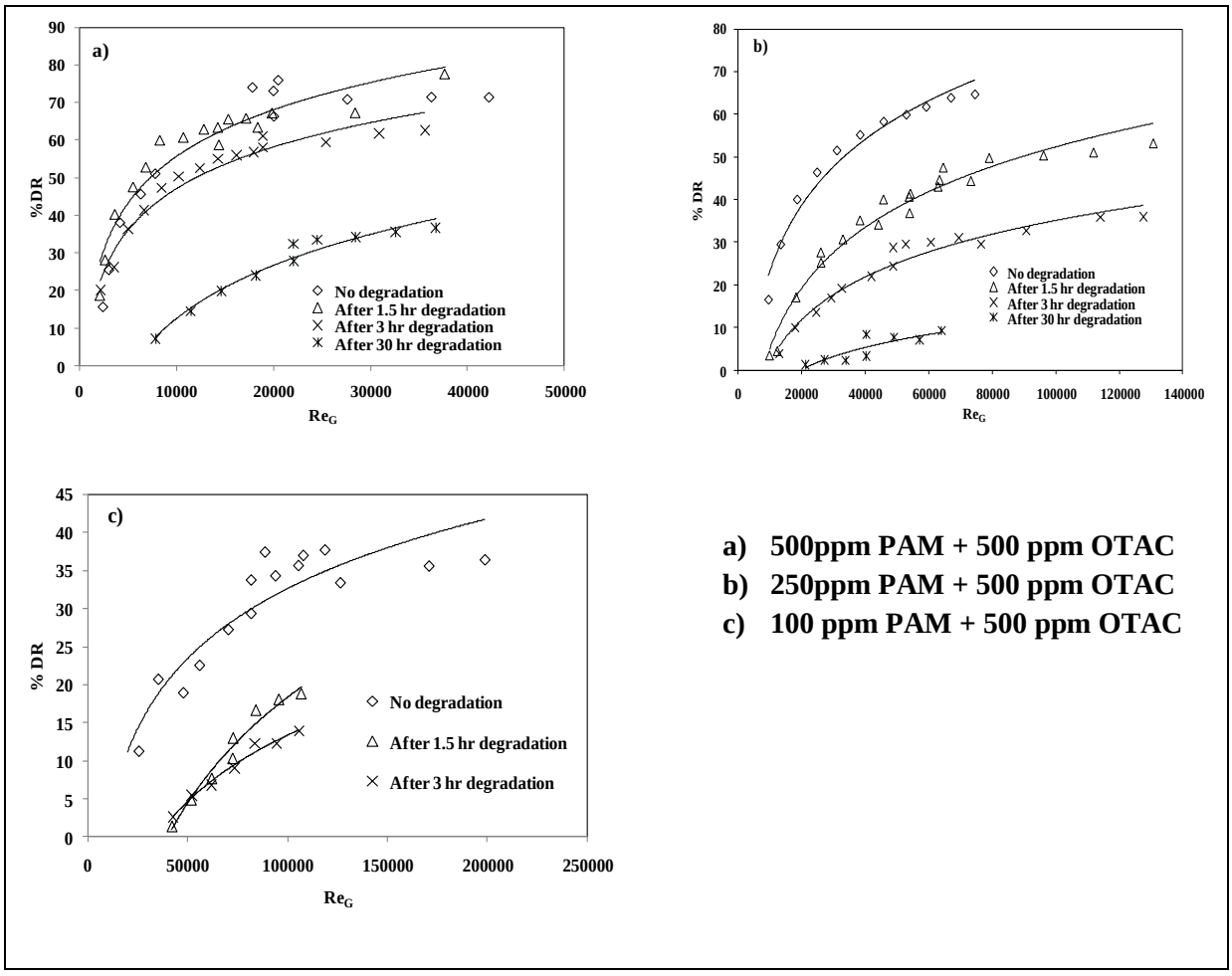

Figure 6-16 : Effect of degradation on %DR for different PAM /OTAC systems

Figure 6-17 compares %DR verses time for different PAM concentrations at a fixed value of 500 ppm OTAC with pure PAM solution. %DR decreases exponentially for pure PAM solution whereas for PAM / OTAC solutions a sharp decrease in %DR (especially at early time) is followed by a negligible change at later stages. This graph also supports this idea that coiling of polymer not only does not have any advantage for protecting polymer against shear degradation, but also accelerates degradation. In fact, the addition of OTAC to pure PAM solution can decrease the effective PAM macromolecules which eventually contribute to DR. As effective concentration is decreased, the polymer degradation happens faster. Same effect was observed for other pipe diameters.

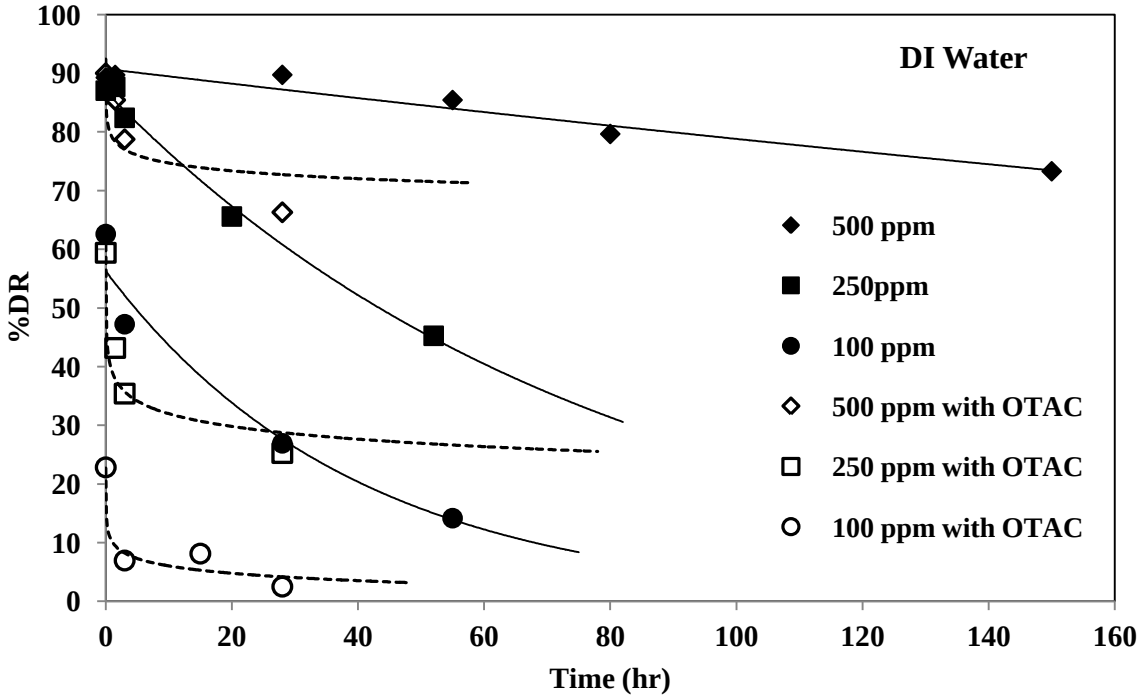

Figure 6-17: Effect of degradation on %DR vs. time in different solutions of PAM+500 ppm OTAC systems in DI water (D=34.8)

6.2.1.3 Effect of NaSal

OTAC in combination with NaSal can be suitable drag reducer in turbulent flow but it does not show any DR up to 1000 ppm OTAC+NaSal (MR=2). The presence of NaSal in the solution can decrease the repulsive effect of OTAC head groups by shielding them. Since micelle formation starts at very low OTAC concentration, in presence of salt the system can get benefit from formation of rod like micelle on the back bone of the polymer chain. This might be a good idea to increase the stability of polymer chain against shear degradation. Using NaSal could potentially lead to some interesting results.

A series of experiments were conducted using NaSal as salt. Some results are presented in Figure 6-18. This graph depicts the effect of NaSal on friction factor variation for 250 ppm PAM / 500 ppm OTAC system. With a MR=2 (molar ration of salt to OTAC) a lower friction factor was observed at Reynolds higher than 10,000 in comparison to the equivalent

PAM / OTAC system. This increase in %DR does not look to be the effect of free OTAC micelles since at this concentration all OTAC monomer would go to react with negative charges (Refer to bench scale experiment).

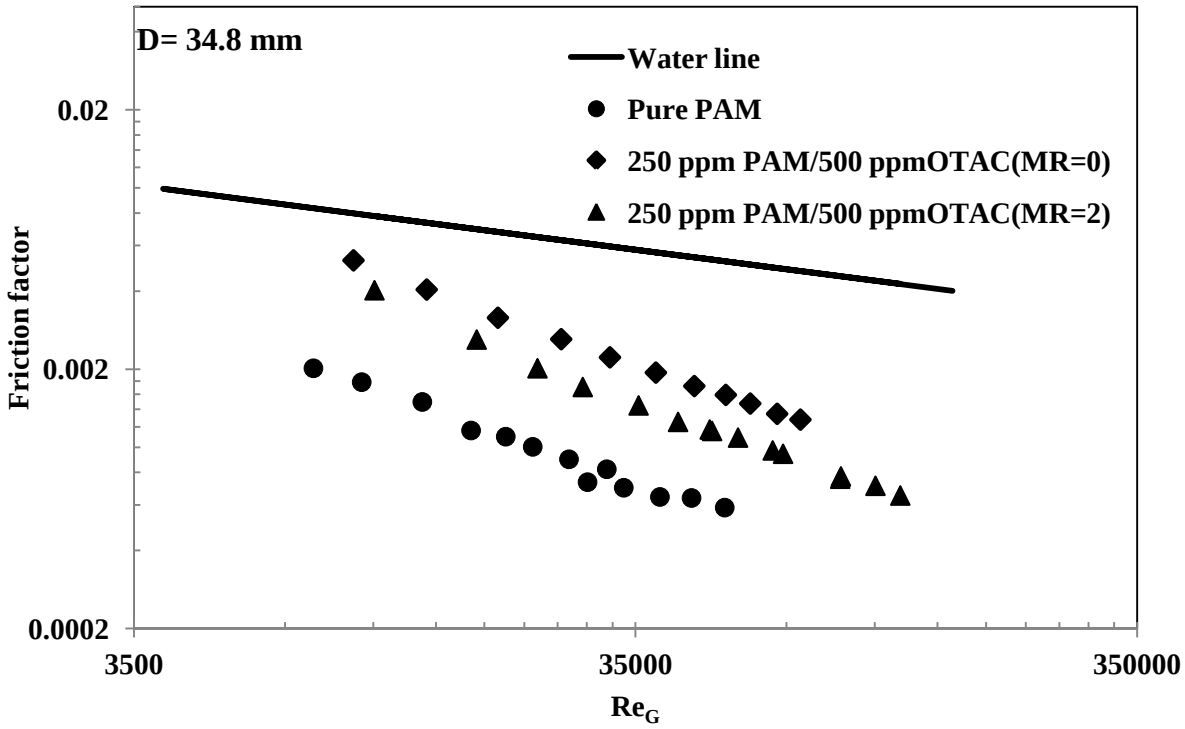

Figure 6-18: Effect of NaSal on friction factor of 250 ppm PAM / 500 ppm OTAC in DI

Figure 6-19 shows same system shown in Figure 6-18 after 30 hr. The hat seems that the presence of salt can cause a relative stability against shear degradation compare to PAM / OTAC solution. This system still has no preference in comparison to pure PAM against degradation which gives lower friction factor and better DR after 30 hr.

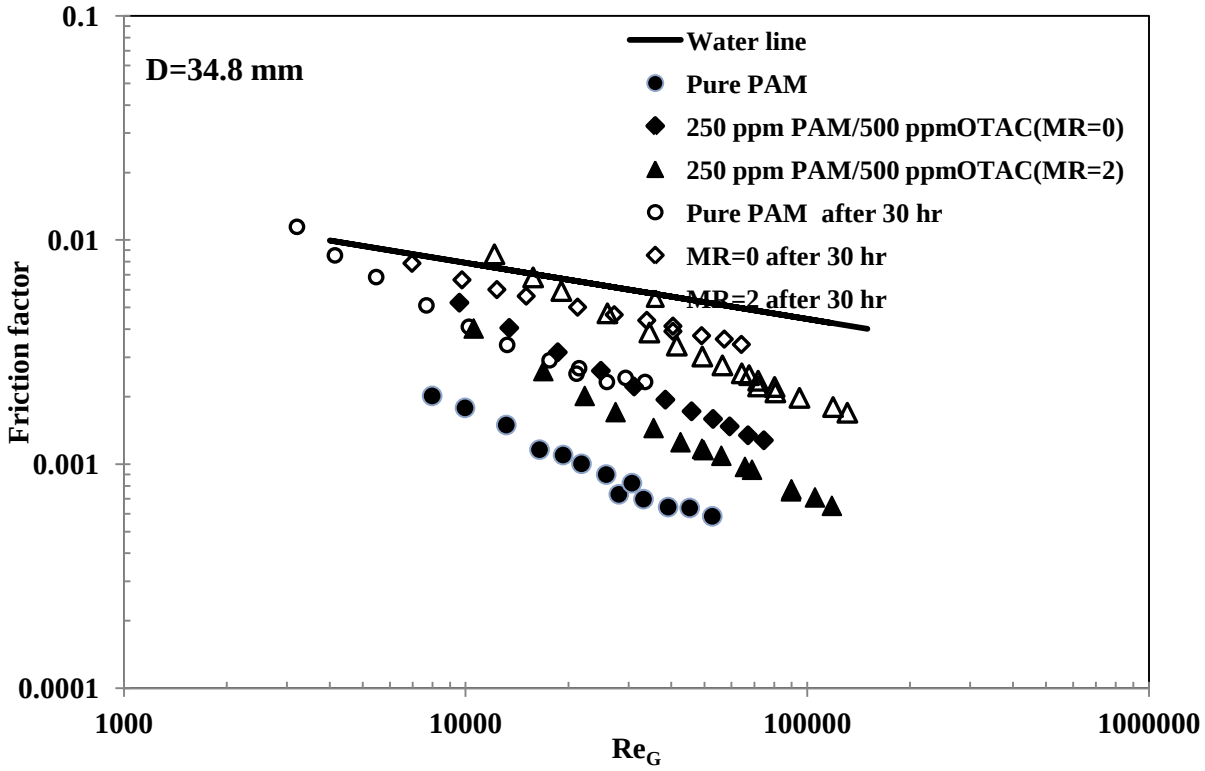

Figure 6-19: Effect of degradation on friction factor of 250 ppm PAM / 500 ppm OTAC in DI water after 30 hr degradation

6.2.2 Solution in tap water

6.2.2.1 Effect of OTAC concentration

In Chapter 5 a complete comparison was done on drag reduction for pure PAM in tap and DI water. Some experiments using tap water as solvent were conducted for different PAM / OTAC systems. With regards to the bench-scale results it would be expected to observe lower DR for PAM / OTAC in tap water in comparison to DI water.

Figure 6-20 shows the effect of OTAC concentration on drag reduction behaviour of 500 ppm PAM solution in tap water. The OTAC concentration is varied from 100 ppm to 800 ppm. The surfactant has negligible effect on the drag reduction behaviour of polymer solution. The friction factor at any given Re_G has the same value regardless of the

concentration of OTAC. Since tap water is a poor solvent for the anionic PAM, the PAM chains in tap water are already collapsed. The addition of a high concentration of OTAC (800 ppm OTAC) is expected to cause further shrinkage of anionic PAM chains, but it seems that the degree of shrinkage due to OTAC addition is not large. Therefore, little change in the drag reduction ability of 500 ppm PAM in tap water is observed upon addition of OTAC.

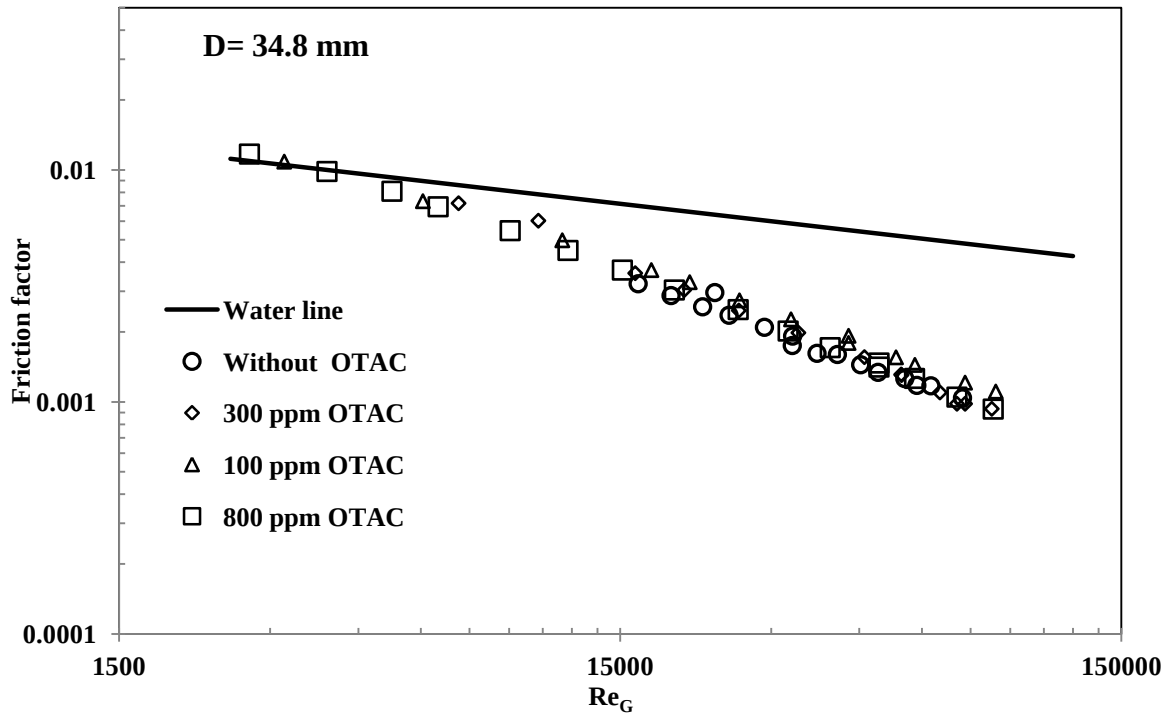

Figure 6-20: Friction factor vs. Reynolds number for 500 ppm PAM and different amount of OTAC

Figure 6-21 summarizes the effect of OTAC addition on the drag reduction behaviour of PAM solutions in tap water. This graph shows friction factor vs. Reynolds number data for three PAM concentrations of 100ppm, 250 ppm and 500 ppm, with and without OTAC addition. Hollow points show the data with OTAC and solid points are data without OTAC. For any given PAM concentration, the friction factor values are almost the same with and without OTAC.

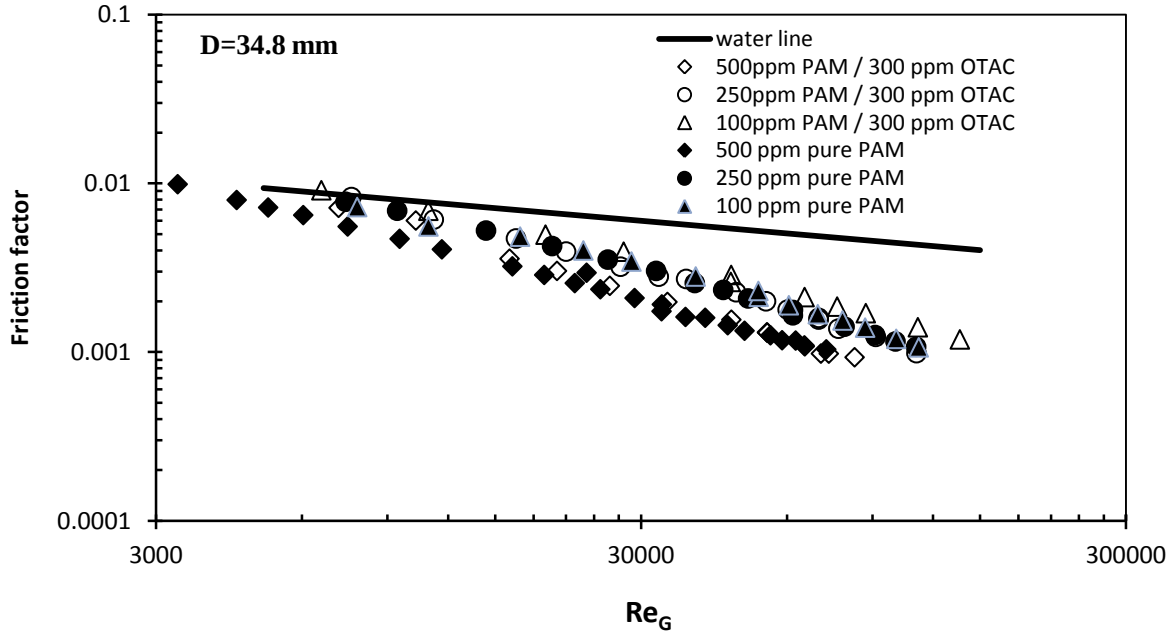

Figure 6-21: Friction factor vs. Re_G for different solutions of PAM with 300 ppm of OTAC

6.2.2.2 Mechanical degradation

Figure 6-22 shows %DR versus time for different concentrations of pure PAM in tap water. DR behavior of the pure PAM in tap water, exhibits the same behavior as the PAM / OTAC solutions in DI water. This similarity is much more evident for higher OTAC concentrations. It means that PAM macromolecules are already collapsed in tap water and not much more coiling is expected to happen upon addition of OTAC monomers.

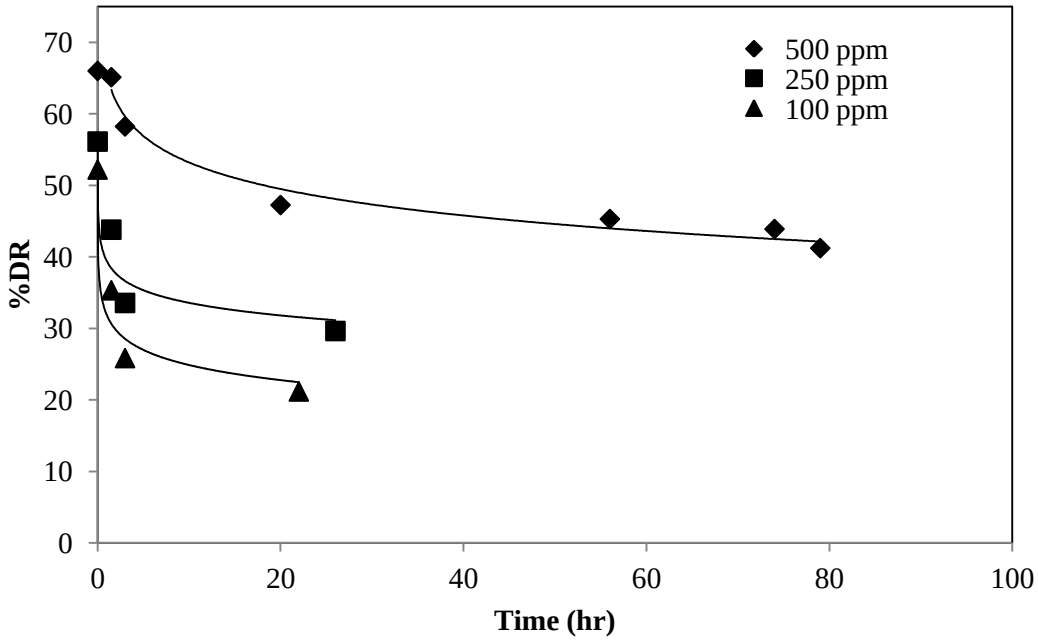

Figure 6-22: %DR vs. time for pure PAM in tap water

Power law parameters have been tabulated in Table 6-2 for 500 ppm PAM /OTAC system. The addition of 100 ppm OTAC slightly increases the value of n. No more change in n and k index was observed for higher OTAC amounts. These results are compatible with other results.

Table 6-2: Power law parameters for 500 ppm PAM in tap water

OTAC(ppm)	k	n	R^2
0	0.1726	0.7278	0.9994
100	0.1299	0.7497	0.9849
300	0.1299	0.7497	0.9849
800	0.1299	0.7497	0.9849

Figure 6-23 shows friction factor versus Reynolds number for 500 ppm PAM / OTAC solutions after 70 hr in tap water. This graph depicts that 500 ppm PAM/ OTAC solutions in tap water lose their drag reduction capability at the same rate as pure 500 PAM in tap water. Same trend was observed for other pipe diameters.

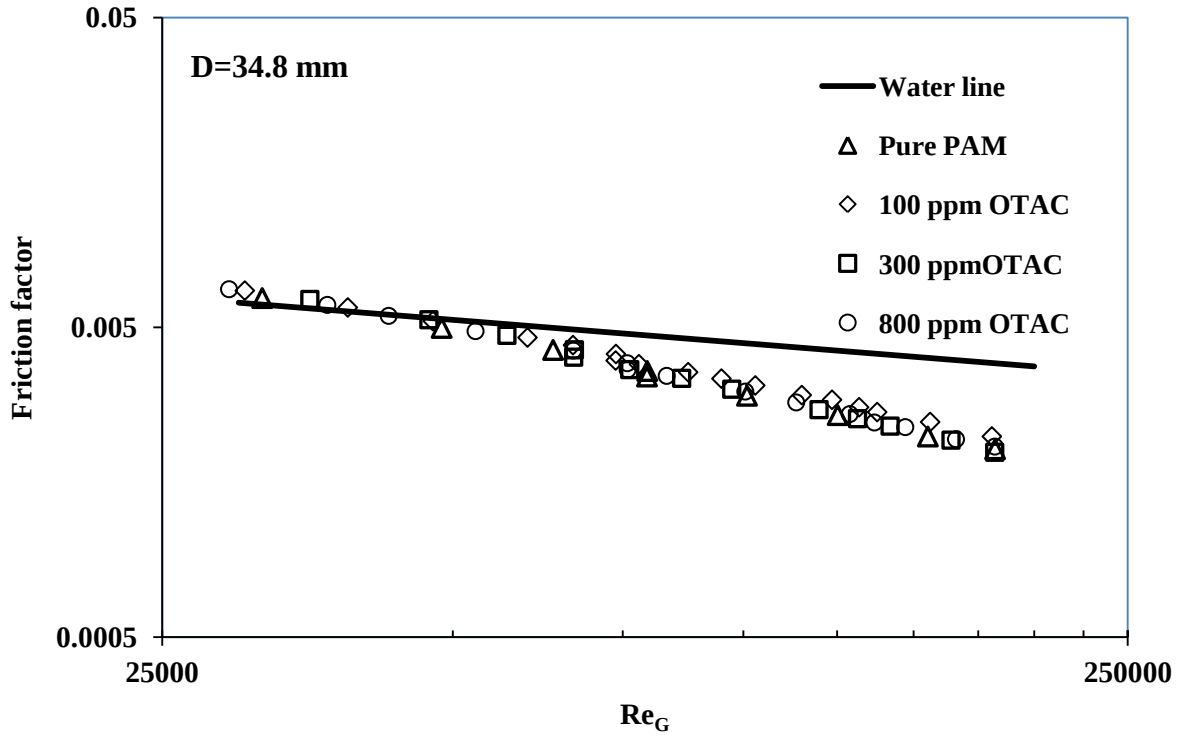

Figure 6-23: Friction factor vs. Re_G for 500 ppm PAM / OTAC solutions after 70 hr in tap water

6.3 Summary

The synergistic effects of combined polymer-surfactant were experimentally investigated for the purpose of drag reduction. The interactions between polyacrylamide (as an anionic drag reducer polymer) and octadecyltrimethylammonium chloride (as a cationic surfactant) were studied in DI and Tap water. The following conclusions can be drawn from this experimental work:

- Strong interactions occur between PAM and OTAC molecules. The CMC (critical micelle concentration) of surfactant increases in the presence of PAM due to the transfer of OTAC molecules to oppositely charged PAM chains.

- At high PAM concentrations, PAM chains are less accessible to OTAC molecules due to the formation of an interconnected network of polymer chains. Consequently, the surfactant is less effective in neutralizing the polymer chains at high PAM concentrations.
- The charge neutralization of polymer chains by OTAC molecules render the polymer chains less polar and insoluble in DI water. Consequently, the drag reduction capability of PAM is reduced upon the addition of OTAC. At high PAM concentrations, the effect of surfactant on drag reduction behaviour becomes less due to inaccessibility of PAM chains to surfactant molecules.
- The presence of cations in tap water makes the tap water a poor solvent for PAM compared with DI water. The addition of OTAC to PAM solutions in tap water causes further shrinkage of anionic PAM chains but the degree of shrinkage is not large. Therefore, little change in the drag reduction ability of PAM/tap-water solutions takes place upon the addition of OTAC.

Chapter 7
Interaction of Cationic Surfactant (OTAC) with Nonionic Polymer (PEO)

Same procedure as section Bench Scale 4.1 was used for the bench- scale experiments. All the bench scale and pipeline flow experiment were done at 25^{o}C±0.5.

7.1 Bench Scale Results

7.1.1 Viscosity

The low shear relative viscosity of mixed polymer-surfactant system as a function of OTAC concentration is shown in Figure 7-1. The relative viscosity for 500 ppm PEO system first increases with the addition of small amount (100 ppm) of OTAC and then becomes constant with further increase in surfactant concentration up to 1000 ppm. The increase in relative viscosity beyond this point (1000 ppm) can be attributed to the formation of free micelles in the solution. In the case of 1000 ppm PEO system, the relative viscosity is almost constant up to a surfactant concentration of 800 ppm. With further increase in surfactant concentration, the relative viscosity exhibits a minimum and then it continues to increase. The increase in relative viscosity at high OTAC concentrations is due to the formation of free micelles. The relative viscosity for 2000 ppm PEO system shows a maximum at 800 ppm OTAC. It then shows a minimum around 1000 ppm OTAC. With further increase in OTAC concentration, the relative viscosity increases due to the formation of free micelles. Similar patterns were observed by Prajapati (2009) for the same system with different molecular weight.

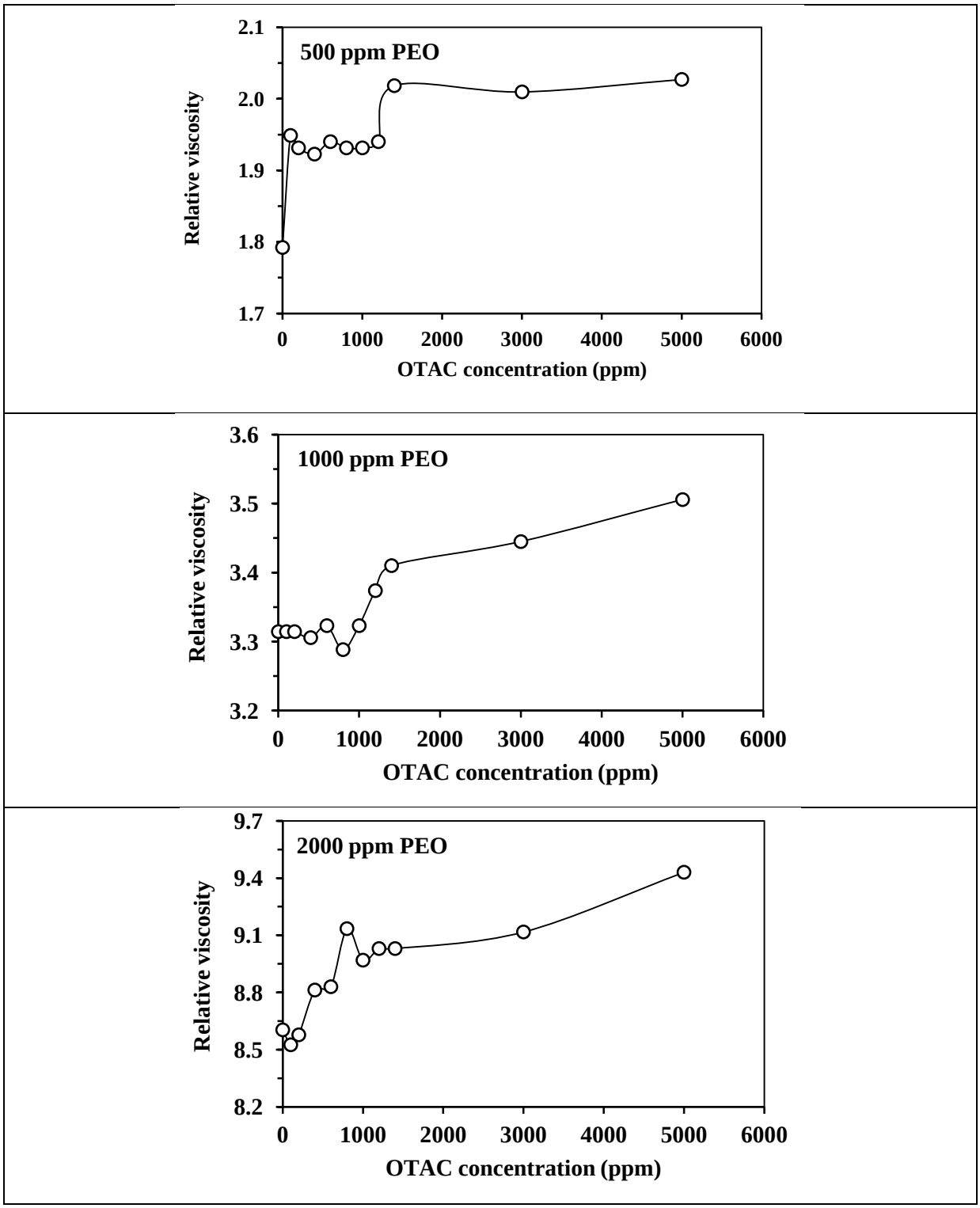

Figure 7-1 : Relative viscosity vs. OTAC concentration for PEO / OTAC + NaSal (MR=2) systems at 25°C

The overlap concentration (C*) where the polymer chains begin to overlap with each other is approximately 1500 ppm for the PEO used in the present work. When the polymer concentration is less than C*, the polymer chains are not able to reach each other to bond and form an intermolecular connection. For the 500 ppm PEO solution, the polymer concentration is less than C* and therefore, the addition of OTAC results in the formation of multiple OTAC micelles on a single polymer chain. The polymer chains undergo expansion due to electrostatic repulsion between micelles present on the same polymer chain. The expansion of the polymer chains results in an increase in the viscosity. This explanation is consistent with the necklace model proposed by Nagarjan (1980) and extended by Nilsson (Nilsson et al. 2000). When the polymer concentration is higher than C*, the intermolecular interactions become more significant. In this case, different polymer chains interact with the developing micelles on other macromolecules resulting in an increase in the intermolecular connections. Consequently, an increase in the viscosity takes place. The number of micelles in the solution increases with further addition of OTAC. Therefore, the three-dimensional intermolecular structure disappears and the relative viscosity decreases near the CMC point. The increase in relative viscosity past the CMC point is mainly due to the formation of free micelles in the solution.

7.1.2 Surface tension

Figure 7-2 shows surface tension vs. OTAC concentration for pure surfactant system (with NaSal) and mixed system (PEO / OTAC+NaSal (MR=2)). The surface tension data does not show any change in the CMC point due to the presence of polymer in the surfactant system.

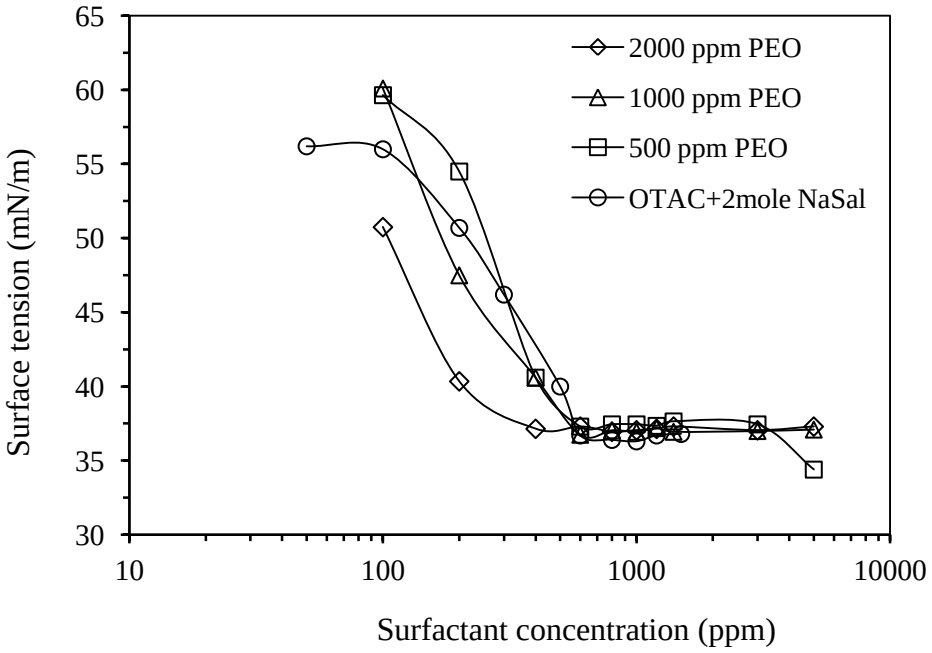

Figure 7-2: Surface tension for PEO / OTAC+ NaSal (MR=2)

7.2 Pipeline Results

7.2.1 Synergistic effect of PEO/OTAC on DR

The pipeline experiments were conducted for three levels of PEO concentration (500, 1000, and 2000 ppm) and two levels of surfactant concentration (1000 and 2500 ppm).

Figure 7-3 shows friction factor versus Re number for 500 ppm PEO / 1000 ppm OTAC +NaSal (MR=2). The slop of friction factor vs. Re_G changes for Re>150000. The data points after this Re shown by empty points.

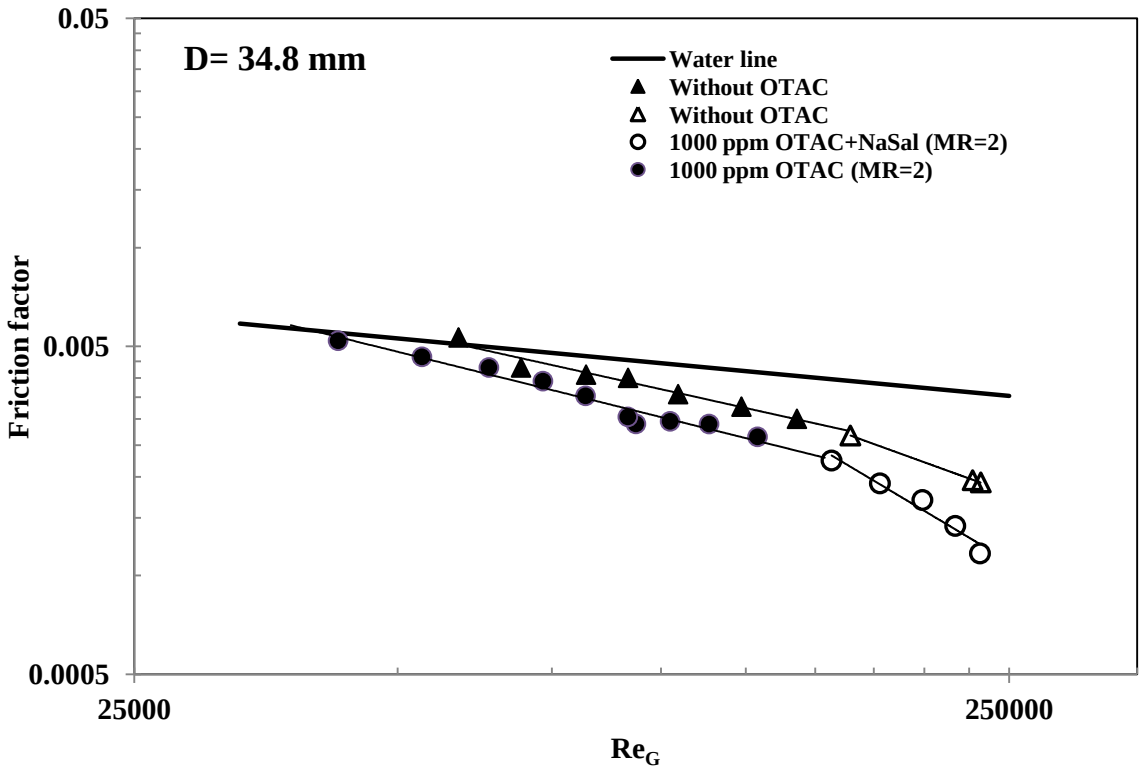

Figure 7-3: Friction factor Vs. Re_G for 500 ppm PEO / 1000 ppm OTAC +NaSal (MR=2) at 25°C

The addition of OTAC (+ NaSal) decreases the friction factor values at the same level of Re_G ;in other words, drag reduction is enhanced upon the addition of OTAC. The friction factor is lower for 500 ppm PEO /1000 ppm OTAC (MR=2) system compared with pure PEO solution at the same Re_G. Also the onset of drag reduction (see Table 7-1) occurs at a lower Re_G value for 500 ppm PEO / OTAC (MR=2) as compared with pure 500 ppm PEO.

Table 7-1: Onset of drag reduction for 500 ppm PEO / 1000ppm OTAC + NaSal (MR=2) and pure 500 ppm PEO solution

Solution	Re_G
500 ppm PEO	57740
500 pm PEO /1000 ppm OTAC (MR=2)	39850

It is interesting to note that the slope of the friction factor plot changes around Re_G =150000 for both systems (pure PEO and mixed PEO/OTAC). However, the mixed system containing OTAC has a steeper slope than that of pure PEO.

Figure 7-3 further reflects the enhancement of drag reduction upon addition of surfactant to the polymer solution. The % decrease in friction factor upon the addition of surfactant is plotted as a function of Re_G. The addition of OTAC to PEO can decrease the friction factor by as much as 35% at high Re_G.

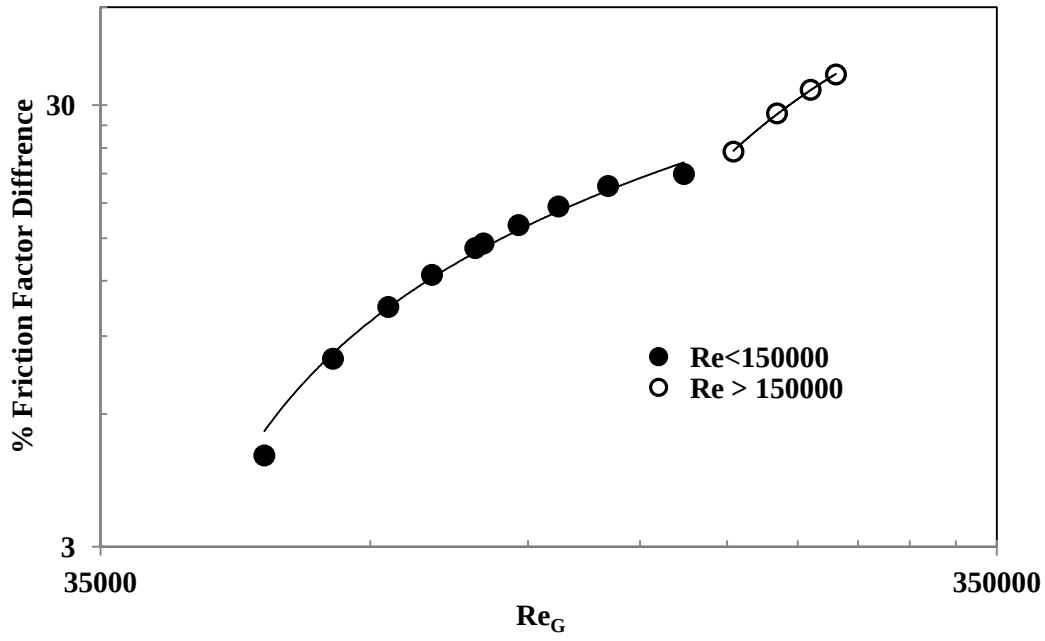

Figure 7-4: Friction factor difference between 500 ppm PEO / OTAC+NaSal (MR=2) and pure 500 ppm PEO

It should be noted that the mixed PEO and OTAC / NaSal system exhibits larger drag reduction (lower friction factors) than both of the individual systems (PEO without surfactant and OTAC/NaSal without polymer). This can be seen clearly in Figure 7-5. Thus the mixed system exhibits a good synergistic effect.

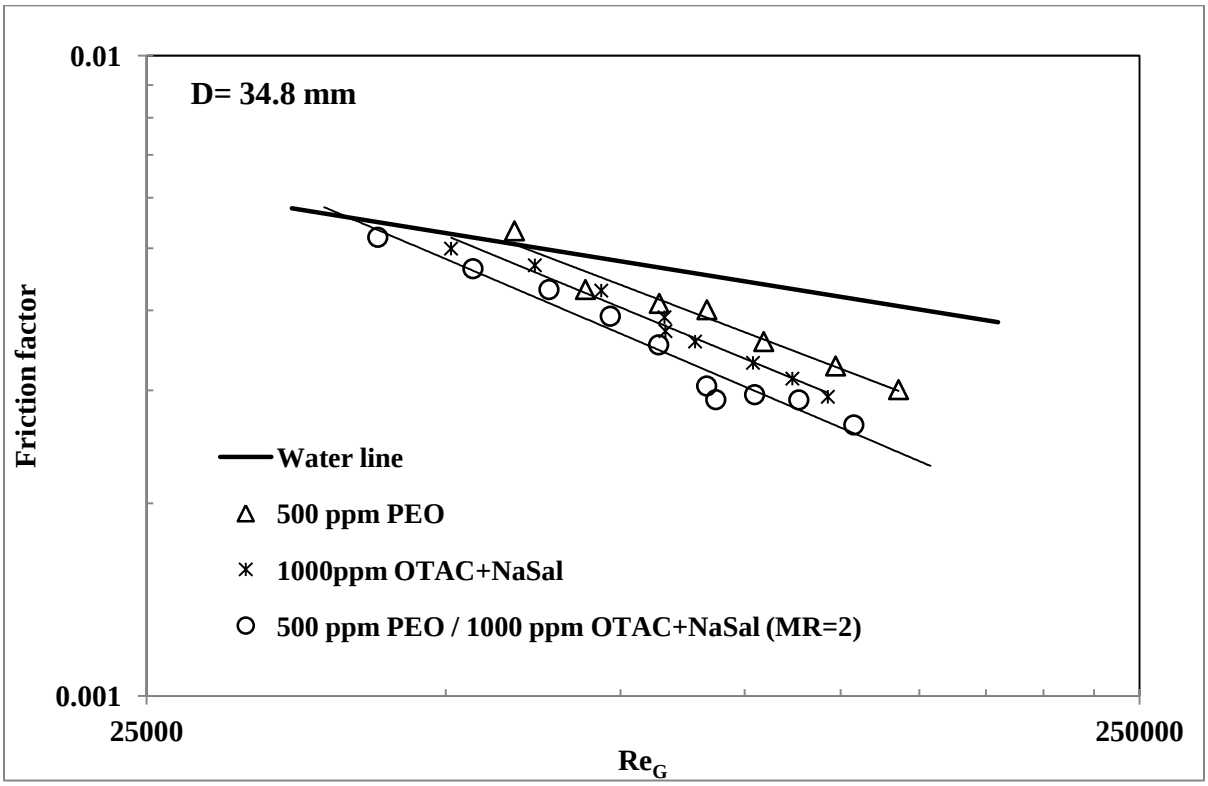

Figure 7-5: Friction factor vs. Re_G for OTAC+Nasal compare to combined PEO / OTAC and pure PEO

The synergy between polymer and surfactant in reducing drag could be due to the formation of a new shear-induced state (SIS) in mixed polymer-surfactant systems under turbulent conditions. It is entirely possible that in turbulent flow, the cylindrical micelles of the surfactant become attached to the back bone of polymer chains and form a three dimensional interconnected network structure possessing viscoelastic properties and hence resulting in suppression of turbulence. Figure 7-6 shows schematically the evolution of the microstructure with the increase in shear stress.

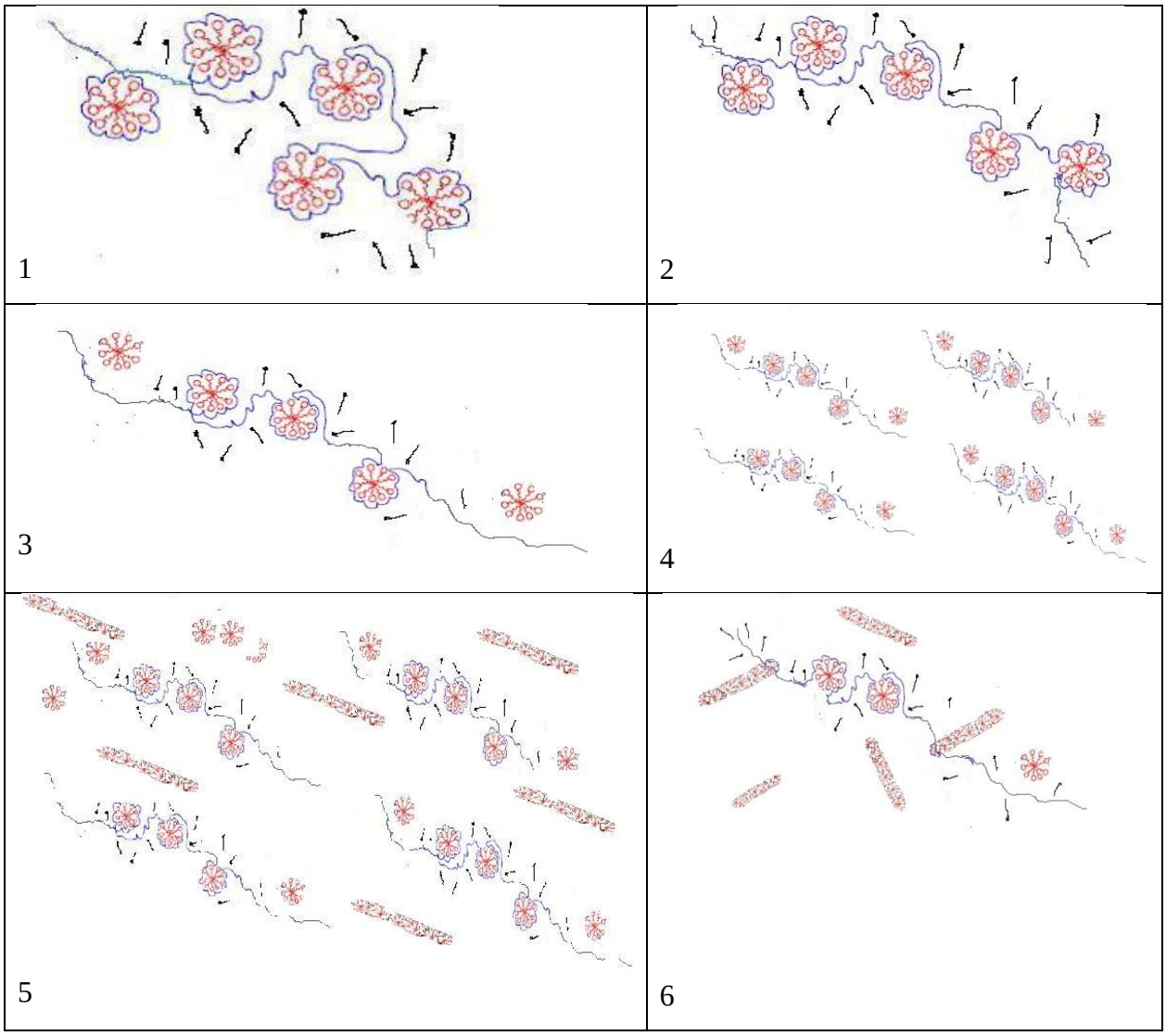

Figure 7-6: Proposed model for new microstructure formed by increasing shear stress

According to the proposed microstructure, the increase in the length of the cylindrical micelles is expected to impart more flexibility and viscoelasticity to the solution. One way to increase the micelle length is to increase the surfactant concentration. For this reason, a new set of experiments was conducted using the same polymer concentration (500 ppm) and a higher surfactant concentration of 2500 ppm OTAC + NaSal (MR=2). Figure 7-7 shows variations of friction factor and drag reduction (DR) with Re_G for the pure and mixed polymer/surfactant systems. With the increase in the surfactant concentration, an increase in the synergistic effect is clearly observed (also see Figure 7-5).

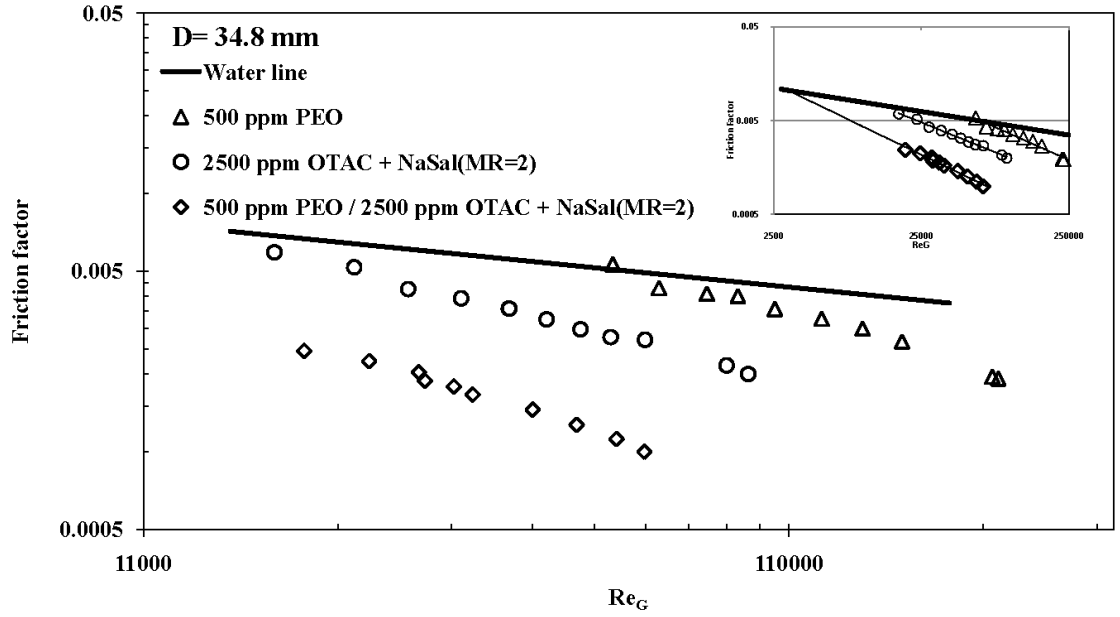

a) Friction factor vs. Re_G

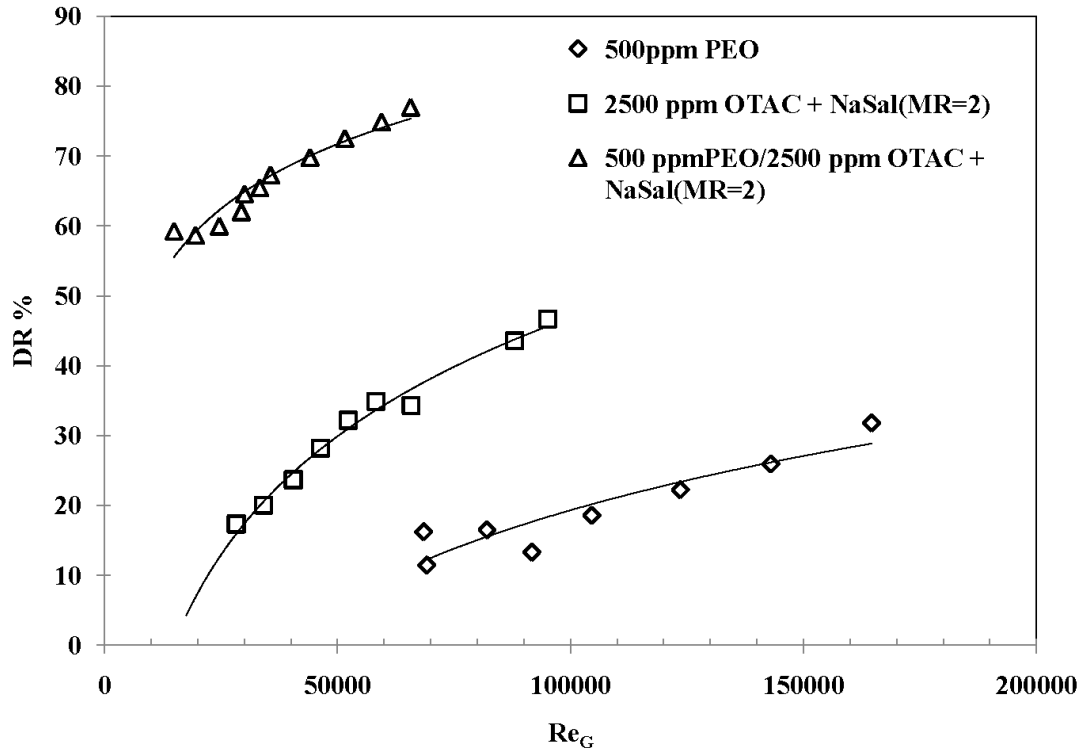

b) %DR vs. Re_G

Figure 7-7: Friction factor and %DR vs. Re_G for solution of 500 ppm PEO / 2500 ppm OTAC + NaSal (MR=2) compare to pure 500 ppm PEO solution and 2500 ppm OTAC + NaSal (MR=2) solution

Table 7-2 shows the % Friction Factor Difference between 2500ppm OTAC+ NaSal (MR=2) PEO and 500 ppm PEO/ 2500 ppm OTAC+NaSal (MR=2) for Re_G in the turbulent flow regime. The average difference is almost 58.1%. In other words, the friction factor is reduced by about 59% upon addition of surfactant to the polymer. This table was prepared using the best fitted curve on friction factor data. Most of this huge difference in friction factor data can be attributed to forming a new structure during the interaction between PEO and OTAC.

Table 7-2: Friction factor difference between (2500ppm OTAC+NaSal (MR=2)) and (500 ppm PEO/ 2500 ppm OTAC+NaSal (MR=2))

Re_G	Friction Factor		Friction factor difference percentage (%)
	2500ppm OTAC+NaSal (MR=2)	500 ppm PEO /2500ppm OTAC+NaSal (MR=2)	
30000	0.004266	0.001886	55.8
35000	0.003869	0.001678	56.6
40000	0.003555	0.001517	57.3
45000	0.003299	0.001387	58.0
50000	0.003086	0.001281	58.5
55000	0.002905	0.001191	59.0
60000	0.002749	0.001115	59.4
65000	0.002613	0.00105	59.8
		Average	**58.1**

Figure 7-8 shows friction factor and %DR versus Re_G for 1000 ppm PEO / 1000 ppm OTAC + NaSal (MR=2). For this combination of polymer and surfactant concentrations the interaction is not strong enough to result in a significant increase in drag reduction.

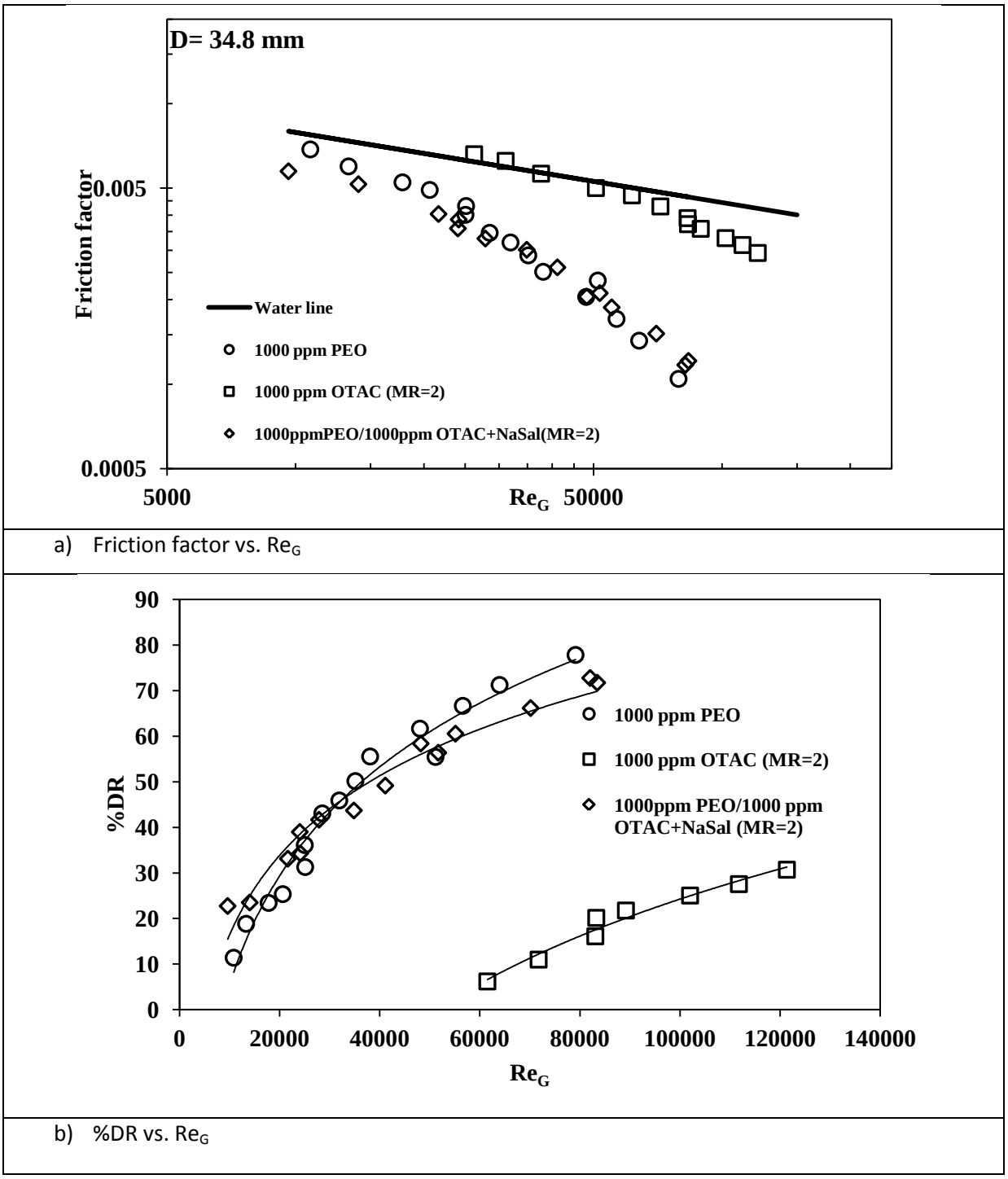

Figure 7-8: Friction factor and %DR vs. Re_G for 1000 ppm PEO / 1000 ppm OTAC + NaSal (MR=2) compared to pure 1000 ppm PEO solution and 1000 ppm OTAC + NaSal (MR=2) solution

A significant increase in drag reduction occurs when the surfactant concentration is increased from 1000 to 2500 ppm OTAC (see Figure 7-9) for the same polymer concentration of 1000 ppm. Also note that the onset of drag reduction is changed from Re_G of ~10000 for pure 1000 ppm PEO to ~4000 for the new combination. The improvement in %DR over the pure polymer solution in the present case is about 10 to 15 percent. As mentioned earlier, when the OTAC concentration is 2500 ppm, it is more likely to form rod-like micelles. These micelles interact with the polymer chains in turbulent flow to form a three-dimensional microstructure possessing viscoelastic properties and resulting in enhanced drag reduction

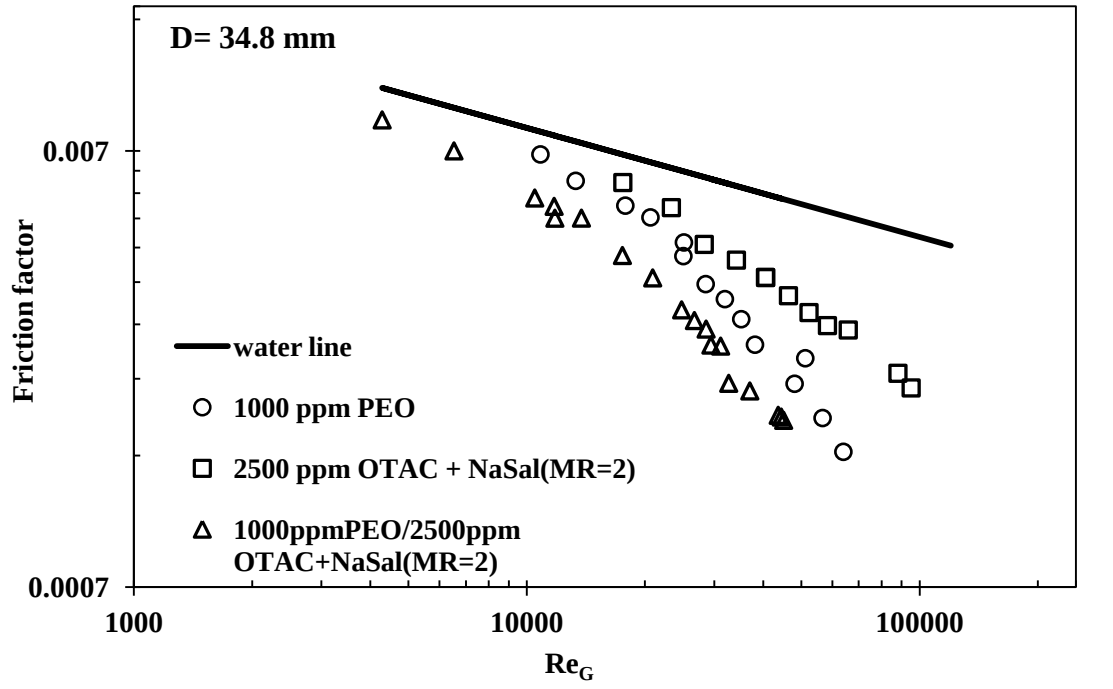

a) Friction factor vs. Re_G

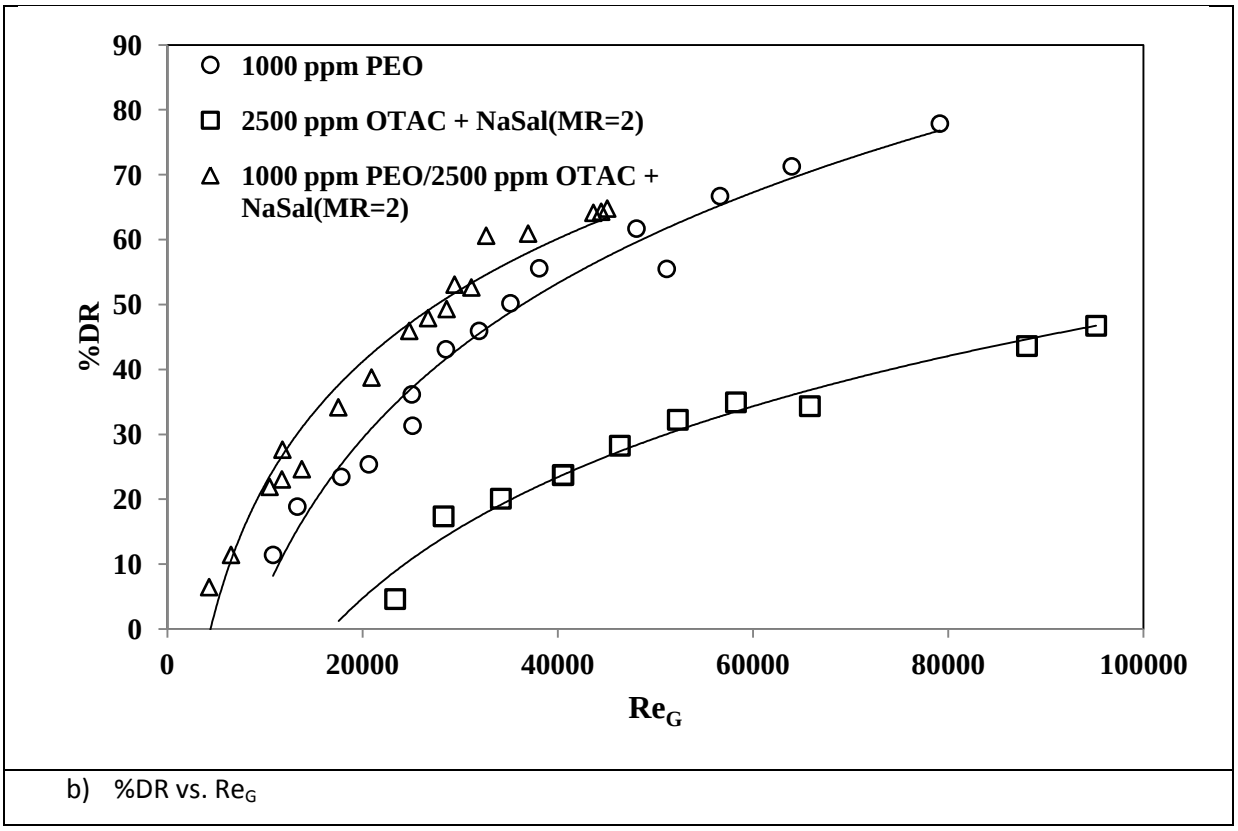

b) %DR vs. Re_G

Figure 7-9: Friction factor and %DR vs. Re for 1000 ppm PEO / 1000 ppm OTAC + NaSal (MR=2) compared to pure 1000 ppm PEO solution and 2500 ppm OTAC + NaSal (MR=2) solution

Figure 7-10 shows the friction factor vs. Re_G data for the mixed system consisting of 2000 ppm PEO/1000 ppm OTAC + NaSal (MR=2), and for the corresponding pure systems (2000 ppm PEO and 1000 OTAC/NaSal(MR=2)). Once again a good synergy is observed between the polymer and the surfactant in reducing the drag. The drag reduction behavior of the system also changes from Type A to Type B upon the addition of surfactant to the polymer.

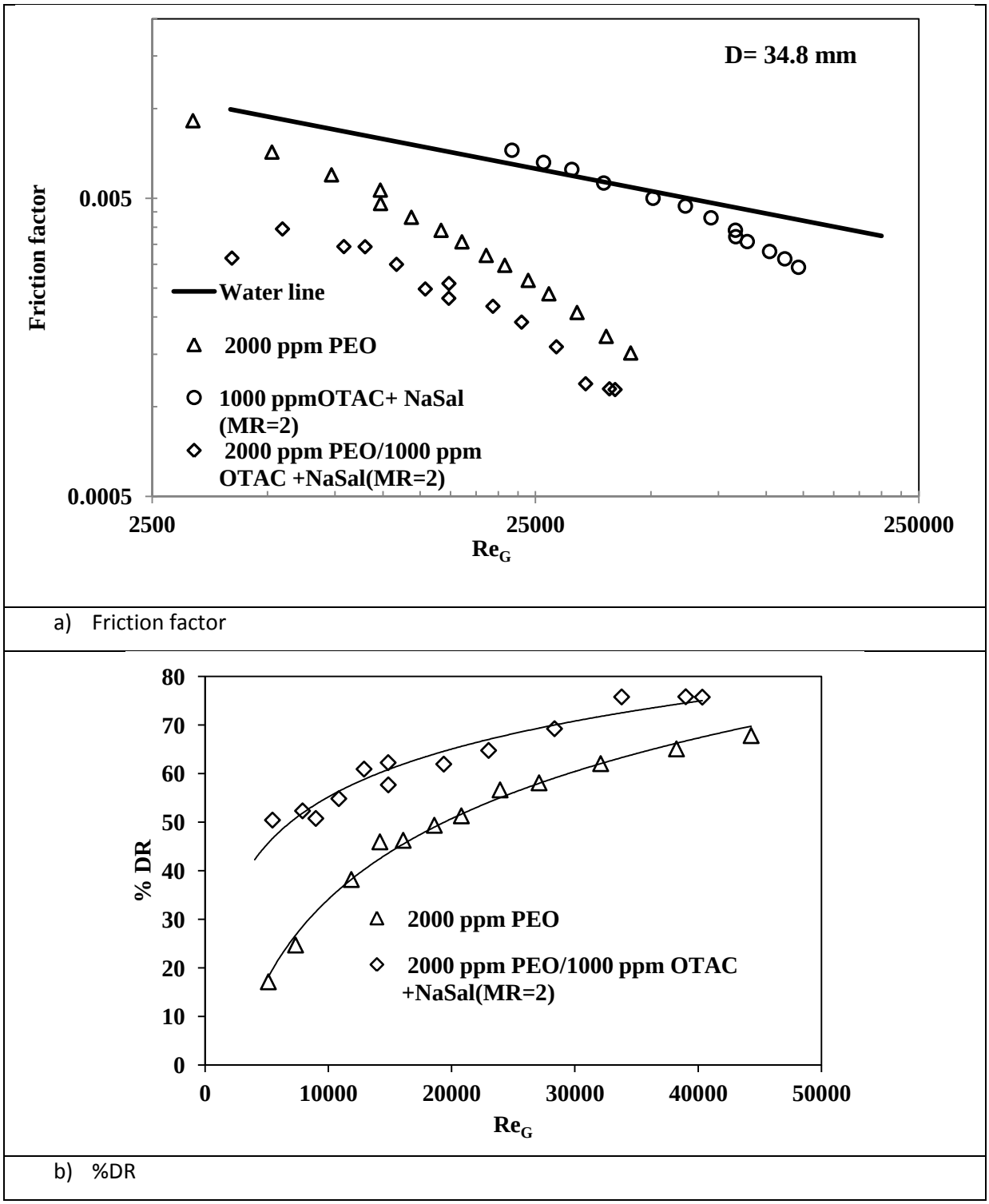

Figure 7-10: Friction factor and %DR vs. Re_G for 2000 ppm PEO/1000 ppm OTAC + NaSal (MR=2)

The percent friction factor difference between pure 2000 ppm PEO and 2000 ppm PEO/ 1000 ppm OTAC+NaSal (MR=2) is given in Table 7-3 for different Re_G numbers in the turbulent flow regime. The average decrease in friction factor upon the addition of surfactant to the polymer is approximately 35%.

Table 7-3: Friction factor difference between pure 2000ppm PEO and 2000 ppm PEO/ 1000 ppm OTAC+NaSal (MR=2)

Re_G	Friction factor		Friction factor different percentage (%)
	2000 ppm PEO	2000ppmPEO/ OTAC+NaSal (MR=2)	
8000	0.005514	0.003682	33.22146
10000	0.004728	0.003141	33.56331
15000	0.003576	0.002353	34.18
20000	0.002933	0.001918	34.61407
25000	0.002515	0.001636	34.94879
30000	0.002218	0.001437	35.22101
35000	0.001994	0.001287	35.45027
40000	0.001819	0.001171	35.64822
		Average difference	**34.60589**

Figure 7-11 shows the effect of surfactant concentration on the friction factor and drag reduction behavior for the mixed surfactant-polymer system with 2000ppm PEO. With the increase in the surfactant concentration, the friction factor decreases and the percent drag reduction increases.

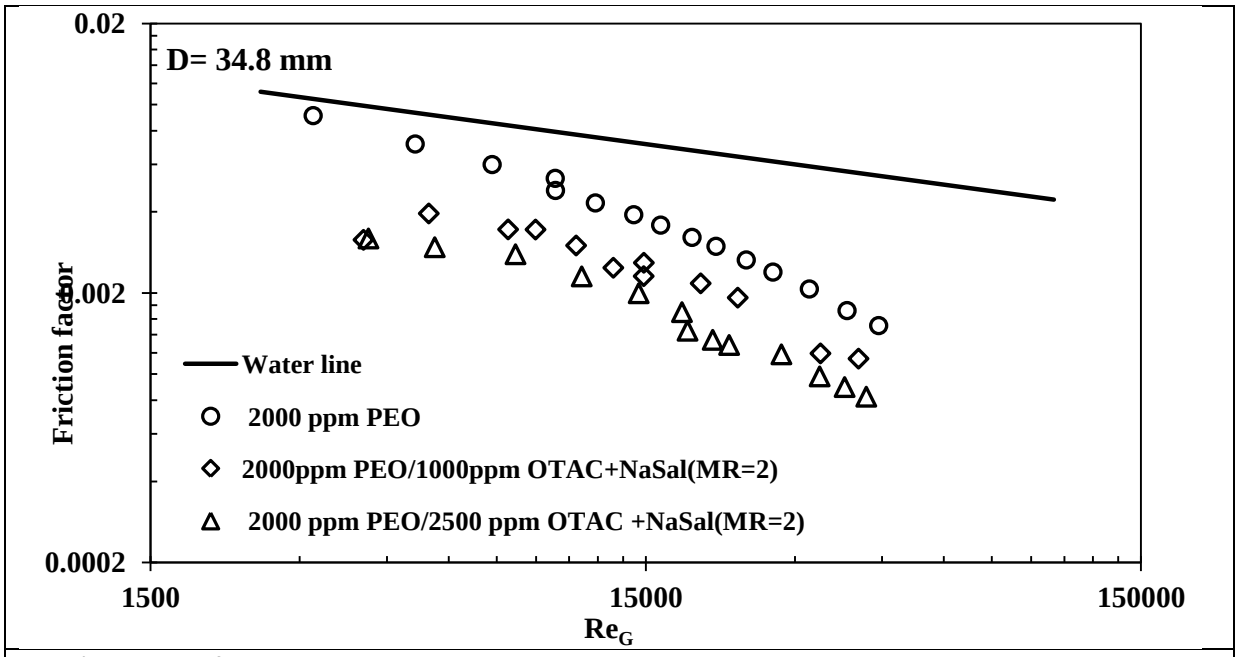

a) Friction factor

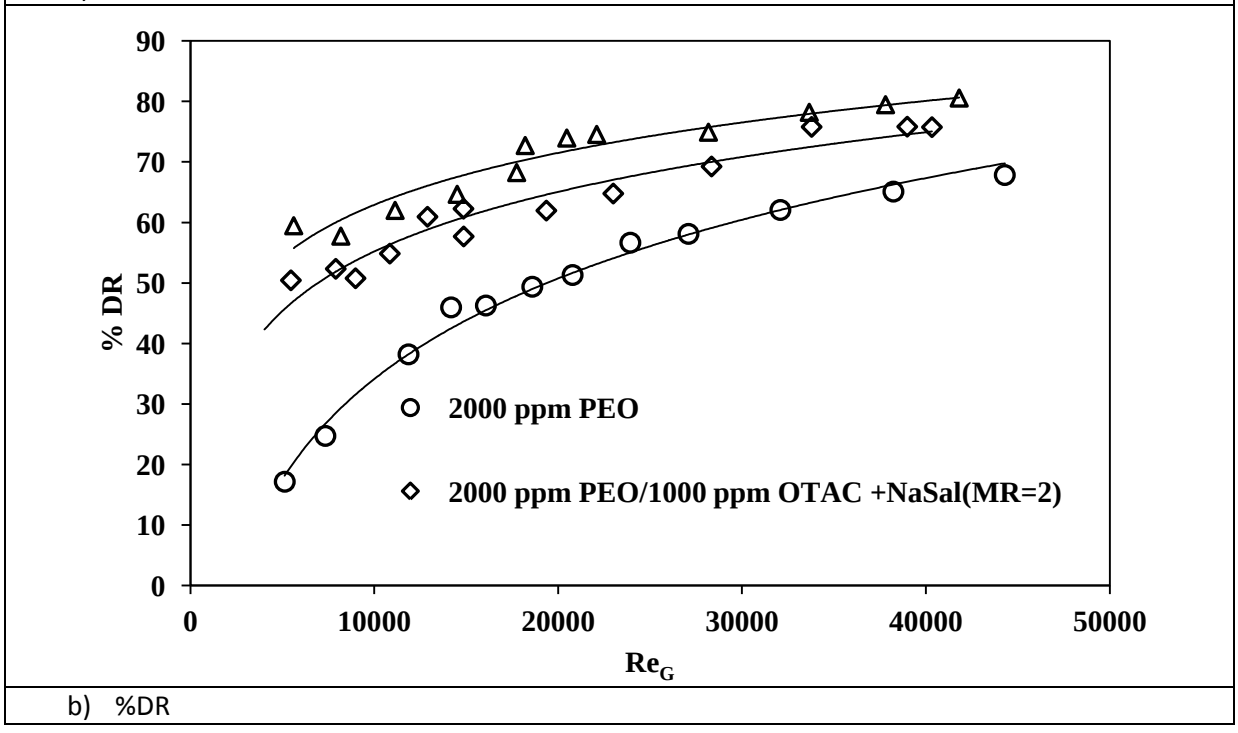

b) %DR

Figure 7-11: Friction factor and %DR vs. Re_G for different PEO/OTAC mixtures

7.2.2 Mechanical degradation of mixture of PEO and OTAC

Figure 7-12 shows the effect of degradation on %DR for 500 ppm PEO/1000 ppm OTAC + NaSal (MR=2) compared with pure 500ppm PEO after 3hr. The mixture loses almost 35-45% of its original drag reduction ability after 3hr whereas the pure PEO almost loses 85% of its DR ability after the same time.

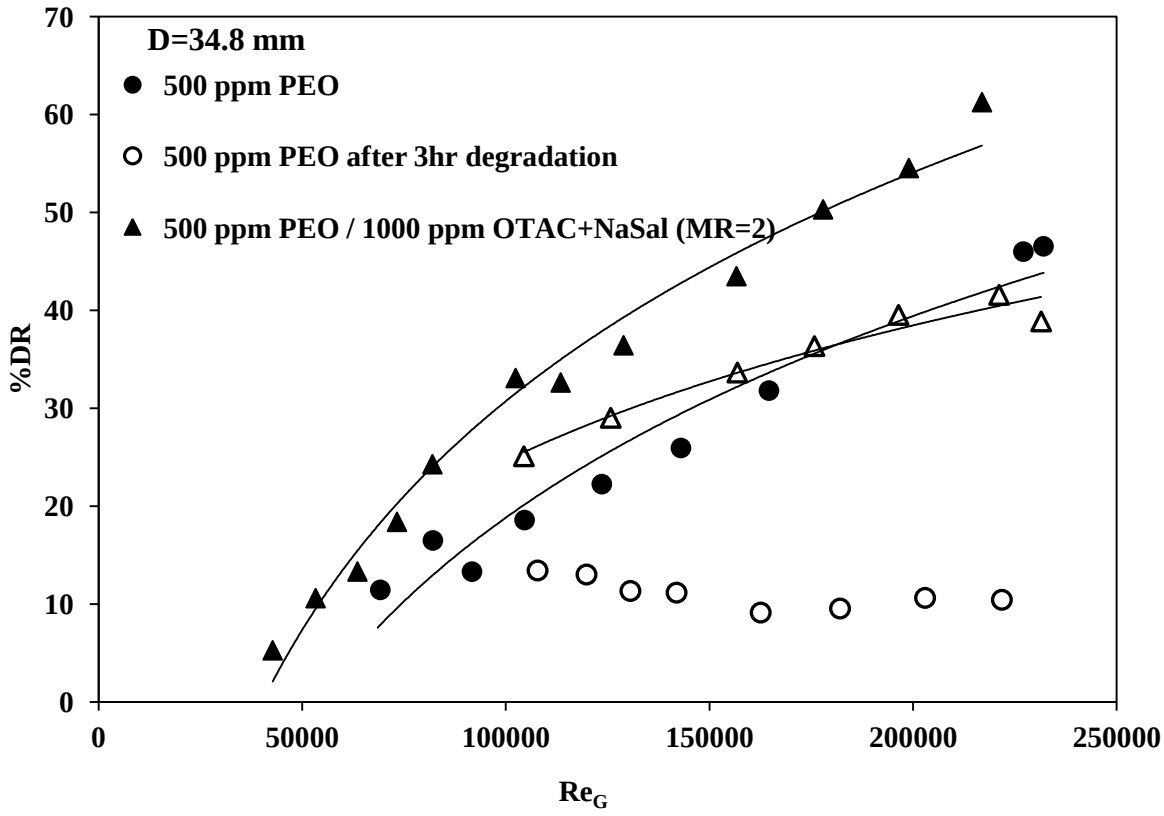

Figure 7-12: Effect of PEO degradation on DR of PEO/OTAC

It seems that the addition of OTAC can delay degradation of PEO in DI water. When the OTAC concentration is increased to 2500 ppm, PEO shows more resistance against shear degradation (i.e.; mixture shows more %DR at the same time compared to pure PEO) and the effect is more pronounced (Figure 7-13).

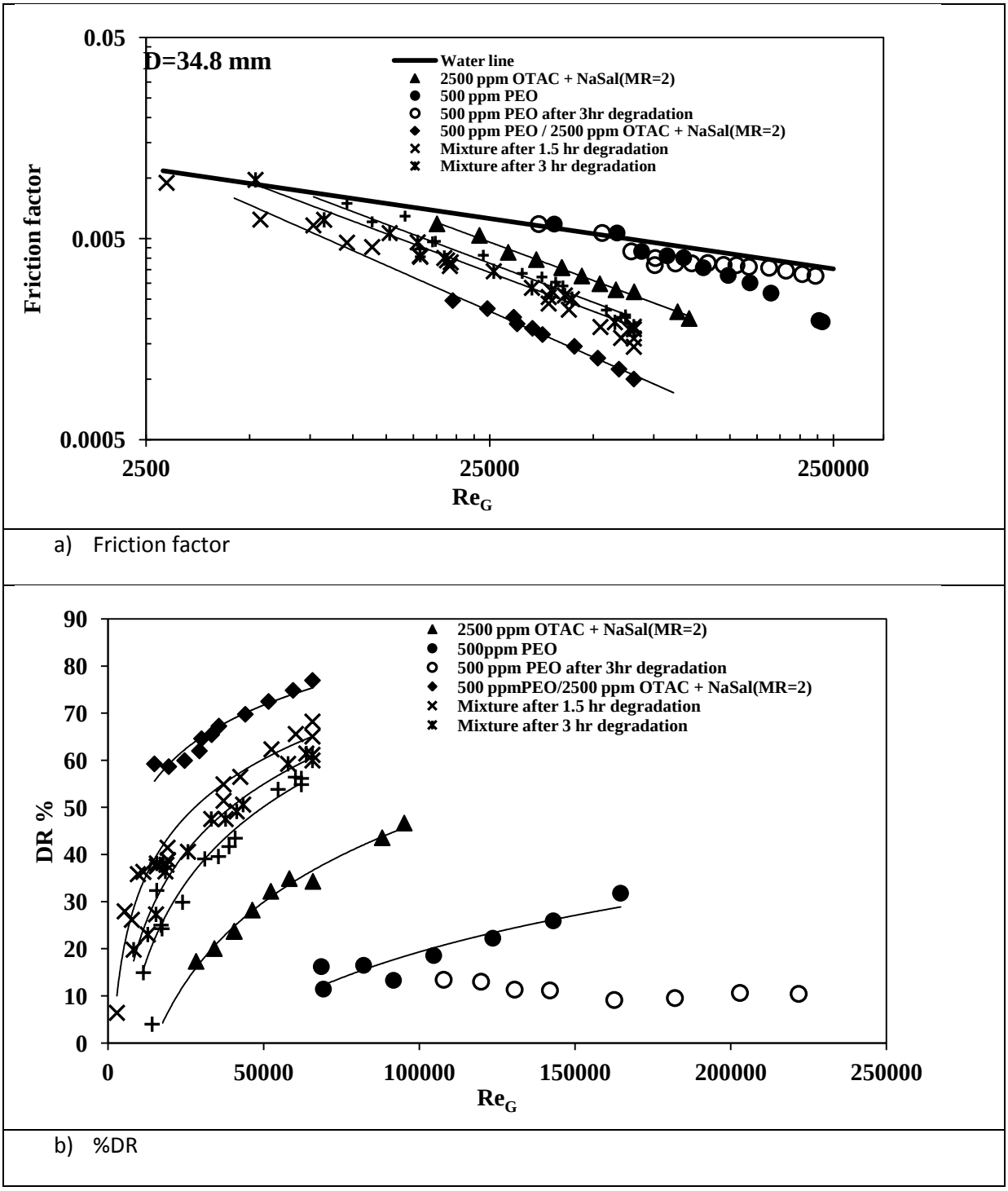

Figure 7-13: Effect of degradation on friction factor and %DR for mixture of PEO/OTAC compared with corresponding pure system

Table 7-4 shows average lost of %DR ability of this system after 3 and 24 hr continuous degradation. While pure 500 ppm PEO almost loses its %DR ability (i.e.; %DR is negligible) after 3hr, the mixture of this solution with OTAC /NaSal (MR=2) just loses ~%17 of its DR ability. The mixture shows ~70% of original %DR (~%30 lost) after 24 hr. This amount is even higher than %DR capability of OTAC/NaSal (MR=2). This means that the new structure can stabilize the polymer and postpone the degradation of PEO.

Table 7-4: %DR capability lost for mixture of 500ppmPEO/2500ppm OTAC+NaSal (MR=2)

Re_G	Lost percentage in DR of mixture after 3 hr	Lost percentage in DR of mixture after 24 hr
30000	21.0	41.1
35000	19.4	37.5
40000	18.0	34.6
45000	16.9	32.2
50000	16.0	30.1
55000	15.1	28.3
60000	14.4	26.7
Average lost	**17.3**	**32.9**

Figure 7-14 shows friction factor vs. Re_G for 1000 ppm PEO combined with 1000ppmOTAC/NaSal (MR=2). The friction factor data was compared at start of experiment and after 3 hr degradation. The trends are almost the same except that the mixture shows a small break in friction factor and fall on OTAC system data line for lower Re_G. The result is consistent for this system as no considerable increase in %DR was observed for this mixture compared with corresponding pure polymer and surfactant solution.

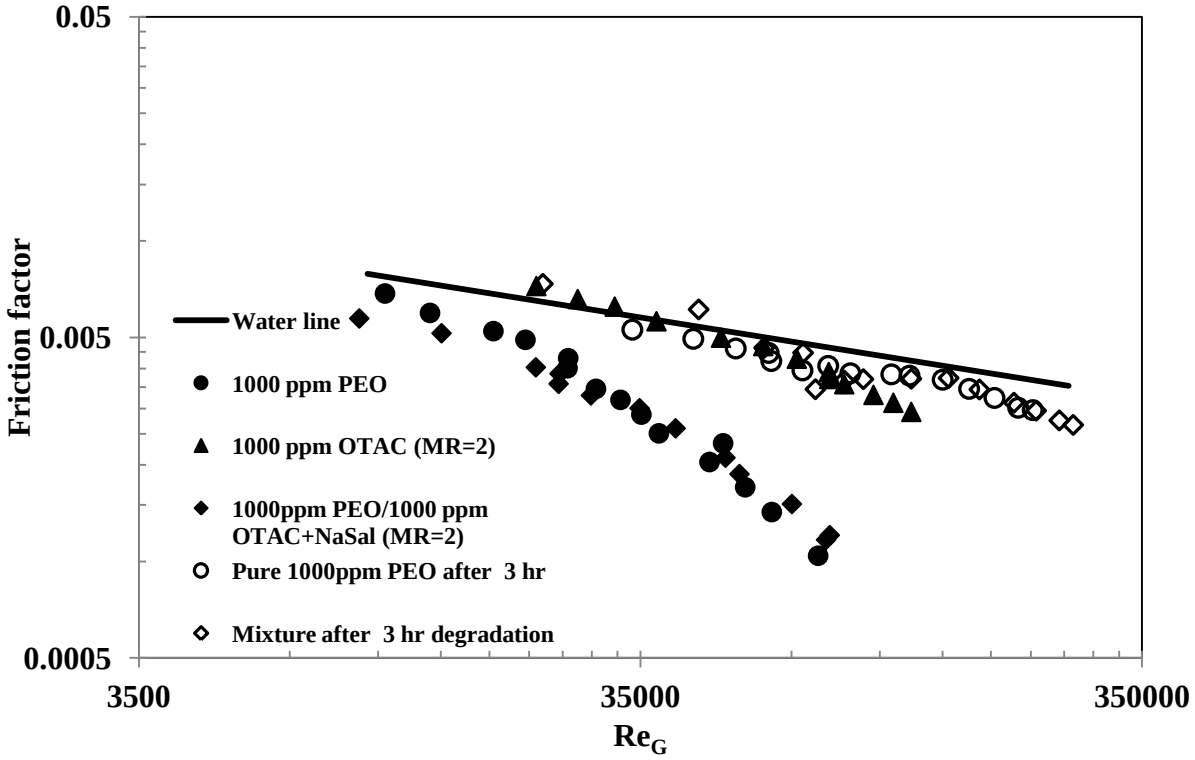

Figure 7-14: Effect of mechanical degradation of friction factor for PEO/OTAC System along with pure PEO solution

For 2000 ppm PEO resistance against mechanical degradation was improved by addition of OTAC system into the pure PEO solution. This improvement is remarkable but is not as much as the amount observed in the case of 500ppm PEO /2500ppm OTAC (see Figure 7-15).

As a whole OTAC can improve the properties of solution (such as hydrodynamic radius) to better resist against mechanical degradation compared with that of the pure polymer solution. As mentioned earlier in this chapter, OTAC micelles which attached to the backbone of polymer chains can cause those chains to be further extended. Polymers with extended chains are more resistant to mechanical degradation

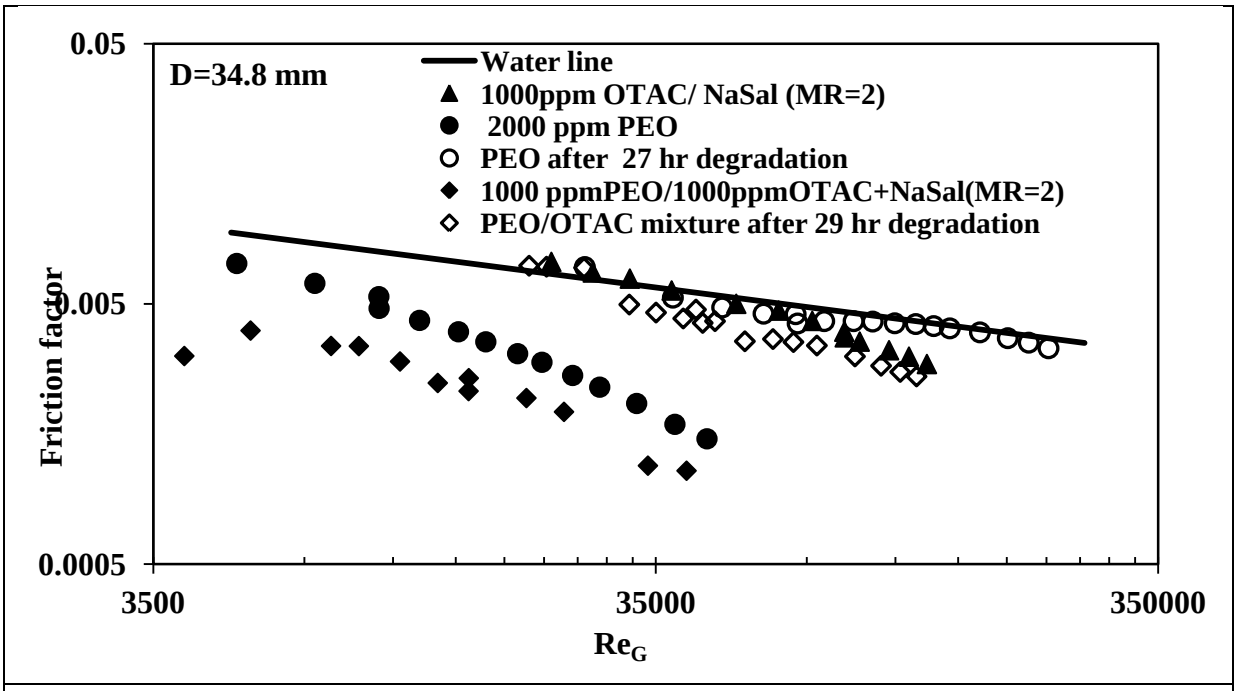

a) Friction factor vs. Re_G

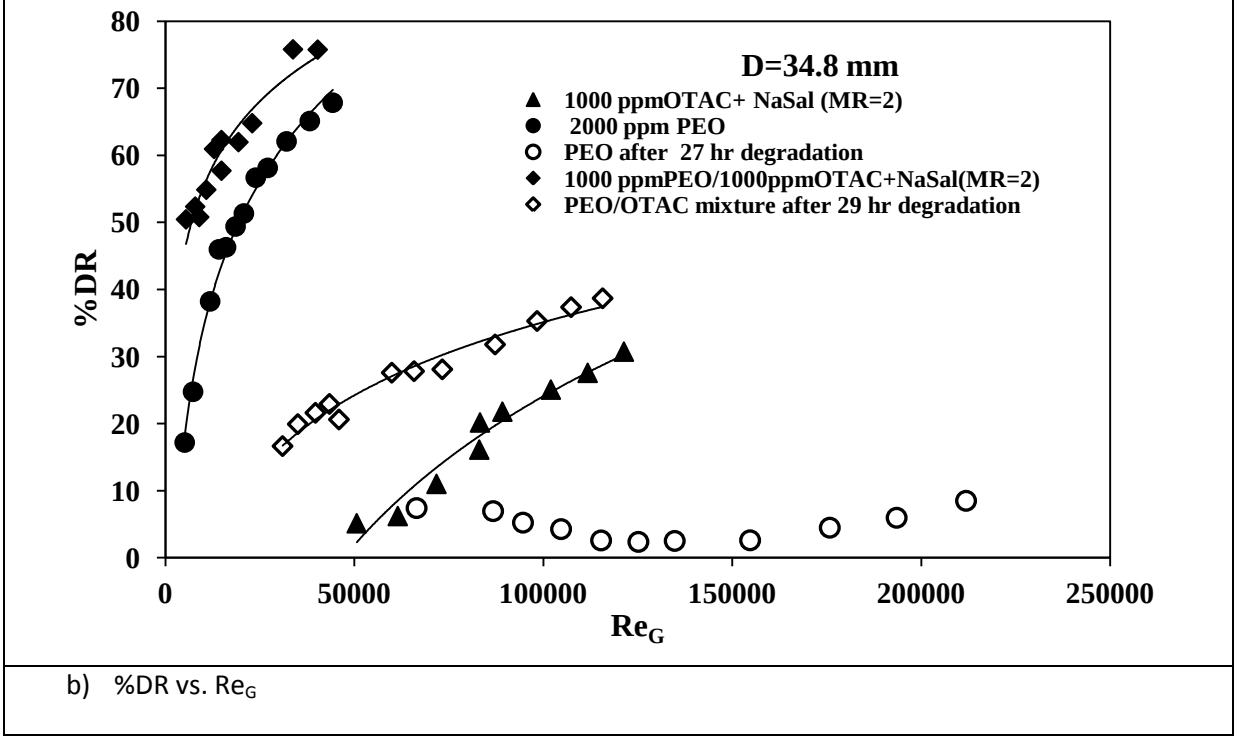

b) %DR vs. Re_G

Figure 7-15: variation of friction factor and %DR with time for 2000 ppmPEO/1000ppm OTAC (MR=2)

7.3 Summary

The synergistic effects of non-ionic polymer (PEO) and cationic surfactant (OTAC+NaSal) on drag reduction in turbulent pipeline flow were investigated experimentally. The following conclusions can be drawn from the experimental work:

- The relative viscosity measurements indicate a moderate interaction between the polymer and the surfactant. No measurable interaction was revealed by surface tension measurement. The critical micelle concentration (CMC) of the surfactant does not change due to the presence of PEO in the solution.
- The pipeline data show considerable synergistic effects so that the mixed polymer-surfactant system gives a significantly higher drag reduction (lower friction factors) as compared to pure polymer or pure surfactant. Addition of surfactant to the polymer always increases the extent of drag reduction; however the impact is more pronounced at low PEO concentration and high surfactant concentration.
- The enhancement of drag reduction upon the addition of surfactant to the polymer is explained in terms of a new microstructure shown in Figure 7-6.
- Addition of OTAC can improve the resistance against shear degradation. This improvement is more pronounced in the case of lower PEO concentration along with higher OTAC concentration.

Chapter 8
Interaction of Anionic Surfactant (SDS) with Nonionic Polymer (PEO)

The bench scale and pipeline flow experiments presented in this chapter follow the same procedure as explained in chapter 4 of this study. All the bench scale and pipeline flow experiments were done at $25^{o}C \pm 0.5$.

8.1 Bench Scale Experiments

The PEO was dissolved in DI water in order to prepare a stock solution at 0.3%- 0.5 % polymer concentration. Also, SDS was dissolved in DI water before being added to the polymer to make a 2% SDS stock solution. 400ml of SDS/polymer/DI solution at various concentrations was synthesized and then mixed to ensure homogeneity throughout the solution. Three different solutions of PEO (i.e. 500 ppm, 1000 ppm, 2000 ppm) were prepared and SDS solution was added to them. The characterizations of the surfactant and surfactant/polymer solutions were presented in terms of conductivity, surface tension, and relative viscosity.

8.1.1 Conductivity

Electrical conductivity measurement can be used to declare any change in solution behavior when an ionic surfactant is added to aqueous solutions. Figure 8-1 shows conductivity measurements for pure SDS and different mixtures of PEO/SDS in DI water at 25˚C. By evaluating the trend lines, and calculating the points of intersection, the CAC/CMC and polymer saturation points were determined and tabulated in Table 8-1. It is obvious that the CAC values generally decreased as the concentration of PEO increased. For solution containing 500 ppm and 1000 ppm of PEO, CAC's are almost similar but different to CMC value of pure SDS. For 2000 ppm PEO solution a lower CAC value compared to other concentration was observed. Many studies have shown that CAC, in general, is less than the

critical micelle concentration (CMC) of the surfactant (Jones 1967; Nagarajan 1989). Increasing of PEO can increase the possible sites for micellization which result in decrease in CAC values. In this case it can be deduced that aggregated state of the SDS on the backbone of PEO is a more stable energy condition for the SDS monomers thanpolymer-free micelles.

It is proved that the polymer chains are saturated at the well known polymer saturation point (PSP). At this particular point, the monomer concentration reaches the point beyond which polymer-free micelles form again. For different PEO/SDS mixtures, PSP values are shown in Table 8-1. By increasing polymer concentration from 500 ppm to 2000 ppm the PSP increased with an SDS concentration changes from 2781 ppm to 3277 ppm. The value of the PSP depends on the concentration of polymer. Since more surfactant monomers are needed for higher concentrations of polymer to saturate the polymer chains, it is expected that while polymer concentration is increased the PSP will increase as well The PSP values obtained from the experiments are in good agreement with the theory described at this study work.

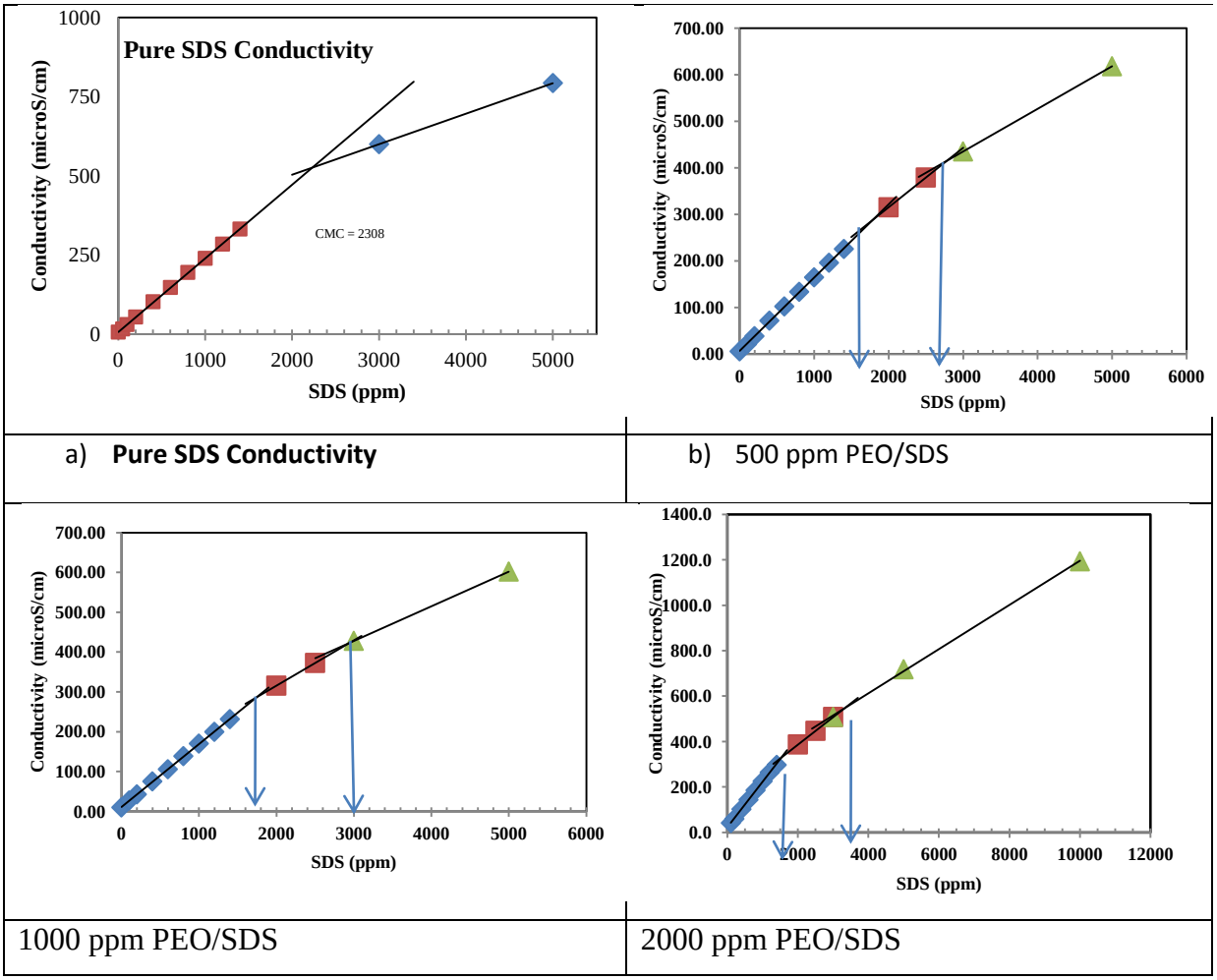

Figure 8-1: Conductivity vs. SDS concentration for different PEO/SDS mixtures

Table 8-1: CAC/CMC and PSP number for SDS and PEO/SDS mixtures using conductivity method

Solution	CAC /CMC number (ppm)	PSP number (ppm)
Pure SDS in DI WATER	2308	-
500 ppm PEO/SDS	1769	2781
1000 ppm PEO /SDS	1744	2944
2000 ppm PEO /SDS	1454	3277

8.1.2 Viscouse behavior of solutions

The relative viscosities, measured for different combinations of PEO and SDS, are shown in Figure 8-2 as a function of SDS concentration. The viscosity is initially constant up to a surfactant concentration of about 2000 ppm. A sharp rise in the viscosity occurs when SDS concentration is increased above 2000 ppm. This surfactant concentration where a sharp increase in viscosity begins (2000 ppm) is only slightly higher than the CAC. The rise in viscosity implies a change in the conformation of the polymer molecules. By adding SDS to PEO solution, the SDS monomers find alternative places on the backbone of polymer to form micelles. SDS monomers have smaller head group compared to OTAC head group. This can help SDS diffuse better and make micelles on the backbone of polymer chain. The PEO coils undergo expansion when they interact with SDS monomers/ micelles. The repulsive force between the adjacent surfactant micelles on the same polymer chain causes the chain to expand.

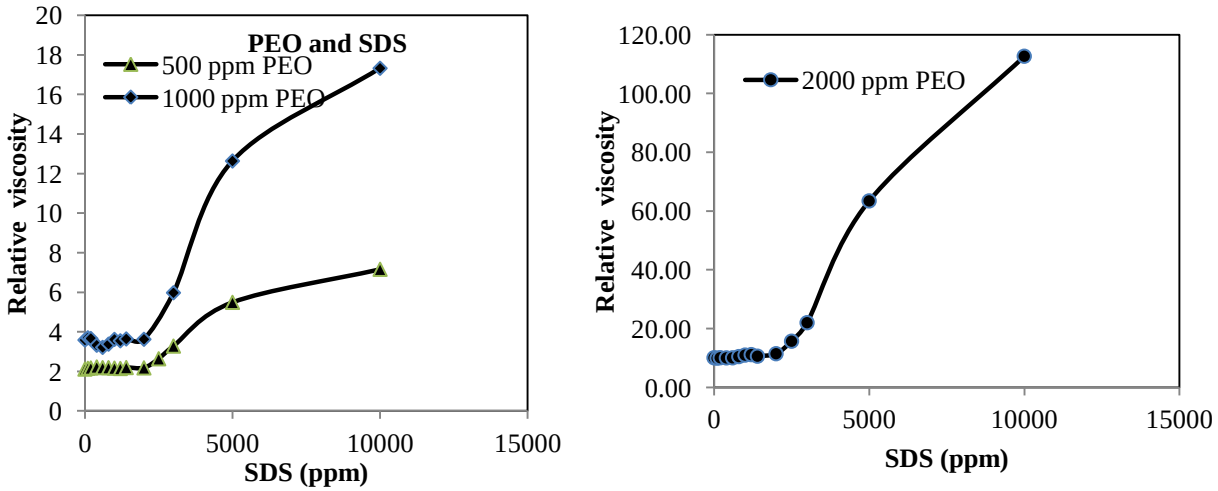

Figure 8-2: Relative viscosity of PEO solution with different amount of SDS

These observations are consistent with other studies. For example, the work of Francois et al. (1985) on mixtures of nonionic polymer (PEO) and SDS revealed an increase in viscosity near the CAC of the system.

Figure 8-3 shows the mechanism for the expansion of polymer coils upon the addition of surfactant. This mechanism is consistent with the "necklace and beads" model proposed by Shirahama et al. (1974) and Nagarajan (1980). Here the beads are the SDS clusters formed along the polymer chain (necklace).

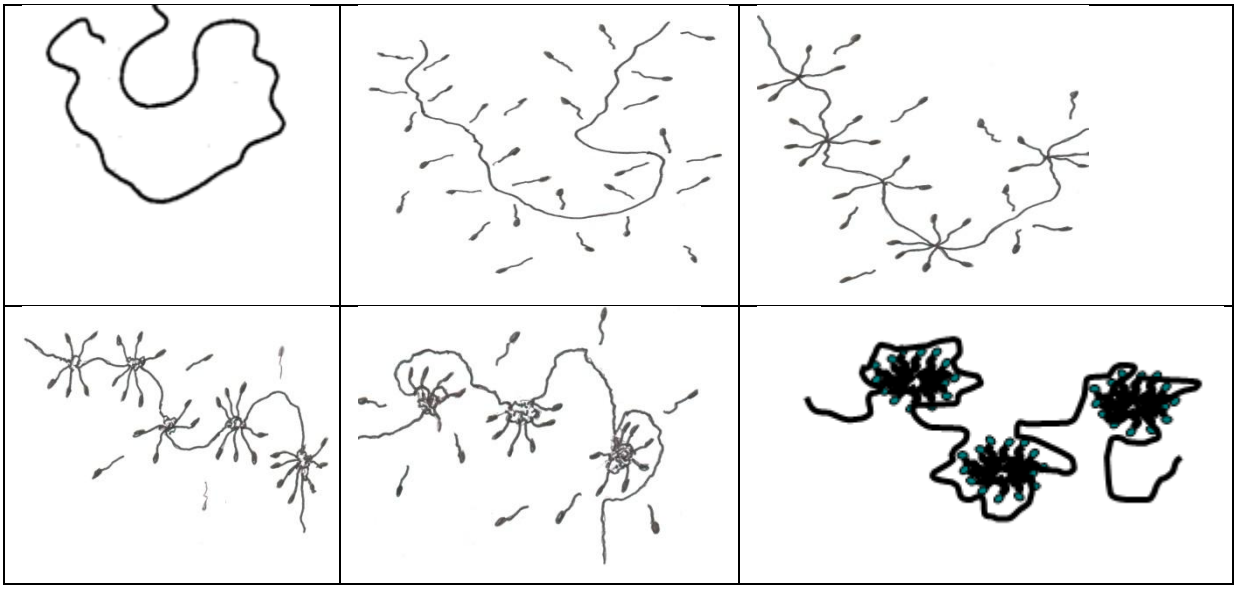

Figure 8-3: Necklace model

Figure 8-4 shows apparent viscosity for different PEO /SDS mixtures. Apparent viscosities are consistent with relative viscosity data. All the solutions show increase in apparent viscosity when SDS concentration reaches 2000 ppm. It means at any given shear rate, the apparent viscosity generally increases with the increase in surfactant (SDS) concentration. Also it's clear that for 500 ppm and 1000 ppm PEO solutions, addition of SDS changes the behavior of fluids and the solutions become more shear-thinning (as reflected in the slope of apparent viscosity versus shear rate plot). In this case mixtures show shear thinning effect when SDS >2000 ppm. Although, 2000 ppm PEO solution approaches to shear tinning behavior at the beginning of interaction process, but addition of SDS causes an increase in viscosity and shear thinning effect (k increases and n decreases).

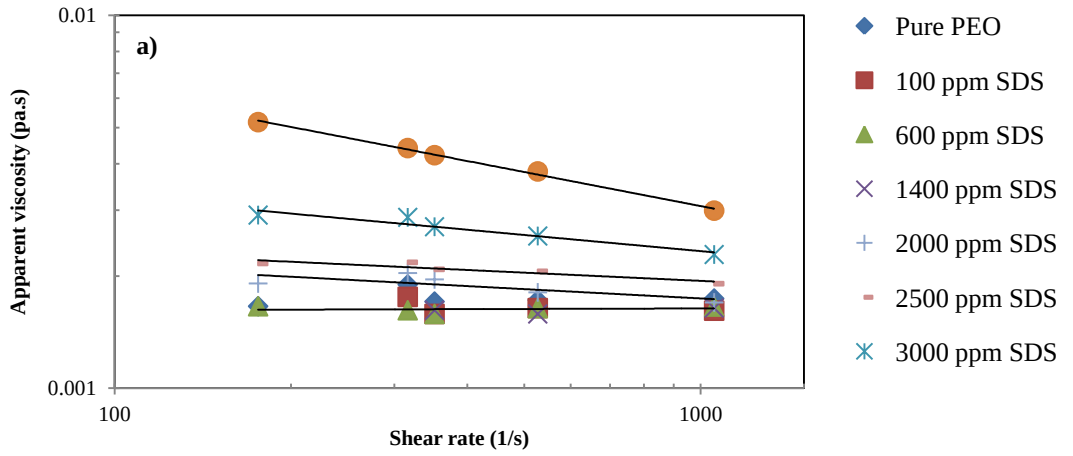

a) 500 ppm PEO

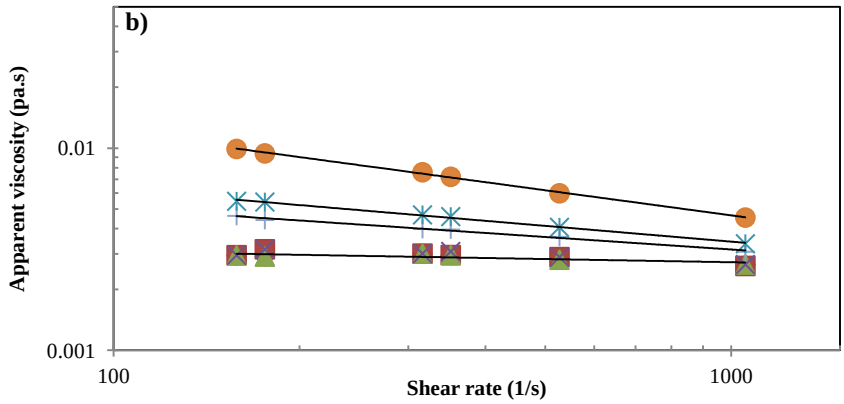

b) 1000 ppm PEO

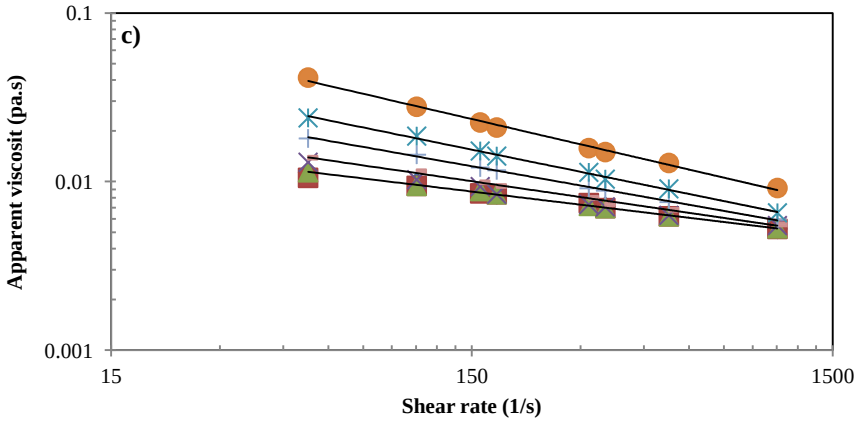

c) C) 2000 ppm PEO

Figure 8-4: Apparent viscosity of PEO/SDS mixtures

8.1.3 Surface tension

Figure 8-5 shows the experimental surface tension data for pure surfactant solution and mixed polymer-surfactant systems at three different concentrations of PEO. From the plots, the values of CMC, CAC, and PSP are determined as shown in the figure. The values are summarized in Table 8-2. Although the values are not exactly the same as those obtained by the conductivity method, the trends are consistent with the conductivity measurements. As PEO itself is surface-active, it may have affected the surface tension results to some extent and resulted in the observed deviations.

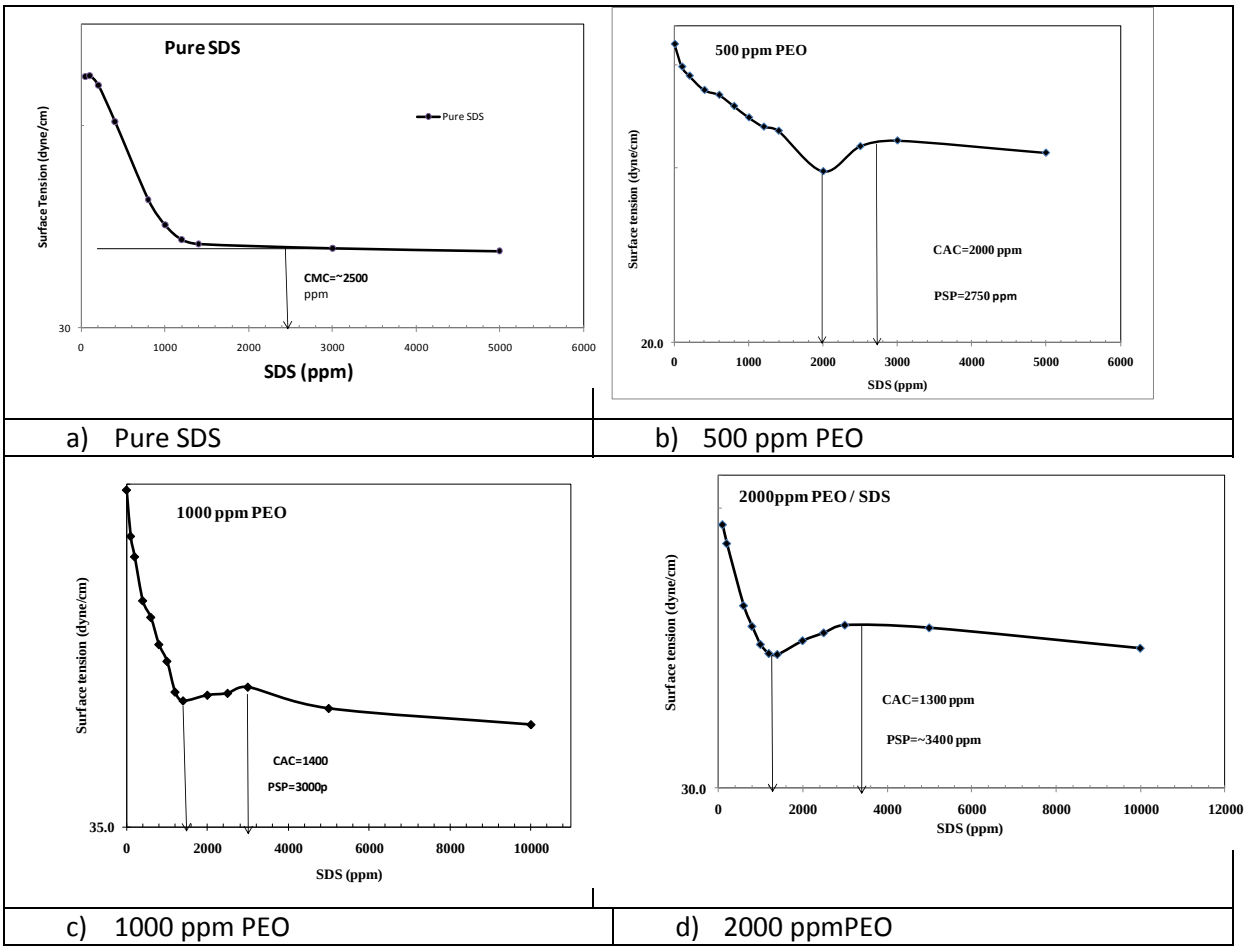

Figure 8-5: surface tension results for different mixture of PEO/SDS

Table 8-2: Approximation values of CAC and PSP using surface tension method

Solution	CMC or CAC (ppm)	PSP (ppm)
Pure SDS in DI WATER	2500	-
500 ppm PEO/SDS	2000	2750
1000 ppm PEO /SDS	1400	3000
2000 ppm PEO /SDS	1300	3400

8.2 Pipeline Behavior Study

The experiments were designed at three concentration levels for PEO (500, 1000, and 2000 ppm) and three concentration levels for surfactant (1000, 3000 and 5000 ppm).

Figure 8-6 shows friction factor and %DR vs. Re_G for PEO/SDS mixtures containing 500ppm PEO and different levels of SDS concentration. Increasing the SDS concentration reduces the friction factor and increases the %DR. The increase in %DR with the increase in SDS concentration is large up to a surfactant concentration of 3000 ppm. Above 3000 ppm, the increase in %DR with the increase in SDS concentration is small. It should be noted that the PSP is close to 3000 ppm SDS for 500 ppm PEO solution (see Table 8-1). Thus %DR increases with SDS concentration up to the PSP and then levels off.

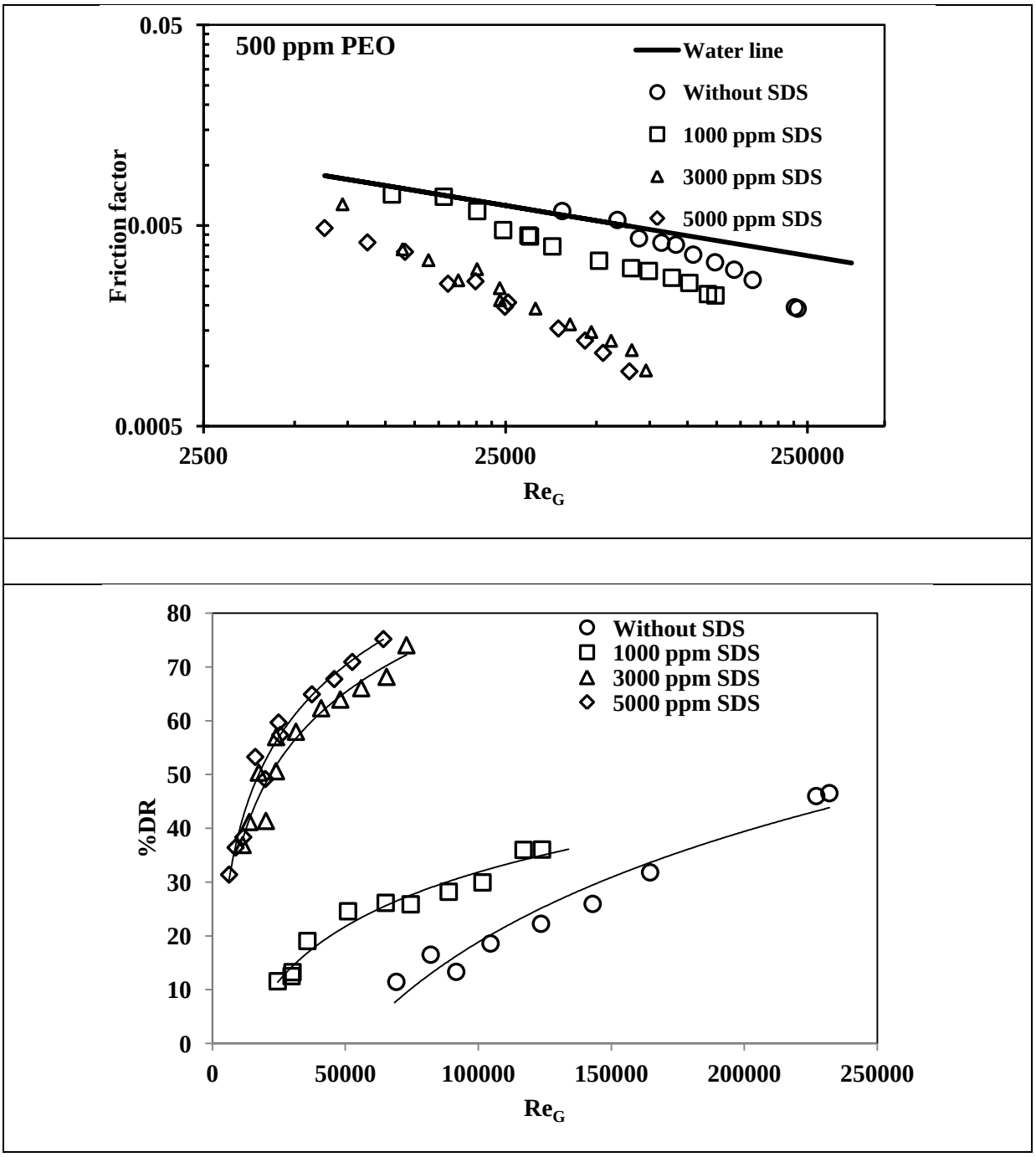

Figure 8-6: Friction factor and %DR vs. Re_G for 500ppm PEO/SDS mixtures

Table 8-3 presents friction factor difference (%FFD) for 500ppm PEO/SDS mixtures compared to pure 500 ppm PEO. The average shows an increase in %FDD (i.e. decrease in

the friction factor of the mixtures) with the increase in SDS concentration. The CAC value of SDS in 500 ppm PEO is 1769 to 2000 ppm based on conductivity and surface tension meaurements. It is interesting to note that the drag reduction synergy between polymer and surfactant occurs even at a relatively low surfactant concentration of 1000 ppm which is well below the CAC. In general, CAC is a point at which stable aggregation formation occurs. Chain conformation of polymer molecules can be started even at early stage of surfactant addition but it might be not stable to be detected by regular methods such as conductivity and surface tension. In the case of 500 ppm PEO, which is a dilute polymer solution with a viscosity close to water, the polymer molecules are mostly coiled. Negative charge of SDS monomers which are attached to polymer chains can probably help the chains experience a considerable expansion. This observation indicates that the interaction between the surfactant and the polymer under turbulent flow conditions begins at a much lower surfactant concentration than expected. In other words, the CAC value under turbulent flow conditions is lower than the CAC value under quiecent conditions. The local mixing action of turbulent flow enhances the diffusion of surfactant molecules to the polymer chains.

DR is improved by the stretched chain. In this regard, the amount of decrease in friction factor (%FFD) is not considerable compared to %FFD for 3000ppm of SDS (~70%). PSP for 500 ppm PEO solution happened at about 2750ppm of SDS. Addition of 3000 ppm SDS usually saturates the polymer chains. It was proved that the binding of charged surfactant micelles to flexible non-ionic polymers leads to a considerable change in the hydrodynamic properties of the solution. Charli et al. showed that a good binding between formed micelles and PEO chains happens upon addition of the anionic surfactant sodium dodecyl sulfate (SDS) to PEO. The hydrodynamic radius increases. The phenomenon takes place because the polymer coil expands. The main reason for this expansion is the electrostatic repulsions between the bound micelles on backbone of PEO chains(Chari et al. 1994; Chari et al. 1995). Although, the polymer chains are not fully extended, but even partial expansion of polymer chains will behave much better compared to original chains against the turbulence eddies. Consequently, more eddies will be dampened and suppressed by this new complex structure. DR for mixture of 500ppm PEO and 5000ppm SDS does not change considerably compared

to the DR for mixture of 500ppmPEO and 3000ppmSDS does. This can be attributed to this reason that the PSP happens at about 3000 ppm that results in maximum chain expansion. No more conformation change happens for higher SDS concentrations. That's why %FFD for 5000 ppm SDS shows negligible variation (almost 3%) compared to %FFD for 3000ppm SDS does. Experimental data shows that adding SDS to PEO solution has no effect on the %DR magnitude and DR behaviour of solution. Table 8-4 summarizes the onset Re_G values for PEO/SDS mixtures at a fixed polymer concentration of 500 ppm. It is observed that the onset of DR is lower if SDS concentration increases. As polymer chains in the complex are more extended compared to the polymer chains in pure PEO solution, DR will onset at lower Re_G.

Table 8-3: % Friction factor difference between pure 500 ppm PEO and 500ppm PEO/SDS mixtures for some of Re_G

Re_G	**%FFD (5000 ppm SDS)**	**%FFD (3000 ppm SDS)**	**%FFD (1000 ppm SDS)**
15000	60.1	53.4	0.0
20000	65.0	59.5	17.2
25000	68.4	63.7	21.5
30000	70.9	66.7	24.9
35000	72.8	69.2	27.6
40000	74.4	71.1	29.9
50000	76.9	74.1	33.6
60000	79.3	76.9	38.0
70000	79.3	77.0	35.9
80000	79.3	77.1	34.1
90000	79.3	77.2	32.5
100000	79.3	77.3	31.0
Average	**73.7**	**70.3**	**27.2**

Table 8-4: Onset of DR for 500ppm PEO/SDS mixtures

SDS concentration(ppm)	Without SDS	1000 ppm	3000 ppm	5000 ppm
Onset of DR (Re_G)	58000	9100	4900	3200

Figure 8-7 shows friction factor and %DR vs. Re_G for PEO/SDS mixtures at a fixed PEO concentration of 1000 ppm. The addition of 1000 ppm SDS to 1000 ppm PEO has a little effect on the friction factor. As the CAC value for 1000 ppm PEO solution is around 1400 ppm to 1744 ppm SDS (1400 ppm based on surface tension and 1744 ppm based on conductivity), it is not surprising that there is little effect on DR at 1000 ppm SDS. The question may arise when 1000ppmPEO/1000ppmSDS mixture is compared with 500ppmPEO/1000ppmSDS mixture. The CAC for both systems approximately fall in the same range. As pointed out earlier, some researchers believe that interaction of surfactant and polymer starts in early stage of surfactant addition however no stable cluster is made till CAC. This temporary structure may have some effects on DR. A noticeable increase in DR is observed for 500 ppm PEO/1000 SDS compared to pure500ppmPEO. Effect of surfactant on polymer chain conformation at the early stage of SDS addition is almost the same for both 1000ppmPEO and 500ppmPEO. This conformation change may not be enough to make a considerable effect on DR of 1000ppm PEO solution. It has to be taken into consideration that pure 1000 ppm PEO solution shows 70% more DR than pure 500ppm PEO does. It means that the later solution is not a good drag reducer like the pure 1000ppm PEO. In this case, any small change in polymer chain conformation can show itself in the form of an improvement in DR.

Increasing the SDS concentration to 3000 ppm increases the DR substantially. As the PSP value for 1000ppm PEO solution is about 3000 ppm SDS, the addition of 3000 ppm SDS has a large effect on friction factor and %DR. Above the PSP value, the effect of SDS addition (for example, 5000 ppm SDS) on friction factor and %DR is only moderate. The PEO solution (1000 ppm PEO) containing high concentrations of SDS (3000ppm and 5000ppm) also show a different DR behavior. These systems act as Type B drag reducers

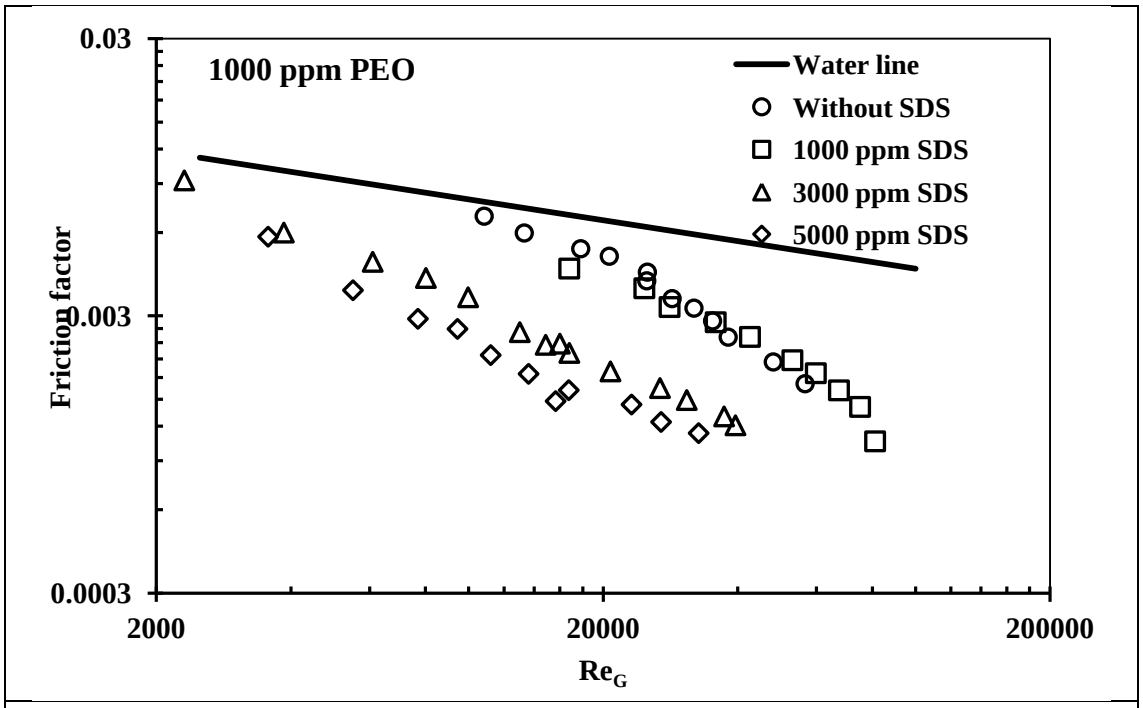

a)

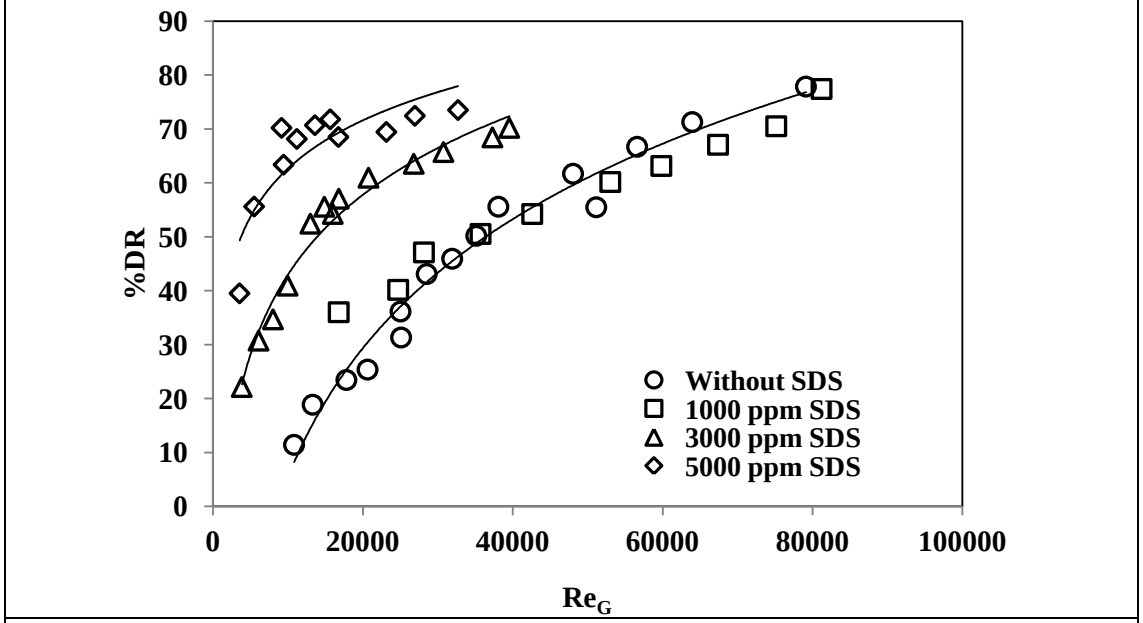

b)

Figure 8-7: Friction factor and %DR vs. Re_G for 1000ppm PEO/SDS mixtures

whereas the corresponding pure PEO solution (1000 ppm PEO) behaves as a Type A drag reducer. Type A drag reduction is typical for coiled polymer molecules. For these systems the onset of DR occurs when the wall shear stress reaches a certain value. On the other hand, Type B drag reduction usually happens for extended polymer molecules, which exhibit drag reduction immediately after transition from laminar to turbulent flow (Gasljevic et al. 2001).

Table 8-5 shows friction factor diffrence (%FFD) upon the addition of SDS to 1000 ppm PEO solution. The average values show an increase for solution with 3000 ppm and 5000 ppm of SDS. The friction factor is reduced by an average of 52 % upon the addition of 3000 ppm SDS to the PEO solution. The %FFD is small (average of 4.3%) for SDS concentration of 1000 ppm which is below the CAC value. Also the increase in %FFD upon increasing the SDS concentration from 3000 ppm to 5000 ppm is moderate as the SDS concentration exceeds the PSP value.

Table 8-5: %Friction factor difference between pure 1000 ppm PEO and 1000ppm PEO/SDS mixtures for some of Re_G

Re_G	%FFD (5000 ppm SDS)	%FFD (3000 ppm SDS)	%FFD (1000 ppm SDS)
15000	68.8	58.1	5.0
25000	66.8	54.9	4.6
30000	66.1	53.7	4.4
35000	65.4	52.6	4.3
40000	64.8	51.7	4.2
45000	64.3	50.8	4.1
50000	63.9	50.1	4.1
60000	63.1	48.7	3.9
70000	62.3	47.6	3.8
Average	**65.1**	**52.0**	**4.3**

Figure 8-8 shows friction factor and %DR vs. Re_G for PEO/SDS mixtures containing 2000 ppm PEO. The addition of 1000 ppm SDS to this 2000ppm PEO solution results in a significant increase in %DR. The CAC value for 2000 ppm PEO solution is 1300 to 1454 ppm SDS (1300 ppm SDS based on surface tension and 1454 ppm SDS based on conductivity). This indicates that under turbulent flow conditions, the interaction between the surfactant molecules and the polymer chains occurs even below the CAC value obtained under quiescent condition. Upon increasing the SDS concentration from 3000 ppm to 5000 ppm, the increase in %DR is not large. Also the solutions with high SDS concentrations of 3000 ppm and 5000 ppm exhibit Type B of drag reduction behavior. Figure 8-8 also shows that increase in %DR for 2000ppm PEO/1000ppm SDS depends on Re_G, as Re_G increases the mixture exhibits same %DR as pure 2000 ppm PEO solution.

One possible reason for a smaller increase in %DR upon increasing the SDS concentration from 3000 to 5000 ppm is that the polymer molecules are saturated with surfactant. The PSP value of 2000 ppm PEO solution is 3277 ppm SDS based on conductivity measurements and 3400 ppm SDS based on surface tension measurements. Furthermore, at high concentrations of SDS, the viscous effect (increase in solution apparent viscosity) counteracts the drag reduction effect. Using power law equation, viscosity parameters were calculated and tabulated in Table 8-6. When SDS concentration reaches 5000ppm, k increases an order of magnitude compare to pure PEO solution. The consistent index k undergoes a jump from 0.087 to 0.3221 when the SDS concentration is increased from 3000 ppm to 5000 ppm. This increase is much more than what is observed for other SDS concentrations. At this stage viscosity effect will be more pronounced and will change the behavior of mixture. For this type of solutions, somebody would expect to observe Type B behavior in case of DR. %DR will remain constant for all Re after a certain Re (Gasljevic et al. 2001). This behavior was seen for 3000 ppm and 5000 ppm of SDS.

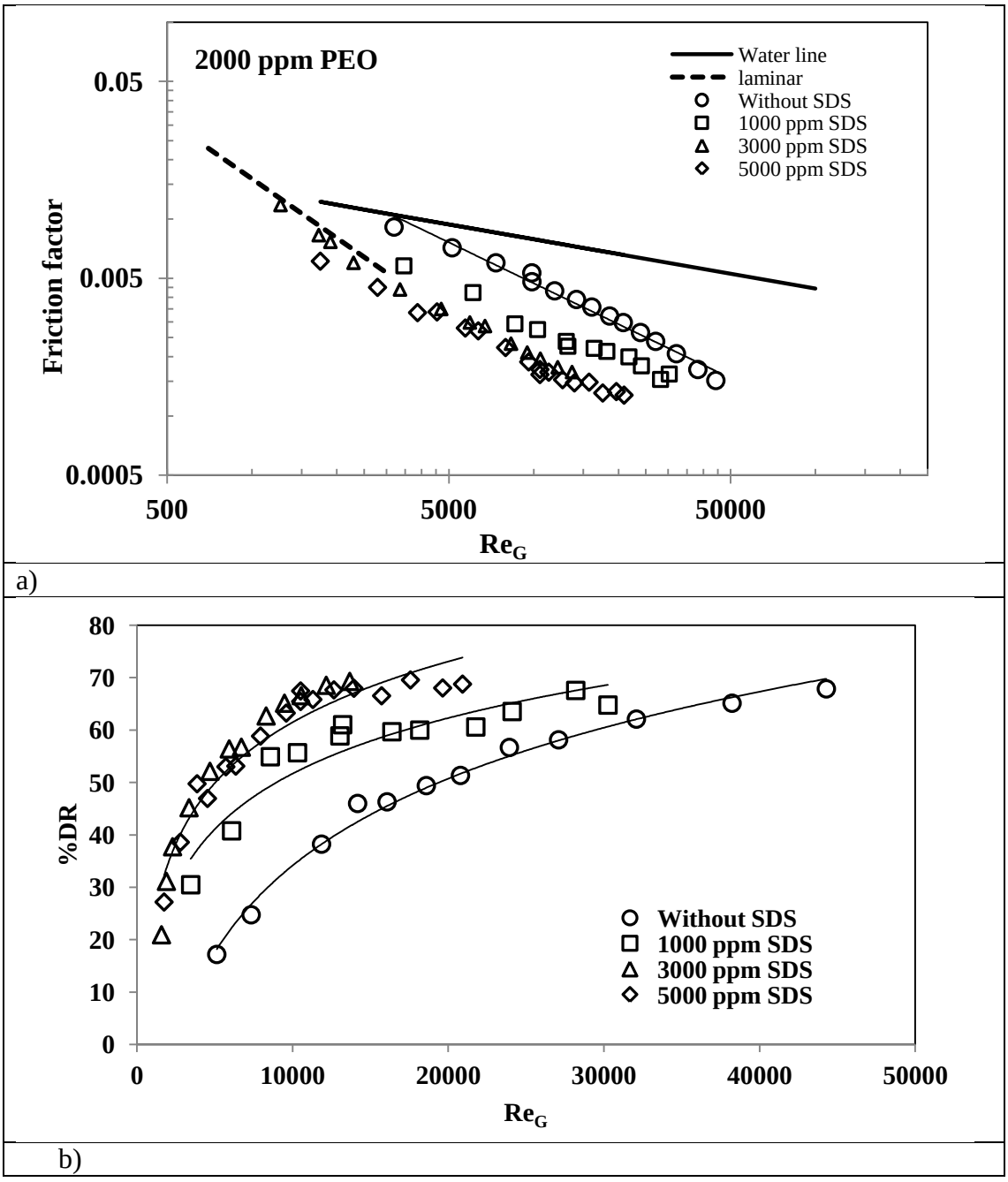

Figure 8-8: %Friction factor and %DR vs. Re_G for 2000ppm PEO/SDS mixtures

Table 8-6: Power law parameters for 2000ppm PEO/SDS mixtures

2000ppmPEO/SDS	k	n
Without SDS	0.0508	0.6481
1000 ppm SDS	0.0465	0.6994
3000 ppm SDS	0.087	0.6451
5000 ppm SDS	0.3221	0.4801

Table 8-7 shows %FFD for 2000 ppm PEO/SDS compared to 2000ppm PEO for some of Re_G. The average %FFD is increased for 5000 ppm SDS compared to 1000 ppm SDS but will remain almost the same as 3000 ppm of SDS. The average %FFD is 37.4 at 1000 ppm SDS, 56.6 at 3000 ppm SDS, and 59.8 at 5000 ppm. As mentioned earlier, there occurs only a small increase in %FFD when SDS concentration is increased from 3000 to 5000 ppm due to saturation of polymer chains with SDS molecules.

Table 8-7: %Friction factor difference between pure 2000 ppm PEO and 2000ppm PEO/SDS mixtures for some of Re_G

Re_G	%FFD (5000 ppm SDS)	%FFD (3000 ppm SDS)	%FFD (1000 ppm SDS)
5000	61.1	55.5	42.5
7500	60.5	56.0	40.0
10000	60.0	56.4	38.2
12500	59.6	56.7	36.8
15000	59.3	57.0	35.6
17500	59.1	57.2	34.6
20000	58.9	57.3	33.7
Average	**59.8**	**56.6**	**37.4**

8.3 Mechanical Degradation

PEO degrades very fast when it goes under high shearing. According to Figure 5-15 and (also Figure 8-9) 500ppm and 1000 ppm of pure PEO solutions lose thire DR ability by 85% when they goe under shear degradation for 3 hr. In the case of 2000 ppm PEO, this reduction in DR ability is lower (almost 60%) but it is still a remarkable reduction.

In this study, the effect of SDS addition to PEO solutions on mechanical degradation was investigated. Different PEO/SDS mixtures were prepared and degraded under the same conditions (in 34.8 mm pipe with same Re). No change in degradation behavior was observed for solution containing 1000 ppm SDS over a wide range of PEO concentrations. Therefore, no data has been presented for those series in this chapter. In case of 3000 ppmSDS/PEO and 5000 ppm SDS /PEO, mechanical degradation was studied. The results are shown in Figure 8-9 and Figure 8-10.

Figure 8-9 shows the effect of PEO degradation on friction factor and %DR of 500 ppm PEO/SDS mixtures. The results show that pure 500 ppm PEO degrades much faster compared to PEO/SDS mixtures (see Table 8-8). While 500 ppm PEO solution loses almost 70% of DR ability, same polymer solution containing 3000 ppm SDS and 5000 ppm SDS loses ~40% and ~22% of DR capability, respectively. A remarkable point in the table is the difference between %DR of 3000ppm and 5000 ppm SDS solution. These two solutions show almost the same DR before degradation but 5000 ppm solution acts better at the early stage of degradation (till 3hr) and then after 24 hr degradation shows same reduction in DR ability as the 3000ppm SDS solution. SDS micelles on the backbone of PEO chains can make the polymer chain to extend more. As the chains extend the %DR improves but will be limited (%DR is almost same for 3000 ppm and 5000 ppm of SDS).On the other hand by increasing the SDS concentration the number of extended chains is increased. When the polymer chains undergo mechanical degradation, concentration of extended chains is a crucial key against degradation (and consequently DR ability). This will be more pronounced at the early stage of degradation.

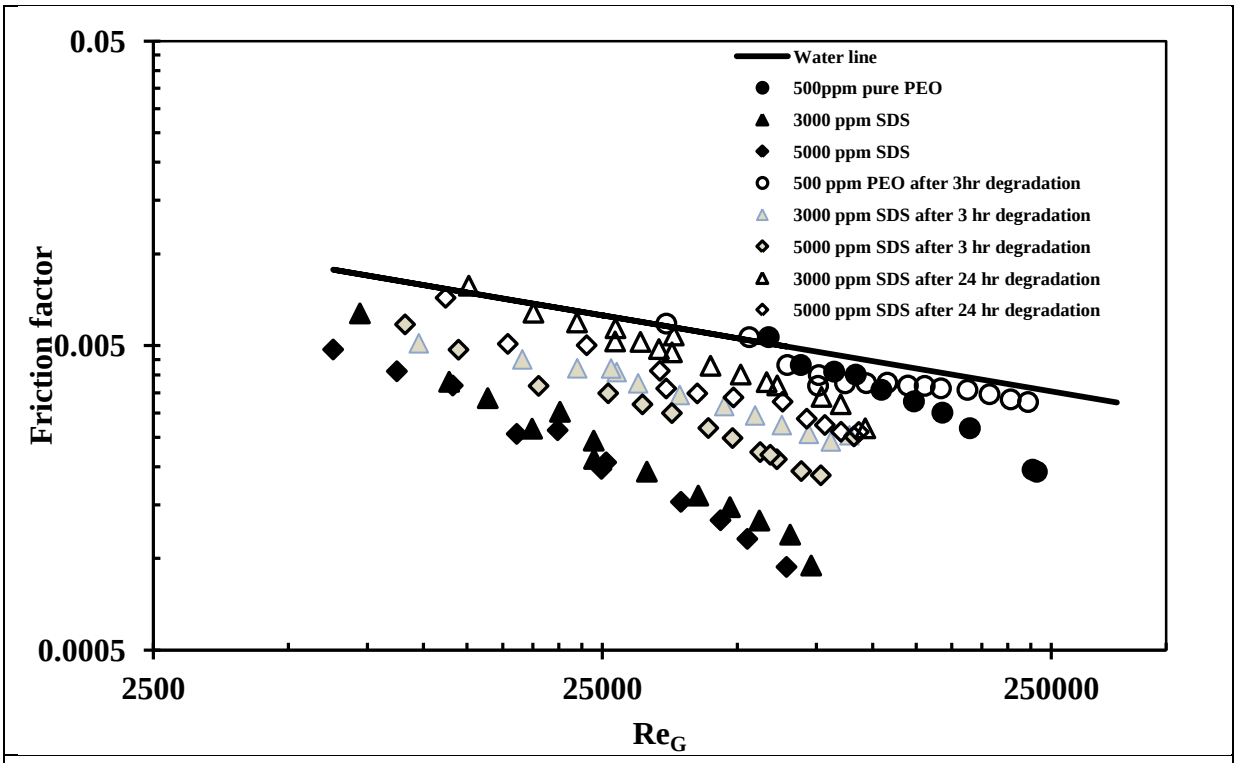

a

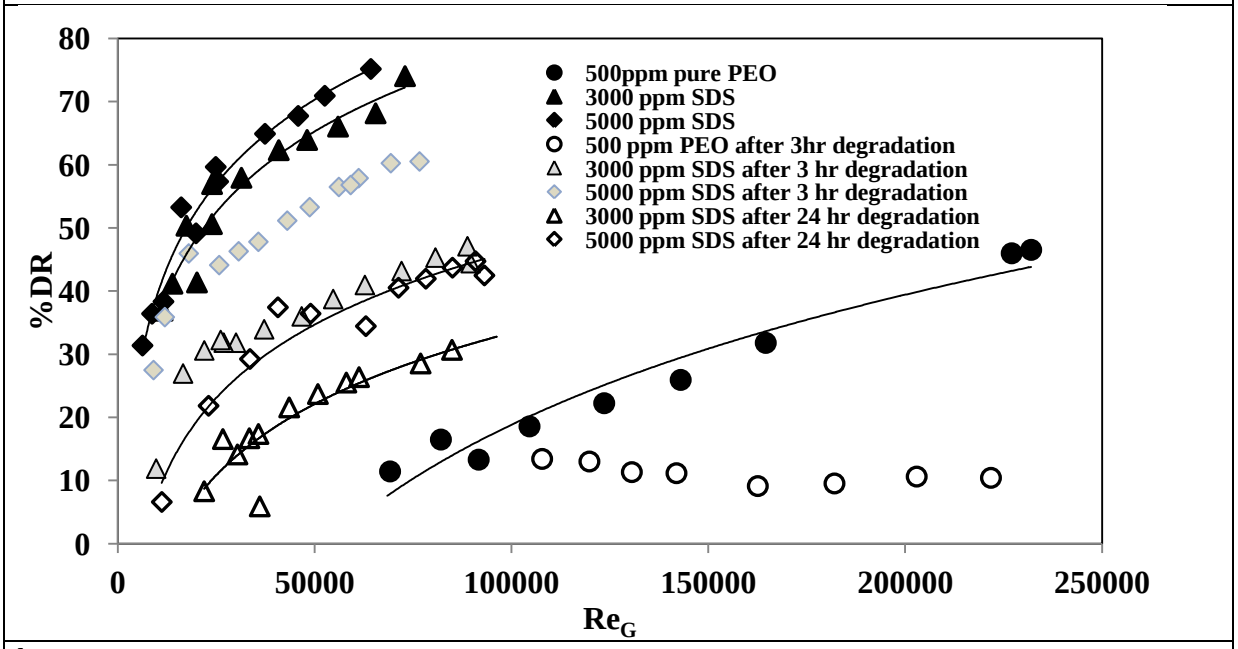

b

Figure 8-9: Effect of degradation on friction factor and %DR of 500ppmPEO solutions with different amount of SDS

Table 8-8: Average reduction in %DR for (500ppmPEO/SDS) mixtures in different times

Tim(hr)	Reduction of DR for pure 500ppmPEO (%)	Reduction of DR for solution with 3000 ppm SDS (%)	Reduction of DR for solution with 5000 ppm SDS(%)
After 3hr	70.8	41.5	22.4
After 24 hr	90.2	67.4	51.3

Figure 8-10 shows the influence of mechanical shearing on friction factor and DR for 1000ppm PEO /SDS mixture at different times. Addition of SDS improves the resistance against mechanical degradation. Table 8-9 shows the average reduction in DR for 1000ppmPEO/SDS solutions. In the case of 5000 ppm SDS solution, a decrease of ~17% and ~37% was observed after 3hr and 24 hr of degradation, in DR ability respectively. This is a great improvement in resistibility against degradation correspondence to pure 1000ppm PEO which shows a ~68% reduction in DR ability in early stage of degradation (afetr3 hr). For 3000ppm SDS, the DR ability was decreased ~40% and ~70% after 3 and 24 hr, respectively. Improvements in degradation resistance compared to pure PEO may still be observed but these improvements will not be as pronounced as for 5000 ppm SDS values.

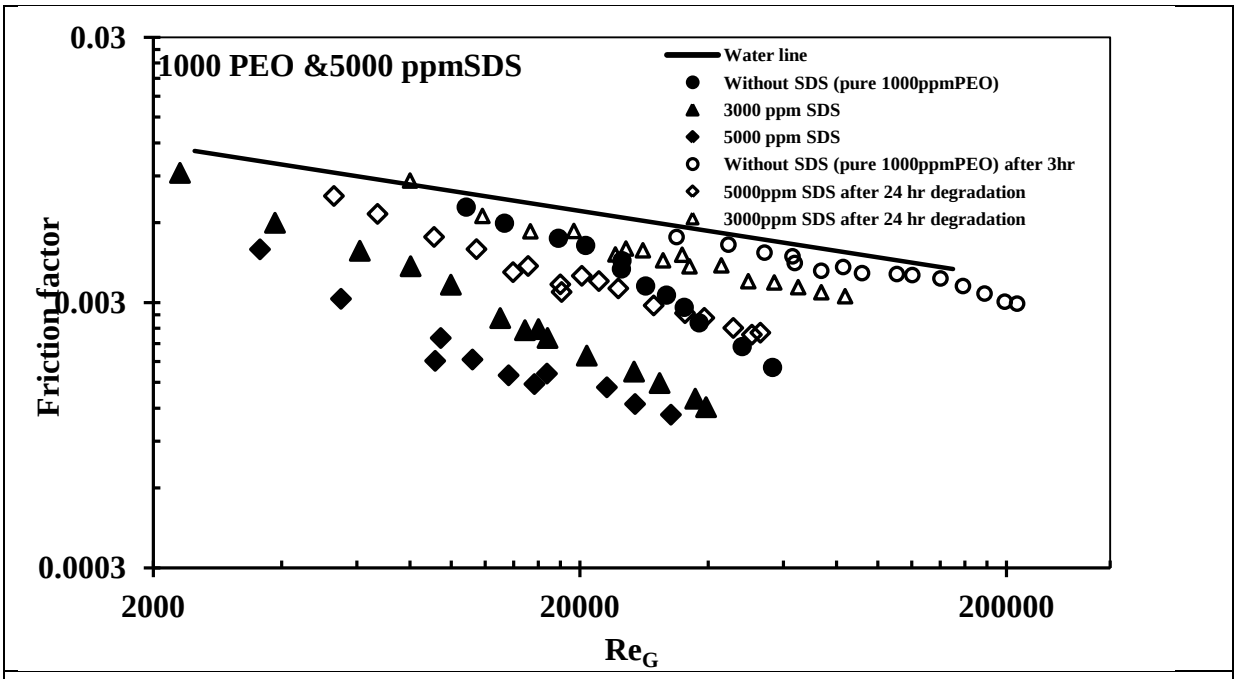

a

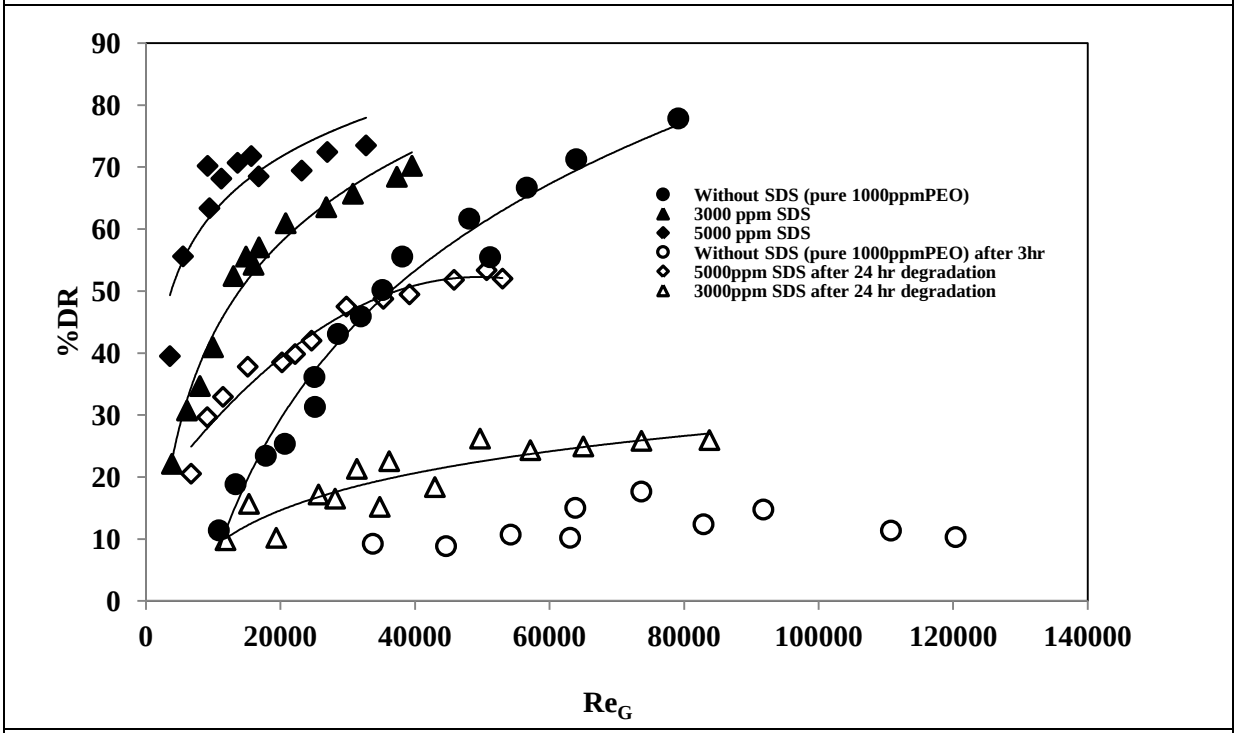

b

Figure 8-10: Effect of degradation on friction factor and %DR of 1000ppm PEO solutions with different amount of SDS

Table 8-9: Average reduction in %DR for (1000ppm PEO/SDS) mixtures in different times

Tim(hr)	Reduction of DR for pure 500ppmPEO (%)	Reduction of DR for solution with 3000 ppm SDS (%)	Reduction of DR for solution with 5000 ppm SDS (%)
after 3hr	68.2	40.2	17.1
after24hr	80.2	71.4	37.6

8.4 Summary

The synergistic effects of PEO /SDS were experimentally investigated for the purpose of drag reduction. The interactions between PEO (as a non-ionic drag reducer polymer) and SDS (as an anionic surfactant) were studied in the DI water. The following conclusions can be drawn from this experimental work:

- The plot of electrical conductivity of PEO/SDS mixture versus SDS concentration shows two break points. The first break point occurs at critical aggregation concentration (CAC) of SDS and the second break point occurs at polymer saturation point (PSP) where the PEO molecules are saturated with the surfactant molecules. As PEO concentration is increased the CAC decreases but the PSP increases. The CAC and PSP values obtained by surface tension measurements are similar to those obtained by the conductivity method.
- Relative viscosity showed a remarkable increase compared to pure PEO solution. This increase can be attributed to change in hydrodynamic radius of complex. Formation of micelles on backbone of polymer can extend the polymer chains.
- The pipeline flow was exhibited a considerable increase in DR for 500 ppm of PEO/SDS mixtures compared to DR of 500 ppm pure PEO.

- In the case of 1000 ppm PEO, by addition of 1000 ppm SDS no increase in DR was observed. %FFD improved almost 50 and 60 percent for solution with 3000ppm and 5000ppm SDS respectively. Polymer solution behavior was changed to Type B.
- The PEO/SDS with 2000 ppm PEO complexes act differently under the shear stress compared to the quiescent condition, Indicating that under turbulent flow conditions, the interaction between the surfactant molecules and the polymer chains occurs even below the CAC value obtained under quiescent condition.
- The addition of surfactant always improves the extent of DR up to PSP; however the impact was more pronounced for lower PEO concentration level (500 ppm) with the higher surfactant concentrations. It seems the interaction between the polymer and surfactant starts at a lower surfactant concentration as a result of high turbulent shear stress which causes polymer chains to stretch.
- Addition of SDS will improve the resistance of PEO against mechanical degradation. This effect is more pronounced at higher SDS concentration (5000 ppm).

Chapter 9
Conclusions and Recommendations

9.1 Conclusions

- Considerable energy savings resulting from a reduction in pumping power can be achieved using both polymers and some types of surfactants.
- DR requires higher concentrations of surfactant compared with the required polymer concentration.
- The advantage of surfactant over polymer additives is due to the different nature of the mechanical degradation they experience. Mechanical degradation is the permanent loss of drag-reducing ability of a polymeric solution after exposure to supercritical shear or elongation stresses. Surfactants regain their DR ability when the supercritical shear is removed or decreased to lower values.
- The charge neutralization of PAM polymer chains by OTAC molecules decreases the drag reduction capability of PAM. At high PAM concentrations, the effect of surfactant on drag reduction behaviour becomes less due to inaccessibility of PAM chains to surfactant molecules.
- The presence of cations in tap water makes the tap water a poor solvent for anionic polymers (PAM) compared with DI water. The addition of OTAC to PAM solutions in tap water causes further shrinkage of anionic PAM chains but the degree of shrinkage is not large. Therefore, little change in the drag reduction ability of PAM/tap-water solutions takes place upon the addition of OTAC.
- In the case of non-ionic polymer / cationic surfactant, a moderate interaction between the polymer and the surfactant was observed. The critical micelle concentration (CMC) of the surfactant does not change due to the presence of PEO in the solution.
- The pipeline data show considerable synergistic effects for the mixed non-ionic polymer (PEO) /cationic surfactant (OTAC) system and gives a significantly higher drag reduction (lower friction factors) as compared with pure polymer or

pure surfactant. However, the impact is more pronounced at low PEO concentration and high surfactant concentration.

- The enhancement of drag reduction upon the addition of surfactant to the polymer is explained in terms of a new microstructure shown in Figure 7-6.
- In the case of non-ionic polymer (PEO)/ anionic surfactant (SDS), stronger interaction was observed compared to cationic surfactant. The addition of surfactant always improves the extent of DR up to PSP. Same as PEO/OTAC system, the impact was more pronounced for lower PEO concentration level with the higher surfactant concentrations.
- It seems the interaction between the polymer and surfactant starts at a lower surfactant concentration in pipeline flow as a result of high turbulent shear stress which causes polymer chains to stretch.
- Addition of OTAC and SDS improve the resistance against shear degradation. This effect is more pronounced for anionic surfactant compared to cationic surfactant especially at higher concentration of surfactant.

9.2 Recommendations

- ***To study the effect of temperature****:* The pipeline flow of polymer/surfactant mixtures was investigated under constant temperature. As temperature can have different effect on surfactant CMC and DR, one could test the system with highest performance under different temperature condition.
- ***To study combinations of amphoteric and non-ionic surfactant with non-ionic polymers****:* This can be a capable system to observe different behaviour in drag reduction.
- ***Study replacement of current used surfactant with biodegradable surfactants***
- ***To explore drag reduction mechanisms for new combinations*****:** The mechanism of drag reduction in pure polymer and surfactant are still ongoing research. For these new combinations mechanism of drag reduction might be different than those for pure polymer and pure surfactant. This area need to be explored.
- ***To correlate drag reduction with molecular weight distribution of the polymer*****:** Molecular weight distribution is a key role in drag reduction. Relation of molecular weight distribution with polymer degradation and effect of surfactant addition on this subject is interesting for drag reduction point of view.
- ***Visualization of polymer/surfactant microstructures:*** Using Cryo-TEM or 3D image technique can help to visualised the structure of possible polymer/surfactant microstructure.

Bibliography

Aguilar, G., K. Gasljevic and E. Matthys "Reduction of friction in fluid transport: experimental investigation." Revista mexicana de física **52**(5): 444-452 (2006).

Aguilar, G., K. Gasljevic and E. F. Matthys "Asymptotes of maximum friction and heat transfer reductions for drag-reducing surfactant solutions." International journal of heat and mass transfer **44**(15): 2835-2843 (2001).

Anthony, O. and R. Zana "Interactions between water-soluble polymers and surfactants: effect of the polymer hydrophobicity. 2. Amphiphilic polyelectrolytes (polysoaps)." Langmuir **12**(15): 3590-3597 (1996).

Bai, G., M. Nichifor and M. Bastos "Cationic Polyelectrolytes as Drug Delivery Vectors: Calorimetric and Fluorescence Study of Rutin Partitioning†." The Journal of Physical Chemistry B **114**(49) (2010).

Bai, G., M. Nichifor, A. Lopes and M. Bastos "Thermodynamic characterization of the interaction behavior of a hydrophobically modified polyelectrolyte and oppositely charged surfactants in aqueous solution: Effect of surfactant alkyl chain length." The Journal of Physical Chemistry B **109**(1): 518-525 (2005).

Benrraou, M., B. Bales and R. Zana "Effect of the nature of the counterion on the interaction between cesium and tetraalkylammonium dodecylsulfates and poly (ethylene oxide) or poly (vinylpyrolidone)." Journal of colloid and interface science **267**(2): 519-523 (2003).

Berman, N. S. "Drag reduction by polymers." Annual Review of Fluid Mechanics **10**(1): 47-64 (1978).

Bewersdorff, H. W. "Rheology of drag reducing surfactant solutions." ASME-PUBLICATIONS-FED **237**: 25-30 (1996).

Bewersdorff, H. W. and D. Ohlendorf "The behaviour of drag-reducing cationic surfactant solutions." Colloid & Polymer Science **266**(10): 941-953 (1988).

Brackman, J. C. and J. B. F. N. Engberts "Effect of surfactant charge on polymer-micelle interactions: n-dodecyldimethylamine oxide." Langmuir **8**(2): 424-428 (1992).

Brostow, W., H. Ertepinar and R. Singh "Flow of dilute polymer solutions: chain conformations and degradation of drag reducers." Macromolecules **23**(24): 5109-5118 (1990).

Brostow, W., H. E. H. Lobland, T. Reddy, R. P. Singh and L. White "Lowering mechanical degradation of drag reducers in turbulent flow." Journal of materials research **22**(1): 56-60 (2007).

Carreau, P. J. "Rheological equations from molecular network theories." Journal of Rheology **16**: 99 (1972).

Chari, K., B. Antalek, M. Lin and S. Sinha "The viscosity of polymer–surfactant mixtures in water." The Journal of Chemical Physics **100**: 5294 (1994).

Chari, K., B. Antalek and J. Minter "Diffusion and scaling behavior of polymer-surfactant aggregates." Physical review letters **74**(18): 3624-3627 (1995).

Cho, S. H., C. S. Tae and M. Zaheeruddin "Effect of fluid velocity, temperature, and concentration of non-ionic surfactants on drag reduction." Energy conversion and management **48**(3): 913-918 (2007).

Cho, Y. and J. P. Harnett "Non-Newtonian fluids in circular pipe flow." Advances in heat transfer **15**: 59-141 (1982).

Choi, H. J., C. A. Kim, J. I. Sohn and M. S. Jhon "An exponential decay function for polymer degradation in turbulent drag reduction." Polymer degradation and stability **69**(3): 341-346 (2000).

Dan, A., S. Ghosh and S. P. Moulik "Physicochemistry of the Interaction between Inulin and Alkyltrimethylammonium Bromides in Aqueous Medium and the Formed Coacervates." The Journal of Physical Chemistry B **113**(25): 8505-8513 (2009).

Den Toonder, J., M. Hulsen, G. Kuiken and F. Nieuwstadt "Drag reduction by polymer additives in a turbulent pipe flow: numerical and laboratory experiments." Journal of Fluid Mechanics **337**(-1): 193-231 (1997).

Deo, P., N. Deo, P. Somasundaran, A. Moscatelli, S. Jockusch, N. J. Turro, K. Ananthapadmanabhan and M. F. Ottaviani "Interactions of a hydrophobically modified polymer with oppositely charged surfactants." Langmuir **23**(11): 5906-5913 (2007).

Diamant, H. and D. Andelman "Onset of self-assembly in polymer-surfactant systems." EPL (Europhysics Letters) **48**: 170 (1999).

Dodge, D. and A. Metzner "Turbulent flow of non Newtonian systems." AIChE Journal **5**(2): 189-204 (1959).

Escudier, M., F. Presti and S. Smith "Drag reduction in the turbulent pipe flow of polymers." Journal of non-newtonian fluid mechanics **81**(3): 197-213 (1998).

Feitosa, E., W. Brown and P. Hansson "Interactions between the Non-ionic Surfactant C12E5 and Poly (ethylene oxide) Studied Using Dynamic Light Scattering and Fluorescence Quenching." Macromolecules **29**(6): 2169-2178 (1996).

Fishman, M. and F. Elrich "Interactions of aqueous poly (N-vinylpyrrolidone) with sodium dodecyl sulfate. II. Correlation of electric conductance and viscosity measurements with equilibrium dialysis measurements." The Journal of Physical Chemistry **79**(25): 2740-2744 (1975).

Francois, J., J. Dayantis and J. Sabbadin "Hydrodynamical behaviour of the poly (ethylene oxide)-sodium dodecylsulphate complex." European polymer journal **21**(2): 165-174 (1985).

Frohnapfel, B., P. Lammers, J. Jovanovi and F. Durst "Interpretation of the mechanism associated with turbulent drag reduction in terms of anisotropy invariants." Journal of Fluid Mechanics **577**(-1): 457-466 (2007).

Gasljevic, K., G. Aguilar and E. Matthys "On two distinct types of drag-reducing fluids, diameter scaling, and turbulent profiles." Journal of non-newtonian fluid mechanics **96**(3): 405-425 (2001).

Goddard, E. D. and K. P. Ananthapadmanabhan, Interactions of surfactants with polymers and proteins, CRC press Boca Raton, FL (1993).

Graham, M. "Drag reduction in turbulent flow of polymer solutions." Rheology Reviews: 143 (2004).

Gyr, A. and H. W. Bewersdorff, Drag reduction of turbulent flows by additives, Kluwer Academic (Dordrecht and Boston) (1995).

Hansson, P. and B. Lindman "Surfactant-polymer interactions." Current opinion in colloid & interface science **1**(5): 604-613 (1996).

Harada, A. and K. Kataoka "Supramolecular assemblies of block copolymers in aqueous media as nanocontainers relevant to biological applications." Progress in polymer science **31**(11): 949-982 (2006).

Harwigsson, I. and M. Hellsten "Environmentally acceptable drag-reducing surfactants for district heating and cooling." Journal of the American Oil Chemists' Society **73**(7): 921-928 (1996).

Hellsten, M. "Drag-reducing surfactants." Journal of Surfactants and Detergents **5**(1): 65-70 (2002).

Hinch, E. "Mechanical models of dilute polymer solutions in strong flows." Physics of Fluids **20**: S22 (1977).

Hormnirun, P., A. Sirivat and A. Jamieson "Complex formation between hydroxypropylcellulose and hexadecyltrimethylamonium bromide as studied by light scattering and viscometry." Polymer **41**(6): 2127-2132 (2000).

Hunston, D. and J. Zakin "Flow assisted degradation in dilute polystyrene solutions." Polymer Engineering & Science **20**(7): 517-523 (1980).

Indartono, Y., H. Usui, H. Suzuki and Y. Komoda "Temperature and diameter effect on hydrodynamic characteristic of surfactant drag-reducing flows." Korea-Australia Rheology Journal **17**(4): 157-164 (2005).

Jiang, W. and S. Han "Viscosity of nonionic polymer/anionic surfactant complexes in water." Journal of colloid and interface science **229**(1): 1-5 (2000).

Jones, M. N. "The interaction of sodium dodecyl sulfate with polyethylene oxide." Journal of colloid and interface science **23**(1): 36-42 (1967).

Jönsson, B., B. Lindman, K. Holmberg and B. Kronberg, Surfactants and polymers in aqueous solution, John Wiley & Sons Chichester, UK (1998).

Jovanovi , J., M. Pashtrapanska, B. Frohnapfel, F. Durst, J. Koskinen and K. Koskinen "On the mechanism responsible for turbulent drag reduction by dilute addition of high polymers: Theory, experiments, simulations, and predictions." Journal of fluids engineering **128**: 118 (2006).

Kim, S. (2003). Turbulent drag reduction behavior of pseudoplastic fluids in straight pipes. Canada, University of Waterloo (Canada). **Ph.D.:** 335.

Kogej, K. and J. Škerjanc "Fluorescence and conductivity studies of polyelectrolyte-induced aggregation of alkyltrimethylammonium bromides." Langmuir **15**(12): 4251-4258 (1999).

Kwak, J. C. T., Polymer-surfactant systems, Volume 77 of Surfactant science series, Marcel Dekker (Ed.), New York (1998).

Liaw, G. C., J. L. Zakin and G. K. Patterson "Effects of molecular characteristics of polymers on drag reduction." AIChE Journal **17**(2): 391-397 (1971).

Lin, Z., Y. Zheng, H. Davis, L. Scriven, Y. Talmon and J. Zakin "Unusual effects of counterion to surfactant concentration ratio on viscoelasticity of a cationic surfactant drag reducer." Journal of non-newtonian fluid mechanics **93**(2-3): 363-373 (2000).

Lumley, J. "Drag reduction by additives." Annual Review of Fluid Mechanics **1**(1): 367-384 (1969).

Lumley, J. "Drag reduction in turbulent flow by polymer additives." Journal of Polymer Science: Macromolecular Reviews **7**(1): 263-290 (1973).

Ma, C. and C. Li "Interaction between polyvinylpyrrolidone and sodium dodecyl sulfate at solid/liquid interface." Journal of colloid and interface science **131**(2): 485-492 (1989).

Masuda, Y., K. Hirabayashi, K. Sakuma and T. Nakanishi "Swelling of poly (ethylene oxide) gel in aqueous solutions of sodium dodecyl sulfate with added sodium chloride." Colloid & Polymer Science **280**(5): 490-494 (2002).

Matras, Z., T. Malcher and B. Gzyl-Malcher "The influence of polymer-surfactant aggregates on drag reduction." Thin Solid Films **516**(24): 8848-8851 (2008).

Metzner, A. and A. Metzner "Stress levels in rapid extensional flows of polymeric fluids." Rheologica Acta **9**(2): 174-181 (1970).

Metzner, A. and M. G. Park "Turbulent flow characteristics of viscoelastic fluids." Journal of Fluid Mechanics **20**(02): 291-303 (1964).

Metzner, A. and J. Reed "Flow of non newtonian fluids—correlation of the laminar, transition, and turbulent flow regions." AIChE Journal **1**(4): 434-440 (1955).

Minatti, E. and D. Zanette "Salt effects on the interaction of poly (ethylene oxide) and sodium dodecyl sulfate measured by conductivity." Colloids and Surfaces A: Physicochemical and Engineering Aspects **113**(3): 237-246 (1996).

Mya, K. Y., A. M. Jamieson and A. Sirivat "Effect of temperature and molecular weight on binding between poly (ethylene oxide) and cationic surfactant in aqueous solutions." Langmuir **16**(15): 6131-6135 (2000).

Mysels, K. J. "Napalm. Mixture of Aluminum Disoaps." Industrial & Engineering Chemistry **41**(7): 1435-1438 (1949).

Nagarajan, R. "Thermodtnamics of surfactant-polymer interactions in dilute aqueous solutions." Chemical Physics Letters **76**(2): 282-286 (1980).

Nagarajan, R. (1989) "Association of nonionic polymers with micelles, bilayers, and microemulsions." The Journal of Chemical Physics **90** DOI: DOI:10.1063/1.456041.

Nikas, Y. and D. Blankschtein "Complexation of nonionic polymers and surfactants in dilute aqueous solutions." Langmuir **10**(10): 3512-3528 (1994).

Nilsson, S., M. Goldraich, B. Lindman and Y. Talmon "Novel organized structures in mixtures of a hydrophobically modified polymer and two oppositely charged surfactants." Langmuir **16**(17): 6825-6832 (2000).

Ohlendorf, D., W. Interthal and H. Hoffmann "Surfactant systems for drag reduction: physico-chemical properties and rheological behaviour." Rheologica Acta **25**(5): 468-486 (1986).

Pal, R. "Rheology of polymer-thickened emulsions." Journal of Rheology **36**: 1245 (1992).

Prajapati, K. "Interactions between drag reducing polymers and surfactants." MSc Thesis(University of Waterloo) (2009).
Prandtl, L., The essentials of fluid dynamics, Blackie & Son Limited (1963).
Prud'homme, R. K. and G. G. Warr "Elongational flow of solutions of rodlike micelles." Langmuir **10**(10): 3419-3426 (1994).
Ptasinski, P., F. Nieuwstadt, B. Van Den Brule and M. Hulsen "Experiments in turbulent pipe flow with polymer additives at maximum drag reduction." Flow, Turbulence and Combustion **66**(2): 159-182 (2001).
Qi, Y. and J. L. Zakin "Chemical and rheological characterization of drag-reducing cationic surfactant systems." Industrial & engineering chemistry research **41**(25): 6326-6336 (2002).
Rehage, H. and H. Hoffmann "Viscoelastic surfactant solutions: model systems for rheological research." Molecular Physics **74**(5): 933-973 (1991).
Romani, A. P., M. H. Gehlen and R. Itri "Surfactant-polymer aggregates formed by sodium dodecyl sulfate, poly (N-vinyl-2-pyrrolidone), and poly (ethylene glycol)." Langmuir **21**(1): 127-133 (2005).
Rothstein, J. P. "Strong flows of viscoelastic wormlike micelle solutions." Rheol. Rev: 1–42 (2008).
Ruckenstein, E., G. Huber and H. Hoffmann "Surfactant aggregation in the presence of polymers." Langmuir **3**(3): 382-387 (1987).
Savins, J. "A stress-controlled drag-reduction phenomenon." Rheologica Acta **6**(4): 323-330 (1967).
Schwuger, M. "Mechanism of interaction between ionic surfactants and polyglycol ethers in water." Journal of colloid and interface science **43**(2): 491-498 (1973).
Sellin, R. and E. Loeffler Drag reduction measurements with Poly (Acrylic Acid) under different solvent pH and salt conditions.(1977).
Sellin, R. H. J. and M. Ollis "Effect of pipe diameter on polymer drag reduction." Industrial & engineering chemistry product research and development **22**(3): 445-452 (1983).
Shah, S. N. and Y. Zhou "Maximum Drag Reduction Asymptote of Polymeric Fluid Flow in Coiled Tubing." Journal of fluids engineering **131**: 011201 (2009).
SHIRAHAMA, K., K. TSUJII and T. TAKAGI "Free-boundary electrophoresis of sodium dodecyl sulfate-protein polypeptide complexes with special reference to SDS-polyacrylamide gel electrophoresis." Journal of Biochemistry **75**(2): 309 (1974).
Sreenivasan, K. R. and C. M. White "The onset of drag reduction by dilute polymer additives, and the maximum drag reduction asymptote." Journal of Fluid Mechanics **409** (2000).
Stoll, M., H. Al-Shureqi, J. Finol, S. Al-Harthy, S. Oyemade, A. de Kruijf, J. Van Wunnik, F. Arkesteijn, R. Bouwmeester and M. Faber Alkaline-Surfactant-Polymer Flood: From the Laboratory to the Field. SPE EOR Conference at Oil & Gas West Asia, Muscat, Oman.(2010), DOI: 10.2118/129164-MS.
Streeter, V. L., E. B. Wiley and K. W. Bedford (1998). Fluid mechanics, WCB, McGraw-Hill.

Suksamranchit, S. and A. Sirivat "Influence of ionic strength on complex formation between poly (ethylene oxide) and cationic surfactant and turbulent wall shear stress in aqueous solution." Chemical Engineering Journal **128**(1): 11-20 (2007).

Suksamranchit, S., A. Sirivat and A. M. Jamieson "Polymer-surfactant complex formation and its effect on turbulent wall shear stress." Journal of colloid and interface science **294**(1): 212-221 (2006).

Sung, J. H., S. T. Lim, C. Am Kim, H. Chung and H. J. Choi "Mechanical degradation kinetics of poly (ethylene oxide) in a turbulent flow." Korea-Australia Rheology Journal **16**(2): 57-62 (2004).

Tabor, M. and P. G. Gennes "A cascade theory of drag reduction." EPL (Europhysics Letters) **2**: 519 (1986).

Tamano, S., M. Itoh, K. Kato and K. Yokota "Turbulent drag reduction in nonionic surfactant solutions." Physics of Fluids **22**: 055102 (2010).

Tesauro, C., B. Boersma, M. Hulsen, P. Ptasinski and F. T. M. Nieuwstadt "Events of high polymer activity in drag reducing flows." Flow, Turbulence and Combustion **79**(2): 123-132 (2007).

Thalberg, K., B. Lindman and G. Karlstroem "Phase diagram of a system of cationic surfactant and anionic polyelectrolyte: tetradecyltrimethylammonium bromide-hyaluronan-water." Journal of Physical Chemistry **94**(10): 4289-4295 (1990).

Thomas, A. and K. Wilson "New analysis of non newtonian turbulent flowndashyield power law fluids." The Canadian Journal of Chemical Engineering **65**(2): 335-338 (1987).

Thuresson, K., B. Nystroem, G. Wang and B. Lindman "Effect of surfactant on structural and thermodynamic properties of aqueous solutions of hydrophobically modified ethyl (hydroxyethyl) cellulose." Langmuir **11**(10): 3730-3736 (1995).

Thuresson, K., O. Söderman, P. Hansson and G. Wang "Binding of SDS to ethyl (hydroxyethyl) cellulose. Effect of hydrophobic modification of the polymer." The Journal of Physical Chemistry **100**(12): 4909-4918 (1996).

Tiederman, W. The effect of dilute polymer solutions on viscous drag and turbulent structure.(1989).

Toms, B. Some observations on the flow of linear polymer solutions through straight tubes at large Reynolds numbers, North Holland, Amsterdam.(1948).

Touhami, Y., D. Rana, G. Neale and V. Hornof "Study of polymer-surfactant interactions via surface tension measurements." Colloid & Polymer Science **279**(3): 297-300 (2001).

Trabelsi, S. and D. Langevin "Co-adsorption of carboxymethyl-cellulose and cationic surfactants at the air-water interface." Langmuir **23**(3): 1248-1252 (2007).

Usui, H., T. Itoh and T. Saeki "On pipe diameter effects in surfactant drag-reducing pipe flows." Rheologica Acta **37**(2): 122-128 (1998).

Usui, H., T. Kamada and H. Suzuki "Surfactant drag reduction caused by a cationic surfactant with excess addition of counter-ions." Journal of Chemical Engineering of Japan **37**(10): 1232-1237 (2004).

Vanapalli, S. A., S. L. Ceccio and M. J. Solomon "Universal scaling for polymer chain scission in turbulence." Proceedings of the National Academy of Sciences **103**(45): 16660 (2006).

Villetti, M. A., C. I. D. Bica, I. T. S. Garcia, F. V. Pereira, F. I. Ziembowicz, C. L. Kloster and C. Giacomelli "Physicochemical Properties of Methylcellulose and Dodecyltrimethylammonium Bromide in Aqueous Medium." The Journal of Physical Chemistry B **115**(19) (2011).

Virk, P. "Drag reduction fundamentals." AIChE Journal **21**(4): 625-656 (1975).

Virk, P. and E. W. Merrill (1969). "The Onset of Dilute Polymer Solution Phenomena". in Viscous Drag Reduction ,CS Wells(Ed.), , Plenum Press, New York**:** p107-130.

Virk, P. and D. Wagger (1989). Aspects of mechanisms in type B drag reduction. Structure of Turbulence and Drag Reduction, IUTAM Symposium Zurich, Switzerland.

Warholic, M., H. Massah and T. Hanratty "Influence of drag-reducing polymers on turbulence: effects of Reynolds number, concentration and mixing." Experiments in fluids **27**(5): 461-472 (1999).

Wei, T. and W. Willmarth "Examination of< em> v-velocity fluctuations in a turbulent channel flow in the context of sediment transport." Journal of Fluid Mechanics **223**(-1): 241-252 (1991).

Wilson, K. and A. Thomas "Analytic Model of Laminar Turbulent Transition for Bingham Plastics." The Canadian Journal of Chemical Engineering **84**(5): 520-526 (2006).

Wilson, K. C. and A. D. Thomas "A new analysis of the turbulent flow of non newtonian fluids." The Canadian Journal of Chemical Engineering **63**(4): 539-546 (1985).

Witte, F. M. and J. B. F. N. Engberts "Perturbation of SDS and CTAB micelles by complexation with poly (ethylene oxide) and poly (propylene oxide)." The Journal of Organic Chemistry **52**(21): 4767-4772 (1987).

Yan, P. and J. X. Xiao "Polymer-surfactant interaction: differences between alkyl sulfate and alkyl sulfonate." Colloids and Surfaces A: Physicochemical and Engineering Aspects **244**(1-3): 39-44 (2004).

Yoo, S. S. (1974). Heat transfer and friction factors for non-Newtonian fluids in turbulent pipe flow, University of Illinois at Chicago Circle.

Yu, B. and Y. Kawaguchi "Parametric study of surfactant-induced drag-reduction by DNS." International journal of heat and fluid flow **27**(5): 887-894 (2006).

Yu, J., J. Zakin and G. Patterson "Mechanical degradation of high molecular weight polymers in dilute solution." Journal of Applied Polymer Science **23**(8): 2493-2512 (1979).

Zakin, J. and D. Hunston "Effects of solvent nature on the mechanical degradation of high polymer solutions." Journal of Applied Polymer Science **22**(6): 1763-1766 (1978).

Zakin, J., Y. Zhang and W. Ge "Drag Reduction by Surfactant Giant Micelles." SURFACTANT SCIENCE SERIES **140**: 473 (2007).

Zakin, J., Y. Zhang, W. Ge, R. Zana and E. Kaler (2007). Giant Micelles: Properties and Applications, CRC Press Taylor and Francis Group, New York.

Zakin, J. L. (2010) "Polymer and Surfactant Drag Reduction in Turbulent Flows." Polymer Physics: From Suspensions to Nanocomposites and Beyond DOI: 10.1002/9780470600160.ch2.

Zakin, J. L., and Chang,Jl Nature Physical Science **239**(26) (1972).

Zakin, J. L., B. Lu and H. W. Bewersdorff "Surfactant drag reduction." Reviews in Chemical Engineering **14**(4-5): 253-320 (1998).

Zakin, J. L., B. Lu and H. W. BewersdorS "Surfactant Drag Reduction." Reviews in Chemical Engineering **14**(4-5): 67 (1998).

Zakin, J. L. and H. L. Lui "VARIABLES AFFECTING DRAG REDUCTION BY NONIONIC SURFACTANT ADDITIVES†." Chemical Engineering Communications **23**(1): 77-88 (1983).

Zakin, J. L., J. Myska and Z. Chara "New limiting drag reduction and velocity profile asymptotes for nonpolymeric additives systems." AIChE Journal **42**(12): 3544-3546 (1996).

Zakin, J. L., M. Poreh, A. Brosh and M. Warshavsky Exploratory study of friction reduction in slurry flows.(1971).

Zakin, J. L., Y. Zhang and Y. Qi "Drag Reducing Agents." (2006).

Zana, R., W. Binana-Limbelé, N. Kamenka and B. Lindman "Ethyl (hydroxyethyl) cellulose-cationic surfactant interactions: electrical conductivity, self-diffusion and time-resolved fluorescence quenching investigations." The Journal of Physical Chemistry **96**(13): 5461-5465 (1992).

Zhang, H., D. Wang and H. Chen "Experimental study on the effects of shear induced structure in a drag-reducing surfactant solution flow." Archive of Applied Mechanics **79**(8): 773-778 (2009).

Zhang, X., D. Taylor, R. Thomas and J. Penfold "The role of electrolyte and polyelectrolyte on the adsorption of the anionic surfactant, sodium dodecylbenzenesulfonate, at the air-water interface." Journal of colloid and interface science **365**(2): P:656-664 (2011).

Zhang, Y. (2005). Correlations among surfactant drag reduction, additive chemical structures, rheological properties and microstructures in water and water/co-solvent systems, The Ohio State University,Phd Thesis.

Zhang, Y., Y. Qi and J. L. Zakin "Headgroup effect on drag reduction and rheological properties of micellar solutions of quaternary ammonium surfactants." Rheologica Acta **45**(1): 42-58 (2005).

Zhang, Y., J. Schmidt, Y. Talmon and J. L. Zakin "Co-solvent effects on drag reduction, rheological properties and micelle microstructures of cationic surfactants." Journal of colloid and interface science **286**(2): 696-709 (2005).

Zheng, Y., Z. Lin, J. Zakin, Y. Talmon, H. Davis and L. Scriven "Cryo-TEM imaging the flow-induced transition from vesicles to threadlike micelles." The Journal of Physical Chemistry B **104**(22): 5263-5271 (2000).

Appendix A

Physical and chemical properties of materials used in this thesis

Octadecy trimethyl ammonium chloride

Identification

Name	Octadecy trimethyl ammonium chloride
Synonyms	Octadecyltrimethylammonium chloride; Steartrimonium chloride; Stearyl trimethyl ammoium chloride; Trimethyloctadecylammonium chloride; Aliquat 7
Molecular Structure	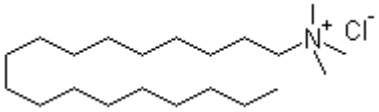
Molecular Formula	$C_{21}H_{46}N{\cdot}Cl$
Molecular Weight	348.05
CAS Registry Number	112-03-8
EINECS	203-929-1

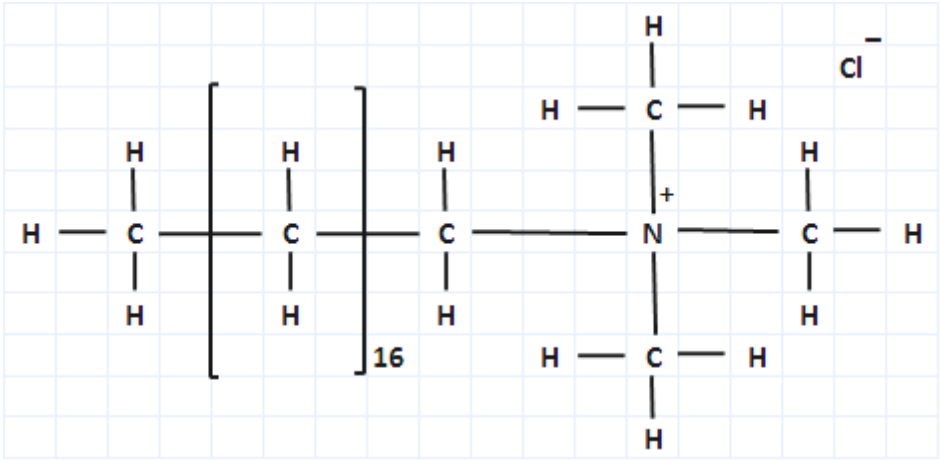

Molekula S.a.r.l.
Z.I. du Chapelier
St. Jean-de-Soudain
38110 La Tour du Pin
France
Tel: +33 (0) 6 19 11 96 97
Fax: +33 (0) 4 74 97 43 68

Molekula Ltd.
Technology House, Old Forge Road
Ferndown Industrial Estate
Wimborne Dorset BH21 7RR
United Kingdom
Tel: +44 (0) 1202 86 3000
Fax: +44 (0) 1202 86 3003

Molekula Life Sciences (P) Ltd
'Kanchan', 10, Umanagar
Begumpet,
Hyderabad 500 016
A.P. India
Tel: +91 (0) 40 6662 6366
Fax: +91 (0) 40 6682 6366

Molekula GmbH
Werk Nienburg
Grosse Drakenburger Str. 93-97
31582 Nienburg/Weser
Deutschland
Tel: +49 (0) 5021 988 341
Fax: +49 (0) 5021 988 342

Certificate of Analysis

Product	Octadecyltrimethylammonium chloride
Product Number	61986888(M67752390)
CAS Number	112-03-8
Batch Number	60802
Physical Appearance	White Powder
Purity(HPLC)	98.65%
Moisture	0.2%

molekula July 2007

SAFETY DATA SHEET

Product name:	STAC	Page:	1/7
Revision Date:	2010-02-25	Print date:	2010-03-24
		SDS-ID:	GB-EN/8.1

1. IDENTIFICATION OF THE SUBSTANCE/PREPARATION AND OF THE COMPANY/UNDERTAKING

Product name: STAC Container size: 20 kg

Application: Cosmetics industry.

Supplier:
FeF Chemicals A/S
København svej 216
DK-4600 Køge
Tel:+45 56 67 10 00
www.fefchemicals.com

Responsible for safety data sheet authoring. Any questions to the contents of this safety data sheet should be sent to:
SDS_info@dhigroup.com

2. HAZARDS IDENTIFICATION

The product is classified:
67/548/EEC: Xn;R22 Xi;R38-41 N;R50
GHS/CLP: Acute Tox. 4;H302 - Skin Irrit. 2;H315 - Eye Dam. 1;H318 - Aquatic Acute 1;H400

Human health: Harmful if swallowed. Causes serious eye damage. Causes skin irritation.

Environment: Very toxic to aquatic life.

3. COMPOSITION/INFORMATION ON INGREDIENTS

The product contains: quaternary ammonium compounds.

67/548/EEC

%:	CAS-No.:	EC No.:	Chemical name:	Hazard classification:	Notes:
100	112-03-8	203-929-1	Trimethyloctadecylammonium chloride	Xn;R22 Xi;R38-41 N;R50	

GHS/CLP

%:	CAS-No.:	EC No.:	Chemical name:	Hazard classification:	Notes:
100	112-03-8	203-929-1	Trimethyloctadecylammonium chloride	Acute Tox. 4;H302 - Skin Irrit. 2;H315 - Eye Dam. 1;H318 - Aquatic Acute 1;H400	

MATERIAL SAFETY DATA SHEET

1. Product and Company Identification

Material name	**STEPWET DF-95**
Version #	29
Revision date	09-13-2011
Product code	0615
Chemical class	Alkyl sulfate
Manufacturer	Stepan Company 22 West Frontage Road Northfield, IL 60093
Emergency	Medical 800-228-5635 Chemtrec 800-424-9300 Chemtrec Int'l 703-527-3887
General information	General (847) 446-7500

2. Hazards Identification

Emergency overview

WARNING
Product may form explosive dust/air mixtures if high concentration of product dust is suspended in air.
Contact with eyes may cause irritation. Contact with skin may cause irritation. May cause irritation of respiratory tract.

Potential health effects

Eyes	Moderately irritating to the eyes.
Skin	This product may cause irritation to the skin.
Inhalation	Inhalation of dusts may cause respiratory irritation.
Ingestion	Ingestion of large amounts may produce gastrointestinal disturbances including irritation, nausea, and diarrhea.

3. Composition / Information on Ingredients

Components	CAS #	Percent
Sodium sulfate	7757-82-6	< 3.5
Water	7732-18-5	< 2
_Lauryl alcohol	112-53-8	< 3.5
_Sodium chloride	7647-14-5	< 2
_Sodium lauryl sulfate	151-21-3	> 93

4. First Aid Measures

First aid procedures

Eye contact	Hold eyelids apart and immediately flush eyes with plenty of water for at least 15 minutes . Get medical attention immediately.
Skin contact	For skin contact flush with large amounts of water. Get medical attention if irritation develops or persists. Immediately take off all contaminated clothing. Wash clothing separately before reuse.
Inhalation	If symptoms are experienced, remove source of contamination or move victim to fresh air. If symptoms persist, get medical attention. If the affected person is not breathing, apply artificial respiration. If breathing is difficult, give oxygen. Get medical attention immediately.
Ingestion	If ingestion of a large amount does occur, seek medical attention. Do NOT induce vomiting.

5. Fire Fighting Measures

Flammable properties

Dust accumulation from this product may present an explosion hazard in the presence of an ignition source. Fire hazard. Class II Dust for National Electric Code (NFPA 70)

Stepan

Product Bulletin

AGRICULTURE

STEPWET® DF-95 and DF-95 Needles

Product Name

Chemical Description

Sodium Lauryl Sulfate

CAS Registry No.

151-21-3

Applications

STEPWET DF-95 is a high active anionic wetting agent. The product is available as a spray dried powder, STEPWET DF-95, or extruded needles, STEPWET DF-95 Needles. Both products are free flowing and provide rapid, efficient granule wetting and breakup when added to a pesticide. STEPWET DF-95 wetting agents can be used in water dispersible granules and wettable powders.

Typical Properties

		STEPWET DF-95	STEPWET DF-95 Needles
Appearance		Free flowing white powder	Free flowing white needles
Activity, %		93	93
Moisture, %		2	2
pH, 1% in H_2O		9.8	9.8
Density, lb./cu. ft.		25	38
Flash Point, °C (°F)		>94 (>201)	>94(>201)
RVOC, U.S. EPA, %		0	0
Solubility	Water	Soluble	Soluble
	Methanol	Insoluble	Insoluble
	Kerosene	Insoluble	Insoluble
	Xylene	Insoluble	Insoluble

Other Data

DOT Classification ..... Non Hazardous

Biodegradability

Products are readily biodegradable. A detailed biodegradability statement is available upon request.

Toxicity

STEPWET DF-95 wetting agents are slightly toxic orally (LD_{50} is between 0.8-1.1 g/kg) and cause moderate skin and eye irritation at 10% active.

Storage & Handling

Normal safety precautions (i.e. gloves and safety goggles) should be employed when handling STEPWET DF-95 wetting agents. Contact with the eyes and prolonged contact with the skin should be avoided. To avoid inhalation of particles, wear a dust mask when handling. Wash thoroughly after handling materials.

Storage Information: It is recommended that STEPWET DF-95 wetting agents be stored in sealed containers and kept in a dry place.

Standard Packaging: STEPWET DF-95 is available in drums (200 lb, 91 kg) and in bulk quantities. STEPWET DF-95 Needles is available in bags (55 lb, 25 kg).

Clearances

STEPWET DF-95 wetting agents are approved for use as inert ingredients under U.S. EPA 40 CFR 180.910 and 180.930.

STEPWET DF-95 wetting agents are listed in Europe (EINECS 205-788-1), Japan (ENCS 2-1679), Canada (DSL 151-21-3), and Australia (AICS 151-21-3).

March 2009
Supercedes: June 2003

2. COMPOSITION INFORMATION

Component	CAS #	Amount (%W/W)
Poly(ethylene oxide)	25322-68-3	>= 95 %
Fumed silica (generic)	112945-52-5	<= 3%
Calcium as mixed salts	Not available	<= 1%
BHT	128-37-0	<= 0.1%
Ammonia	7664-41-7	<= 0.02%
Monoethylamine	75-04-7	<= 0.02%
Ethylene oxide	75-21-8	<= 0.001%

3. HAZARDS IDENTIFICATION

3.1 EMERGENCY OVERVIEW

Appearance White to off-white

Physical State Powder

Odor Ammoniacal

Hazards of product WARNING! CAUSES EYE IRRITATION.
STATIC IGNITION HAZARD CAN RESULT FROM HANDLING AND USE.
DUST DISPERSED IN AIR MAY BE IGNITED AND BURN RAPIDLY.
PLASTIC CONTAINER, IF PRESENT, MAY CAUSE STATIC IGNITION HAZARD.
SLIPPERY WHEN WET.

3.2 POTENTIAL HEALTH EFFECTS

hyperdrill® AF 207

ANIONIC DRY SHALE INHIBITOR

DESCRIPTION

HYPERDRILL® AF 207 is a high molecular weight, medium charge, polyacrylamide supplied as a dry granular powder. It has excellent handling characteristics, mixes easily and dissolves quickly when added to water-based fluid systems.

TYPICAL PROPERTIES

Appearance:	White Granular Powder
Ionic Character:	Anionic
Bulk Density:	0.8 gr/cc (50 lbs./cu. ft.)
pH of 0.5% Soln. @ 25°C:	6.0 - 8.0

APPLICATIONS

HYPERDRILL® AF 207 is a very versatile polymer which can be used for oil, gas, water well and mineral drilling. It can be added to fresh, KCL or sea water based drilling fluid systems. **HYPERDRILL® AF 207** functions primarily as a:

- SHALE INHIBITOR
- VISCOSIFIER
- FLOW LINE FLOCCULANT
- FRICTION REDUCER/LUBRICANT
- FOAM STABILIZER

PRINCIPAL FUNCTIONS

Shale Inhibitor

HYPERDRILL® AF 207 can be used alone or in conjunction with KCL to stabilize active shales by decreasing the shale's tendency to absorb water, swell and slough-off. As an additional benefit, fluid loss is often reduced when using this product. The recommended dosage rate is 0.25 - 1.0 ppb as supplied.

Viscosifier

The addition of 0.5 - 1.0 ppb of **HYPERDRILL® AF 207** is a cost effective way to generate viscosity in fresh or low salinity drilling fluids. It's shear thinning capacity assures maximum power at the bit under high shear while retaining excellent carrying capacity under low shear conditions.

Flow Line Flocculant

HYPERDRILL® AF 207 can also be utilized for clear water or low solids drilling. The addition of a 0.5% solution of **HYPERDRILL® AF 207** into the flow line or just prior to any mechanical separation equipment will greatly enhance the removal of drill solids.

Friction Reducer

The addition of **HYPERDRILL® AF 207** into a drilling fluid will help reduce turbulent flow, friction and power losses at points of high shear. Lowering turbulent flow also helps reduce erosion and washouts of fragile geologic structures.

Foam Stabilizer

HYPERDRILL® AF 207 assists in foam drilling by creating a very stable foam, thereby increasing foam life. This results in enhanced cuttings removal and reduced water requirements. The product is compatible with most commonly used foamers.

PACKAGING

HYPERDRILL® AF 207 is supplied in 50 lb. (net), multi-walled, polyethylene-lined, paper bags, packed 30 to a shrink-wrapped pallet or in 1500 lb. (net) bulk bags.

STORAGE

HYPERDRILL® AF 207 should be stored inside under cool dry conditions. When stored under these conditions, the product has a shelf life of at least one year.

HEALTH AND SAFETY

HYPERDRILL® AF 207 exhibits a low order of toxicity. However, precautions should be taken to avoid inhalation, ingestion or contact with skin or eyes. For additional information, see the relevant MSDS.

SPILLS: Polymer spills are extremely slippery and therefore hazardous. They should be addressed immediately. Dry polymer spills should be left dry, swept up and disposed of according to local, state or federal regulations. If the polymer becomes wet, an absorbent material should be applied to the spill, then swept up and discarded. **Do not add water to a spill.**

TDS/207/V2/1-97

hychem, inc.

10014 North Dale Mabry Highway, Suite 213, Tampa, FL 33618 • Tel: (813) 963-6214 • FAX: (813) 960-0175

Appendix B

Apparatus specification

1- Pressure transducers

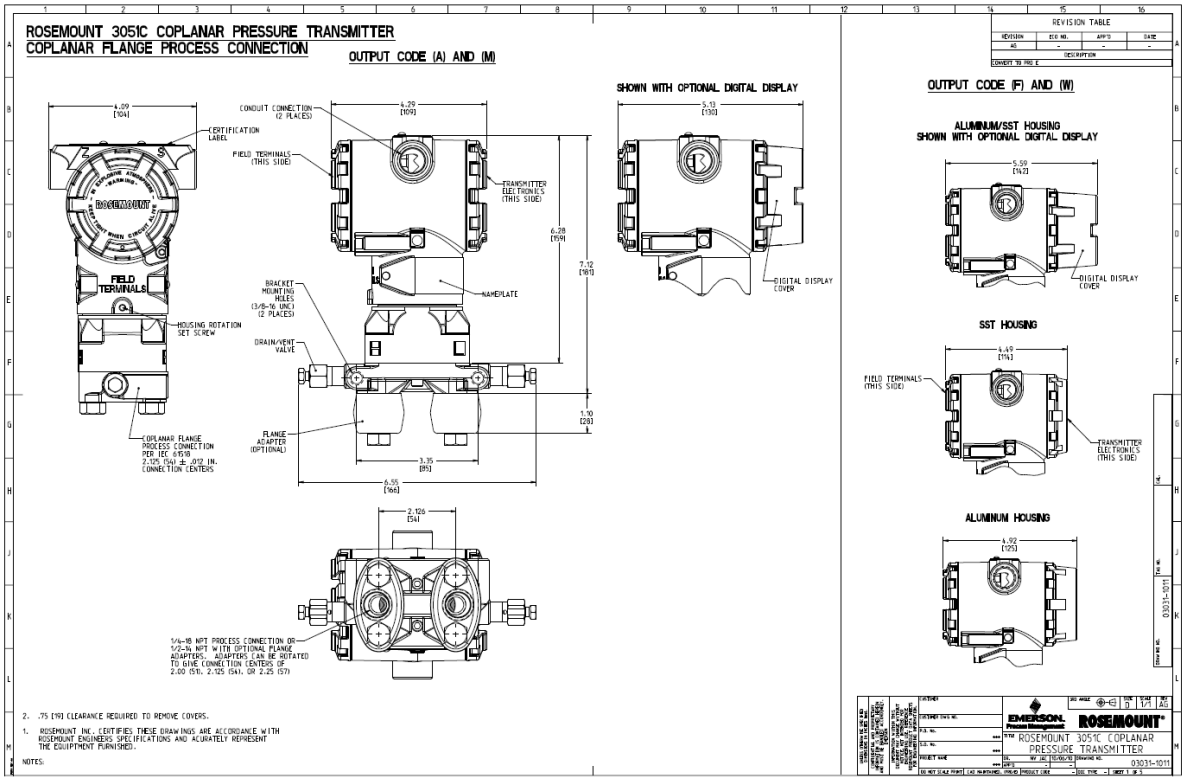

Manifold Operation

⚠ Improper installation or operation of manifolds may result in process leaks, which may cause death or serious injury.

Always perform a zero trim on the transmitter/manifold assembly after installation to eliminate any shift due to mounting effects. See Section 4 Operation and Maintenance, "Sensor Trim Overview" on page 4-5.

Three and five-valve configurations shown:

In normal operation the two block valves between the process and instrument ports will be open and the equalizing valve will be closed.

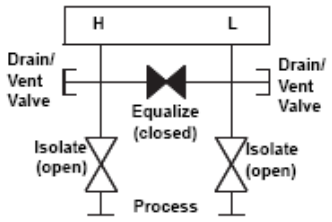

1. To zero the 3051S, close the block valve to the low pressure (downstream) side of the transmitter first.

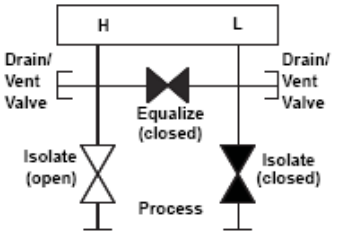

2. Open the center (equalize) valve to equalize the pressure on both sides of the transmitter. The manifold valves are now in the proper configuration for zeroing the transmitter.

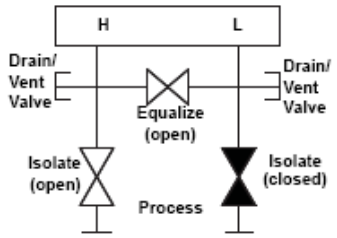

3. After zeroing the transmitter, close the equalizing valve.

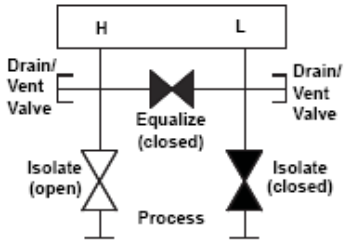

4. Open the block valve on the low pressure side of the transmitter to return the transmitter to service.

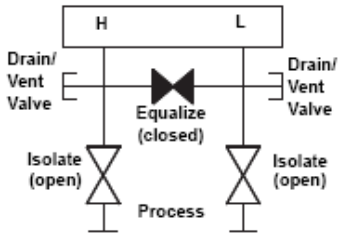

Transmitter Total Performance

Total performance is based on combined errors of reference accuracy, ambient temperature effect, and line pressure effect.

Models		Ultra	Classic	Ultra for Flow[1]
3051S_CD	Ranges 2-3	±0.1% of span; for ±50°F (28°C) temperature changes; 0-100% relative humidity, up to 740 psi (51 bar) line pressure (DP only), from 1:1 to 5:1 rangedown	±0.15% of span; for ±50°F (28°C) temperature changes; 0-100% relative humidity, up to 740 psi (51 bar) line pressure (DP only), from 1:1 to 5:1 rangedown	±0.1% of reading; for ±50°F (28°C) temperature changes; 0-100% relative humidity, up to 740 psi (51 bar) line pressure, over 8:1 DP turndown from URL
3051S_CG	Ranges 2-5			
3051S_CA	Ranges 2-4			
3051S_T	Ranges 2-4			
3051S_L		*Use Instrument Toolkit or the QZ Option to quantify the total performance of a remote seal assembly under operating conditions.*		

(1) Ultra for Flow is only available for 3051S_CD Ranges 2-3.

Long Term Stability

Models		Ultra and Ultra for Flow[1]	Classic
3051S_CD	Ranges 2-5	±0.20% of URL for 10 years; for ±50°F (28°C) temperature changes, up to 1000 psi (68,9 bar) line pressure	±0.125% of URL for 5 years; for ±50°F (28°C) temperature changes, up to 1000 psi (68,9 bar) line pressure
3051S_CG	Ranges 2-5		
3051S_CA	Ranges 1-4		
3051S_T	Ranges 1-5		

(1) Ultra for Flow is only available on 3051S_CD ranges 2-3.

2-Flowmeter

KROHNE

CERTIFICATE ISSUED BY
Krohne Ltd
Rutherford Drive
Park Farm Industrial Estate
Wellingborough
Northants NN8 6AE
Tel: +44 (0) 1933 408 500
Fax: +44 (0) 1933 408 501

CERTIFICATE OF CALIBRATION
CALIBRATION-ZERTIFIKAT
CERTIFICAT DE CALIBRATION
In acc. with / gemäß / selon ISO /IEC 17025

Date of issue: 02/02/2007
Date of calibration: 01/02/2007
Certificate No: 02400932_R029228/M
Page 1 of 1 pages

SENSOR DATA

Type	:	OPTIMASS 7050C S25			
Ser. No	:	02400932			
Tag No	:				
CF1	:	19.1	CF11	:	28.491686
CF2	:	513.85	CF12	:	-26.241611
CF3	:	300	CF13	:	112.20409
CF4	:	18.14304	CF14	:	0
CF5	:	313238.5	CF15	:	-2.4570854
CF6	:	-20.782412	CF16	:	0
CF7	:	315.39438	CF17	:	-0.45
CF8	:	0	CF18	:	0
CF9	:	23.636065	CF19	:	173.51563
CF10	:	1073.5414	CF20	:	4961.3838

TEST EQUIPMENT DATA

Weighing Scale Type	:	ID1+/KCC300
Scale Serial Number	:	2492804/2491654
Scale Calibration Date	:	19/09/2006
Scale Certificate Number	:	PT1509
Calibration Fluid	:	Water
No. Of Calibration Points	:	3
No. Of Test Runs/Point	:	Minimum 2
Flow Rig Uncertainty (1)	:	0.035%

The calibration was performed in mass flow rigs using static weighing techniques in start / stop operation. All weighing scales are annually calibrated by a UKAS accredited laboratory.

CALIBRATION RESULT – KALIBRIER RESULTAT – RESULTATS DE TESTS

The following data is the average of several flow runs at each cardinal point.

FLOW RATE (% Nominal)	SET FLOW RATE (kg/h)	MEASURED MASS (kg)	ACTUAL MASS (kg)	ERROR (% Rate)
12	4295	162.5344	162.1093	0.262
51	17462	199.5293	199.3558	0.087
78	26962	183.8033	183.6455	0.086

Name Signature

TUV UKQA

ISO 9001 CERT No GB00187

(1) The reported expanded uncertainty is based on a standard uncertainty multiplied by a coverage factor k=2, providing a level of confidence of approximately 95%. The uncertainty evaluation has been carried out in accordance with UKAS requirements. The equipment complies with the stated specification, as data sheet 7.02445.24.00, at the measured points, due allowance having been made for the uncertainty of measurements, comprising of flow rig uncertainty and specified repeatability.

FE-Serial No	FE-SW	BE-Serial No	BE-SW	Connections
00604566	V2.0	00632862	V1.28	1" ANSI 150 lb

QUALITY DOCUMENT DO NOT DESTROY!

Vertical mounting

Horizontal mounting

Upward sloping installation

Avoid mounting the meter with long vertical drops after the meter. This could cause siphoning and cause measurement errors.

Avoid mounting the meter at the highest point in the pipeline. Air or gas can accumulate here and cause faulty measurements

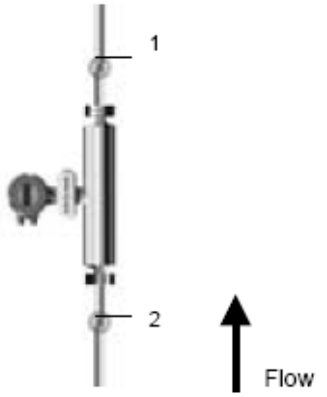

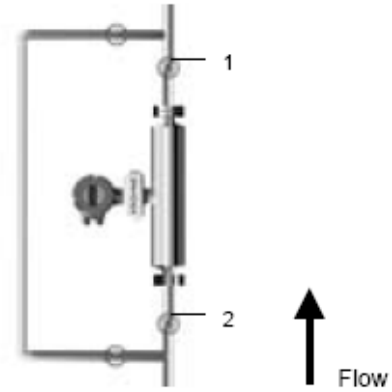

1 Valve for zeroing flow meter
2 The second valve is recommended if the pump is switched off to prevent reverse flow

To enable a good zero to be done, it is recommended that a shut-off valve be installed downstream of the flow meter.

Secondary Pressure containment
The 7000 and 7100 Series meters are supplied with secondary pressure containment as standard.

Allowable maximum secondary containment pressures are as follows:

7000 Series	63 bar at 20°C
	914 psig at 70°F
7100 Series	30 bar (63 bar optional) at 20°C
	435 psig (914 psig optional) at 70°F

If the user suspects that the primary tube has failed, the unit must be depressurised and removed from service as soon as possible.

Note:
In the 7000 Series there are high pressure feed through seals and 'O' rings that might not be compatible with the process fluid for an extended period if a primary tube fails.
It is important to remove the meter ASAP

It is the users responsibility to ensure that the materials used are compatible with this product. Other 'O' ring materials are available on request.

1.2 MFS 7000 Single Straight Tube Meter

- Tighten flange bolts evenly.
- Observe min and max pipe end loads at end of this section.

The use of reducers at the flanges is allowed. Extreme pipe size reductions should be avoided due to possibility of cavitation and degassing.

There are no additional installation requirements for the MFS 7000 sensors. Fixing of flexible hoses directly on the meter is allowed.

1.2.1 Ambient / Process temperatures

The specified and approved ambient and process temperatures must be observed (see specifications).

Note:
Where meters are mounted in direct sunlight, it is recommended to install a sunshade. This is particularly important in countries with high ambient temperatures.

The maximum differential temperature between the process and ambient temperature without insulation is 130°C or 265°F for Titanium and 80°C or 115°F for Hastelloy and Stainless Steel meters.

3- Conductivity

Product Specifications

The Thermo Scientific Orion 3-Star Plus conductivity meters work for a variety of applications and liquid purities.

Thermo Scientific Orion 3-Star Plus

Conductivity Meters

Features and Benefits

- Simultaneous display of conductivity, resistivity, TDS or salinity and temperature measurements on the backlit LCD
- The Thermo Scientific Orion SMART STABILITY™ and SMART AVERAGING™ functions for automatically optimized accuracy, precision and response time
- Meet all U.S. Pharmacopeia (USP) requirements
- Accept cell constants from 0.001 to 199.9 cm^{-1}
- Compatible with 2-electrode and 4-electrode conductivity cells
- Temperature calibration capability
- Conductivity / TDS / salinity / resistivity calibration of up to 5 points
- Reading reference temperatures at 5 °C, 10 °C, 15 °C, 20 °C or 25 °C
- Storage of up to 10 individually password-protected methods for easy retrieval of operation procedures
- Datalog up to 1000 points with time and date stamp
- RS232 port for easy data downloading and software updates
- Benchtop units can control an autosampler and the 096010 stirrer probe (*each sold separately*)
- Benchtop units are splashproof with an IP54-rated housing and include a universal power supply
- Portable units are waterproof with an IP67-rated housing and run for over 2,000 hours on four AA batteries
- 3 year meter warranty

Part of Thermo Fisher Scientific

Thermo SCIENTIFIC

Thermo Scientific Orion 3-Star Plus Conductivity Meters

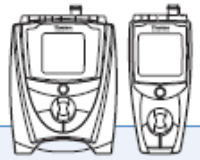

Conductivity	Range	0.000 to 3000 mS/cm, auto resolution with cell constant dependence
	Resolution	4 significant digits down to 0.001 µS/cm, cell constant dependent
	Relative Accuracy	0.5% ± 1 digit or 0.01 µS/cm, whichever is greater
	Cell Constants	0.001 to 199.9
Resistivity	Range	0.0001 to 100 Megohm
	Resolution	Automatic
	Relative Accuracy	0.5 % ± 1 digit
Salinity	Range	0.1 to 80.0 ppt NaCl equivalent, 0.1 to 42 ppt practical salinity
	Resolution	0.1
	Relative Accuracy	± 0.1 ± 1 digit
TDS	Range	0 to 19999
	Resolution	1 mg/L
	Relative Accuracy	± 0.5 % ± 1 digit
Temperature	Range	- 5 to 105 °C
	Resolution	0.1 up to 99.9 °C, 1.0 over 99.9 °C
	Relative Accuracy	± 0.1 °C

Meters Only

Cat. No.	Package
1114000	Includes benchtop meter, universal power and user guide
1214000	Includes portable meter, batteries and user guide

Benchtop Meter Kits

Cat. No. / *Application*	Sensor (s)	Accessories and Solutions
1114001 / *Fresh Water Wastewater*	• 013005MD DuraProbe conductivity cell, K = 0.475, 1 µS/cm to 200 mS/cm	• 1413 µS/cm conductivity standard (5 x 60 mL bottles) • Swing arm electrode stand
1114002 / *Ultra Pure Water*	• 013016MD Conductivity cell, K = 0.1, includes flow cell, 0.01 µS/cm to 300 µS/cm	• 100 µS/cm conductivity standard (5 x 60 mL bottles) • Swing arm electrode stand
1114003 / *Ultra Pure Water*	• 013016MD Conductivity cell, K = 0.1, includes flow cell, 0.01 µS/cm to 300 µS/cm	• 100 µS/cm conductivity standard (5 x 60 mL bottles) • Conductivity calibration resistor kit • Star Navigator 21 software with RS232 computer cable • Swing arm electrode stand

Portable Meter Kits

Cat. No. / *Application*	Sensor (s)	Accessories and Solutions
1214001 / *Fresh Water Wastewater*	• 013005MD DuraProbe conductivity cell, K = 0.475, 1 µS/cm to 200 mS/cm	• 1413 µS/cm conductivity standard (10 x 15 mL pouches) • Hard field case
1214002 / *Ultra Pure Water*	• 013016MD Conductivity cell, K = 0.1, includes flow cell, 0.01 µS/cm to 300 µS/cm	• 100 µS/cm conductivity standard (5 x 60 mL bottles)
1214003 / *Fresh Water Wastewater*	• 013610MD Conductivity cell, K = 0.55, includes 3 meter cable, 10 µS/cm to 200 mS/cm)	• 1413 µS/cm conductivity standard (10 x 15 mL pouches) • Hard field case
1214004 / *Ultra Pure Water*	• 013016MD Conductivity cell, K = 0.1, includes flow cell, 0.01 µS/cm to 300 µS/cm	• 100 µS/cm conductivity standard (5 x 60 mL bottles) • Hard field case
1214501 / *Fresh Water Wastewater*	• 013005MD DuraProbe conductivity cell, K = 0.475, 1 µS/cm to 200 mS/cm	• 1413 µS/cm conductivity standard (10 x 15 mL pouches) • Soft field case
1214503 / *Fresh Water Wastewater*	• 013610MD DuraProbe conductivity cell, K = 0.55, includes 3 meter cable, 10 µS/cm to 200 mS/cm	• 1413 µS/cm conductivity standard (10 x 15 mL pouches) • Soft field case
1214504 / *Ultra Pure Water*	• 013016MD Conductivity cell, K = 0.1, includes flow cell, 0.01 µS/cm to 300 µS/cm	• 100 µS/cm conductivity standard (5 x 60 mL bottles) • Soft field case
1214101 / *Fresh Water Wastewater*	• 013005MD DuraProbe conductivity cell, K = 0.475, 1 µS/cm to 200 mS/cm	—

S-3STARCD-E 0408 RevA

Environmental Instruments
Water Analysis Instruments

North America
166 Cummings Center
Beverly, MA 01915 USA
Toll Free: 1-800-225-1480
Tel: 1-978-232-6000
Dom. Fax: 1-978-232-6015
Int'l Fax: 978-232-6031

Europe
Denmark House, Angel Drove
Ely, Cambridgeshire
England, CB7 4ET
Tel: 44-1353-666111
Fax: 44-1353-666001

Asia Pacific
Blk 55, Ayer Rajah Crescent
#04-16/24, Singapore 139949
Tel: 65-6778-6876
Fax: 65-6773-0836

www.thermo.com/water

4-Tensiometer

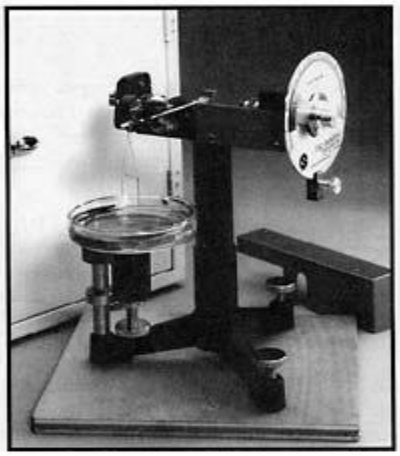

Direct Reading – circular scale is graduated in dynes/cm

Reproducible Results – readings can be reproduced to within +/- 0.05 dyne/cm. This precision instrument provides precise readings of upward interfacial and surface tensions by the ring method to values reproducible to within + /- 0.05 dyne/cm. It is specified for determining interfacial tension of oil against water by the ring method (ASTM Std. D971); for testing solutions of surface-active agents (ASTM Std. C1331); for testing synthetic rubber lattices (ASTM Std. D1417); and for determining the surface tension of industrial water and industrial wastewater (ASTM Std. D1590). **(Source:** http://www.cscscientific.com/surface-tension/tensiometer/ **)**

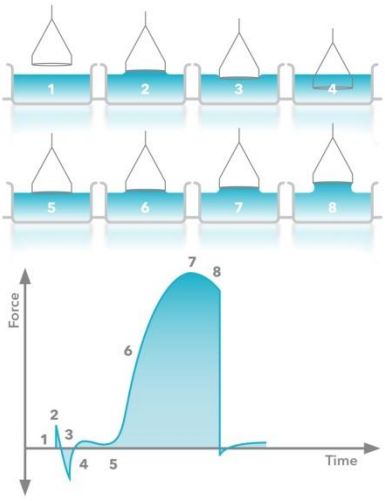

Source:

http://www.attension.com/surface-tension.aspx

1- The ring is above the surface and the force is zeroed.
2- The ring hits the surface and there is a slight positive force due to the adhesive force between ring and surface.
3- The ring must be pushed through the surface (due to the surface tension) which causes a small negative force.
4- The ring breaks through the surface and a small positive force is measured due to the supporting wires of the ring.
5- When lifted through the surface the measured force starts to increase.
6- The force keeps increasing until
7- The maximum force is reached
8- After the maximum there is a small decrease of in the force until the lamella breaks.

A	Knurled Knob	J	Wire Retaining Screw
B	Sample Table Adjustment Screw	K	Rear Clamp Spring Support
C	Dial Clamp	L	Base Leveling Screw
D	Adjustable Stops	M	Torsion Arm
F	Fine Adjustment Screw	R	Cap
G	Adjustment Nut	S	Dial
H	Hook	T	Sample Table
I	Index	V	Vernier
		Y	Torsion Wire Cover

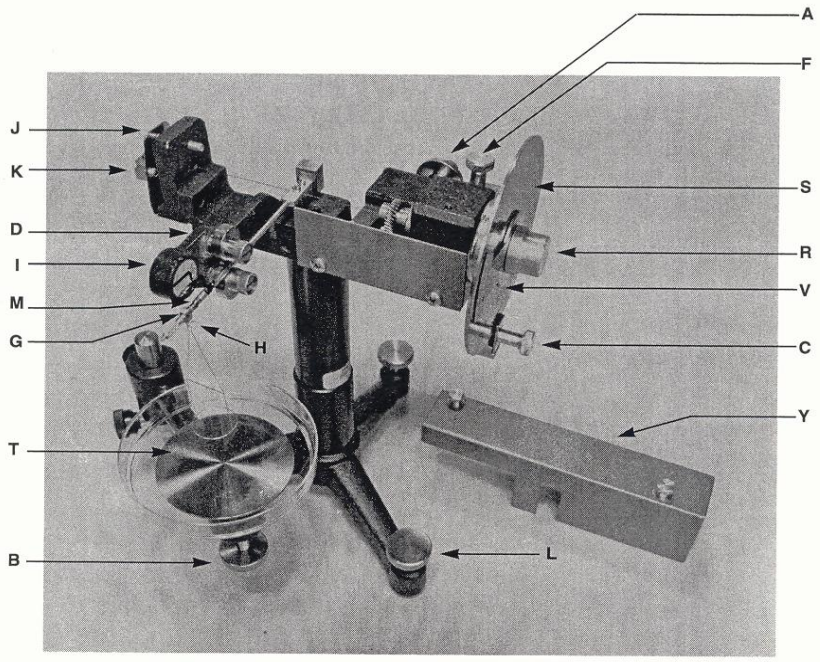

FIG. 1 – TENSIOMETER NO. 70535

Source: http://www.cscscientific.com/surface-tension/tensiometer/

A	Knurled Knob	L	Base Leveling Screw
B	Sample Table Adjustment Screw	M	Torsion Arm
C	Dial Clamp	N	Knurled Release
D	Adjustable Stops	P	Vertical Arm
E	Counter Weight	R	Cap
F	Fine Adjustment Screw	S	Dial
G	Adjustment Nuts	T	Sample Table
I	Index	V	Vernier
J	Wire Retaining Screw	X	Clamping Jaws
K	Rear Clamp Spring Support	Y	Torsion Wire Cover

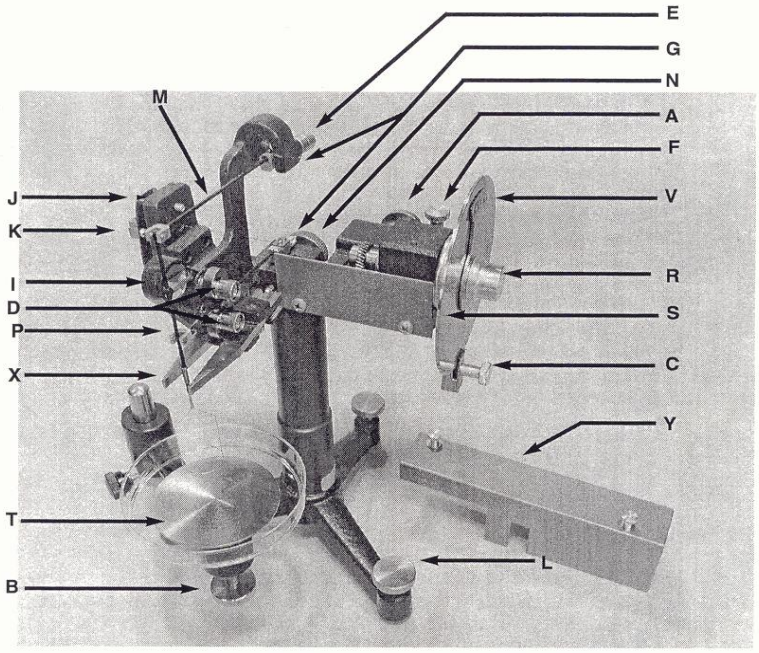

FIG. 2 - TENSIOMETER NO. 70545

Source: http://www.cscscientific.com/surface-tension/tensiometer/

Appendix C: Bench scale and Pipeline flow experimental data

a) Bench scale data

Specific viscosity of pure PEO in DI water

PEO ppm	Time(sec) Average	Specific Viscosity
50	119.04	0.035
100	128.03	0.1133
200	149.88	0.303
500	217.54	0.892
700	272.83	1.372
1000	379.74	2.302
1200	447.31	2.890
1400	520	3.522
1700	744.66	5.475
2000	1018.00	7.852
Pure water	115.00	-

500 ppm PEO apparent viscosity

Shear rate(1/s)	Dial Reading	Shear stress(Pa)	Apparent viscosity(Pa.s)
175.7	6.5	0.203	0.00116
316.3	8.5	0.379	0.00120
351.5	8.5	0.379	0.00108
527.2	11.5	0.644	0.00122
1054.4	19	1.305	0.00124

1000ppm PEO apparent viscosity

Shear rate(1/s)	Dial Reading	Shear stress(Pa)	Apparent viscosity(Pa.s)
158.2	10.0	0.512	0.00324
175.7	10.5	0.556	0.00316
316.3	15.5	0.996	0.00315
351.5	16.0	1.040	0.00296
527.2	22.0	1.569	0.00298
1054.4	38	2.978	0.00283

2000 ppm PEO apparent viscosity

Shear rate(1/s)	Dial Reading	Shear stress(Pa)	Apparent viscosity(Pa.s)
105.4	14	0.864	0.00819
158.2	18	1.216	0.00769
175.7	19	1.305	0.00742
316.3	28	2.097	0.00663
351.5	30	2.274	0.00647
527.2	39	3.067	0.00582
105.4	14	0.864	0.00819

Average relative viscosity of PAM in DI water

PAM	Time(sec)	Relative viscosity	Specific viscosity
20	147	1.371	0.397
40	180	1.683	0.715
60	217	2.031	1.069
80	250	2.335	1.380
100	288	2.688	1.740

150	385	3.600	2.668
200	489	4.566	3.653
250	610	5.698	4.806
300	743	6.941	6.073
400	1077	10.070	9.261
600	1950	18.224	17.571
800	3304	30.879	30.467
1000	5326	49.776	49.724
water	107.2		

Average relative viscosity of PAM in tap Water

PAM concentration ppm	Average viscosity in sec	Relative viscosity	Specific viscosity
100	136.9	1.23	0.229
300	214.5	1.93	0.927
500	305.5	2.74	1.744
700	427.2	3.84	2.837
900	591.2	5.31	4.310
1000	702.3	6.31	5.308
1300	1126.6	10.12	9.119
1700	2272.0	20.41	19.409
	111.3	<------ Tap Water	

Surfactant concentration ppm	DI water	Average Conductivity microS/cm	Avg. Surface Tension	Average Viscosity in sec	Relative Viscosity
0	400	6.5	71.1		
50	399	16.5	59.7	108.72	0.95
100	398	30.4	60.7	109.29	0.95
200	396	54.2	57.5	112.83	0.98
400	392	102.4	49.1	110.43	0.96
600	388	147.5	52.4	115.47	1.00
800	384	195	48.2	111.87	0.97
1000	380	239.5	48.1	106.63	0.93
1200	376	284.4	44.1	111.71	0.97
1400	372	332	43.5	114.75	1.00
3000	340	600	41.6	114.57	1.00
5000	300	793	40.8	116.77	1.02
10000	4525.0	1252		**DI Water** 115.03	

Average conductivity of pure OTAC

OTAC ppm	Conductivity
0	5.6
249.4	100.7
522.0	221
1112.5	425
1599.0	588
2104.7	752

2367.6	842
3077.3	1068
3568.0	1222
4053.7	1375
4965.6	1652
5437.4	1793
5904.5	1912
6345.1	1992
6868.5	2076
7770.3	2191
8214.8	2248
9070.2	2362

Average conductivity of OTAC +NaSal (MR=2)

OTAC ppm	Conductivity
60	44.8
100	67.1
159	99.7
249	151.8
348	207.3
495	290.7
544	318
593	346
642	373
690	401
787	453
980	533
1076	571
1267	646
1362	684
1456	722
1550	759

1644	796
1830	866
2015	939
2199	1010

Shear viscosity of 1000 ppm OTAC +NaSal

speed	Omega	Shear rate	Dial Reading	
			MR=1.5	MR=2
60	6.283	105.4372	5.5	
90	9.4245	158.1558	6.5	7
100	10.47167	175.7286	7	8
180	18.849	316.3116	7.5	8.5
200	20.94333	351.4573	8	9
300	31.415	527.1859	10	10
600	62.83	1054.372	15	15.5

Shear viscosity of 2500 ppm OTAC +NaSal

speed	Omega	Shear rate	Dial Reading		
			MR=1	MR=1.5	MR=2
60	6.283	105.4372	6.5	6.5	7
90	9.4245	158.1558	7.5	9	9
100	10.47167	175.7286	8	9.5	9.5
180	18.849	316.3116	8	10.5	12
200	20.94333	351.4573	9	11	13.5
300	31.415	527.1859	10.5	14	15.5
600	62.83	1054.372	16.5	23	25.5

Shear viscosity of 5000 ppm OTAC +NaSal

speed	Omega	Shear rate	Dial Reading		
			MR=1	MR=1.5	MR=2
60	6.283	105.4372	6	9.5	10.5
90	9.4245	158.1558	8.5	13	13.5
100	10.47167	175.7286	8.5	13.5	14
180	18.849	316.3116	9	19	20
200	20.94333	351.4573	9.5	20.5	21
300	31.415	527.1859	12	28	29.5
600	62.83	1054.372	20	48	52

OTAC+NaSal power law parameters

Solution	n	k
1000 ppm(MR=1)	0.989	0.0011
1000 ppm (MR=1.5)	0.986	0.0011
1000 ppm (MR=2)	0.989	0.0011
2500 ppm (MR=1)	0.924	0.0017
2500 ppm(MR=1.5)	0.914	0.0029
2500 ppm (MR=2)	0.882	0.0071
5000 ppm(MR=1)	0.98	0.0014
5000 ppm(MR=1.5)	0.887	0.0081
5000 ppm (MR=2)	0.866	0.0098

Average relative viscosity of PAM/OTAC systems

500 ppm PAM				250 ppm PAM		100 ppm PAM		
OTAC (pm)	flow time(s)	Relative viscosity	OTAC (ppm)	flow time(s)	Relative viscosity	OTAC (ppm)	flow time(s)	Relative viscosity
0	1864.15	16.21	0	807.42	7.02	0	317.32	2.76
50	1592.87	13.85	100	559.36	4.86	100	165.73	1.44
100	1381.38	12.01	200	454.71	3.95	200	141.57	1.23
200	1163.80	10.12	300	369.61	3.21	300	128.92	1.12
400	888.26	7.72	500	212.87	1.85	500	123.05	1.07
600	589.26	5.12	800	117.30	1.02			
800	388.26	3.38	1000	118.45	1.03			
1000	278.76	2.42						
1200	179.86	1.56						
1400	120.75	1.05						
1600	118.38	1.03						
Water	115							

Apparent viscosity of 500 ppm PAM and different OTAC concentrations

Apprent viscosity						
Shear rate(1/s)	No OTAC	100 ppm	200 ppm	400 ppm	800 pppm	1000 ppm
102.1	0.0185					
153.2	0.0154	0.0144	0.012328	0.00686	0.003443	0.002076
170.2	0.0136	0.0136	0.011095	0.006789	0.003714	0.001868
306.4	0.0103	0.0103	0.010264	0.005139	0.003088	0.001857
340.4	0.0102	0.0095	0.009542	0.004932	0.003087	0.001725
510.6	0.0082	0.0081	0.007184	0.004518	0.002673	0.001545
1021.3	0.0059	0.0059	0.005232	0.003489	0.002362	0.001439

Power law parameter (n) for PAM/OTAC system

OTAC(ppm)	1000ppm	500ppm
0	0.5232	0.4746
100	0.5035	0.5641
200	0.5128	0.6018
400	0.5659	0.7677
600	0.6085	0.9899
800	0.7524	1
1000	1	1

Average relative viscosity of PAM/OTAC in tap water

	100ppm		500ppm		1000ppm	
OTAC (ppm)	Flow time(s)	Relative viscosity	Flow time(s)	Relative viscosity	Flow time(s)	Relative viscosity
50	125.9	1.099	193.4	1.689	410.5	3.585
100	126.0	1.100	193.4	1.689	406.5	3.550
300	124.7	1.089	188.0	1.642	413.2	3.609
500	124.9	1.091	184.5	1.612	363.8	3.177
700	117.5	1.026	167.4	1.462	322.4	2.815
1000	114.5	1.000	131.6	1.149	249.5	2.179
1300	114.8	1.002	126.9	1.109	203.3	1.776
1600	116.7	1.019	133.6	1.167	163.7	1.430
2000	116.3	1.016	119.7	1.046	133.2	1.164
2500	117.2	1.024	125.6	1.097	127.8	1.116
Pure water 114.5						

Average conductivity of PAM/OTAC systems

	conductivity(mS/cm)	
OTAC(ppm)	500ppm	1000ppm
100	658.2	1280.5
500	783.1	1388
1000	917	1522
3000	1538	2100
5000	2095	2703
9000	2915	3556
13000	3401	4050
18000	4050	4660
21000	4380	5040
25000	4920	5560

Average relative viscosity of different PEO/OTAC systems

	500 ppm		1000 ppm		2000 ppm	
OTAC(ppm)	Flow time(s)	Relative viscosity	Flow time(s)	Relative viscosity	Flow time(s)	Relative viscosity
0	206	1.79	381	3.314	989	8.604
100	224	1.95	381	3.314	980	8.525
200	222	1.93	381	3.314	986	8.578
400	221	1.92	380	**3.306**	1013	8.813
600	223	1.94	382	3.323	1015	8.830
800	222	1.93	378	3.288	1050	9.134
1000	222	1.93	382	3.323	1031	8.969
1200	223	1.94	388	3.374	1038	9.030
1400	232	2.02	392	3.410	1038	9.030
3000	231	2.01	396	3.445	1048	9.117
5000	233	2.03	403	3.506	1084	9.430

Average Surface tension (dyne/cm) for PEO/OTAC systems

OTAC (ppm)	500 ppm	1000 ppm	2000 ppm
100	50.8	59.65	60.1
200	40.4	54.5	47.5
400	37.2	40.6	40.6
600	37.3	37.3	36.75
800	37.0	37.45	37.05
1000	37.1	37.45	36.95
1200	37.2	37.35	37.2
1400	37.3	37.65	36.95
3000	37.1	37.45	37
5000	37.3	34.4	37.1

Pure SDS Average conductivity

SDS(ppm)	Conductivity (mS/cm)
0	6.5
50	16.48
100	30.4
200	54.2
400	102.4
600	147.5
800	195
1000	239.5
1200	284.4
1400	332
3000	600
5000	793

Average conductivity of PEO/SDS systems

	Conductivity		
SDS(ppm)	500 ppm	1000 ppm	2000 ppm
0	5.6	9.52	6.6
100	20.97	27.03	41.5
200	38.2	42.4	59.6

400	71.5	75	102
600	102.1	105.5	143.5
800	133.4	138.4	185.3
1000	164.6	169.9	225
1200	195.9	199.4	263.7
1400	225.5	231.3	297
2000	315	315.5	387
2500	379	372.5	447
3000	435	428	508
5000	618	602	718
10000	------	- - ----	1193

Average relative viscosity change for 500 ppm PEO and different amount of SDS

SDS(ppm)	Flow time(s)	Relative viscosity
0	222.5	2.119
100	226.6	2.158
200	228.5	2.176
400	233.8	2.226
600	230.2	2.192
800	230.1	2.192
1000	227.8	2.169
1200	225.7	2.150
1400	230.6	2.197
2000	228.8	2.179
2500	277.3	2.641
3000	344.6	3.282
5000	576.7	5.493
10000	752.2	7.164

Average relative viscosity change for 1000 ppm PEO and different amount of SDS

SDS(ppm)	Flow time(s)	Relative viscosity
0	383.9	3.588
100	395.9	3.700
200	392.2	3.665

400	355.6	3.323
600	344.0	3.215
800	361.5	3.378
1000	387.3	3.619
1200	379.7	3.549
1400	389.7	3.642
2000	387.8	3.625
3000	639.4	5.976
5000	1352.0	12.636
10000	1853.5	17.322

Average relative viscosity change for 2000 ppm PEO and different amount of SDS

SDS(ppm)	Flow time(s)	Relative viscosity
0	1122.8	10.115
100	1107.6	9.979
200	1123.2	10.119
400	1117.1	10.064
600	1120.2	10.092
800	1167.0	10.514
1000	1223.1	11.019
1200	1241.5	11.185
1400	1181.5	10.644
2000	1275.5	11.491
2500	1747.4	15.742
3000	2446.5	22.041
5000	7045.0	63.468
10000	12507.0	112.676

Average surface tension of pure SDS solutions

SDS	Average Surface tension (dyne/cm)
50	71.1
100	71.4
200	69.1
400	61.0
800	46.6

1000	42.7
1200	40.6
1400	40.1
3000	39.5
5000	39.1

Average surface tension of 500 ppm PEO and different amount of SDS solutions

SDS	Average Surface tension (dyne/cm)
0	65.2
100	59.6
200	57.5
400	54.4
600	53.3
800	51.0
1000	48.8
1200	47.0
1400	46.3
2000	39.4
2500	43.5
3000	44.5
5000	42.4

Average surface tension of 1000 ppm PEO and different amount of SDS solutions

SDS	Average Surface tension (dyne/cm)
0	64.3
100	59.2
200	57.0
400	52.7
600	51.1
800	48.7
1000	47.2
1200	44.7
1400	44.0
2000	44.4

2500	44.6
3000	45.1
5000	43.4
10000	42.1

Average surface tension of 2000 ppm PEO and different amount of SDS solutions

SDS	Average Surface tension (dyne/cm)
1	65.5
100	57.6
200	55.0
600	47.1
800	44.8
1000	42.8
1200	41.9
1400	41.8
2000	43.2
2500	44.1
3000	44.9
5000	44.6
10000	42.4

b) Pipeline flow data

Pure water in pipe (D=34.8 mm)

flow(kg/s)	Pressure drop(Pa)	Re_G	Friction factor
1.56	2284.1	57219	0.004812624
1.44	1987.6	52729	0.004931643
1.32	1702.2	48295	0.005034654
1.23	1495.0	44871	0.005122161
1.17	1368.4	42794	0.00515461
1.13	1276.7	41447	0.00512672
1.07	1116.1	39146	0.005024482
1.04	1134.8	38023	0.005414706
0.94	1004.8	34375	0.005866335
0.90	939.4	32915	0.005981587
0.90	909.7	32859	0.005812093
0.82	825.6	30109	0.006282478
0.74	700.7	27134	0.006565585
0.70	612.4	25675	0.006408685
0.61	478.2	22307	0.006629206
0.52	363.5	18996	0.006949737
0.43	277.7	15909	0.007570119
0.28	139.3	10795	0.008245094

Pure water in pipe (D=22.02 mm)

flow(kg/s)	Pressure drop(Pa)	Re_G	Friction factor
3.61	97971.4	208641	0.00393499
2.53	51698.7	146202	0.004228784
2.17	39594.1	125360	0.004405136
1.97	33280.3	114096	0.004469832
1.59	22762.9	92189	0.004682892
3.30	86023.9	190814	0.004130875
3.26	84018.1	188508	0.004133868
3.21	81628.6	185847	0.004132124
3.10	76797.2	179195	0.004181532
2.97	71634.5	171657	0.004250545
2.87	67553.1	166069	0.004282642
2.75	62652.0	158974	0.004334391

2.57	55989.3	148686	0.00442804
2.37	48280.1	137067	0.004493105
2.28	46082.4	131745	0.004642033
2.13	41338.3	123142	0.004766304
2.14	41634.8	123675	0.004759269
2.02	38041.8	116845	0.00487173
1.93	35129.1	111612	0.004930437
1.83	28640.8	105581	0.004492145
1.81	31466.3	104428	0.005044899
1.71	28850.1	99018	0.005144705
1.72	26376.1	99284	0.004678351
1.58	22973.9	91302	0.004818551
1.49	20697.0	85981	0.004894988
1.39	17909.5	80304	0.004855668
1.39	18108.6	80127	0.004931414
1.30	15450.9	75160	0.004782126
1.26	14974.7	72588	0.00496903
1.17	13303.9	67710	0.005073605
1.13	12672.0	65138	0.005221774
1.01	10135.4	58220	0.00522806
0.89	8248.2	51213	0.005498381
0.81	7079.5	47045	0.005592683
0.74	6421.6	43054	0.006057046
0.67	5330.8	38708	0.006220621
0.64	5001.8	36845	0.006441744
0.57	3512.8	33209	0.005569071
0.55	3157.8	31613	0.005524774
0.49	2586.5	28420	0.005599048
0.47	2231.5	27096	0.005314163
0.47	2563.6	27096	0.006104807
0.44	2330.8	25259	0.006387325
0.38	1777.0	22110	0.006355722
0.33	1454.2	19135	0.006943879
0.30	1180.7	17385	0.006829685
0.25	896.1	14674	0.007276788
0.20	553.8	11437	0.007402788
0.14	308.3	8200	0.008017249
0.11	208.9	6450	0.008780081

from viscosity n= 0.4694

from viscosity k= 0.1697

500 ppm PAM in DI water (D= 34.8 mm)

flow(kg/s)	Pressure drop(Pa)	Re_G	Friction factor	%DR
4.55	3407.0	35894	0.000848353	75.7
3.72	2929.9	26404	0.001089677	71.4
3.72	2929.9	26404	0.001089677	71.4
2.84	2407.4	17497	0.001532875	64.3
2.57	1965.4	14938	0.001538648	65.8
2.28	1519.2	12446	0.001509681	68.1
1.99	1465.3	10152	0.001900276	62.2
1.71	1175.7	8058	0.002061844	61.7
1.39	922.3	5850	0.002458154	58.3
1.16	809.5	4408	0.003122732	51.2
0.84	589.0	2704	0.004303489	41.7
0.58	461.0	1549	0.006974985	19.6

from viscosity n= 0.5121

from viscosity k= 0.0922

250 ppm PAM in DI water (D= 34.8 mm)

flow(kg/s)	Pressure drop(Pa)	Re_G	Friction factor	%DR
4.76	2572.4	52730	0.00058597	81.2
4.29	2282.8	45273	0.000638292	80.4
3.89	1895.5	39158	0.000644146	81.1
3.48	1645.5	33169	0.000698981	80.4
3.11	1382.8	28089	0.000734481	80.4
3.30	1746.5	30679	0.000823935	77.4
2.94	1510.8	25795	0.000899814	76.5
2.63	1349.2	21838	0.001005102	75.0
2.42	1249.8	19293	0.001099851	73.7
2.17	1066.3	16455	0.001162149	73.4
1.87	1016.6	13154	0.001497045	67.9
1.55	834.0	9959	0.001785062	64.7
1.34	700.1	7979	0.002018726	62.6

from viscosity n= 0.5296

from viscosity k= 0.0506

100 ppm PAM in DI water (D= 34.8 mm)

flow(kg/s)	Pressure drop(Pa)	Re_G	Friction factor	%DR
3.26	3405.8	48871	0.001652417	48.2
2.97	3034.5	42678	0.001770218	46.6
2.71	2664.1	37287	0.001867481	45.8
2.37	2460.4	30580	0.002258681	38.2
2.14	2244.9	26259	0.002535322	33.6
1.84	1694.3	21009	0.002591825	36.4
1.53	1435.0	16125	0.00314587	28.5
1.22	1244.8	11570	0.004286361	11.5
1.01	924.0	8769	0.0046389	11.6
0.71	612.5	5159	0.006326918	3.4

n= 0.4694

k= 0.1697

Degraded 500 ppm PAM in DI water after 3 hr(D= 34.8 mm)

flow(kg/s)	Pressure drop(Pa)	Re_G	Friction factor	%DR
3.09	2078.2	19890	0.001119199	72.9
2.79	2088.3	16966	0.001384408	68.0
2.49	1806.3	14247	0.001504442	67.0
2.18	1539.4	11647	0.001668366	65.5
1.91	1393.8	9502	0.00197078	61.6
1.72	1744.0	8125	0.003025773	43.6
1.42	1096.6	6029	0.002809878	52.0
1.13	958.5	4266	0.003859706	40.3
0.86	761.6	2779	0.005366626	26.7
0.67	706.8	1931	0.008015267	1.5

n= 0.5231

k= 0.1140

Degraded 500 ppm PAM in DI water after 28 hr(D= 34.8 mm)

flow(kg/s)	Pressure drop(Pa)	Re_G	Friction factor	%DR
3.32	2474.7	23258	0.001156707	70.7
2.83	2076.5	18407	0.001332249	68.5

2.56	1982.2	15863	0.001555548	64.8
2.28	1812.2	13325	0.001800805	61.2
2.13	1695.2	12111	0.001917227	59.9
1.75	1467.0	9004	0.002478611	52.4
1.43	1282.7	6727	0.003216629	43.2
1.00	936.7	3930	0.004862938	26.6
0.74	774.2	2511	0.007375188	2.2

n= 0.5577

k= 0.0844

Degraded 500 ppm PAM in DI water after 55 hr(D= 34.8 mm)

flow(kg/s)	Pressure drop(Pa)	Re_G	Friction factor	%DR
3.32	2736.5	25036	0.001282636	70.5
2.88	2287.8	20480	0.001416751	69.2
2.59	2042.8	17549	0.001567258	67.3
2.31	1797.9	14874	0.001734782	65.5
1.90	1557.9	11200	0.002227894	59.0
1.67	1281.0	9320	0.002363337	58.7
1.37	1122.7	7001	0.003079844	50.3
1.19	993.1	5740	0.00358856	45.3
0.94	850.8	4042	0.004999567	30.9
0.60	590.7	2106	0.008572159	1.3

n= 0.6035

k= 0.0605

Degraded 500 ppm PAM in DI water after 80 hr(D= 34.8 mm)

flow(kg/s)	Pressure drop(Pa)	Re_G	Friction factor	%DR
3.30	3520.3	21933	0.001668466	63.0
3.02	3132.2	19215	0.001764704	62.3
2.72	2807.2	16369	0.001950107	60.1
2.52	2574.9	14503	0.002095218	58.6
2.28	2349.3	12485	0.002325126	55.9
1.95	2110.2	9819	0.002858395	49.3
1.78	1832.4	8538	0.002979635	49.2
1.50	1519.2	6555	0.003489165	44.8
1.17	1160.6	4480	0.004383306	37.6
0.88	835.6	2918	0.00552604	30.3

0.77	736.3	2356	0.006437957	23.5
0.67	679.1	1918	0.007770812	12.8
0.57	583.9	1487	0.009318002	2.6

n= 0.5881

k= 0.0641

Degraded 500 ppm PAM in DI water after 150 hr(D= 34.8 mm)

flow(kg/s)	Pressure drop(Pa)	Re_G	Friction factor	%DR
3.28	3709.7	26708	0.001771403	58.5
3.03	3401.6	23782	0.001914539	56.5
2.75	3054.8	20743	0.002086633	54.4
2.48	2816.5	17924	0.002366231	50.4
2.17	2469.7	14886	0.002699267	46.2
1.87	2046.2	12019	0.003028038	43.2
1.62	1740.6	9862	0.003408675	39.5
1.38	1451.0	7811	0.003953907	34.3
1.16	1228.8	6146	0.004702399	26.9
0.86	794.4	4034	0.00551851	23.8
0.74	674.0	3276	0.00628897	18.0
0.55	506.5	2166	0.008489597	1.5

n= 0.5121

k= 0.0922

Fresh 250 ppm PAM in DI water after (D= 34.8 mm)

flow(kg/s)	Pressure drop(Pa)	Re_G	Friction factor	%DR
4.76	2572.4	52730	0.00058597	81.2
4.29	2282.8	45273	0.000638292	80.4
3.89	1895.5	39158	0.000644146	81.1
3.48	1645.5	33169	0.000698981	80.4
3.11	1382.8	28089	0.000734481	80.4
3.30	1746.5	30679	0.000823935	77.4
2.94	1510.8	25795	0.000899814	76.5
2.63	1349.2	21838	0.001005102	75.0
2.42	1249.8	19293	0.001099851	73.7
2.17	1066.3	16455	0.001162149	73.4
1.87	1016.6	13154	0.001497045	67.9
1.55	834.0	9959	0.001785062	64.7
1.34	700.1	7979	0.002018726	62.6

n= 0.5816

k= 0.0496

Degraded 250 ppm PAM in DI water after 3 hr(D= 34.8 mm)

flow(kg/s)	Pressure drop(Pa)	Re_G	Friction factor	%DR
3.30	2243.2	36288	0.001059237	81.5
3.02	1944.4	31993	0.001096574	81.4
2.75	1780.2	27928	0.001216009	80.1
2.44	1503.2	23588	0.001302942	79.6
2.16	1393.8	19891	0.001536358	76.9
1.89	1286.9	16443	0.001855212	73.4
1.60	1115.1	13020	0.002234187	69.8
1.28	1007.4	9457	0.003168063	60.5
1.03	796.9	6963	0.003859208	55.4
0.82	622.6	5053	0.004738033	49.4
0.72	608.3	4144	0.006122826	37.8

n= 0.5816

k= 0.0496

Degraded 250 ppm PAM in DI water after 28 hr(D= 34.8 mm)

flow(kg/s)	Pressure drop(Pa)	Re_G	Friction factor	%DR
3.12	4413.2	33523	0.00233022	60.1
2.85	3823.3	29399	0.002429229	59.7
2.61	3068.7	25915	0.002329367	62.6
2.26	2504.8	21123	0.002536727	61.3
2.28	2714.6	21490	0.002683123	58.9
1.98	2223.8	17609	0.002910738	57.6
1.62	1740.6	13233	0.003408675	53.7
1.35	1457.8	10221	0.004108607	47.7
1.11	1212.8	7678	0.005116616	39.4
0.87	1006.5	5473	0.006845176	25.5
0.72	849.9	4144	0.008554606	13.1

n= 0.5296

k= 0.0506

Fresh 100 ppm PAM in DI water after (D= 34.8 mm)

flow(kg/s)	Pressure drop(Pa)	Re_G	Friction factor	%DR
3.26	3405.8	48871	0.001652417	48.2
2.97	3034.5	42678	0.001770218	46.6
2.71	2664.1	37287	0.001867481	45.8
2.37	2460.4	30580	0.002258681	38.2
2.14	2244.9	26259	0.002535322	33.6
1.84	1694.3	21009	0.002591825	36.4
1.53	1435.0	16125	0.00314587	28.5
1.22	1244.8	11570	0.004286361	11.5
1.01	924.0	8769	0.0046389	11.6
0.71	612.5	5159	0.006326918	3.4

n= 0.5566

k= 0.0382

Degraded 100 ppm PAM in DI water after 3 hr(D= 34.8 mm)

flow(kg/s)	Pressure drop(Pa)	Re_G	Friction factor	%DR
3.05	4855.6	49285	0.002697213	49.1
2.82	4213.7	44140	0.002726957	50.0
2.53	3502.4	37812	0.002808671	50.4
2.53	3703.8	37812	0.002970217	47.6
2.26	3102.7	31950	0.00314225	46.8
1.94	2428.4	25725	0.00332071	46.8
1.66	1908.2	20532	0.003566131	46.0
1.40	1474.6	15994	0.003895512	44.5
1.12	1045.3	11615	0.004301684	43.5
0.84	765.8	7716	0.005554578	34.1
0.73	665.6	6281	0.006420733	27.6

n= 0.6735

k= 0.0132

Degraded 100 ppm PAM in DI water after 28 hr(D= 34.8 mm)

flow(kg/s)	Pressure drop(Pa)	Re_G	Friction factor	%DR
2.91	5879.1	63528	0.003579515	28.1
2.68	5124.5	56993	0.0036748	28.1
2.42	4248.4	49674	0.003748071	29.2
2.10	3302.9	41208	0.003862156	30.3

1.86	2608.9	35057	0.003892676	32.6
1.86	2842.6	35019	0.004248361	26.4
1.54	2122.0	27270	0.004623995	24.8
1.25	1562.2	20804	0.005119238	22.2
0.99	1128.6	15113	0.005987846	16.0
0.70	667.3	9632	0.006982815	12.4
0.59	560.4	7595	0.008389501	0.9

n= 0.7162

k= 0.0180

Fresh 500 ppm PAM in tap water (D= 34.8 mm)

flow(kg/s)	Pressure drop(Pa)	Re_G	Friction factor	%DR
5.06	5159.2	72274	0.001039625	72.6
4.52	4638.7	62493	0.001172397	70.3
4.29	4213.7	58596	0.001177351	70.7
4.11	4135.6	55444	0.001259477	69.1
3.74	3632.5	49027	0.001339928	68.2
3.51	3459.0	45262	0.001445044	66.4
3.23	3242.1	40671	0.001600012	63.9
3.00	2834.5	37040	0.001618221	64.4
2.75	2565.5	33059	0.00174856	62.7
2.75	2823.2	33106	0.001919906	59.0
2.49	2518.5	29089	0.002095046	56.8
2.19	2203.6	24724	0.002361564	53.3
2.08	2492.4	23159	0.002957515	42.6
1.99	1983.1	21897	0.002567733	50.9
1.78	1768.4	18939	0.002870647	47.2
1.58	1571.4	16282	0.003228143	43.0
1.22	1176.6	11650	0.00407195	34.2
1.04	993.9	9533	0.004700672	28.0
0.86	800.3	7448	0.005559447	20.3
0.64	576.3	5107	0.007208057	6.6

n= 0.7388

k= 0.0130

Degraded 500 ppm PAM in tap water after 24 hr (D= 34.8 mm)

flow(kg/s)	Pressure drop(Pa)	Re_G	Friction factor	%DR

3.20	5141.8	48077	0.002588869	38.9
3.05	4820.9	45217	0.002675244	37.9
2.93	4560.6	43075	0.002733339	37.3
2.78	4248.4	40196	0.002841337	36.1
2.67	4031.5	38189	0.002924403	35.1
2.53	3753.9	35794	0.003017701	34.2
2.39	3519.7	33215	0.003185605	31.9
2.25	3233.5	30783	0.003301536	30.8
2.24	3345.2	30704	0.003429645	28.2
2.09	3058.1	28156	0.003596965	26.4
1.95	2777.8	25809	0.003750873	25.0
1.86	2601.8	24184	0.003894957	23.5
1.74	2414.1	22283	0.004114817	20.9
1.61	2168.3	20172	0.004327628	19.0
1.45	1891.3	17656	0.004662827	15.8
1.33	1693.5	15949	0.004905625	13.8
1.20	1467.9	13963	0.005250228	11.0
1.01	1150.5	11168	0.005864241	6.3
0.84	886.1	8920	0.006451267	3.0

n= 0.7647

k= 0.0110

Degraded 500 ppm PAM in tap water after 56 hr (D= 34.8 mm)

flow(kg/s)	Pressure drop(Pa)	Re_G	Friction factor	%DR
4.99	9609.1	9000	0.001989074	45.6
4.61	8316.6	8533	0.002016128	46.3
4.46	8030.4	8346	0.002078752	45.2
4.28	7588.0	8110	0.002138467	44.4
4.09	7180.3	7870	0.002211392	43.4
4.10	7241.0	7882	0.00222009	43.1
3.77	6416.9	7446	0.002328649	42.0
3.51	5870.5	7097	0.002456751	40.2
3.32	5471.4	6832	0.002562137	38.8
3.05	4916.3	6460	0.002717239	36.8
2.75	4265.7	6026	0.002897605	34.9
2.52	3745.3	5670	0.003047547	33.5
2.36	3441.7	5424	0.003192464	31.9
2.36	3582.6	5422	0.003327529	29.0

2.19	3245.9	5154	0.003502925	27.1
2.00	2892.3	4852	0.00373349	24.5
1.77	2492.4	4475	0.004088028	20.6
1.58	2131.2	4139	0.004403754	17.7
1.41	1809.7	3838	0.00467733	15.7
1.26	1551.2	3554	0.005033988	12.6
1.15	1366.8	3344	0.00531473	10.5
1.01	1138.7	3070	0.005699342	7.9
0.87	924.0	2765	0.006306313	3.2

n= 0.7647

k= 0.0110

Degraded 500 ppm PAM in tap water after 75 hr (D= 34.8 mm)

flow(kg/s)	Pressure drop(Pa)	Re_G	Friction factor	%DR
4.98	9721.8	83111	0.002019862	44.8
4.24	7752.8	68176	0.002219817	42.5
3.42	5913.8	52274	0.002603013	37.2
2.76	4430.5	40012	0.003006208	32.4
2.17	3172.8	29807	0.003467715	28.0
2.17	3310.7	29833	0.003613355	24.9
1.74	2469.7	22603	0.004224418	18.5
1.33	1710.3	16279	0.004977271	12.1
0.87	907.2	9595	0.006213323	4.7

n= 0.8107

k= 0.0061

Fresh 250 ppm PAM in tap water (D= 34.8 mm)

flow(kg/s)	Pressure drop(Pa)	Re_G	Friction factor	%DR
flow(kg/s)	pdiff(psi)	Re genral	Friction	Real DR
5.04	5298.0	110741	0.001076719	71.6
4.64	4829.5	100389	0.001157653	70.2
4.27	4482.6	91137	0.0012642	68.3
3.78	3936.1	78829	0.001416812	65.8
3.08	3042.6	61670	0.001654957	62.5
3.08	3274.5	61706	0.001779286	59.6
2.57	2679.3	49874	0.00208256	55.3
2.33	2467.1	44307	0.002340006	51.3

2.08	2159.9	38713	0.002570492	48.3
1.78	1872.0	32221	0.003033509	41.9
1.47	1484.7	25614	0.003539176	36.1
1.18	1145.4	19664	0.004258695	28.2
0.90	834.8	14367	0.005261347	18.2
0.63	538.5	9423	0.006898143	3.8

n= 0.8107

k= 0.0061

Degraded 250 ppm PAM in tap water after 3 hr (D= 34.8 mm)

flow(kg/s)	Pressure drop(Pa)	Re_G	Friction factor	%DR
4.96	10233.6	108738	0.002144651	43.7
4.49	9053.9	96726	0.002310232	41.1
4.00	7830.8	84256	0.002520202	38.0
3.72	6989.4	77197	0.002605952	37.4
3.32	5991.9	67487	0.002800671	35.0
2.97	5098.4	59011	0.00298652	33.0
2.66	4482.6	51931	0.003255345	29.4
2.46	3953.4	47340	0.003354561	29.0
2.10	3155.4	39223	0.003673598	25.9
2.11	3293.0	39257	0.003828204	22.8
1.77	2601.0	32023	0.004258776	18.5
1.56	2163.2	27500	0.004575915	15.8
1.32	1695.2	22436	0.005048912	11.9
1.05	1203.5	17221	0.005593001	8.9
0.85	884.5	13301	0.006346101	3.3

n= 0.8107

k= 0.0061

Degraded 250 ppm PAM in tap water after 24 hr (D= 34.8 mm)

flow(kg/s)	Pressure drop(Pa)	Re_G	Friction factor	%DR
4.93	10997.0	108098	0.002327608	39.0
4.41	9409.6	94688	0.002488544	36.9
3.95	7969.6	82989	0.002631019	35.6
3.67	7241.0	76100	0.002765533	33.8
3.38	6599.1	69048	0.002968172	30.7
3.08	5662.3	61743	0.003073705	30.3

2.66	4569.3	51753	0.003337532	27.7
2.39	3884.0	45663	0.00350182	26.5
2.00	2964.6	37022	0.00380341	24.4
2.00	3152.4	37022	0.004044401	19.6
1.75	2573.2	31464	0.004339948	17.3
1.46	1949.4	25328	0.004735429	14.7
1.21	1445.1	20306	0.005090556	13.4
0.99	1070.5	15917	0.005679659	9.3

n= 0.8107

k= 0.0061

Fresh 100 ppm PAM in tap water (D= 34.8 mm)

flow(kg/s)	Pressure drop(Pa)	Re_G	Friction factor	%DR
5.09	6338.9	112107	0.001261988	71.7
4.65	5471.4	100745	0.001303742	69.1
4.11	5124.5	86913	0.0015653	65.3
3.75	4604.0	78069	0.00168444	62.8
3.40	4170.3	69420	0.001858847	60.7
3.03	3736.6	60502	0.002098821	57.2
2.69	3302.9	52429	0.002360402	53.7
2.68	3221.4	52358	0.00230748	49.8
2.09	2379.6	38883	0.002811225	43.4
1.62	1747.4	28661	0.0034479	35.9
1.33	1384.5	22810	0.004010642	29.7
1.04	1009.1	16894	0.004843257	21.5
0.72	557.8	10932	0.0055666	19.4
0.54	411.3	7794	0.007251676	3.8

n= 0.8107

k= 0.0061

Degraded 100 ppm PAM in tap water after (D= 34.8 mm)

flow(kg/s)	Pressure drop(Pa)	Re_G	Friction factor	%DR
4.80	13382.4	175537	0.002996014	22.1
4.11	10476.5	150560	0.003188194	20.9
3.90	9617.8	142534	0.003265774	20.4
3.59	8516.1	131533	0.003395647	19.2

3.28	7397.1	119970	0.003545393	18.0
2.98	6330.2	109194	0.00366244	17.7
2.67	5263.3	97856	0.003791665	17.7
2.33	4152.9	85227	0.003944129	17.9
1.97	3138.1	72149	0.004158604	17.8
1.97	3277.0	72149	0.00434274	14.1
1.67	2499.1	60980	0.004636277	13.0
1.22	1497.3	44758	0.00515603	12.0
0.89	887.0	32523	0.00578493	10.5
0.61	513.2	22363	0.007078953	2.4

n= 0.6481

k= 0.0508

Fresh 2000 ppm PEO in DI water (D= 34.8 mm)

flow(kg/s)	Pressure drop(Pa)	Re_G	Friction factor	%DR
5.36	8429.4	44292	0.001512434	72.2
4.81	7709.4	38236	0.001719357	69.6
4.22	7154.3	32089	0.002067839	65.0
3.73	6434.3	27091	0.002389099	61.2
3.40	5939.8	23929	0.002649991	58.3
3.06	5419.4	20788	0.002977332	54.7
2.82	4959.7	18596	0.003213231	52.5
2.53	4439.2	16072	0.003568574	49.1
2.31	4031.5	14181	0.003900387	46.1
2.02	3424.3	11863	0.004313625	43.0
1.76	2895.2	9855	0.004798365	39.5
1.76	3205.4	9844	0.005321854	32.9
1.42	2336.7	7341	0.005987284	29.8
1.09	1640.4	5133	0.007137154	23.5
0.77	1036.0	3194	0.009094737	13.5

n= 0.9650

k= 0.0037

Degraded 2000 ppm PEO in DI water after 1.5 hr(D= 34.8 mm)

flow(kg/s)	Pressure drop(Pa)	Re_G	Friction factor	%DR
6.33	19853.4	80179	0.0025556	59.4
5.75	17788.9	72667	0.002769321	55.4

5.15	15776.5	64840	0.00306101	49.8
5.10	16062.8	64181	0.003178692	47.0
4.48	13295.7	56052	0.00341819	43.7
4.00	11361.3	49842	0.003664829	40.2
3.44	9175.4	42654	0.003999059	35.7
3.05	7596.6	37700	0.0042029	33.9
2.85	6729.2	35134	0.004266349	34.2
2.54	5558.2	31131	0.004451902	33.0
2.23	4604.0	27203	0.004785511	29.2
2.07	4343.8	25208	0.005231126	21.8
1.75	3302.9	21233	0.005541348	20.2
1.73	3362.9	20964	0.005782886	15.7
1.43	2603.5	17207	0.006557103	6.5
1.17	1845.0	13952	0.006968231	5.5
0.65	1036.8	7601	0.01266275	3.3

n= 0.9834

k= 0.0029

Degraded 2000 ppm PEO in DI water after 3 hr (D= 34.8 mm)

flow(kg/s)	Pressure drop(Pa)	Re_G	Friction factor	%DR
6.33	21562.3	89770	0.002776913	39.2
5.85	19463.1	82980	0.002926053	37.1
5.32	17415.9	75338	0.003166399	33.6
4.73	15152.0	66784	0.003491945	28.9
4.16	12376.2	58665	0.003680733	27.5
3.77	10840.8	53021	0.003934039	24.4
3.45	9418.2	48482	0.004075771	23.4
3.19	8299.3	44825	0.004190668	22.8
2.82	6954.7	39535	0.004496009	19.8

n= 0.9834

k= 0.0029

Degraded 2000 ppm PEO in DI water after 27 hr (D= 34.8 mm)

flow(kg/s)	Pressure drop(Pa)	Re_G	Friction factor	%DR
6.33	26168.3	211903	0.003370108	8.5
5.78	22950.1	193539	0.003542509	5.9
5.25	19714.6	175846	0.003685571	4.5

4.62	16080.1	154760	0.003880074	2.6
4.03	12645.1	134809	0.004020098	2.5
3.74	11127.1	125194	0.004101114	2.4
3.44	9617.8	115323	0.004176951	2.6
3.13	7987.0	104733	0.004204845	4.2

n= 0.9425

k= 0.0042

Fresh 1000 ppm PEO in DI water (D= 34.8 mm)

flow(kg/s)	Pressure drop(Pa)	Re_G	Friction factor	%DR
6.06	7431.8	79134	0.001043307	77.8
4.01	7301.7	51157	0.002339138	55.5
4.95	6798.6	63963	0.001427425	71.3
4.41	6451.6	56614	0.00170626	66.7
3.78	5670.9	48058	0.002044597	61.7
3.03	4491.2	38097	0.002512522	55.6
2.81	4413.2	35150	0.002874796	50.2
2.57	4092.2	31935	0.003196025	45.9
2.31	3580.4	28537	0.003459393	43.1
2.04	3242.1	25041	0.004010814	36.1
2.05	3505.1	25120	0.004310208	31.3
1.70	2760.1	20645	0.004919182	25.4
1.48	2223.8	17819	0.005235364	23.4
1.12	1462.0	13320	0.005967462	18.8
0.92	1137.0	10834	0.006860192	11.4

n= 0.9990

k= 0.0011

degraded 1000 ppm PEO in DI water after 3 hr (D= 34.8 mm)

flow(kg/s)	Pressure drop(Pa)	Re_G	Friction factor	%DR
6.33	23062.9	211954	0.002968736	19.4
5.92	20530.0	198271	0.003019627	19.3
5.31	17719.5	177800	0.003240244	15.8
4.73	14987.1	158257	0.003458448	12.7
4.19	12558.3	140156	0.003693955	9.5
3.59	9539.7	120361	0.003803776	10.3
3.31	8151.8	110747	0.003838552	11.4

2.74	5644.9	91779	0.003868875	14.8
2.48	4855.6	82888	0.0040793	12.4
2.20	3710.6	73638	0.003948795	17.7
1.91	2981.9	63823	0.004223152	15.0
1.88	3085.1	63053	0.004476584	10.2
1.62	2356.0	54216	0.00462254	10.7
1.33	1710.3	44611	0.004954398	8.9
1.01	1044.4	33723	0.005291227	9.2

n= 1

k= 0.0011

Fresh 500 ppm PEO in DI water (D= 34.8 mm)

flow(kg/s)	Pressure drop(Pa)	Re_G	Friction factor	%DR
6.34	15013.2	232009	0.001924139	46.5
6.21	14605.5	227070	0.001954212	46.0
4.50	10502.5	164597	0.002674384	31.8
3.91	8915.1	142987	0.003008212	26.0
3.38	7249.7	123566	0.003275618	22.3
2.86	5670.9	104594	0.003576137	18.6
2.51	4794.8	91684	0.003935119	13.3
2.24	3806.0	82086	0.003896727	16.5
1.87	2782.4	68503	0.004090524	16.2
1.89	2991.6	69176	0.004312857	11.5

n= 1

k= 0.0011

Degraded 500 ppm PEO in DI water after 3 hr (D= 34.8 mm)

flow(kg/s)	Pressure drop(Pa)	Re_G	Friction factor	%DR
6.06	23245.1	221793	0.003259925	10.5
5.55	19853.4	202934	0.003325835	10.6
4.98	16617.9	182053	0.003459016	9.6
4.44	13694.7	162576	0.003574462	9.1
3.88	10554.6	141921	0.00361513	11.2
3.57	9106.0	130582	0.003684097	11.4
3.27	7683.4	119805	0.003692951	13.0
2.95	6356.2	107794	0.003773866	13.4
2.65	5107.1	96792	0.003760706	16.0

n= 0.9728

k= 0.0010

1000 ppm OTAC + NaSal (MR=1),T=20C , in DI water (D= 22.02 mm)

flow(kg/s)	Pressure drop(Pa)	Re_G	Friction factor	%DR
2.13	23739.5	150367	0.002741109	31.7
1.92	19567.2	135136	0.002781544	32.5
1.71	15950.0	120394	0.002839201	33.1
1.52	13035.4	106582	0.002941721	32.7
1.32	10346.4	91718	0.003128004	31.1
1.16	8403.3	80748	0.003255688	30.5
1.01	7136.9	70255	0.003625909	25.3
0.85	5792.4	58499	0.004203455	17.3
0.72	4361.1	49074	0.004455529	16.1
0.58	3216.1	39482	0.005018013	10.5
0.46	2444.1	31233	0.006018725	
0.46	2243.2	31126	0.005560958	6.5
0.31	1169.9	20926	0.006282998	4.3
0.37	1566.4	25057	0.005923629	5.7

n= 0.9728

k= 0.0010

1000 ppm OTAC + NaSal (MR=1),T=25C , in DI water (D= 22.02 mm)

flow(kg/s)	Pressure drop(Pa)	Re_G	Friction factor	%DR
1.99	26810.2	140134	0.003550986	13.0
1.80	21701.0	126374	0.003514993	16.1
1.59	18005.8	111660	0.003711369	14.1
1.37	14024.3	95566	0.003913889	12.9
1.22	11560.8	84584	0.004092054	11.7
1.05	9071.3	72438	0.004342108	9.8
0.84	6373.6	57739	0.004744468	6.9
0.70	4777.5	47886	0.005119531	4.1
0.54	2782.4	36584	0.005036046	11.8
0.54	2961.3	36584	0.005359849	6.2
0.44	2042.0	29526	0.005610175	6.9

n= 0.9728

k= 0.0010

1000 ppm OTAC + NaSal (MR=1.5),T=25C , in DI water (D= 22.02 mm)

flow(kg/s)	Pressure drop(Pa)	Re_G	Friction factor	%DR
2.08	24598.3	133763	0.00296283	28.3
1.90	21111.2	121741	0.003054537	27.8
1.70	17684.8	108845	0.003182097	26.8
1.53	14969.8	97294	0.003351184	25.1
1.33	12107.3	84379	0.003576459	22.8
1.16	9886.7	73308	0.003840495	20.0
0.92	6963.4	57726	0.004307447	15.5
0.84	6035.3	52293	0.004525708	13.4
0.74	5003.0	46185	0.004777907	11.3
0.66	4187.6	41276	0.004977496	10.2
0.59	3250.8	36284	0.004966326	13.2
0.58	3435.3	35991	0.005331651	7.0
0.49	2550.5	30240	0.005555744	7.3
0.41	1877.8	25292	0.005792519	7.5

n= 0.9728

k= 0.0010

1000 ppm OTAC + NaSal (MR=1.5),T=20C , in DI water (D= 22.02 mm)

flow(kg/s)	Pressure drop(Pa)	Re_G	Friction factor	%DR
2.26	21310.7	145104	0.002190716	45.9
2.06	18196.6	132347	0.002237646	46.0
1.92	16158.2	122649	0.002304308	45.4
1.71	13564.6	109348	0.002418906	44.3
1.53	11456.7	97494	0.002554468	42.9
1.30	9010.6	82182	0.002802023	39.9
1.07	6668.5	67242	0.003064756	37.5
0.89	5324.0	55749	0.003524589	31.4
0.79	4560.6	49631	0.003786136	28.5
0.66	3493.7	40982	0.004210888	24.2
0.66	3655.8	40982	0.004406305	20.6
0.56	2947.8	34819	0.004879704	15.6
0.46	2265.9	28394	0.005579973	8.3
0.36	1561.3	21911	0.006368602	1.9
0.28	947.6	17009	0.00632847	8.5
0.36	1510.8	22103	0.00605831	6.5
3.81	67989.2	248381	0.00245422	30.6

3.41	52152.1	221790	0.002346895	35.5
2.73	33123.3	176815	0.002317319	39.8
1.37	11425.9	86778	0.003195878	30.6

n= 0.9728

k= 0.0010

1000 ppm OTAC + NaSal (MR=2),T=20C , in DI water (D= 22.02 mm)

flow(kg/s)	Pressure drop(Pa)	Re_G	Friction factor	%DR
2.32	19671.3	149058	0.001919036	52.3
2.16	17589.4	138823	0.001970871	51.8
1.99	15594.3	127900	0.002049603	50.9
1.80	13313.0	114785	0.002160039	49.7
1.62	11474.0	103116	0.002293811	48.0
1.40	9374.9	88979	0.002497415	45.4
1.24	8004.3	78689	0.002708755	42.6
1.02	6191.4	64364	0.003098525	37.5
0.93	5514.8	58617	0.003311188	34.8
0.84	4690.8	52786	0.003453758	33.7
0.76	4248.4	47661	0.003816202	28.6
0.64	3259.5	39512	0.004218134	24.7
0.63	3448.7	39414	0.004484654	20.0
0.56	2915.8	34428	0.004933877	14.9
0.45	2179.2	27617	0.005664077	7.6
0.37	1610.1	22586	0.006190906	3.9
0.29	1029.3	17392	0.006582027	4.3
3.93	63000.9	256815	0.00213099	39.3
3.60	50983.6	234613	0.00205647	42.7
2.49	24821.1	160634	0.002093294	47.0

n= 0.9728

k= 0.0010

1000 ppm OTAC + NaSal (MR=2),T=25C , in DI water (D= 22.02 mm)

flow(kg/s)	Pressure drop(Pa)	Re_G	Friction factor	%DR
2.11	23930.3	135786	0.002799344	32.0
1.95	21050.5	124870	0.002898926	31.0
1.78	18986.0	114080	0.003117664	27.5
1.58	15958.7	100906	0.003327756	24.9
1.41	13469.1	89279	0.003564652	22.0

1.21	10693.4	76296	0.003842994	19.2
0.99	8091.1	62281	0.004317007	13.7
0.88	6607.8	55452	0.004420142	14.1
0.79	5887.8	49532	0.004906867	7.3
0.70	4803.5	43925	0.005058176	7.3
0.63	3918.7	39414	0.005095832	9.1
0.56	3051.3	34624	0.005106578	11.8
0.56	3242.5	34624	0.005426523	6.3
0.47	2404.8	29268	0.005582553	7.6
0.37	1621.1	22972	0.006030656	6.0
0.30	1095.8	18159	0.006442553	5.3

n= 0.9239

k= 0.0017

2500 ppm OTAC + NaSal (MR=1),T=20C , in DI water (D= 22.02 mm)

flow(kg/s)	Pressure drop(Pa)	Re_G	Friction factor	%DR
2.19	21874.5	131072	0.002376197	42.8
2.01	19055.4	119572	0.002455165	42.2
1.81	16886.8	106692	0.002689108	38.5
1.61	14388.6	93824	0.002909487	35.5
1.44	12436.9	83180	0.00314565	32.4
1.21	9878.0	68949	0.00354095	27.4
1.01	7822.2	57060	0.003986105	22.0
0.84	6035.3	46443	0.004509128	16.2
0.74	5176.5	40787	0.004923156	11.4
0.67	4439.2	36537	0.00518022	9.3
0.53	3007.9	28674	0.005506929	9.3
0.46	2434.3	24446	0.005994591	5.1
0.40	1903.9	20876	0.006287571	4.3
0.30	1191.7	15645	0.006727173	4.8
0.25	876.0	12864	0.007114783	4.1

n= 0.9239

k= 0.0017

2500 ppm OTAC + NaSal (MR=1),T=25C , in DI water (D= 22.02 mm)

flow(kg/s)	Pressure drop(Pa)	Re_G	Friction factor	%DR
1.86	22742.0	109415	0.003977724	8.4

1.80	19055.4	105720	0.003683594	15.9
1.59	15993.4	92958	0.003920157	13.4
1.41	12419.5	81653	0.004186884	10.4
1.19	9418.2	67819	0.004590881	6.2
1.02	6980.8	57525	0.004727593	7.3
0.86	5419.4	47635	0.004975535	7.0
0.75	4100.9	41060	0.00509077	8.3
0.65	3294.2	35457	0.005059876	12.1
0.57	3425.2	30894	0.00525052	11.9
0.57	2564.0	30983	0.005430158	8.8
0.49	1950.2	25850	0.005691488	8.6
0.42	1220.4	22004	0.005840486	10.0
0.32	879.4	16495	0.006243598	10.4
0.26		13451	0.006574024	10.4

n= 0.9126

k= 0.0029

2500 ppm OTAC + NaSal (MR=1.5),T=25C , in DI water (D= 22.02 mm)

flow(kg/s)	Pressure drop(Pa)	Re_G	Friction factor	%DR
2.07	24086.5	78473	0.002935661	37.8
1.88	21362.7	70419	0.003177501	34.5
1.68	18691.1	62563	0.0034558	30.8
1.51	16279.6	55461	0.003756656	27.0
1.30	13590.6	47400	0.004186571	21.8
1.08	10563.2	38492	0.004772039	15.4
0.89	7683.4	31212	0.005104172	14.1
0.75	5731.7	25969	0.005340106	14.2
0.61	3866.7	20753	0.005441153	17.3
0.55	3198.8	18661	0.005472848	19.0
0.55	3376.3	18548	0.005841295	13.7
0.48	2670.9	16031	0.006042856	13.9
0.39	1845.0	12833	0.006285284	15.3
0.28	1065.5	9059	0.006887205	14.9
0.34	1435.0	10879	0.00662426	14.4

n= 0.9126

k= 0.0029

2500 ppm OTAC + NaSal (MR=1.5),T=20C , in DI water (D= 22.02 mm)

flow(kg/s)	Pressure drop(Pa)	Re_G	Friction factor	%DR
2.26	19992.2	86211	0.002049597	55.5
2.04	18014.5	77083	0.002268929	52.1
1.87	15871.9	70168	0.00237632	51.0
1.68	14050.3	62315	0.002616828	47.7
1.46	11942.5	53498	0.00294472	43.3
1.25	9973.4	45159	0.003358511	38.0
1.10	8620.2	39447	0.003722493	33.6
0.85	6312.8	29747	0.004581144	23.8
0.78	5627.6	27127	0.004838746	21.4
0.71	4890.3	24469	0.00508292	19.5
0.62	3953.4	21094	0.00539897	17.6
0.57	3450.3	19112	0.00564966	15.9
0.56	3376.3	18943	0.005619654	16.5
0.49	2823.2	16365	0.006149898	12.0
0.39	2050.4	12833	0.006985045	5.9
0.36	1749.9	11581	0.007199349	5.5
0.30	1269.2	9538	0.007462179	6.7

n= 0.7960

k= 0.0072

2500 ppm OTAC + NaSal (MR=2),T=20C , in DI water (D= 22.02 mm)

flow(kg/s)	Pressure drop(Pa)	Re_G	Friction factor	%DR
2.26	19506.4	82662	0.001999797	57.1
2.06	17511.4	73823	0.002166249	54.8
1.87	15741.8	65745	0.002360713	52.1
1.71	14197.8	59044	0.002545488	49.8
1.53	12593.0	51906	0.002796618	46.6
1.30	10363.7	42504	0.003207633	41.7
1.14	8889.1	36128	0.003603841	37.1
0.93	6885.3	28296	0.004188982	31.2
0.78	5679.6	22868	0.004922144	23.4
0.68	4491.2	19329	0.00514619	23.2
0.59	3632.5	16307	0.005520424	21.0
0.58	3595.2	16154	0.005550528	20.8
0.47	2572.4	12637	0.005971449	19.9
0.42	2116.1	11032	0.006155077	20.2
0.34	1522.6	8400	0.006964787	15.6

n= 0.7960

k= 0.0072

2500 ppm OTAC + NaSal (MR=2),T=25C , in DI water (D= 22.02 mm)

flow(kg/s)	Pressure drop(Pa)	ReG	Friction factor	%DR
2.08	23817.6	74819	0.00288151	39.7
1.86	20608.1	65226	0.003131502	36.7
1.70	18456.9	58724	0.003339009	34.2
1.48	15394.8	49665	0.003678829	30.5
1.25	12254.7	40639	0.004086408	26.6
1.04	9366.2	32460	0.00453638	22.9
0.82	6642.5	24564	0.005111634	19.0
0.77	5913.8	22705	0.005186378	19.4
0.67	4682.1	19224	0.005413911	19.3
0.57	3528.4	15795	0.005654055	19.8
0.57	3690.3	15591	0.006042678	14.5
0.47	2688.5	12391	0.006447828	13.9
0.37	1821.4	9373	0.006945467	13.5
0.30	1294.4	7312	0.00745648	12.7

n= 0.9895

k= 0.0014

5000 ppm OTAC + NaSal (MR=1),T=20C , in DI water (D= 22.02 mm)

flow(kg/s)	Pressure drop(Pa)	ReG	Friction factor	%DR
2.06	24095.1	91995	0.002962989	34.7
1.88	21492.9	83563	0.003196854	31.2
1.68	18769.1	75002	0.003457609	27.6
1.49	16158.2	66314	0.00379797	22.9
1.30	13521.2	57569	0.004204701	17.6
1.08	10667.3	47807	0.004791699	10.3
0.85	7561.9	37587	0.00546782	3.6
0.66	4768.8	29171	0.0056946	5.8
0.58	3727.9	25552	0.005785833	7.4
0.51	2921.2	22416	0.005875319	9.0
0.51	3095.2	22416	0.006225211	3.6
0.39	1961.2	17312	0.006577643	4.5
0.33	1406.4	14257	0.006927036	4.2

0.26	972.0	11412	0.007437817	2.7

n= 0.9895

k= 0.0014

5000 ppm OTAC + NaSal (MR=1),T=25C , in DI water (D= 22.02 mm)

flow(kg/s)	Pressure drop(Pa)	ReG	Friction factor	%DR
1.91	27243.9	85290	0.003891472	15.8
1.71	23331.8	75968	0.004190632	11.9
1.51	19671.3	67141	0.004511683	8.1
1.30	15681.1	57638	0.004864853	4.6
1.11	11751.6	49112	0.005004742	5.7
0.92	8229.9	40533	0.005124991	8.0
0.70	4968.3	31016	0.005254575	11.7
0.59	3658.5	25962	0.005502272	11.6
0.59	3709.7	26030	0.005550363	10.8
0.48	2626.3	21190	0.005904173	9.8
0.40	1862.7	17380	0.006199042	9.9
0.35	1499.9	15343	0.006388679	10.0

n= 0.8870

k= 0.0081

5000 ppm OTAC + NaSal (MR=1.5),T=25C , in DI water (D= 22.02 mm)

flow(kg/s)	Pressure drop(Pa)	ReG	Friction factor	%DR
2.01	24103.8	32766	0.003124627	46.8
1.77	20720.8	28534	0.003443859	43.3
1.62	18621.7	25801	0.00370863	40.5
1.38	15290.7	21571	0.004201164	35.6
1.24	13399.7	19077	0.004591097	31.7
1.09	11153.1	16512	0.004953405	28.9
0.88	8221.2	13045	0.005576533	24.6
0.77	6763.9	11258	0.005979306	22.0
0.65	5237.2	9376	0.006431592	19.9
0.57	4213.7	8133	0.006680221	19.7
0.50	3302.9	6982	0.006889405	20.3
0.50	3463.0	6982	0.007223534	16.4
0.44	2799.7	6060	0.007532047	15.9
0.32	1580.7	4215	0.00816518	16.7
0.24	919.0	3079	0.008346964	21.3

n= 0.8870

k= 0.0081

5000 ppm OTAC + NaSal (MR=1.5),T=20C , in DI water (D= 22.02 mm)

flow(kg/s)	Pressure drop(Pa)	ReG	Friction factor	%DR
2.16	19931.5	35563	0.002230127	61.2
1.97	18049.2	32070	0.002431717	58.8
1.78	16297.0	28671	0.002685326	55.8
1.63	15056.5	26046	0.002948163	52.6
1.39	12679.8	21678	0.003453016	47.0
1.20	10962.3	18393	0.004010713	40.9
0.99	8871.8	14884	0.004748246	33.6
0.83	7258.3	12261	0.005503348	26.7
0.75	6390.9	10983	0.005905851	23.5
0.68	5566.9	9793	0.006321118	20.4
0.58	4369.8	8230	0.006782079	18.2
0.49	3363.6	6792	0.007373018	15.3
0.49	3551.4	6815	0.007736143	11.0
0.39	2244.9	5221	0.007892785	15.1

n= 0.8662

k= 0.0098

5000 ppm OTAC + NaSal (MR=2),T=20C , in DI water (D= 22.02 mm)

flow(kg/s)	Pressure drop(Pa)	ReG	Friction factor	%DR
2.10	20382.5	33206	0.002412246	58.8
1.86	18274.7	28819	0.002776933	54.2
1.72	17121.0	26400	0.003036771	51.0
1.48	14900.4	22243	0.00357549	44.7
1.32	13460.5	19512	0.004069476	39.1
1.12	11396.0	16295	0.00473458	32.3
0.95	9600.4	13471	0.005579342	23.9
0.79	7640.0	10957	0.006391879	17.2
0.66	5948.5	8909	0.007169641	11.8
0.58	4838.2	7742	0.007469542	11.3
0.51	3910.1	6710	0.007770426	11.0
0.51	3709.7	6710	0.007372266	15.5
0.43	3065.7	5473	0.008726758	5.0
0.35	2074.8	4290	0.009074626	7.0
0.28	1426.6	3417	0.009321995	9.8

n= 0.8662

k= 0.0098

5000 ppm OTAC + NaSal (MR=2),T=25C , in DI water (D= 22.02 mm)

flow(kg/s)	Pressure drop(Pa)	ReG	Friction factor	%DR
1.97	24424.8	30772	0.003306111	44.6
1.80	22273.5	27821	0.003601572	41.1
1.57	19246.2	23901	0.004068269	36.0
1.44	17285.8	21563	0.004381427	32.8
1.16	13295.7	16953	0.005151101	25.6
0.97	10450.5	13768	0.005844366	19.9
0.82	8334.0	11465	0.006437231	15.7
0.76	7093.5	10477	0.006423498	17.7
0.66	5697.0	8909	0.006866447	15.6
0.58	4612.7	7696	0.007197023	14.7
0.50	3476.4	6460	0.00738642	16.2
0.50	3672.7	6460	0.007803553	11.4
0.41	2545.4	5141	0.008091138	13.3
0.32	1759.1	3990	0.008746525	12.0
0.26	1148.8	3104	0.008894664	16.0

n= 0.9728

k= 0.0011

1000 ppm OTAC + NaSal (MR=2),T=20C , in DI water (D= 38.4 mm)

flow(kg/s)	Pressure drop(Pa)	ReG	Friction factor	%DR
3.23	4239.7	127721	0.002100273	49.7
2.96	3771.3	116752	0.002225188	47.9
2.82	3649.8	111401	0.002359497	45.4
2.82	3709.7	111401	0.002398205	44.5
2.52	3377.2	99233	0.00273469	38.6
2.28	2984.9	89638	0.002946259	35.5
2.00	2567.3	78221	0.003303869	30.1
1.70	2117.8	66052	0.003788048	23.1
1.40	1680.9	54307	0.004401617	14.9
1.17	1365.2	45057	0.005142406	5.2

n= 0.7960

k= 0.0072

2500 ppm OTAC + NaSal (MR=2),T=20C , in DI water (D= 38.4 mm)

flow(kg/s)	Pressure drop(Pa)	ReG	Friction factor	%DR

3.12	5237.2	58247	0.002778964	45.4
2.85	4690.8	52294	0.00297716	43.0
2.58	4196.3	46354	0.003253958	39.6
2.31	3701.9	40573	0.003581484	35.7
2.30	3695.4	40508	0.003584738	35.6
2.00	3051.4	34170	0.003926808	32.4
1.71	2424.2	28301	0.004266472	30.0
1.46	2137.1	23340	0.005180544	18.9
1.15	1520.9	17561	0.005913759	13.8

n= 0.8662

k= 0.0098

5000ppm OTAC + NaSal (MR=2),T=20C , in DI water (D= 38.4 mm)

flow(kg/s)	Pressure drop(Pa)	ReG	Friction factor	%DR
3.00	6798.6	26215	0.003881401	37.5
2.68	6104.7	23067	0.004367703	31.9
2.42	5506.1	20542	0.004833153	26.8
2.17	4855.6	18127	0.005314483	21.9
1.90	4135.6	15620	0.005885423	16.7
1.75	3589.1	14200	0.006042743	16.5
1.72	3709.7	13946	0.00644771	11.3
1.42	2887.2	11247	0.007334417	4.4
1.16	2137.1	8915	0.008178572	4.1

n= 0.9728

k= 0.0011

1000ppm OTAC + NaSal (MR=2),T=20C , in DI water (D= 9.45 mm)

flow(kg/s)	Pressure drop(Pa)	ReG	Friction factor	%DR
0.37	10311.7	56162	0.001453605	71.7
0.34	9348.8	52070	0.001527018	70.8
0.33	9071.3	50627	0.001564969	70.3
0.31	8446.7	47746	0.001633318	69.4
0.30	8013.0	45588	0.001695447	68.6
0.28	7501.2	42955	0.00178213	67.5
0.27	7206.3	41520	0.001829138	66.9
0.26	6894.0	39848	0.001895695	66.1
0.23	5991.9	35318	0.002083968	63.8
0.20	4933.6	29856	0.002379916	60.4
0.17	4031.5	25364	0.002671496	57.3

n= 0.7960

k= 0.0072

2500ppm OTAC + NaSal (MR=2),T=20C , in DI water (D= 9.45 mm)

flow(kg/s)	Pressure drop(Pa)	ReG	Friction factor	%DR
0.34	11352.6	32860	0.001888108	67.8
0.33	11196.5	31965	0.001949581	67.0
0.32	10771.4	30187	0.002062612	65.6
0.30	10303.0	28426	0.002179984	64.2
0.29	9999.4	27379	0.002251895	63.3
0.28	9565.7	25820	0.002374486	61.9
0.25	9452.9	22752	0.002895363	55.0
0.22	7440.5	19259	0.003005976	55.2
0.19	6607.8	16827	0.003340557	51.8
0.16	5185.2	13060	0.003993647	46.0

n= 0.8662

k= 0.0098

5000ppm OTAC + NaSal (MR=2),T=20C , in DI water (D= 9.45 mm)

flow(kg/s)	Pressure drop(Pa)	ReG	Friction factor	%DR
0.30	13434.4	11944	0.002842551	62.4
0.28	12888.0	11254	0.003028968	60.5
0.28	12506.3	10842	0.003139124	59.5
0.26	11864.4	10159	0.003339905	57.6
0.24	11170.4	9415	0.003596367	55.2
0.23	10702.0	8945	0.003771465	53.6
0.22	10077.5	8278	0.004071323	50.8
0.20	9314.2	7552	0.004424387	47.8
0.19	8585.5	6964	0.004705194	45.6
0.17	7900.2	6446	0.004961882	43.7

n= 0.5301

k= 0.1078

Fresh 500 ppm PAM + 300 ppm OTAC in DI water (D= 34.8 mm)

flow(kg/s)	Pressure drop(Pa)	Re_G	Friction factor	%DR
4.49	4291.7	36594	0.001098092	68.3
4.28	3953.4	34175	0.001110185	68.6
4.00	3389.6	30934	0.001090042	70.1

3.77	3224.8	28305	0.00117025	68.7
3.59	3261.0	26362	0.001303603	65.8
3.31	2770.2	23373	0.001304447	67.0
3.04	2551.3	20608	0.001425839	65.2
2.78	2322.3	18060	0.0015532	63.5
2.53	2084.9	15790	0.00167401	62.2
2.30	1945.2	13714	0.001891977	58.9
3.30	2921.7	23325	0.001379637	65.1
2.77	2473.0	18016	0.001659482	61.0
2.57	2163.2	16086	0.001693527	61.5
2.26	1733.9	13340	0.001751203	62.3
1.98	1557.9	11013	0.00204231	58.4
1.61	1286.9	8086	0.002568429	52.2
1.37	1116.0	6401	0.003061369	46.7
1.13	1042.7	4789	0.00424461	32.1
0.88	742.2	3361	0.004891074	29.4
0.73	722.0	2556	0.006906741	7.9
0.59	451.8	1846	0.006728345	18.4

n= 0.5261

k= 0.1255

Fresh 500 ppm PAM + 300 ppm OTAC in DI water (D= 34.8 mm)

flow(kg/s)	Pressure drop(Pa)	Re_G	Friction factor	%DR
3.23	2738.2	19850	0.001356468	67.2
2.92	2446.1	17170	0.001475272	65.8
2.71	2184.3	15343	0.001534588	65.6
2.40	1943.5	12815	0.001743293	62.9
2.12	1696.8	10700	0.001944201	60.7
1.78	1313.0	8267	0.002135007	60.0
1.56	1260.8	6820	0.002661689	52.8
1.35	1114.3	5503	0.003147685	47.6
1.02	811.2	3618	0.004048018	40.3
0.82	690.0	2615	0.005349781	28.2
0.70	608.3	2069	0.006478944	18.8
4.98	3709.7	37675	0.000770275	77.6
3.06	2816.5	18379	0.001548898	63.4
2.59	2441.0	14367	0.001874969	58.8
2.58	2149.2	14255	0.001668531	63.4

4.12	4014.2	28440	0.001220672	67.3

n= 0.7526

k= 0.0102

Fresh 500 ppm PAM +800 ppm OTAC in DI water (D= 34.8 mm)

flow(kg/s)	Pressure drop(Pa)	Re_G	Friction factor	%DR
5.08	4421.8	99871	0.000882461	74.7
4.87	4213.7	94671	0.000916194	74.1
4.44	3780.0	84295	0.000990025	72.8
4.04	3519.7	74983	0.001112192	70.4
3.60	3042.6	64892	0.001212161	69.0
3.60	3224.0	64892	0.001284401	67.1
3.18	3295.5	55707	0.001676917	58.8
2.80	2678.4	47429	0.001763962	58.5
2.44	2491.6	39993	0.002156879	51.5
1.94	1844.2	30100	0.002517812	47.6
3.31	3261.0	58433	0.001536981	61.8
2.85	2710.4	48632	0.001714736	59.4
2.44	2271.0	40087	0.001958546	56.0
1.97	1773.5	30605	0.002357547	50.7
1.67	1471.2	24918	0.002719344	46.2
1.36	1107.6	19289	0.00308645	42.9
1.11	1051.1	15022	0.004373773	24.4
1.01	892.0	13261	0.004533043	24.2
0.87	696.7	10984	0.0047888	23.8
0.73	537.6	8821	0.005252256	21.2

n= 0.5301

k= 0.1078

Fresh 500 ppm PAM + 300 ppm OTAC in DI water (D= 22.02 mm)

flow(kg/s)	Pressure drop(Pa)	Re_G	Friction factor	%DR
4.03	26402.5	93952	0.000852026	67.7
3.55	21284.7	78251	0.00088091	68.3
3.17	16852.1	66164	0.000876335	70.0
2.93	14787.6	58821	0.000902451	70.1
2.67	12246.1	51370	0.000898588	71.4
2.29	9088.6	41101	0.000903322	73.1
2.02	7162.9	34192	0.000914523	74.1

2.34	9912.7	42442	0.000943142	71.6
2.04	7501.2	34497	0.000946206	73.2
1.72	5601.6	26818	0.00099533	73.8
1.47	4465.2	21340	0.001082692	73.3
1.24	3467.7	16612	0.001182237	72.9
1.02	2851.8	12529	0.001427201	69.8
1.02	2931.0	12529	0.001466837	69.0
0.86	2628.8	9687	0.001866966	63.4
0.72	2277.7	7415	0.002327029	57.8
0.55	1936.8	5076	0.003313671	46.1
0.47	1677.5	4056	0.003894079	40.6
0.33	1363.5	2399	0.006469636	15.3

n= 0.5301

k= 0.1078

Fresh 500 ppm PAM +500 ppm OTAC in DI water (D= 22.02 mm)

flow(kg/s)	Pressure drop(Pa)	Re_G	Friction factor	%DR
2.18	12905.3	38147	0.001419693	58.6
1.98	10997.0	33093	0.001467847	58.9
1.80	9227.4	28706	0.001494595	59.8
1.59	7648.7	23944	0.001585702	59.6
1.42	6035.3	20236	0.00157313	61.8
1.18	4525.9	15535	0.001690407	62.0
1.03	3407.0	12750	0.001664822	64.6
0.81	2426.8	8933	0.001924349	63.1
4.02	34762.8	93637	0.001126966	57.3
3.75	29931.5	84584	0.00111431	59.0
2.93	20408.3	58867	0.001244162	58.8
2.94	19766.7	59093	0.001198759	60.3
2.41	13850.8	44208	0.0012467	62.0
2.08	11396.0	35611	0.001376683	60.6

n= 0.7526

k= 0.0102

Fresh 500 ppm PAM +800 ppm OTAC in DI water (D= 22.02 mm)

flow(kg/s)	Pressure drop(Pa)	Re_G	Friction factor	%DR
2.40	15958.7	86803	0.001453023	59.8
2.18	14336.6	77075	0.001579365	57.7

2.00	12957.4	69437	0.001687411	56.0
1.81	11630.2	61250	0.001852027	53.4
1.57	9904.0	51270	0.002097599	49.6
1.34	8143.1	42022	0.002372523	46.0
1.18	7067.5	35992	0.002639665	42.3
0.96	5540.8	27594	0.003168651	35.5
0.77	4430.5	21134	0.003885533	26.4
0.66	3736.6	17332	0.004503626	19.1
0.54	3155.4	13642	0.005582971	5.9
0.54	3081.7	13498	0.005546042	6.8
0.41	2509.2	9556	0.007856774	0.0
0.29	2068.1	6162	0.013084578	0.0
4.28	36334.6	178944	0.001037184	65.2
3.91	33662.9	160033	0.001149375	62.6
3.65	31060.6	146766	0.001218363	61.2
3.42	27747.0	135019	0.001244159	61.3
3.04	23670.1	116598	0.001342757	59.8
2.75	21206.6	103237	0.001462216	57.7

n= 0.5775

k= 0.0421

Fresh 250 ppm PAM +300 ppm OTAC in DI water (D= 34.8 mm)

flow(kg/s)	Pressure drop(Pa)	Re_G	Friction factor	%DR
5.10	2864.5	81323	0.000568569	80.6
4.66	2386.3	71546	0.000567119	81.3
4.25	1898.1	62731	0.000542675	82.8
2.31	1551.2	26360	0.001500758	62.8
3.43	1216.2	46390	0.000531479	84.5
3.04	1158.9	39086	0.000644409	82.2
2.56	969.5	30566	0.000761714	80.3
2.86	1361.0	35685	0.00086007	76.8
2.59	1249.8	31140	0.000956591	75.2
2.25	1098.3	25393	0.001119883	72.6
1.97	828.9	21074	0.001098475	74.5

n= 0.6769

k= 0.0130

Fresh 250 ppm PAM +500 ppm OTAC in DI water (D= 34.8 mm)

flow(kg/s)	Pressure drop(Pa)	Re_G	Friction factor	%DR
3.30	2425.9	74643	0.001279856	64.7
3.05	2204.5	67079	0.001347556	63.9
2.77	2009.2	59283	0.001476006	61.7
2.55	1746.5	52992	0.001593816	59.9
2.28	1507.4	45858	0.00172392	58.3
2.00	1254.9	38438	0.001942883	55.2
1.70	1051.1	31132	0.002224441	51.5
1.44	819.6	24887	0.002613631	46.4
1.16	642.0	18613	0.0031617	40.1
0.90	500.6	13421	0.00406008	29.5
0.70		9590	0.005261454	16.6

n= 0.8907

k= 0.0020

Fresh 250 ppm PAM +800 ppm OTAC in DI water (D= 34.8 mm)

flow(kg/s)	Pressure drop(Pa)	Re_G	Friction factor	%DR
4.76	13339.0	183224	0.003032671	20.6
4.33	12011.9	164914	0.003301786	15.8
3.92	10311.7	147700	0.003457699	14.2
3.42	8802.4	126950	0.003877901	7.3
3.11	6868.0	114318	0.003655064	14.9
2.84	5835.8	103307	0.003727927	15.4
2.59	4898.9	93083	0.003776285	16.5
2.24	3753.9	79585	0.003838189	18.4
2.02	3051.3	70767	0.003855449	20.4
2.06	3416.7	72319	0.004151584	13.8
1.67	2401.5	57424	0.004422488	13.3
1.45	1901.4	48845	0.004687733	11.8
1.13	1290.2	37041	0.005237822	8.0
0.93	955.2	29897	0.005706093	5.0

n= 0.7740

k= 0.0040

Fresh 100 ppm PAM +500 ppm OTAC in DI water (D= 34.8 mm)

flow(kg/s)	Pressure drop(Pa)	Re_G	Friction factor	%DR
3.07	4864.2	118720	0.002651049	25.1
2.84	4309.1	107850	0.002746737	24.4
2.54	3710.6	93900	0.002964845	21.3
2.27	3086.0	81677	0.003095761	20.8
2.27	3291.3	81677	0.003301715	15.5
2.00	2752.5	70243	0.003531374	13.1
1.66	2134.6	55840	0.003981995	7.8
1.46	1796.2	47680	0.004335796	3.7
1.14	1152.2	35132	0.004577085	6.1
4.69	10133.9	198978	0.002378484	23.0
4.14	8321.7	170932	0.002502513	22.2
3.24	5676.5	126462	0.002790751	19.9
2.79	4264.9	105430	0.002821143	22.8
2.42	3263.4	88643	0.002864566	25.1

n= 0.5775

k= 0.0421

Degraded 250 ppm PAM +300 ppm OTAC in DI water after 20 hr (D= 22.02 mm)

flow(kg/s)	Pressure drop(Pa)	Re_G	Friction factor	%DR
2.25	20425.9	71589	0.002117003	34.6
2.04	17580.8	62588	0.002201028	34.5
2.05	17606.8	62655	0.002200981	34.5
1.85	14909.1	54148	0.002288155	34.6
1.66	12506.3	46449	0.002381286	34.8
1.49	10554.6	39870	0.002491084	34.6
1.24	7822.2	30639	0.002673435	34.8
1.08	6269.5	25176	0.00282423	34.8
0.86	4413.2	18397	0.003089907	34.7
0.76	3580.4	15190	0.003281869	34.3
0.68	3182.7	13044	0.003613945	30.6
0.55	2430.1	9783	0.004134734	26.8
0.46	1861.0	7521	0.004582816	24.6
0.35	1296.1	5030	0.005618854	17.4

n= 0.6769

k= 0.0130

Degraded 250 ppm PAM +500 ppm OTAC in DI water after 20 hr (D= 22.02 mm)

flow(kg/s)	Pressure drop(Pa)	Re_G	Friction factor	%DR
1.99	25630.5	93967	0.0033895	0.4
1.80	21701.0	82078	0.003521002	0.0
1.61	18188.0	70864	0.003684768	0.0
1.40	14466.7	59039	0.003862298	0.0
1.20	11300.6	48337	0.004081946	1.6
1.01	8325.3	38341	0.004268297	3.2
0.83	5957.2	29669	0.004500169	3.9
0.70	4456.5	23611	0.004754702	6.3
0.59	3276.8	18814	0.004928255	1.4
0.59	3433.6	18749	0.005190962	3.2
0.51	2654.0	15461	0.005370241	4.1
0.42	1939.3	12103	0.005681886	4.6
0.35	1418.2	9449	0.006040848	5.8

n= 0.8907

k= 0.0020

Degraded 250 ppm PAM +500 ppm OTAC in DI water after 20 hr (D= 22.02 mm)

flow(kg/s)	Pressure drop(Pa)	Re_G	Friction factor	%DR
2.02	28761.9	129704	0.003700153	3.3
1.87	24719.7	119456	0.003688876	5.6
1.47	17225.1	91577	0.004150559	0.7
1.32	14570.8	81271	0.004354223	0.0
1.13	10884.2	68415	0.004436629	1.5
0.97	8047.7	57611	0.004472206	4.9
0.87	6633.8	50981	0.004595616	5.3
0.79	5584.2	46112	0.004635878	6.9
0.66	3667.2	37886	0.004338782	17.1
0.56	2895.2	31161	0.004871972	11.5
0.56	3064.0	31066	0.005184587	5.9
0.50	2590.9	27662	0.005404313	4.7
0.42	1947.7	23003	0.005665339	4.7
0.32	1154.7	16818	0.005907647	8.3
3.54	70989.1	242018	0.002966122	9.1
3.14	57977.7	212291	0.003068118	9.1
2.75	45908.0	182744	0.003183107	9.2

2.35	35024.4	153662	0.003319356	9.4
1.97	25728.0	126533	0.003460878	10.1
1.56	17199.0	97519	0.003700204	10.1
1.57	16253.6	98158	0.003455877	15.9

n= 1

k= 0.0010

Fresh 500 ppm PEO / 1000 ppm OTAC+NaSal (MR=2) at T=25 C (D= 34.8 mm)

flow(kg/s)	Pressure drop(Pa)	Re_G	Friction factor	%DR
6.33	9079.9	231504	0.001168801	67.5
5.93	9669.8	216910	0.001417855	61.3
5.44	9756.5	198949	0.001700546	54.5
4.86	8767.7	177900	0.001911204	50.3
4.28	7978.3	156627	0.002243643	43.5
3.52	6382.2	128898	0.002650035	36.4
3.10	5410.7	113463	0.002899495	32.6
2.80	4491.2	102405	0.002954587	33.1
2.56	3684.5	93593	0.002901829	0.0
2.50	3709.7	91628	0.003048285	0.0
2.24	3442.8	81974	0.003534601	24.3
2.00	3048.9	73274	0.003917549	18.4
1.74	2525.2	63563	0.004311833	13.3
1.46	1913.2	53292	0.004647494	10.6
1.17	1377.8	42739	0.005203614	5.3

n= 1

k= 0.0010

Degraded 500 ppm PEO / 1000 ppm OTAC+NaSal (MR=2) after 3hr at T=25 C (D= 34.8 mm)

flow(kg/s)	Pressure drop(Pa)	Re_G	Friction factor	%DR
6.33	17095.0	231448	0.002201593	38.9
6.04	15082.6	221120	0.002128108	41.6
5.37	12688.5	196423	0.002268816	39.5
4.80	10997.0	175767	0.002455685	36.4
4.29	9392.2	156851	0.002633704	33.7
3.44	6824.6	125755	0.002977153	29.0
2.85	5202.5	104426	0.003291342	25.1
2.56	4248.4	93705	0.003337872	26.1

n= 0.8587

k= 0.0096

Fresh 500 ppm PEO / 2500 ppm OTAC+NaSal (MR=2) at T=25 C (D= 34.8 mm)

flow(kg/s)	Pressure drop(Pa)	Re_G	Friction factor	%DR
6.33	7761.5	65668	0.000999081	77.0
5.80	7301.7	59436	0.001119329	74.9
5.12	6460.3	51571	0.001270031	72.5
4.46	5618.9	44094	0.001453519	69.8
3.70	4421.8	35607	0.001663717	67.3
3.49	4222.3	33292	0.001787282	65.5
3.19	3710.6	30038	0.001880845	64.6
3.13	3848.8	29362	0.00203022	62.0
2.68	3116.4	24610	0.002239905	60.0
2.19	2274.9	19516	0.002455033	58.7

n= 0.8959

k= 0.0066

Degraded 500 ppm PEO / 2500 ppm OTAC+NaSal (MR=2) after 1.5hr at T=25 C (D= 34.8 mm)

flow(kg/s)	Pressure drop(Pa)	Re_G	Friction factor	%DR
6.33	12350.2	65668	0.001589754	65.1
6.33	11231.2	65668	0.001445715	68.2
5.87	10710.7	60317	0.001600156	65.6
5.20	9522.3	52507	0.001813924	62.3
4.32	8013.0	42489	0.002211988	56.5
3.84	7310.4	37127	0.00255624	51.4
3.84	6781.3	37110	0.002373114	54.9
2.16	3441.7	19250	0.003804502	38.9
2.15	3266.9	19141	0.003647515	41.5
1.80	2581.6	15658	0.004098493	37.5
1.36	1629.5	11372	0.004530745	36.3
1.81	2567.3	15703	0.004055029	38.1
1.17	1275.1	9606	0.004765516	35.9
0.96	1047.8	7670	0.005809509	26.2
0.71	600.8	5378	0.006205183	28.0
0.41	304.4	2868	0.009461561	6.4

n= 0.8811

k= 0.0068

Degraded 500 ppm PEO / 2500 ppm OTAC+NaSal (MR=2) after 3hr at T=25 C (D= 34.8 mm)

flow(kg/s)	Pressure drop(Pa)	Re_G	Friction factor	%DR
6.33	14145.7	65668	0.001820887	60.0
6.33	13729.4	65668	0.001767291	61.2
6.16	13018.1	63691	0.001767942	61.5
5.66	11907.8	57842	0.001914528	59.3
4.40	9392.2	43403	0.002497826	50.6
4.22	8993.2	41355	0.002603144	49.2
3.90	8099.7	37771	0.002748161	47.6
3.48	6668.5	33175	0.002840173	47.6
2.78	5150.5	25692	0.003433291	40.6
2.11	3372.3	18783	0.003891939	37.8
2.08	3355.3	18441	0.003999084	36.4
1.78	2937.7	15430	0.004785282	27.3
1.51	2347.6	12787	0.005315211	23.0
1.03	1267.5	8244	0.006193295	19.8

n= 1

k= 0.0010

Degraded 500 ppm PEO / 2500 ppm OTAC+NaSal (MR=2) after24hr at T=25 C (D= 34.8 mm)

flow(kg/s)	Pressure drop(Pa)	Re_G	Friction factor	%DR
6.02	14676.7	62101	0.002083439	54.9
6.02	14250.7	62101	0.002022968	56.2
5.86	13523.0	60214	0.002026371	56.4
5.38	12387.1	54629	0.002201356	53.8
4.17	9813.4	40846	0.002902816	43.5
4.00	9405.2	38892	0.003031695	41.7
3.69	8491.1	35472	0.003216058	39.6
3.29	7026.8	31087	0.003353742	39.1
2.61	5473.7	23952	0.004125788	29.9
1.97	3654.4	17369	0.004837359	24.3
1.94	3516.1	17043	0.004811249	25.0
1.80	2793.8	15658	0.004435287	32.4
1.81	2567.3	15703	0.004055029	38.1

1.36	2176.7	11372	0.006052214	15.0

n= 0.8888

k= 0.0061

Fresh 1000 ppm PEO / 1000 ppm OTAC+NaSal (MR=2) at T=25 C (D= 34.8 mm)

flow(kg/s)	Pressure drop(Pa)	Re_G	Friction factor	%DR
6.23	8811.0	82060	0.001169647	72.8
6.33	9392.2	83475	0.001208999	71.8
5.41	8594.2	70162	0.001512423	66.2
4.36	6911.4	55153	0.001875777	60.6
4.11	6920.0	51711	0.002109041	56.4
3.86	5922.5	48208	0.002047956	58.4
3.35	5662.3	41132	0.002605512	49.2
2.88	4855.6	34855	0.003010038	43.7
2.36	3563.1	27883	0.003300813	41.7
2.06	2964.6	24041	0.003586107	39.0
2.07	3213.0	24141	0.003857923	34.3
1.88	2764.3	21651	0.004037416	33.1
1.27	1620.2	14045	0.00515707	23.5
0.91	913.1	9627	0.00573531	22.8

n= 0.9728

k= 0.0011

Degraded 1000 ppm PEO / 1000 ppm OTAC+NaSal (MR=2) after3hr at T=25 C (D= 34.8 mm)

flow(kg/s)	Pressure drop(Pa)	Re_G	Friction factor	%DR
6.33	20738.2	255191	0.002669491	24.1
5.95	18916.6	239442	0.002756541	22.8
5.36	16487.8	215239	0.002956617	19.4
4.86	14327.9	194450	0.003131138	16.8
4.16	11569.5	165924	0.003443352	12.0
3.63	9539.7	144035	0.003739671	7.8
3.07	6798.6	121361	0.003720128	12.1
2.48	4413.2	97374	0.003707636	17.1
2.27	3684.5	89205	0.003671288	19.7
1.89	3112.9	73851	0.004480431	6.5
2.00	2676.8	78160	0.003449995	27.0

1.59	2277.7	61763	0.004643068	7.3

n= 0.9728

k= 0.0011

Fresh 1000 ppm PEO / 25000 ppm OTAC+NaSal (MR=2) at T=25 C (D= 34.8 mm)

flow(kg/s)	Pressure drop(Pa)	Re_G	Friction factor	%DR
5.93	11821.0	43646	0.001731043	64.1
6.02	12081.3	44445	0.001714997	64.3
5.14	10110.3	36959	0.001968615	60.9
4.63	8516.1	32661	0.002049464	60.6
4.44	9557.0	31150	0.002494492	52.6
4.23	8715.6	29424	0.002508186	53.0
4.13	9036.6	28610	0.002728671	49.3
3.89	8403.3	26712	0.00285428	47.9
3.65	7822.2	24785	0.003020402	45.9
3.16	6923.4	20918	0.003575146	38.7
2.71	5749.0	17518	0.004023413	34.1
2.21	4641.7	13779	0.004901561	24.6
1.93	3753.9	11740	0.005215688	23.0
1.93	3553.6	11792	0.004899707	27.6
1.75	3229.9	10480	0.005451113	21.9
1.16	1840.0	6527	0.006989344	11.4
0.81	1053.6	4285	0.008231065	6.4

n= 0.7869

k= 0.0218

Fresh2000 ppm PEO / 1000 ppm OTAC+NaSal (MR=2) at T=25 C (D= 34.8 mm)

flow(kg/s)	Pressure drop(Pa)	Re_G	Friction factor	%DR
5.47	6616.4	40332	0.001140328	75.8
4.73	5167.8	33788	0.001192536	75.8
3.44	4413.2	23000	0.001920043	64.8
2.99	3753.9	19360	0.002169667	62.0
2.40	2895.2	14864	0.002586971	57.7
2.40	2579.1	14853	0.002307499	62.3
2.14	2195.2	12896	0.002479227	60.9
1.85	1996.5	10848	0.002998746	54.9
1.43	1360.1	7907	0.003440247	52.3

1.59	1675.8	8982	0.00343593	50.8
1.05	848.3	5468	0.00394204	50.4
0.82	410.5	4036	0.003147133	63.5

n= 0.9780

k= 0.0025

Degraded 2000 ppm PEO / 1000 ppm OTAC+NaSal (MR=2) after 3 hrat T=25 C (D= 34.8 mm)

flow(kg/s)	Pressure drop(Pa)	Re_G	Friction factor	%DR
6.33	18049.2	92579	0.002324477	48.7
6.33	18214.0	92579	0.002345703	48.2
6.30	17988.4	92242	0.002333605	48.5
5.88	16990.9	86113	0.002529145	45.2
5.56	15837.2	81331	0.0026428	43.5
4.49	12306.8	65682	0.003148838	36.2
4.06	10936.2	59440	0.00341668	32.5
3.83	9921.4	56072	0.003483126	32.2
3.09	7215.0	45295	0.003881704	28.3
2.81	6174.1	41119	0.004030645	27.3
2.59	5341.3	37976	0.004088137	27.8
2.26	4048.9	33081	0.004083734	30.3

n= 0.9890

k= 0.0020

Degraded 2000 ppm PEO / 1000 ppm OTAC+NaSal (MR=2) after 24 hrat T=25 C (D= 34.8 mm)

flow(kg/s)	Pressure drop(Pa)	Re_G	Friction factor	%DR
6.33	20395.4	115724	0.002626633	38.7
5.87	18280.5	107389	0.002733918	37.4
5.38	16198.6	98380	0.002886566	35.3
4.77	13844.2	87266	0.003135389	31.8
4.01	10754.5	73290	0.003453173	28.1
3.60	8945.3	65824	0.003560691	27.8
3.28	7615.2	59931	0.003656765	27.6
2.51	5245.9	45954	0.004284297	20.6
2.37	4612.7	43429	0.004218092	22.9
2.17	4014.2	39724	0.004387345	21.6

1.92	3296.4	35065	0.00462376	19.9

n= 0.7120

k= 0.0392

Fresh 2000 ppm PEO / 2500 ppm OTAC+NaSal (MR=2) at T=25 C (D= 34.8 mm)

flow(kg/s)	Pressure drop(Pa)	Re_G	Friction factor	%DR
5.92	5595.9	41812	0.000823918	80.6
5.47	5196.1	37807	0.000894535	79.5
5.00	4751.5	33659	0.000979756	78.2
4.35	4352.5	28176	0.001182883	74.9
3.61	3233.5	22098	0.001281514	74.6
3.40	3000.1	20471	0.00133895	74.0
3.10	2704.3	18210	0.001447533	72.7
3.04	3044.7	17744	0.001696549	68.2
2.60	2618.2	14510	0.001993942	64.7
2.12	2004.1	11134	0.002302782	62.0
1.67	1501.0	8183	0.002782223	57.8
1.25	889.5	5621	0.002954164	59.5

n= 0.7737

k= 0.0093

Fresh 500 ppm PEO / 1000 ppm SDS at T=25 C (D= 34.8 mm)

flow(kg/s)	Pressure drop(Pa)	Re_G	Friction factor	%DR
6.33	17389.9	123942	0.00223849	36.1
6.04	16088.8	117014	0.002274699	36.0
5.38	14510.1	101570	0.002584187	29.9
4.82	12384.9	88866	0.002742788	28.2
4.18	10060.1	74572	0.002965644	25.9
3.75	8334.0	65158	0.003061594	26.1
3.07	6087.3	51004	0.003334249	24.6
2.29	4014.2	35720	0.003930488	19.1
2.00	3407.0	30124	0.004404626	13.3
1.98	3383.1	29784	0.004455537	12.5
1.69	2625.4	24550	0.004738785	11.6

n= 0.9980

k= 0.0010

Degraded 500 ppm PEO / 1000 ppm SD after 24 hr at T=25 C (D= 34.8 mm)

flow(kg/s)	Pressure drop(Pa)	Re_G	Friction factor	%DR
6.26	21033.1	228978	0.003286833	9.0
5.69	17025.6	208154	0.003348952	9.5
4.92	13555.9	179977	0.003626136	5.5
4.46	10875.5	163194	0.003511514	10.7
3.98	10502.5	145625	0.003537947	12.5
3.95	8654.9	144671	0.003461826	14.5
3.47	4812.2	126822	0.003712354	11.3
2.89	4109.6	105773	0.002967342	32.3
2.58	3450.3	94379	0.003182906	29.4
2.35	3397.4	86015	0.00321724	30.3
2.09	2558.9	76361	0.004019543	15.4

n= 0.6761

k= 0.0307

Fresh 500 ppm PEO /3000 ppm SDS at T=25 C (D= 34.8 mm)

flow(kg/s)	Pressure drop(Pa)	Re_G	Friction factor	%DR
6.19	7032.8	72968	0.000946597	74.0
5.70	7544.6	65497	0.001195462	68.2
5.06	6616.4	55952	0.001330053	66.1
4.52	5827.1	48105	0.00147175	63.9
4.00	4977.0	40892	0.001606674	62.3
3.27	4005.5	31421	0.0019252	58.0
2.67	2929.9	23964	0.002120406	57.0
2.67	3355.3	23927	0.002433887	50.6
2.34	3213.0	20123	0.003027491	41.4
2.10	2278.6	17443	0.002664409	50.4
1.77	2036.1	13895	0.003357043	41.2
1.52	1708.6	11400	0.003798682	36.9

n= 0.9068

k= 0.0050

Degraded 500 ppm PEO / 3000 ppm SD after 3 hr at T=25 C (D= 34.8 mm)

flow(kg/s)	Pressure drop(Pa)	Re_G	Friction factor	%DR

6.33	19706.0	89635	0.002536618	44.4
6.27	18491.6	88827	0.002420031	47.1
5.75	16427.1	80694	0.002562774	45.3
5.18	14284.5	72093	0.002738824	43.2
4.57	11925.1	62772	0.002945538	41.0
4.03	9964.7	54728	0.003163142	38.8
3.49	8108.4	46717	0.003438273	36.0
2.83	5835.8	37188	0.003756277	34.0
2.33	4300.4	30043	0.004089562	31.8
2.11	3615.1	26919	0.004202704	31.9
2.05	3431.9	26148	0.004207523	32.3
1.75	2673.4	21986	0.004501007	30.6
1.35	1803.8	16590	0.005083785	27.0
0.83	940.9	9758	0.007002007	11.9

n= 0.9430

k= 0.0036

Degraded 500 ppm PEO / 3000 ppm SD after 24 hr at T=25 C (D= 34.8 mm)

flow(kg/s)	Pressure drop(Pa)	Re_G	Friction factor	%DR
6.33	20755.5	96288	0.002673021	40.4
5.62	19621.8	84898	0.003206715	30.7
5.12	17207.8	76926	0.00338896	28.6
4.13	12207.9	61290	0.003695774	26.4
3.92	11301.4	58067	0.003789575	25.5
3.46	9307.2	50839	0.004013436	23.7
2.99	7417.9	43548	0.004287371	21.6
2.50	6530.6	36065	0.00539259	5.9
2.48	5649.7	35737	0.004746473	17.4
2.32	5103.2	33425	0.004865825	16.7
2.13	4502.1	30402	0.005136045	14.2
1.88	3919.2	26749	0.005696197	7.8
1.88	3535.1	26703	0.00515483	16.6
1.56	2818.0	21960	0.005949355	8.3
1.26	1988.2	17564	0.006405338	6.7

n= 0.6852

k= 0.0313

Fresh 500 ppm PEO /5000 ppm SDS at T=25 C (D= 34.8 mm)

flow(kg/s)	Pressure drop(Pa)	Re_G	Friction factor	%DR
5.99	6521.0	64287	0.000936669	75.2
5.14	5939.8	52592	0.001157978	70.9
4.63	5549.5	45831	0.001333759	67.7
3.97	4682.1	37408	0.001532577	64.9
2.91	3233.5	24893	0.001966627	59.7
2.96	3523.7	25499	0.002066196	57.4
2.45	3077.5	19885	0.002634205	49.2
2.09	2175.0	16120	0.002562015	53.3
1.63	1903.9	11613	0.003693492	38.4
1.31	1371.9	8720	0.004114821	36.4
1.02	983.8	6290	0.004850437	31.4

n= 0.8574

k= 0.0083

Degraded 500 ppm PEO / 5000 ppm SD after 3 hr at T=25 C (D= 34.8 mm)

flow(kg/s)	Pressure drop(Pa)	Re_G	Friction factor	%DR
6.33	14553.4	76657	0.001873367	55.1
5.80	12610.4	69354	0.001934153	54.8
5.19	11075.0	61195	0.002114687	52.1
4.82	10060.1	56163	0.002232207	50.6
5.04	10797.5	59156	0.00218773	50.9
4.26	8733.0	48751	0.002482485	47.0
3.82	7579.3	43055	0.00267802	44.7
3.24	6122.0	35727	0.002998419	41.0
2.84	5020.4	30715	0.003203592	39.4
2.44	4014.2	25767	0.003483715	37.0
1.78	2272.7	18035	0.003682879	39.3
1.24	1456.1	11960	0.00484246	28.2
0.98	1091.6	9094	0.005864118	19.0

n= 0.9782

k= 0.0029

Degraded 500 ppm PEO / 5000 ppm SD after 24 hr at T=25 C (D= 34.8 mm)

flow(kg/s)	Pressure drop(Pa)	Re_G	Friction factor	%DR

6.33	20191.7	93140	0.002600407	42.5
6.18	18604.3	90878	0.002514054	44.7
5.79	16912.8	85023	0.002603692	43.7
5.33	15134.6	78257	0.002740561	42.0
4.87	13234.9	71319	0.0028741	40.5
4.32	11812.3	63022	0.003267752	34.5
3.37	7449.2	48982	0.003374955	36.4
2.81	5341.3	40688	0.003479404	37.4
2.33	4352.5	33582	0.004128167	29.3
1.61	2533.6	23075	0.005008912	21.9
0.80	880.3	11193	0.007171487	6.6

n= 0.9478

k= 0.0040

Fresh 1000 ppm PEO /1000 ppm SDS at T=25 C (D= 34.8 mm)

flow(kg/s)	Pressure drop(Pa)	Re_G	Friction factor	%DR
6.14	7744.1	81219	0.001057487	77.4
5.71	8897.8	75169	0.001407606	70.5
5.15	8299.3	67409	0.001615054	67.1
4.59	7631.3	59840	0.001862377	63.1
4.10	6755.2	53029	0.00207426	60.2
3.33	5410.7	42615	0.002517379	54.2
2.81	4369.8	35721	0.002843441	50.5
2.24	3155.4	28162	0.003226228	47.1
1.98	2880.5	24731	0.003770202	40.2
1.37	1626.1	16795	0.004440953	36.0
0.90	872.7	10798	0.005518818	28.8

n= 0.6051

k= 0.0780

Fresh 1000 ppm PEO /3000 ppm SDS at T=25 C (D= 34.8 mm)

flow(kg/s)	Pressure drop(Pa)	Re_G	Friction factor	%DR
5.42	6894.0	39550	0.001208424	70.2
5.20	6824.6	37305	0.001300801	68.4
4.53	5931.2	30771	0.001489933	65.7
4.10	5376.0	26806	0.001645825	63.5
3.42	4283.1	20770	0.001890301	60.9

2.94	3684.5	16803	0.002203647	57.0
2.83	3709.7	16000	0.002380065	54.2
2.69	3309.8	14876	0.002357295	55.6
2.44	3036.2	13018	0.002618505	52.4
2.02	2768.5	9973	0.003498137	40.9
1.73	2379.6	8024	0.004106552	34.7
1.42	1836.6	6100	0.004695802	30.7
1.02	1214.5	3859	0.005987694	22.1

n= 0.9137

k= 0.0070

Degraded 1000 ppm PEO / 3000 ppm SD after 3 hr at T=25 C (D= 34.8 mm)

flow(kg/s)	Pressure drop(Pa)	Re_G	Friction factor	%DR
6.33	18404.8	60968	0.00236913	48.9
5.80	16097.4	55448	0.002467686	48.1
4.75	12211.4	44638	0.002790663	44.4
4.21	10277.0	39183	0.002985593	42.5
3.57	8134.4	32793	0.003279751	39.6
2.69	5193.9	24030	0.003711807	36.9
2.27	3736.6	20061	0.003723147	39.5
1.98	3377.2	17299	0.004420309	30.9
1.64	2627.1	14042	0.005048709	25.1
1.24	1907.3	10383	0.006390277	12.3
0.95	1085.7	7747	0.006235951	20.5

n= 0.9055

k= 0.0054

Degraded1000 ppm PEO / 3000 ppm SD after 24 hr at T=25 C (D= 34.8 mm)

flow(kg/s)	Pressure drop(Pa)	Re_G	Friction factor	%DR
6.33	24598.3	83764	0.003166372	26.0
5.63	20131.0	73661	0.003277381	25.8
5.02	16748.0	65023	0.003424586	24.9
4.46	13781.4	57150	0.003567481	24.3
3.92	10780.1	49667	0.003606293	26.2
3.44	9487.6	42952	0.004138855	18.4
2.94	6868.0	36160	0.004103326	22.6
2.58	5575.5	31352	0.004323444	21.3

2.83	7067.5	34757	0.004539263	15.2
2.15	4283.1	25662	0.004788903	17.2
2.33	4985.7	28120	0.004716335	16.5
2.04	3667.2	24240	0.004550296	22.4
1.66	2985.1	19373	0.005578887	10.2
1.34	1937.8	15319	0.005562024	15.7
1.06	1379.4	11824	0.006354601	9.8

n= 0.6274

k= 0.0739

Fresh 1000 ppm PEO /5000 ppm SDS at T=25 C (D= 34.8 mm)

flow(kg/s)	Pressure drop(Pa)	Re_G	Friction factor	%DR
5.08	5679.6	32715	0.001132106	73.5
4.42	4699.4	26957	0.001241992	72.4
3.95	4352.5	23152	0.001435762	69.4
3.12	3060.0	16753	0.001617304	68.5
2.97	2531.1	15656	0.001476542	71.8
2.69	2229.7	13620	0.00159349	70.7
2.33	1924.1	11205	0.001827399	68.1
2.06	1807.1	9442	0.002202346	63.4
2.01	1419.0	9163	0.001806708	70.2
1.39	1158.9	5511	0.003095437	55.6
1.01	941.7	3559	0.004756417	39.5

n= 0.7743

k= 0.0267

Degraded 1000 ppm PEO /5000 ppm SD after 3 hr at T=25 C (D= 34.8 mm)

flow(kg/s)	Pressure drop(Pa)	Re_G	Friction factor	%DR
5.58	10060.1	36814	0.001667695	65.4
4.76	9010.6	30299	0.002052545	59.5
4.13	7475.2	25452	0.002263015	57.4
3.66	7084.9	21972	0.002726357	50.6
3.39	5853.1	19991	0.002627871	53.5
2.61	3953.4	14500	0.002997456	51.3
2.25	3155.4	12113	0.003208664	50.3
2.03	2751.7	10682	0.003434987	48.5
1.94	2561.4	10063	0.003524845	48.0

1.68	2297.1	8493	0.004168853	41.2
1.31	1831.5	6260	0.005467854	28.8
1.06	1640.4	4807	0.007535373	8.4
0.87	990.5	3763	0.006784136	22.7

n= 0.9044

k= 0.0086

Degraded 1000 ppm PEO /5000 ppm SD after24 hr at T=25 C (D= 34.8 mm)

flow(kg/s)	Pressure drop(Pa)	Re_G	Friction factor	%DR
6.33	17919.1	53008	0.002306601	52.0
6.07	16210.2	50647	0.002267604	53.4
5.54	14301.9	45801	0.002403814	51.8
4.80	11734.3	39172	0.002623682	49.5
4.36	10103.5	35295	0.00273251	48.7
3.74	7934.9	29803	0.002922187	47.5
3.14	6495.0	24623	0.003389394	42.0
2.86	5714.3	22171	0.003611235	39.8
2.63	5055.1	20222	0.003779146	38.5
2.01	3242.5	15131	0.004115743	37.8
1.56	2256.7	11451	0.004764211	32.9
1.27	1652.2	9108	0.005297142	29.7
0.96	1155.5	6712	0.006468586	20.5
0.77	878.6	5304	0.007557599	12.6

n= 0.6964

k= 0.0465

Fresh 2000 ppm PEO /1000 ppm SDS at T=25 C (D= 34.8 mm)

flow(kg/s)	Pressure drop(Pa)	Re_G	Friction factor	%DR
4.84	7405.8	30265	0.001630764	64.7
4.58	6234.8	28192	0.00153074	67.5
4.06	5749.0	24106	0.00179474	63.5
3.76	5462.8	21772	0.001993735	60.6
3.27	4413.2	18174	0.002125134	60.0
3.02	3901.4	16384	0.002202537	59.7
2.54	2981.9	13044	0.002388407	58.9
2.56	2875.4	13219	0.002256483	61.0
2.12	2390.5	10319	0.002742971	55.7

1.84	1924.1	8574	0.002933575	54.9
1.41	1638.8	6087	0.004226436	40.7
0.92	941.7	3460	0.005777298	30.5

n= 0.9150

k= 0.0080

Degraded 2000 ppm PEO /2000 ppm SD after 3hr at T=25 C (D= 34.8 mm)

flow(kg/s)	Pressure drop(Pa)	Re_G	Friction factor	%DR
6.33	20243.8	52857	0.002605846	50.0
6.07	19289.6	50498	0.0027011	48.7
5.73	18014.5	47429	0.002831545	47.1
5.42	16930.2	44719	0.002965941	45.4
4.92	14978.5	40222	0.003190135	42.8
4.29	12671.1	34647	0.003553146	38.6
4.06	11656.2	32634	0.003649878	37.9
3.11	7683.4	24474	0.004089001	35.3
2.72	6226.1	21154	0.004334837	33.8
2.14	3892.7	16297	0.004383728	37.3
1.80	2895.2	13527	0.004596255	37.3

n= 0.6451

k= 0.0870

Fresh 2000 ppm PEO /3000 ppm SDS at T=25 C (D= 34.8 mm)

flow(kg/s)	Pressure drop(Pa)	Re_G	Friction factor	%DR
3.30	3520.3	13676	0.001668466	69.3
3.02	3132.2	12164	0.001764704	68.5
2.72	2807.2	10555	0.001950107	66.6
2.52	2574.9	9483	0.002095218	65.1
2.28	2349.3	8305	0.002325126	62.7
1.95	2110.2	6714	0.002858395	56.7
1.78	1832.4	5932	0.002979635	56.4
1.50	1519.2	4695	0.003489165	52.1
1.17	1160.6	3352	0.004383306	45.2
0.88	905.5	2293	0.005988112	32.5
0.77	875.2	1898	0.0076525	18.1
0.72	822.2	1726	0.008274994	13.7

n= 0.4801

k= 0.3221

Fresh 2000 ppm PEO /5000 ppm SDS at T=25 C

flow(kg/s)	Pressure drop(Pa)	Re_G	Friction factor	%DR
5.10	6434.3	20920	0.00127406	68.8
4.89	6174.1	19643	0.001328181	68.0
4.55	5245.9	17577	0.001306262	69.5
4.23	5141.8	15720	0.001482937	66.5
3.91	4352.5	13944	0.001469792	68.0
3.67	3979.5	12659	0.001526232	67.6
3.40	3745.3	11308	0.001666382	65.8
3.25	3311.5	10519	0.001620382	67.4
3.25	3516.1	10519	0.00172047	65.4
3.05	3404.1	9597	0.001879575	63.2
2.70	3138.9	7943	0.002222886	58.8
2.33	2844.3	6355	0.002701275	53.1
2.17	2558.9	5718	0.002792852	53.0
1.87	2277.7	4537	0.00337063	46.9
1.68	1832.4	3869	0.003343733	49.7
1.36	1600.9	2790	0.004491559	38.6
1.00	1174.9	1748	0.006099849	27.2